1994

Electro-separations using conducting polymer membranes

Abdolreza Mirmohseni
University of Wollongong

ELECTRO-SEPARATIONS USING CONDUCTING POLYMER MEMBRANES

A thesis submitted in fulfilment of the requirements for the award of the degree of

DOCTOR OF PHILOSOPHY

from

THE UNIVERSITY OF WOLLONGONG

by

ABDOLREZA MIRMOHSENI (B.Sc., M.Sc.)

CHEMISTRY DEPARTMENT

MARCH, 1994

IN THE NAME OF GOD

This is to certify that the work described in this thesis has not been submitted for a higher degree at any other university or institution.

A. Mirmohseni

In Memoriam

I dedicate this thesis to the memory of my beloved friend "***Mehrdad Khanlie***" who always encouraged and helped me well beyond my expectations but sadly did not live to see the final product.

ACKNOWLEDGEMENTS

I would like to express my deep appreciation to Professor Gordon G. Wallace, my supervisor, for his constant assistance and encouragement. I have greatly benefited from discussions and ideas he put forward regarding this investigation.

I am especially indebted to my co-supervisor Dr. William Price for his help and encouragement. This work would not be completed without his efforts.

Many thanks to Dr. Anthony Hodgson for much helpful advice and constructive criticism throughout the course of this work.

The technical assistance of John Reay and Peter Sarakiniotis, Peter Pavlic and Steve Cooper are greatly appreciated.

I would also like to express my gratitude to my colleagues, Chee, Chris, Geoff, Mark, Norm and Trevor, who have patiently proof read parts of the thesis.

The help and friendship of the staff of the Chemistry Department is greatly appreciated. In particular, many thanks are due to Kerry and Louisa.

Many thanks for the financial support provided by the Scholarship Department of the Ministry of Culture and Higher Education of the Islamic Republic of Iran.

Finally my greatest thanks and love goes to my family for all their constant support and encouragement. Special thanks to my wife Maryam for her patient, great understanding and unconditional love and support over the years.

ABSTRACT

Membranes are the basis of many important applications including artificial kidney, purification of water, concentration of aqueous solutions and protein recovery. Much effort has been directed towards making synthetic membrane materials more inert with a view to preventing fouling and extending their lifetime. However once a conventional membrane has been fabricated, its characteristics (such as morphology) are fixed. This is a limitation of conventional membranes.

The present work is concerned with the development of smart separation systems, based on conducting electroactive polymer membranes such as polyaniline and polypyrrole, which are capable of responding to electrical stimuli. This is a novel concept in separation technology differing from conventional membranes due to the nature of the transport mechanism involved. The conducting polymer membranes are used as a working electrode in an electrochemical transport cell. Changes in the oxidation state of the polymers can be induced by application of potential to the membrane and this causes the movement of ions in and out of the polymer. This movement can be used to effect transport and separation processes. In conventional methods (e.g. electro-dialysis) an electrical field is applied across both sides of the film and separation is achieved based on the electrical field generated by passing the current across the membrane.

The major objective of the present investigation was to investigate the transport of organic/inorganic species across conducting polymers using novel electrochemical control. In order to achieve this the improvement of the mechanical properties of the materials, as a primary aim, was considered. Significant achievements obtained can be summarised as follows:

1) Preparation of robust free-standing membranes based on polyaniline, polypyrrole with a variety of counterions and composites was achieved. The effect of growth conditions such as current density, electrolyte concentration and effect of substrate on the membrane properties of the composite films was investigated.

2) As a major objective of the current investigation it was demonstrated that the conducting polymer membranes can be used to transfer species from one side of the membrane to the other with some control over selectivity and flux. This control was achieved using electrochemical devices. Such transport was found to be selective, resulting in the separation of mixtures. Using this approach the electrochemically controlled transport and separation of inorganic acids (e.g. HCl, H_2SO_4 and HNO_3), inorganic salts (such as NaCl and KCl) and a wide range of sulfonated organic compounds across the membranes was shown to be possible. The rate and selectivity of the transport was found to be markedly affected by the electrochemical variables. For example, by altering the electrode configuration and electrochemical waveform the transport of organic anions was significantly increased.

3) In order to study the mechanism of the mass transport in detail a electrochemical quartz crystal microbalance (EQCM) was employed. Using this technique it was shown that the ion movement during redox reactions of polypyrrole films was dependent on the nature of supporting electrolyte, the anion incorporated into the polymer during synthesis and the electrochemical waveform applied. This explained the conditions under which the polymer acts as an anion exchanger or a cation exchanger. Using the information provided by EQCM the transport properties of the membrane can be manipulated. A model to explain the transport mechanism was proposed.

LIST OF PUBLICATIONS

1) A. Mirmohseni, W. E. Price, G. G. Wallace and H. Zhao, "Adaptive Membrane Systems Based on Conductive Electroactive Polymers". *J. Int. Mat. Sys. Struct.*, 4 (1993) 43- 49.

2) R. John, A. Mirmohseni, P. Teasdale and G. G. Wallace, "Interfacial analysis-techniques for the study and characterisation of advanced Materials". *Trends in Analytical Chemistry*, 12(1993) 94- 101.

3) A. Mirmohseni, W. E. Price and G. G. Wallace, "Electrochemically Controlled Transport Across Conducting Polymer Composites. Basis of Smart Membrane Materials "*Polymer Gels and Networks*, 1(1993) 61- 77.

4) A. Mirmohseni, H. Zhao, A. Talaei, W. E. Price and G. G. Wallace, "Scratching the Surface of Intelligent Materials: Characterisation Methods for Conducting Polymer Films". *J. Int. Mat. Sys. Struc.*, In press (1994).

5) A. Mirmohseni, W.E. Price and G.G Wallace. "Electrochemically controlled transport of small charged organic molecules across conducting polymer membranes" J . Memb. Sci. Submitted.

ABBREVIATIONS

A	Surface area
A^-	Anion
ADI	Analog-digital instruments
AFM	Atomic force microscopy
Ag/Ag^+	Silver/silver ion reference electrode
Ag/AgCl	Silver/silver chloride reference electrode
ASTM	American society for testing and materials
1,3 BDSA	1,3-Benzene disulfonic acid, sodium salt
BS	Sodium benzene sulfonate
BQ	Benzoquinone
C(M)	Molar (concentration)
CV	Cyclic voltammetry
DS	Dodecyl sulfate
E	Potential
E_{app}	Applied potential
E_{pa}	Anodic peak potential
E_{pc}	Cathodic peak potential
EQCM	Electrochemical quartz crystal microbalance

ESR	Electron spin resonance spectroscopy
F	Oscillation frequency of a quartz crystal electrode
g	Gram
4HBSA	4-Hydroxy benzene sulfonic acid, sodium salt
HPLC	High performance liquid chromatography
Hz	Hertz
i	Current
ITO	Indium tin oxide
i_p	Peak current
i_{pa}	Anodic peak current
i_{pc}	Cathodic peak current
iR	Ohmic drop
L	Litre
M^+	Cation
mC	Millicoulomb
NDS	Naphthalenedisulfonic acid
NMP	1-methyl-2-pyrrolidinone
PAn/Cl	Polyaniline chloride
PE	Polyelectrolyte

pF	Pico farad
PPy/Cl	Polypyrrole chloride
PPy/BF4	Polypyrrole tetrafluroborate
PPy/NDS	Polypyrrole naphthalenedisulfonate
PPy/PTS	Polypyrrole p-toluene sulfonate
PPy/PVS	Polypyrrole polyvinylsulfonate
PTS	P-toluene sulfonic acid, sodium salt
PVS	Polyvinylsulfonic acid, sodium salt
Q	Charge
QCM	Quartz crystal microbalance
R	Resistance
RVC	Reticulated vitreous carbon
s	Second
S	Siemens
SR	Scan rate
3SBA	3-Sulfobenzoic acid, sodium salt
4SBA	4-Sulfobenzoic acid, sodium salt
SDS	Sodium dodecyl sulfate
SEM	Scanning electron microscopy

TEATFB	Tetraethylammonium tetrafluroborate
THF	Tetrahydrofuran
V	Volt
vs	Versus

SYMBOLS

ΔE	Peak separation
Δm	Mass changes
Ω	Ohm
σ	Conductivity (S cm^{-1})
α	Selectivity factor

TABLE OF CONTENTS

CHAPTER 5

ELECTROCHEMICALLY CONTROLLED TRANSPORT OF SMALL ORGANIC MOLECULES ACROSS CONDUCTING POLYMER MEMBRANES. 130

CHAPTER 6

MECHANISTIC STUDIES USING ELECTROCHEMICAL QUARTZ CRYSTAL MICROBALANCE (EQCM) 167

CHAPTER 1

GENERAL INTRODUCTION

1.1 BACKGROUND REVIEW

Polymer science and technology have been among the most important areas of discovery during the twentieth century[1]. Our bodies, like all forms of life, depend on polymer molecules such as carbohydrates, proteins and nucleic acids. From the earliest times, polymeric materials have been employed to satisfy human needs such as wool, natural rubber, cotton, wood and gums. In the past few decades, there has been an enormous effort to synthesise and characterise polymeric materials. These efforts are perhaps due to the great diversity of physical and chemical properties[2] that they exhibit, in particular having high mechanical strength, thermal stability, elasticity, chemical inertness and electrical insulation. This has resulted in the application of polymers in a wide range of areas.

Over the last decade there has been widespread interest in a new area in polymer science known as conducting polymers, materials having considerable electrical conductivity[3]. Interest in the development of these materials gained momentum[4] in late 1970s, when Shirakawa and co-workers[5,6] synthesised polyacetylene with metallic properties. The conductivity of this polymer was found to increase[7] (~1000 S cm^{-1}) upon doping. Since then remarkable progress has been made in this area.

Figure 1.1 gives the conductivity range of several conducting polymers compared to conventional metals. This group of materials with a backbone of conjugated π-electrons also displays unusual electronic properties such as low energy optical transition, low ionisation potential and high electron affinity[8]. Of particular importance is the fact that they can be oxidised or reduced more easily and more reversibly than conventional polymers.

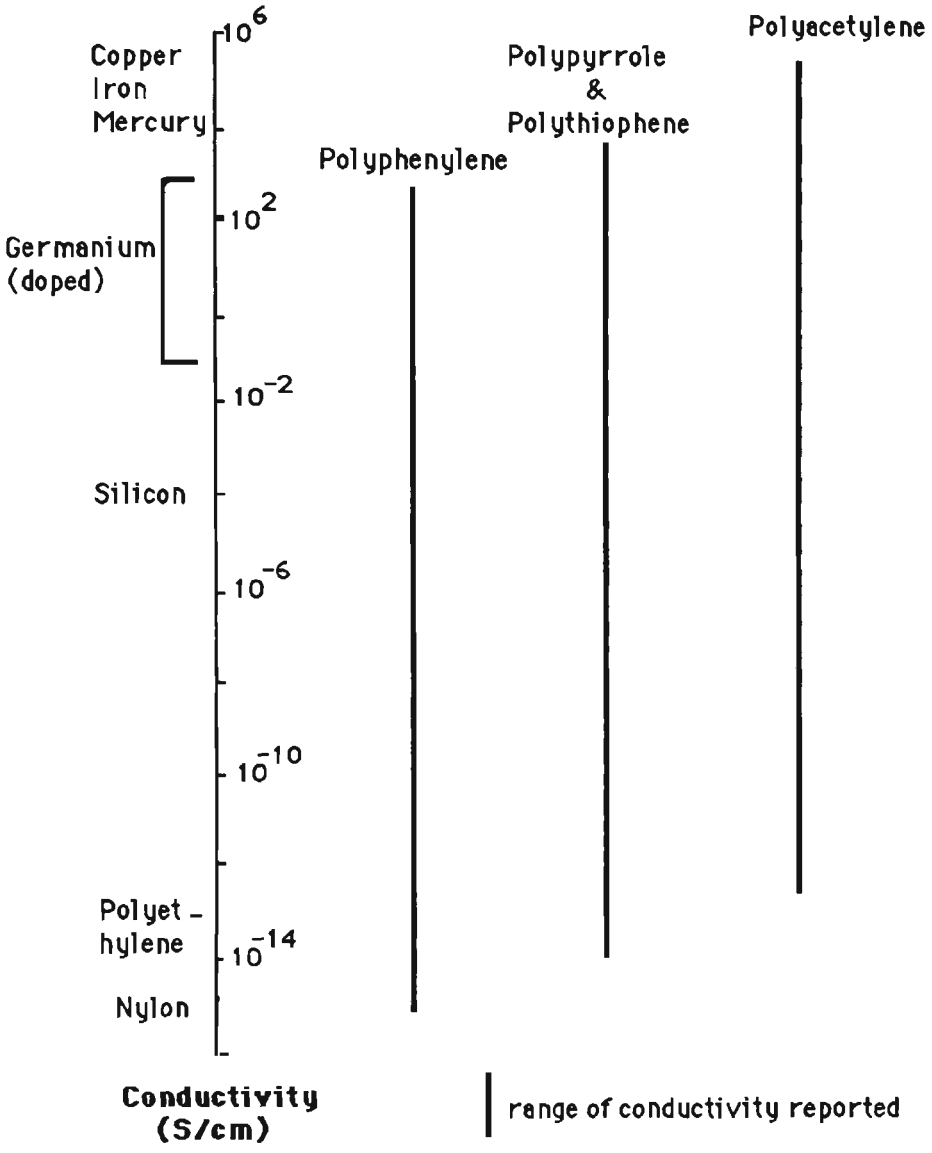

FIGURE 1.1 Comparison of conductivity ranges for conducting polymer systems compared with conventional materials (see reference 3)

The discovery that the doping process can enhance the conductivity of the polymers caused some previously known polymers to be reinvestigated. Two classes of conducting polymers that have attracted considerable attention are polyaniline and polypyrrole. These polymers have high chemical stability and good electrical properties making them suitable for use in rechargeable batteries[9, 10] and sensors[11, 12].

1.2 POLYPYRROLE

1.2.1 SYNTHESIS

Polypyrrole was first[13] prepared as a powder in 1916. However, not much attention was paid to this polymer until 1979 when Diaz and co-workers[14] reported the anodic oxidation of pyrrole in acetonitrile. The product was a flexible, metallic polymer film stable under ambient storage conditions. Since then many groups have investigated the polymer as a conducting material.

Polypyrrole may be polymerised by either chemical[15-18] or electrochemical methods[19-21]. Polypyrrole prepared by electrochemical methods is much more stable than chemically oxidised pyrrole and higher levels of conductivity can be obtained[22]. Electrochemical polymerisation also offers the advantage of homogenous incorporation of dopant counterions into the polymer film as the growth conditions can be more easily controlled[8]. A wide range of counterions can also be employed [23-25]. Furthermore, the morphology and adherence of the polypyrrole layers generated electrochemically can be more easily controlled by manipulation of the electrochemical variables[26]. However, electrochemical synthesis is limited by the fact that the amount of product is restricted by the area of working electrode in the electrochemical apparatus[8]. With chemical polymerisation bulk quantities of polypyrrole in fine powder form can be obtained[27]. For this reason, chemical synthesis may be preferred when large quantities are required.

Electrochemical polymerisation is usually carried out in a conventional three electrode cell. Different modes of synthesis have been employed including constant current[28, 29], constant potential[30-33], potential cycling[11], potential steps[34] or pulsed potential routines at different frequencies[26]. The most commonly used methods are either constant potential (potentiostatic) or

constant current (galvanostatic). The potentiostatic technique has the advantage of allowing synthesis to be controlled at a predetermined optimum potential. The major disadvantage of this method is that it is limited to relatively small polymer samples (electrode areas) due to increasing over-potential effects between the reference and working electrode[35].

Galvanostatic synthesis involves application of a fixed current, but has no control over the resulting potential of the system. The advantage of this technique is that it is independent of the system resistance[35] therefore it is most suited to bulk deposition of films on large surface area electrodes. It has been found that employing this method gives more reproducible films[36].

Mechanism of electropolymerisation of pyrrole. The steps involved in the electropolymerisation of pyrrole have been described in detail by various workers[37-39] and are summarised in Figure 1.2. The polymerisation reaction proceeds when the potential is sufficiently high to oxidise the monomer, resulting in the generation of the radical cation at the anode. Chain propagation proceeds by the coupling of two radical cations and elimination of two protons to produce a neutral dimer[38, 40, 41]. Coupling of a radical cation with a neutral pyrrole can also occur[39].

The potential required to oxidise the dimer and higher oligomers is less than that needed to oxidise the monomer and therefore the dimer is preferably oxidised to produce a radical cation[38]. Then the radical cation reacts with other radical cations to elongate the chain. When the chains becomes sufficiently long they become insoluble and precipitate on the electrode. From elemental analyses, the composition of the final polymer corresponds to the presence of one positive charge (accompanied by counterion) for every 3-4 pyrrole rings on the polymer backbone [42].

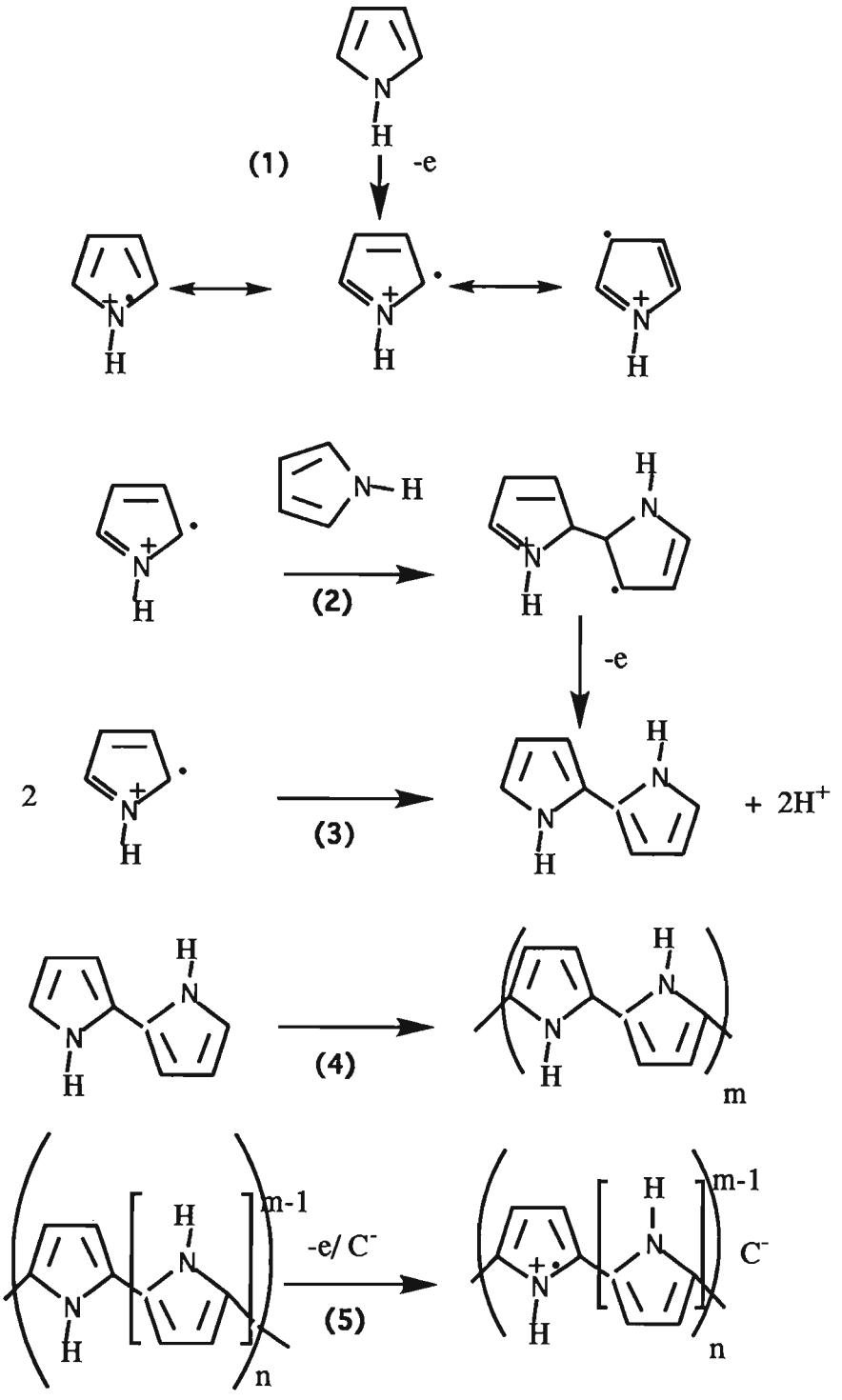

FIGURE 1.2 Mechanism of polymerisation of pyrrole:

(1) Oxidation of monomer and formation of resonance radical cations

(2) Radical-monomer coupling and aromatisation

(3) Radical-radical coupling and aromatisation

(4) Propagation

(5) Doping

The characteristics of electrochemically prepared polypyrrole have been reported to be dependent upon several factors during polymerisation. The counterion employed during electrosynthesis has a substantial effect on both the structural and physical properties of the resulting polymer films, and this has been widely investigated. It has been reported that polypyrrole can be electrochemically prepared with various types of counterions including inorganic salts[24], surfactants[23, 43, 44], polymeric anions[45, 46], aromatic sulfonates[47, 48], electroactive species[49], proteins and other macromolecules[50]. It has been shown that the morphology of the prepared films is controlled by the nature of the counterion[47, 51]. Films containing counterions based on aromatic rings exhibit an anisotropic molecular organisation (orientation of the pyrrole rings parallel to the electrode or growth surface) while polypyrrole prepared using "spherically" shaped counterions such as SO_4^{-2} does not display this behaviour, and exhibit lower electrical conductivity[52]. The electrochemical behaviour of polypyrrole has also been shown to be markedly affected by the type of counterion incorporated[53].

The properties of the polypyrrole films can be changed by varying the magnitude of the current or potential employed during synthesis even when the same electrolyte is employed. For example, it has been shown that the tensile strength of polypyrrole films declines on increasing the current density used for synthesis[28]. However, higher current densities (i.e. 5.0 mA cm^{-2}) produce more uniform and homogeneous films[43]. Increasing the anodic potential (up to 1.5 V vs SCE) during polymerisation leads to an enhancement of both electrical conductivity, as measured by four point-probe technique and the molecular anisotropy[54], as verified by X-ray scattering method. However, the mechanical properties (tensile strength and Young's modulus) decreased[55].

In addition, at a more positive growth potential (~1.0 V) overoxidation of polypyrrole occurs and conductivity is lost[56].

The choice of solvent can have a strong effect on the electrochemical oxidation reaction of pyrrole[42, 57]. Polypyrrole can be prepared in aqueous[9, 58] or organic solvents[24, 59]. The polymerisation of pyrrole proceeds via radical cation intermediates[58] which are generally very reactive species, especially toward nucleophiles. Therefore, aprotic solvents such as acetonitrile, that are poor nucleophiles are often employed. Nucleophilic aprotic solvents, such as dimethylformamide, can only be used if protonic acids are added to decrease the nucleophilicity of the resulting electrolyte[40]. Among the substantial number of solvents that have been tested the most widely used are water and acetonitrile.

It has been shown that the structure of polypyrrole films is influenced by the solution pH during synthesis. With solution pH of ~11 a more uniform surface morphology with fewer and smaller surface defects is produced[35].

The temperature of the preparation also affects the electrical and mechanical properties of the resulting polymer. It was found that the tensile strength of polypyrrole increased with decreasing electrodeposition temperature[57]. This is due to the higher conjugation and order of the chain in the polymer backbone formed at lower temperatures. Films prepared at higher temperatures have also lower conductivities[54].

The use of various substrates including platinum, gold, indium-tin oxide, carbon foil, glassy carbon and stainless steel has been reported[60-62]. Polymerisation onto platinum electrodes has been found to result in smoother and better adhering[14] films. Therefore, it is the most commonly used electrode for polymerisation.

1.2.2 CHEMICAL AND PHYSICAL PROPERTIES OF POLYPYRROLE

1.2.2.1 ELECTRICAL CONDUCTIVITY OF POLYPYRROLE

There has been considerable controversy over the nature and dynamics of the charge carriers in conducting polymers[68]. Although many authors have given a number of theoretical models, none of them gives a completely satisfactory picture for the conduction process[69]. The explanations have included that of a doped organic semiconductor[70, 71], to more advanced descriptions, in which charge transport is considered to occur by tunnelling transitions between localised states[72]. The following is the most frequently encountered description of the mechanism of charge transport.

It was initially assumed that the increase in the conductivity of conjugated polymers such as polypyrrole was due to the removal or addition of electrons from the conduction band (CB) or valence band (VB) as occurs in conventional semiconductors[73]. However, in electrochemically cycled highly conducting polypyrrole films, no ESR absorption signal was detected[74]. If there was an unpaired electron in the CB or VB due to oxidation (with a spin of $\pm 1/2$) the ESR signal should have been detected. Furthermore the observed temperature dependence of dc conductivity could not be explained by the band conduction model[69] as usually is observed for conventional semiconductors. These observations led researchers to suggest that the conductivity might be associated with spinless charge carriers.

Bredas and co-workers were the first who reported changes of the electronic and geometric structures upon polymer oxidation[71]. Their results indicated the appearance of bipolarons upon doping. Shortly after, they showed that polarons and bipolarons are formed upon doping[74]. However, the observation

of high conductivity without paramagnetic susceptibility in heavily oxidised polypyrrole was explained by transport of bipolarons.

The idea of a polaron is familiar in solid state physics. It consists of an electron (or hole) localised in a deformed region of the lattice[75]. The ion radical is sometimes called a soliton in the language of solid-state physics. A polaron is a kind of ion radical where the charge and the spin are mobile and move independently from each other along a single chain without being subject to relaxation or trapping. If it is linked to an elastic bond and thus can not move without exchange of energy the dication is called a bipolaron[76].

In conjugated polymers removal of a single electron generates an electron hole which tends to localise along the polymer chain[77] as shown in Figure 1.3 (b) (formation of a polaron). Polaron states in the band gap result in three allowed optical[78] transitions (Figure 1.4 (a)). Subsequent removal of electrons may lead to more polarons, or, if pairing of charges is energetically favourable and kinetically achievable[78], to bipolarons (Figure 1.3 (c)). Bipolaron states in the band gap result in only two allowed sub gap transitions since the electronic states are either both occupied or both empty (Figure 1.4 (b)). Therefore, the electrochemical oxidation or reduction of polypyrrole gives rise, initially, to an excess concentration of polarons[70] and then to recombination of polarons[79] into bipolarons. This slow process is consistent with the time required for ionic (mass) transport[78].

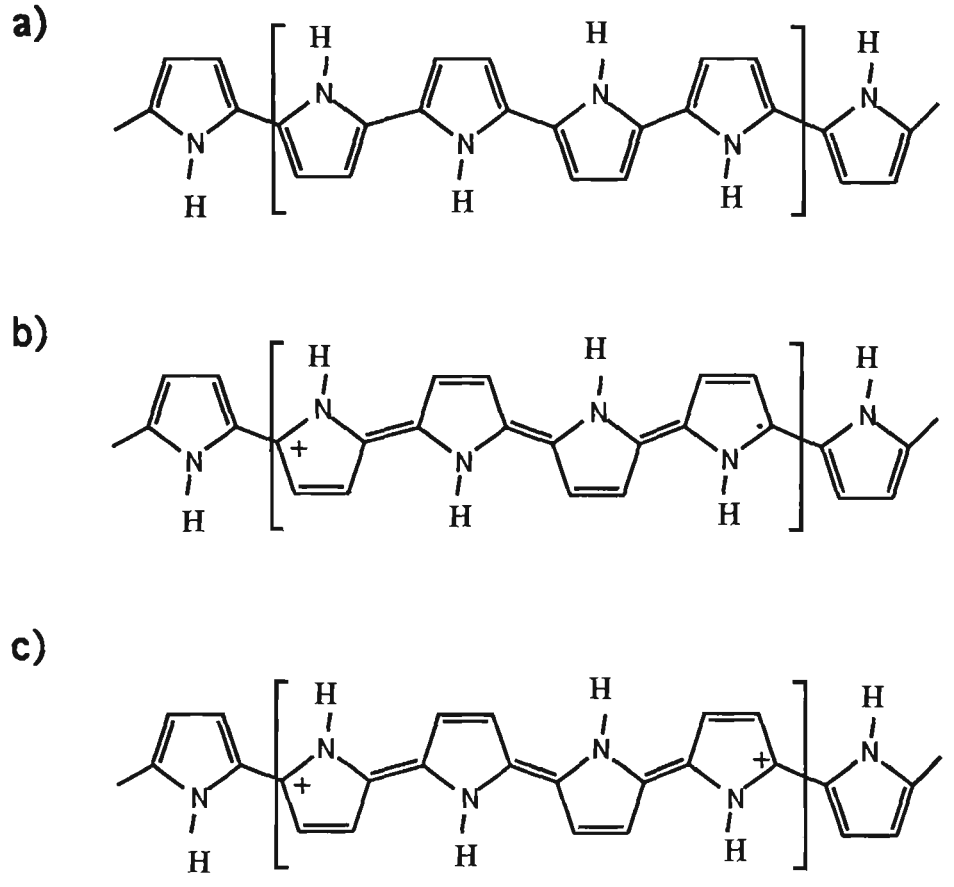

FIGURE 1.3 Formation of polarons (b) and bipolarons (c) from undoped polypyrrole (a).

Polarons and bipolarons are characterised by two experimentally measurable properties[75]. Changes in optical absorption that result from the new energy levels created in the band-gap, and appearance of additional magnetic susceptibility due to the spin of the polaron.

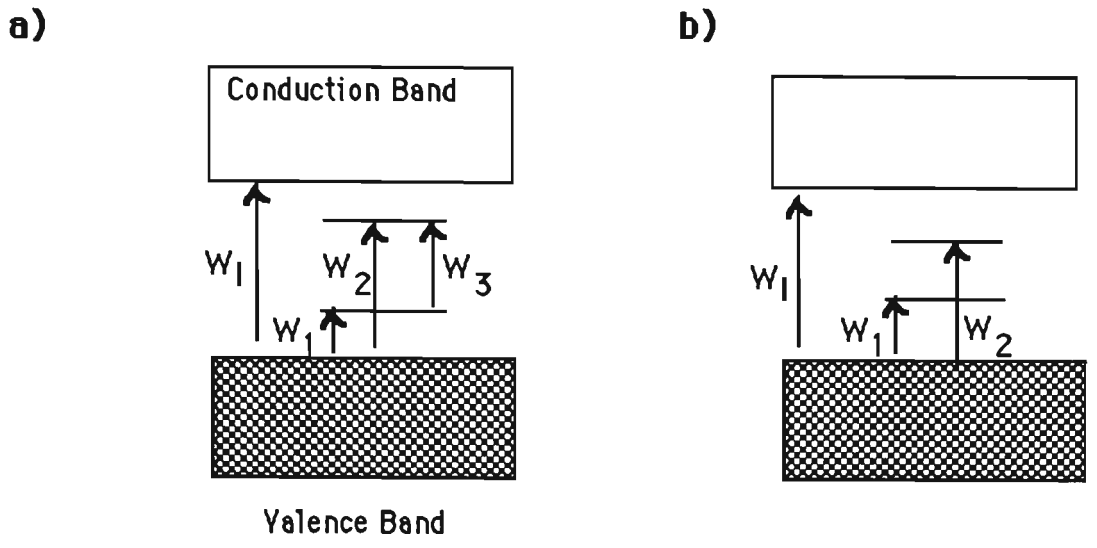

FIGURE 1.4 Energy-level diagram for:
(a) A polaron state showing allowed optical transitions, W_1, W_2, and W_3. W_I is the interband threshold.
(b) A bipolaron state (note the absence of the transition W_3).
Redrawn from reference 78.

1.2.2.2 DOPING PROCESSES IN POLYPYRROLE (ELECTROACTIVITY)

The electrochemical reduction/oxidation of polypyrrole results in the polymer backbone becoming neutralised or positively charged respectively. Consequently, the charge neutrality of the polymer can be conserved by the outward/inward diffusion of anions as shown in Equation 1.1:

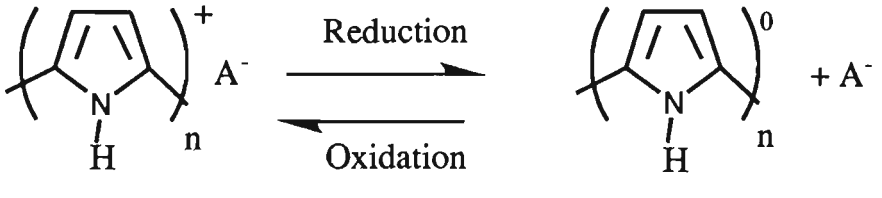

(1.1)

where A^- is the counterion incorporated during synthesis and/or anion incorporated into the polymer from solution. However, more recent studies including advanced techniques such as Electrochemical Quartz Crystal Microbalance[36, 80], a luminescence probe technique[34], electrogravimetric studies[81] and AC impedance measurements combined with cyclic voltammetry[82] have provided evidence of cation movement as well as anion movement in this process. The cation (M^+) motion becomes predominant when the incorporated counterions are relatively immobile[83].

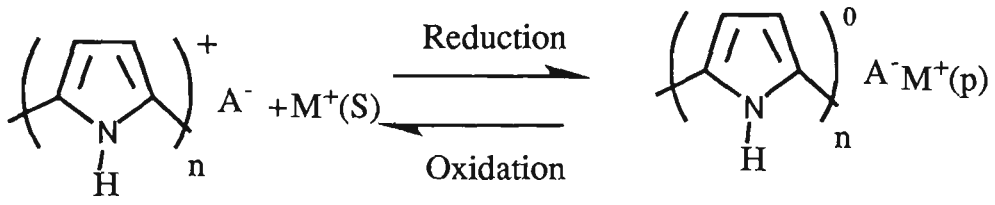

(1.2)

In this case A^- is the immobile counterion and therefore, the inward/outward diffusion of cations (M^+) is likely to occur. This has been shown to be the case for polymers containing polymeric anions where charge balance was maintained by cation movements during the redox process[83, 84]. However, normally a mixture of anion and cation is incorporated/released during the oxidation/reduction of polypyrrole[85, 86].

1.2.2.3 MECHANICAL PROPERTIES OF POLYPYRROLE

To date the range of stand-alone mechanically stable conducting polymer films that can be produced is limited. In this Section the different approaches used to prepare free-standing film of conducting polypyrrole are reviewed.

The counterion incorporated into the polymer during synthesis has a dramatic effect on the mechanical properties[42]. Synthesis of a free-standing film of conducting polypyrrole (PPy) was initially reported by Diaz and co-workers[14]. Since then increasing attention has been paid to further development of these materials with a view to improving the mechanical, electrical and chemical properties. It has been shown[57, 87] that the use of sulfonated aromatics as the counterion during polymerisation produces polymers with excellent mechanical properties and adequate conductivity, so much so that they can be used as stand alone membranes. However, such a restricted choice of counterion limits the modification of the chemical properties of these membranes.

In attempts to extend the range of useful materials studies, aimed at improving the mechanical properties of polypyrrole, the preparation of co-polymers has been considered[88-90]. For example, polypyrrole has been deposited into a host copolymer of vinylidene fluoride and triflouroethylene[88] or has been copolymerised with other monomers[89].

The use of polymer blends that combines the electroactive polymer with an inert host polymer has also been considered. The host polymer can be non-conductive, such as polyvinyl chloride[91-93], or ionically conductive such as Nafion[94-96]. It has been reported that conducting PPy/PVC (polypyrrole-polyvinylchloride) composites can be prepared by electropolymerising pyrrole on a working electrode coated with a layer of PVC. Samples prepared by this method had conductivities as high as 50 S cm^{-1}. Generally, the PPy/Nafion composites have been prepared by casting Nafion from solution onto a substrate such as platinum and then using the precoated electrode as a working electrode onto which conducting polymer was deposited.

Recently, incorporation of anionic polyelectrolytes (APE) as dopants in the conducting polymer material has been suggested[25, 97]. Incorporation of APE in the conducting polymer material has been achieved by electropolymerisation of pyrrole in the presence of potassium polyvinyl sulfate [PVS] or sodium poly styrenesulfonate [PSS]. The APE was incorporated into the PPy chains via entanglement and the mechanical properties were subsequently improved[25].

1.2.2.4 STABILITY OF POLYPYRROLE

Polypyrrole stability has been described with respect to several parameters:

Environmental (storage) stability. Conducting polypyrrole (oxidised form) is stable in air[63] and the conductivity is almost unaffected by hydrostatic pressure[64]. However, the reduced form is very easily oxidised in air or water. For example spectroscopic studies have indicated that reduced neutral polypyrrole (PPy^0) is very unstable in aqueous solution and air[53].

Stability upon acid/base treatment. Detailed investigations on the behaviour of polypyrrole upon acid/base treatment have shown[65, 66] that the doped polypyrrole chain undergoes a deprotonation process with the formation of a quinoid structure in aqueous basic media (with a pKa in the range of 9-11). This causes a profound change in its electronic structure including a decrease in conductivity[57] and a significant change in the optical absorption spectrum[66]. On the contrary, doped polypyrrole in acidic media undergoes a protonation[66] process (with a pKa in the range 2-4). This has little effect on the electronic structure, only a slight increase in conductivity and a small shift in optical absorption spectrum[66] were observed. A slight decrease in mechanical properties was also noted[57]. Cyclic voltammograms obtained using

polypyrrole electrodes also change with an increase in solution pH indicating that the oxidation/reduction processes are affected due to involvement of OH^- anions[53].

Stability at positive potentials. It has been observed that electroactivity of the polypyrrole film decreases after exposure to high potentials and conductivity is lost[56, 67]. This irreversible reaction has been described as overoxidation.

The polypyrrole film is oxidised initially to form a radical cation (polaron). When the applied potential becomes more positive, the radical cation undergoes an oxidation reaction to form a dication (bipolaron). Since the doping density of polypyrrole is about 0.2 to 0.3 per monomer unit in its fully oxidised form[42], two positive charges must be spread over a quinoid unit of 3 to 5 monomer molecules and they will most likely be located at both ends of the unit due to the repulsion[67]. The degradation reaction takes place initially at the end of the unit, where the high density positive charge exists[3]. Degradation proceeds via a nucleophilic attack by water molecules (or any similar species). Then the counterions are expelled and the polymer conjugation is destroyed resulting in a loss of electroactivity and conductivity. It has been shown that the overoxidation process is facilitated by increasing the OH^- concentration[51].

1.3 POLYANILINE

The term polyaniline is descriptive of a class of conducting polymers derived from the base of general composition[98, 99]:

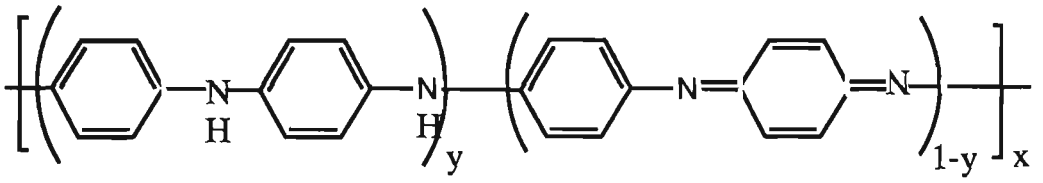

whose average oxidation state is described by the parameter (1-y). In principle y can be varied from one (fully reduced form leucoemeraldine) to zero (fully oxidised form pernigraniline). When an equal number of oxidised and reduced units exist the material is referred to as emeraldine base or salt. It is believed that all or some of the nitrogen atoms (amines or imines) in any of the species can be protonated[98].

1.3.1 SYNTHESIS OF POLYANILINE

Polyaniline has been known for over 150 years[100, 101]. However, it was not studied in any detail until two key developments occurred[102, 103]. Firstly, Diaz and Logan in 1980[102] described an electrochemical method for synthesis of high quality films of polyaniline. They demonstrated that continuously cycling the potential between -0.20 and +0.80 V (versus SCE) in a solution of aniline produced a strongly adherent film on a platinum electrode. The film was insoluble in all common solvents. A few years later MacDiarmid and co workers[103] showed that polyaniline can be doped to highly conducting form upon protonation by protonic acids. Since then there has been much interest in polyaniline with many proposed uses including batteries[104-106], sensors and biosensors[107].

Polyaniline is prepared by direct oxidation of aniline using an appropriate chemical oxidant or by electrochemical oxidation at an appropriate electrode material. The majority of authors have concluded that the characteristics of the polymer depend on the mode of synthesis[108]. For chemical preparation, the use

of various chemical oxidising agents including $(NH_4)_2S_2O_8$[109-111], H_2O_2, $K_2Cr_2O_7$ and KIO_3[112, 113] has been investigated. The yield, conductivity, viscosity of dissolved powder, and the oxidation potential of the polymer have been shown to vary depending on the nature of the oxidising agent employed[113]. In addition, it was shown that the molecular weight of chemically prepared polyaniline increases as the polymerisation temperature decreases[114].

With electrochemical preparation, anodic oxidation is the most common method for the synthesis of polyaniline[108]. The use of potential cycling has been shown to produce films with better adhesion, smoothness and homogeneity[102, 115] as verified by scanning electron micrograph investigations. This method has been used by a number of authors[110, 116-118] while some others have employed constant current or potential[119, 120].

Apart from the mode of synthesis it was shown that the electrochemical properties, structure and morphology of the polyaniline films were dependent upon the nature and concentration of electrolyte anion[115, 121-123], pH[124] and the nature of the substrate employed during synthesis[119].

Electropolymerisation of polyaniline. The first step in the oxidation of aniline is generally thought to be the formation of a radical cation[123, 125, 126] which is independent of the pH of the synthesis media. Then the polymerisation is continued by radical cation coupling[125, 126] resulting in formation of the aniline dimer. The next stage involves the oxidation of dimer to form a radical cation. Finally chain propagation and polymer doping occur as the polymerisation proceeds. The mechanism of polymerisation of aniline has been proposed to occur as shown in Figure 1.5.

It was found that the rate of polyaniline deposition was influenced by the concentration[123] and the nature[124] of the anions used during synthesis.

However, strongly acidic conditions are required in any case for the polymerisation[123] as the formed polyaniline is non-conductive in non-acidic media.

Although the electropolymerisation process shown here occur in acidic media, it has been shown[124] that aniline can be oxidised at pH values greater than 4 provided that a suitable anion is present and a greater potential applied. However, the polymer formed is less conductive and electroactive. At pH>4 the non-protonated form of aniline prevails[124].

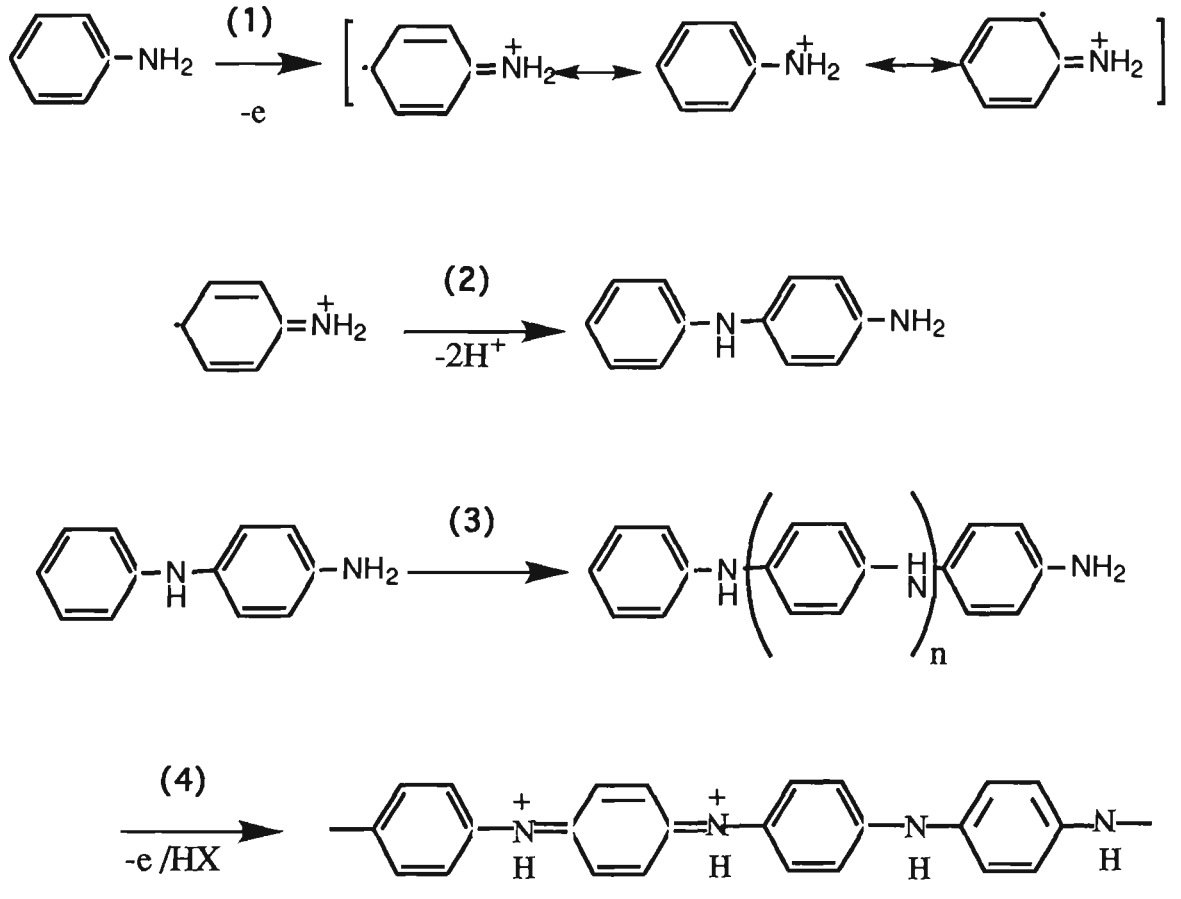

FIGURE 1.5 Mechanism of polymerisation of aniline:
(1) Oxidation of monomer and formation of resonance radical cations
(2) Radical-radical coupling and aromatisation
(3) Propagation
(4) Doping, Propagation/precipitation

1.3.2 CHEMICAL AND PHYSICAL PROPERTIES OF POLYANILINE

1.3.2.1 ELECTRICAL CONDUCTIVITY OF POLYANILINE

The conductivity of polyaniline, unlike that of other conducting polymers such as polypyrrole, depends significantly not only on its redox state (oxidative doping), but on the degree of protonation[140] (non-oxidative doping). The physical mechanism behind this conductivity change has been widely debated. The unusual properties of the emeraldine form of polyaniline has been investigated by various techniques including measurement of relationship between temperature and dielectric constant[141], using optical[142] and spectroscopic[142-144] devices.

Addition of two protons at the nitrogen sites on either side of the quinoid rings in the emeraldine base form results in a spinless bipolaron defect as shown in Figure 1.6 (b). However, it is inconsistent with the measured magnetic susceptibility[138]. Therefore the formation of a polaron (Figure 1.6 (c)) from bipolaron is likely to occur. The existence of polarons have been suggested by a number of authors[142, 143, 145]. The formation of bipolaron is energetically preferred over the formation of two polarons[146, 147], however, it has been suggested that the strong, indirect attractive interaction between electron and positive charge on neighbouring ß (Coulombic interaction) may stabilise the delocalised polaron states[146, 148].

In most cases the model shown here gives satisfactory results. However, there are some exceptions in which the described model is unable to explain, for example formation of bipolarons at lower temperature[141]. Therefore, some other advanced models including formation of metallic islands and conduction due

to charge transport between the islands[141] or three-dimensional electron hopping model[149] have been suggested.

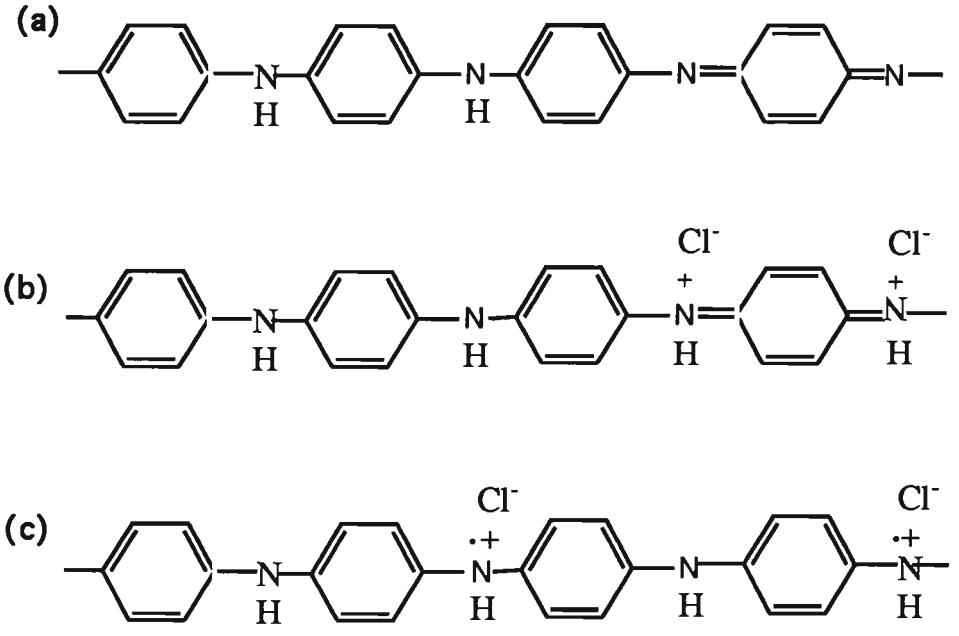

FIGURE 1.6 Emeraldine base polymer:
(a) Unprotonated
(b) Formation of bipolaron
(c) Formation of polaron.

1.3.2.2 DOPING PROCESSES IN POLYANILINE

The redox reactions of polyaniline have been described by a number of authors[98, 99, 135-137]. It has been shown[135, 138] that unlike other conducting polymers such as polypyrrole, the emeraldine base form of polyaniline can be doped to a highly conducting regime in acidic media without removing electrons from the polymer backbone. Since in this process the number of electrons associated with the polymer remains unchanged, it is referred to as non-oxidative doping[99]. The reaction occurring can be shown as:

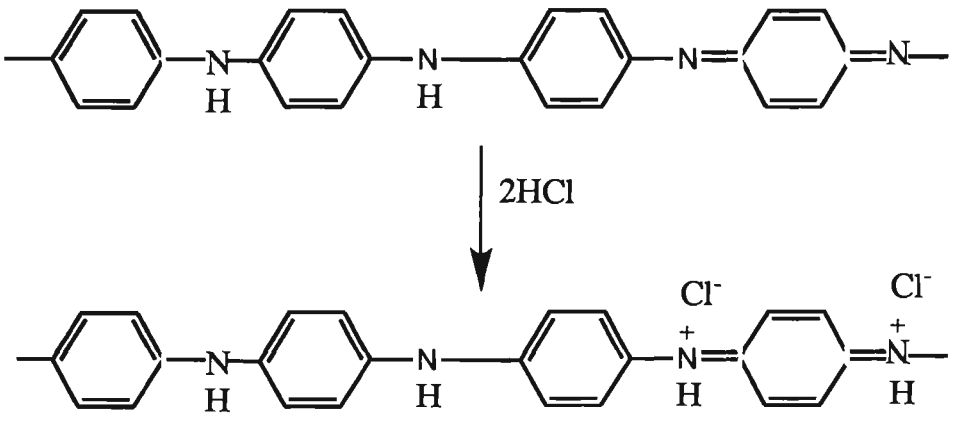

(1.3)

Polyaniline can also undergo oxidative doping. This is a process in which electrons are removed from the polymer backbone. This oxidation is reversible within the potential range that the polymer is stable. The leucoemeraldine base, the completely reduced form of polyaniline, can be oxidised to emeraldine (Equation 1.4 (a,b)) and pernigraniline (fully oxidised form).

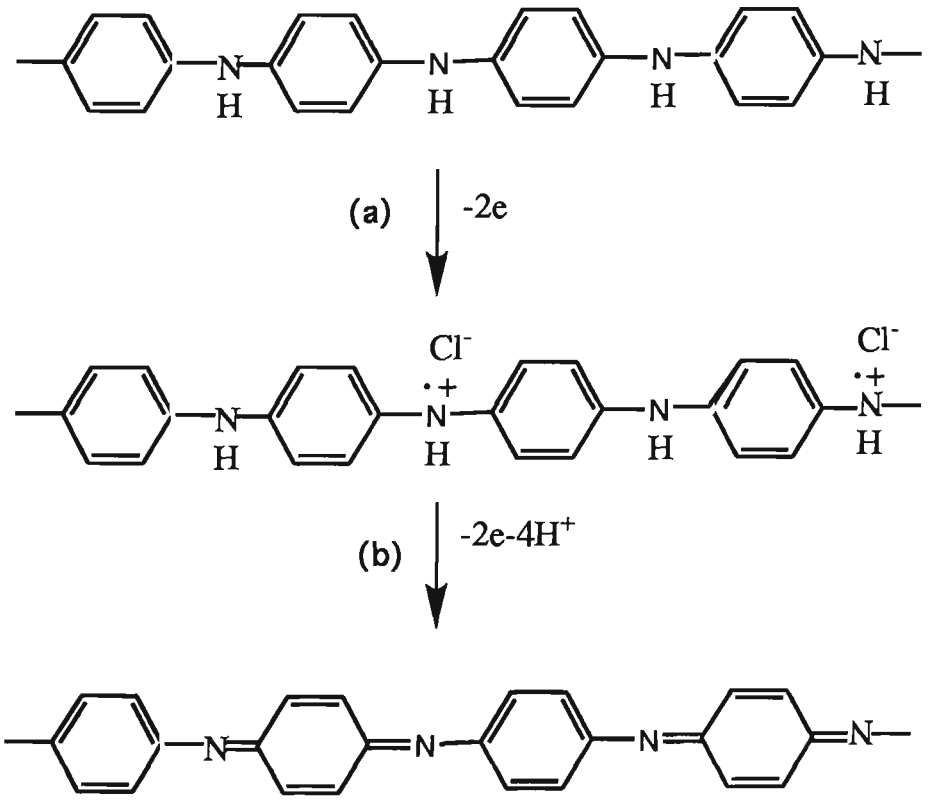

(1.4)

The cyclic voltammogram (CV) of polyaniline in acidic media shows two oxidation/reduction reactions having oxidation potentials of ~0.10 and 0.70 V. The peaks appearing in the CV correspond to the reactions in the above Equations.

As it is clear from Equation 1.4 (a) the oxidation and reduction of leucoemeraldine/emeraldine acid form is independent of pH and hence this process occurs without loss or gain of protons[99]. However, it does not mean that the redox reaction can occur in non-acidic media since there is essentially no protonation at pH values greater than four[118] and the polymer loses its conductivity at higher pH.

With respect to the nature of either oxidative or non-oxidative doping in polyaniline, at least six different phases can be distinguished (Figure 1.7). However, among these forms only the emeraldine salt, is directly obtained after the standard synthesis[139].

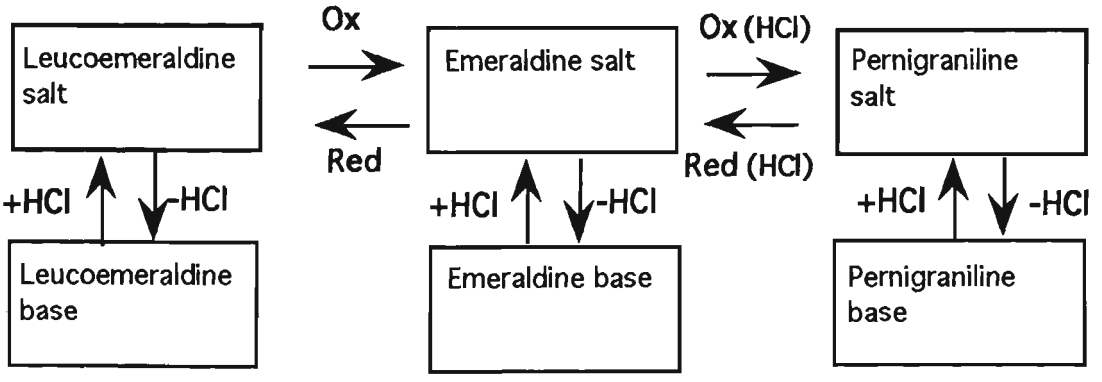

FIGURE 1.7 A diagram of different forms of polyaniline. Horizontal and vertical arrows indicate, respectively, electron transfer (oxidative doping) and proton transfers (non-oxidative doping).

1.3.2.3 SOLUBILITY OF POLYANILINE

It is generally accepted that polyaniline is not completely soluble in most common solvents (aqueous and organic)[108]. However, partial solubility of polyaniline in some organic solvents has been reported[101, 126, 127]. Mohilner and co-workers[126] have shown that the polymer can be dissolved in pyridine, cold 80% acetic acid and in N,N-dimethylformamide (DMF) with production of a bright blue colour solution, but it did not dissolve in glacial acetic acid. These findings were in agreement with the observations of Stilwell and co-workers[127] and Green and co-workers[101]. In addition, the complete solubility of polyaniline in concentrated sulfuric acid was reported by Andreatta and co-workers[128, 129]. Recently MacDiarmid and co-workers[130] showed the solubility of emeraldine base form of polyaniline in 1-methyl-2-pyrrolidinone (NMP) and in dimethylsulfoxide (DMSO). In general, the degree of solubility of polyaniline is strongly dependent on the conditions at which the polymerisation takes place. For example, it was shown[114] that soluble polyaniline can be prepared by optimising the polymerisation conditions including the temperature of polymerisation.

1.3.2.4 STABILITY OF POLYANILINE

As for polypyrrole, irreversible degradation (losing conductivity and electroactivity) of polyaniline in the higher oxidation states has been widely reported[131-134]. The rate of degradation is mainly dependent on the magnitude of the applied potential[118, 133] and the solvent used[133]. It has been shown that p-benzoquinone (BQ) is formed as the final and major soluble product when polyaniline is subjected to anodic potentials higher than a threshold value[131, 132, 134]. The threshold value varied depending on the electrolyte

conditions. The presence of BQ has been verified by UV/visible absorption spectroscopy[131, 132]. A possible mechanism of the reaction is shown in Figure 1.8. The degradation of polyaniline begins by nucleophilic attack of water on the oxidised polyaniline. Then the unstable chain is cleaved into two products. Finally, the BQ is formed through the hydrolysis of the quinoid structure [131].

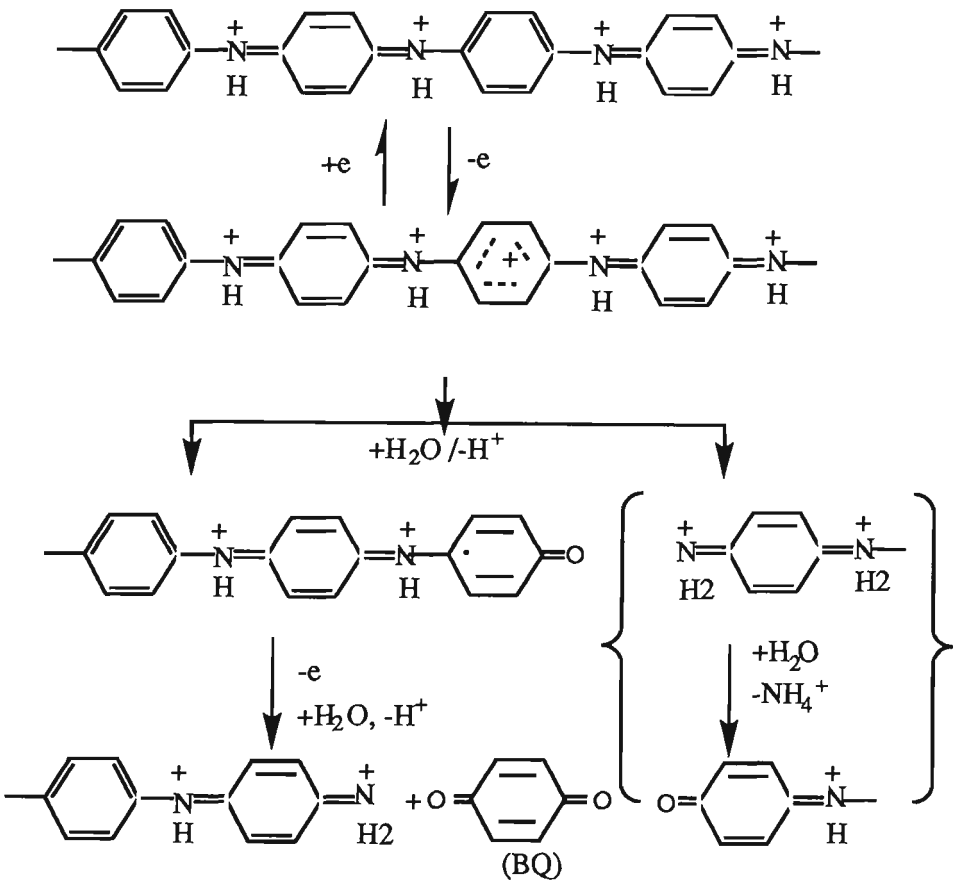

FIGURE 1.8 Mechanism of oxidative degradation of polyaniline (see reference: 132)

1.4 CONDUCTIVE ELECTROACTIVE MEMBRANES

1.4.1 INTRODUCTION TO MEMBRANE TECHNOLOGY

A membrane may be defined as a selective barrier between two homogeneous phases[150]. Membranes can be made of a synthetic or biological product and the most important class of synthetic membrane materials is polymers[150]. Synthetic membranes can be classified[150, 153] according to their utilisation, composition, allowable mode of transport and permselectivity (Table 1.1).

Microfiltration. A process in which water and dissolved species pass through a microporous membrane under a pressure difference of typically 0.7 atm. In this process the retained material is usually particles including bacteria and silica.

Dialysis. Ions and low molecular weight organic compounds (e.g. Urea) pass through the membrane due to concentration differences. Dissolved and suspended material with molecular weight greater than 1000 are retained.

Electrodialysis. As the name implies, electrodialysis (ED) is a dialytic process in which an applied electrical field is used to draw ions across a membrane. Ion separation is effected through the use of selective ion-permeable membranes. All non-ionic and macromolecular species are retained.

Ultrafiltration. Water and salts are separated due to pressure differences of typically 0.7-7.0 atm while all biological materials, colloids and macromolecules are retained.

Gas separation. A high pressure difference of 1.0-100.0 atm is applied between two phases separated by a semipermeable membrane to separate mixtures of gases or vapours.

Reverse osmosis. Reverse osmosis is a process in which an applied pressure is used to reverse the normal osmotic flow of water across a semipermeable membrane. In this process all suspended and dissolved material is retained.

The use of synthetic membranes as employed in modern industrial technologies relies on their physical or chemical properties as determined during synthesis to effect separations[150, 154, 155]. For example, membranes with predetermined pore sizes are used to separate particles or molecules based on size, whilst those with predetermined charge distributions are used to separate ions.

As permselective barriers, synthetic membranes have been employed in a variety of applications (Table 1.1).

1.4.2 CONDUCTIVE ELECTROACTIVE POLYMERS AS MEMBRANES

Much effort has been directed towards making synthetic membrane materials more inert, not dynamic, with a view to preventing fouling and extending their lifetime. However, once a conventional membrane has been fabricated, its characteristics (such as morphology) are fixed[48]. This is a limitation of conventional membranes. If dynamic control of useful membrane characteristics such as ion permeability and molecular selectivity could be achieved, a new dimension in separation technology would be established. Nature has shown that this is possible. Perhaps, the best known example of a smart membrane is the biological cell membrane where specific stimuli initiate changes that facilitate selective transport across the membrane wall. Synthetic membranes that are able to perform according to these principles will be capable of exhanced performance beyond the scope of conventional membranes.

TABLE 1.1 Application and processes for synthetic membranes

Membrane Process	Examples of Application
Microfiltration	Bacteriological analysis of water.
Ultrafiltration	Protein recovery, concentration of macromolecules, waste water purification, laboratory use (tissue-culture).
Dialysis-Hemodialysis	Artificial kidney, purification of polymer solution, controlled chemical release
Electrodialysis	Production of salt and fresh water from sea water, aqueous metallurgy of uranium
Hyperfiltration	Recovery of valuable metal salts from galvanic industry waste water
Gas separation	Separation of helium and oxygen, hydrogen recovery
Membrane distillation	Concentration of aqueous solutions
Pervaporation	Dehydration of organic solvents
Reverse osmosis	Sea water desalination process

In the pursuit of such dynamic systems various workers[156-158] have considered the properties of conducting polymer membrane systems. It has been found that the ionic permeability of polypyrrole coated around a porous metal substrate (a gold minigrid electrode) can be dynamically controlled by an electrical signal[159]. Then it was found that oxidised polypyrrole was permselective[156] to chloride ions in a solution of KCl. These were the first quantitative ionic permeability results on polypyrrole. Similar studies on the ionic permeability of a polypyrrole membrane grown onto Au-coated polycarbonate microfilters also showed that permeability of the polypyrrole membrane can be switched by control of the polypyrrole oxidation state[158].

The membrane properties of polypyrrole were investigated further by measurements of the Volta potential[160, 161], diffusion coefficient[162] and membrane potential[83] . Recently the ability of polypyrrole membrane to measure enzyme activity has also been investigated[163].

Although the above studies have indicated that the dynamic control of the permeability of polypyrrole is possible, investigations into the transport of species across conducting polymers are limited. Only a few reports have been published on using polypyrrole[87, 164, 165] as a free-standing conducting polymer film and hence a permselective barrier. Recently Wang and co-workers[164] demonstrated transport of some monovalent cations such as H^+, Na^+, K^+ and NH_4^+ between two electrolyte solutions when an electrical field between two sides of a polypyrrole film was applied. They showed that the transfer process depends on the size, ionic charge and surface characteristics of the membrane. In other work the permeation of volatile and gaseous compounds through a polypyrrole composite electrode membrane was investigated. It was found that the permeation rates were dependent upon the

redox state of the polymer, a high permeation rate was measured for reduced polypyrrole and a low rate for oxidised polypyrrole[157].

Recently, gas permeability values have been reported for films of polyaniline in the emeraldine oxidation state[165, 166]. The doping procedure, which was found to cause significant concurrent changes in the morphology of the films, resulted in improved gas separation. For example a selectivity value of 207 was obtained for a mixture of H_2/N_2[165, 166] passing through the undoped polyaniline membrane but when it was doped by 4.0 M HCl the value improved to 280.

More recently[87], the transport of potassium chloride across conducting polypyrrole membranes was demonstrated. In particular, the use of an electrical stimulus to initiate and control the rate of transport was demonstrated. In this work a pulsed potential was applied to polypyrrole membranes to initiate transport of KCl across the polymer membrane. A maximum flux of 1.7 $x10^{-9}$ mol cm^{-2} s^{-1} was obtained.

1.5 AIMS OF THIS PROJECT

The development of membrane systems whose transport properties can be regulated by electrochemical stimuli was the main objective of the current investigation. In order to achieve this it is therefore a primary aim to make a variety of free-standing polymer membranes from polyaniline, polypyrrole and composite materials. The inherent reversible electroactivity of the conducting polymer means that the membranes made from such materials are dynamic and by using them as a working electrode and a barrier in a two compartment cell, transport across them may be controlled. This can be basis of an exciting novel method of separation using these polymer membranes.

The system relies on the redox properties of the conducting polymers. It is well established that changes in oxidation state can be induced by application of potential (doping) with ions. When polypyrrole is oxidised the charge neutrality can be maintained either by incorporation of anions from the solution or expulsion of cations into the solution (Equations 1.1 and 1.2). Conversely, when the polymer is reduced the neutrality is maintained by expulsion of anions or/and incorporation of cations. This idea (incorporation and expulsion of species) was used to establish a system which enables transport of ions from one side of the membrane to the other.

This process differs from conventional ion exchange membranes due to the nature of the mechanism of transport. In our system the membranes are in direct electrical contact and are part of the electrical circuit. The movement of ions would be due to redox reactions of the polymer, while in conventional methods an electrical field is applied between two sides of the film and separation is achieved based on the electrical field generated by passing the current through the membrane. In fact the major advantage of the method we employed over the conventional methods was its ability for in-situ or dynamic control of transport. As in this method, unlike the conventional membranes, the structure and morphology of the membranes can be changed during transport by inducing an electrical stimuli.

The work has been divided into the following stages:

1) Diffusion cell design. Chapter 2 describes design and development of a diffusion cell that enables transport studies to be carried out under electrochemical control.

2) Membrane preparation and characterisation. Three different classes of conducting polymer membranes were investigated in this project.

Polyaniline membranes (Chapter 3), polypyrrole based composite membranes (Chapters 4 and 5) and polypyrrole doped with conventional dopants (Chapter 5). The choice of electromembrane material was based upon the electrochemical characteristics required to perform a particular transport function. The membranes were then characterised using a variety of techniques including an atomic force microscopy and scanning electron microscopy.

3) Transport studies. Transport of inorganic and organic salts across the membranes, using electrochemical control, was described (Chapters 3,4 and 5).

4) Mechanistic studies. A series of systematic studies was carried out aimed at better understanding the ion movement accompanying the redox changes in the polymer. To achieve this new techniques such as electrochemical quartz crystal microbalance together with more conventional methods such as cyclic voltammetry and chronoamperometry were employed.

CHAPTER 2

ELECTROMEMBRANE CELL DESIGN AND EXPERIMENTAL METHODS

2.1 INTRODUCTION

As described in Chapter 1, the use of electrochemical control to regulate the transport of ions across conducting polymer membranes is a novel concept. Therefore, a systematic investigation is required to obtain the best electromembrane cell design.

This Chapter also introduces the different experimental techniques that have been employed throughout the work. A brief description of atomic force microscopy (AFM), employed to study the morphology of the membranes is given. Description of particular methods such as Electrochemical Quartz Crystal Microbalance (EQCM) and HPLC that were either developed or investigated in detail, are given in the individual chapters.

2.2 CELL DESIGN FOR PREPARATION AND CHARACTERISATION

The cell design shown in Figure 2.1 was used to prepare conducting polymer membranes. In this set up the working electrode and the auxiliary electrode were parallel to each other and this ensured deposition of uniform films. The working electrode was usually made of a mirror finished stainless steel plate polished with a 1 μm diamond pad (Goodfellow, England). Other working electrodes were considered, when the effect of the substrate material on the membrane properties was investigated (Chapter 4). The electrodes were kept apart at a fixed distance of 2.0 cm. The auxiliary electrode was made of reticulated vitreous carbon (RVC) purchased from Energy Research Generation Inc.

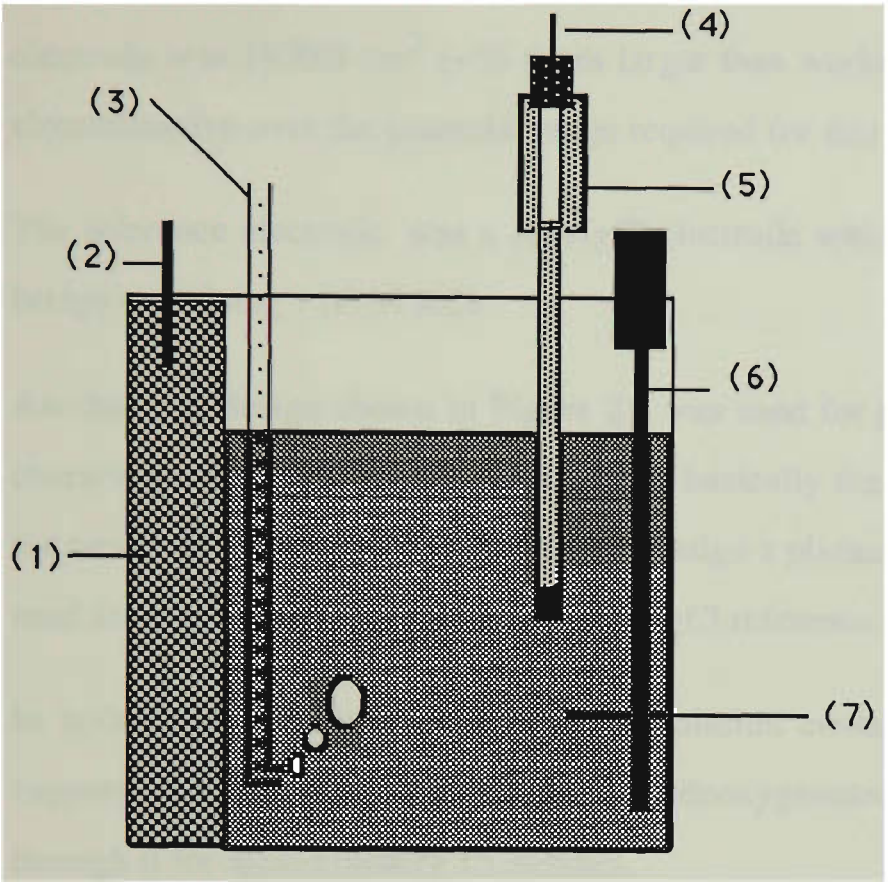

FIGURE 2.1 The electropolymerisation cell used to prepare free-standing membranes.

(1) Auxiliary electrode (RVC).
(2) A gold film auxiliary electrode contact.
(3) Line for input of nitrogen.
(4) Reference electrode.
(5) Saltbridge.
(6) Working electrode (Stainless steel plate).
(7) Polymerisation solution.

The auxiliary electrode must be larger than the working electrode to prevent large current densities being produced there. The working electrode used to prepare membranes had a surface area of 35.0 cm^2 (5.0 cm x 7.0 cm). The use of RVC as the auxiliary electrode was convenient. Since RVC has an open-porous reticulated structure limiting the geometric size required. Therefore while the cell volume was restricted to 150 mL, the surface area of the auxiliary

electrode was 1950.0 cm^2 (~55 times larger than working electrode). RVC is electroinactive over the potential range required for this work[167].

The reference electrode was a Ag/AgCl electrode which was placed in a salt bridge containing 1.00 M KCl.

Another cell design shown in Figure 2.2 was used for polymer synthesis and characterisation on a smaller scale. It was basically the same as the one used for membrane synthesis. However in this design a platinum mesh electrode was used as an auxiliary electrode with a Ag/AgCl reference electrode.

In both designs (Figure 2.1 & 2.2) the solution contains the monomer and supporting electrolyte. The solution was deoxygenated by passing nitrogen through it for approximately 15 minutes.

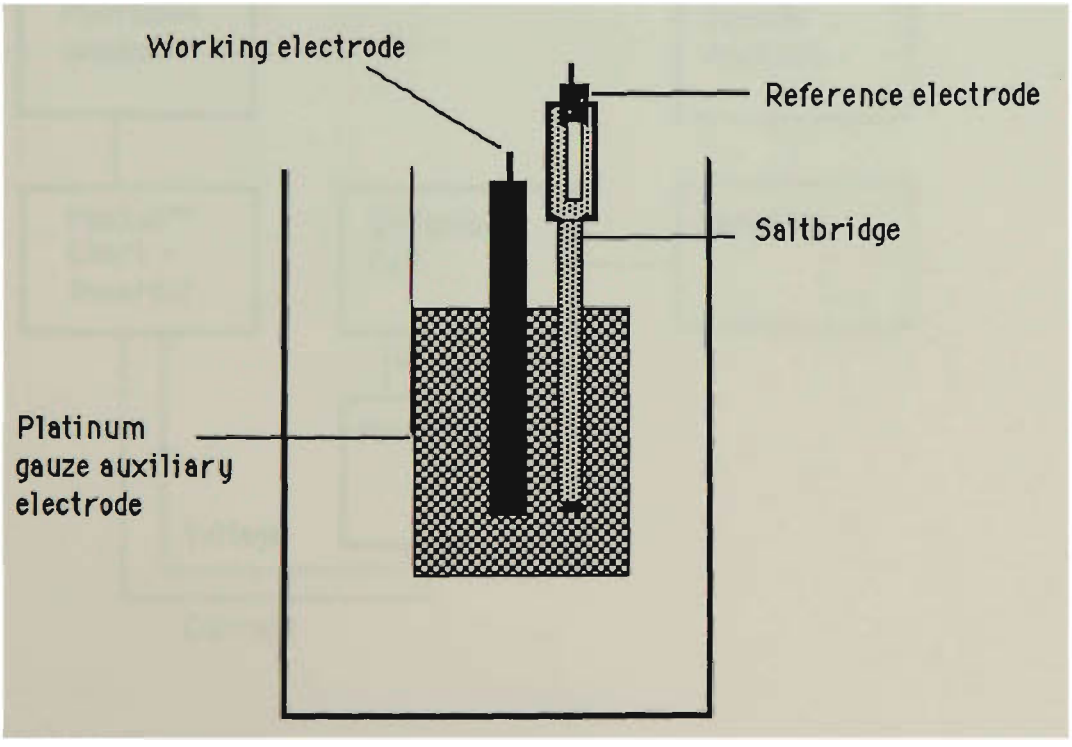

FIGURE 2.2 Alternative cell used for polymer synthesis and characterisation.

2.3 DEVELOPMENT OF INSTRUMENTATION FOR TRANSPORT STUDIES.

Figure 2.3 shows a schematic representation of the experimental set-up used for transport studies throughout this work. Transport was studied with and without electrical stimuli. Electrical stimuli were applied to the conducting membrane using a potentiostat controlled by a pulse generator. The pulse generator was designed and built as part of this investigation in the Science Faculty of the University of Wollongong. The current response due to the applied potential was recorded using a MacLab™ (chart recorder) in combination with a Macintosh computer.

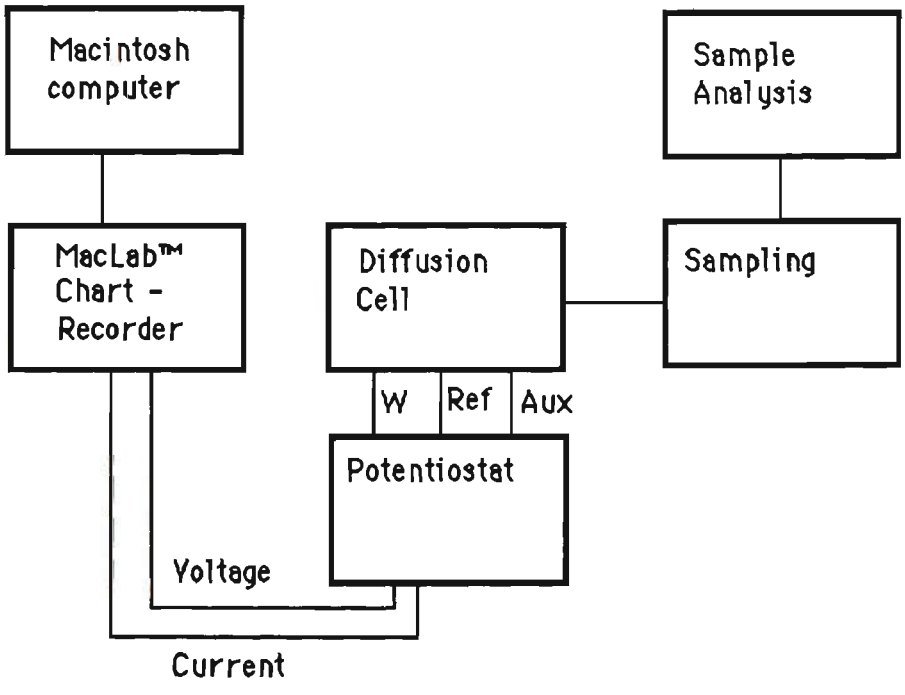

FIGURE 2.3 A block diagram of the experimental set up used to study transport across conducting polymers.

Figure 2.4 shows the basic transport cell designed and constructed for this work. The cell consisted of two compartments separated by the membrane under investigation. The solution in each compartment was stirred using small paddles (A=3.8 cm^2) run off DC motors. To apply electrical stimuli, a three electrode system was used with the membrane acting as the working electrode. A platinum gauze auxiliary electrode and a Ag/AgCl reference electrode were the other two electrodes. Samples were withdrawn from the receiver side of the cell and analysed.

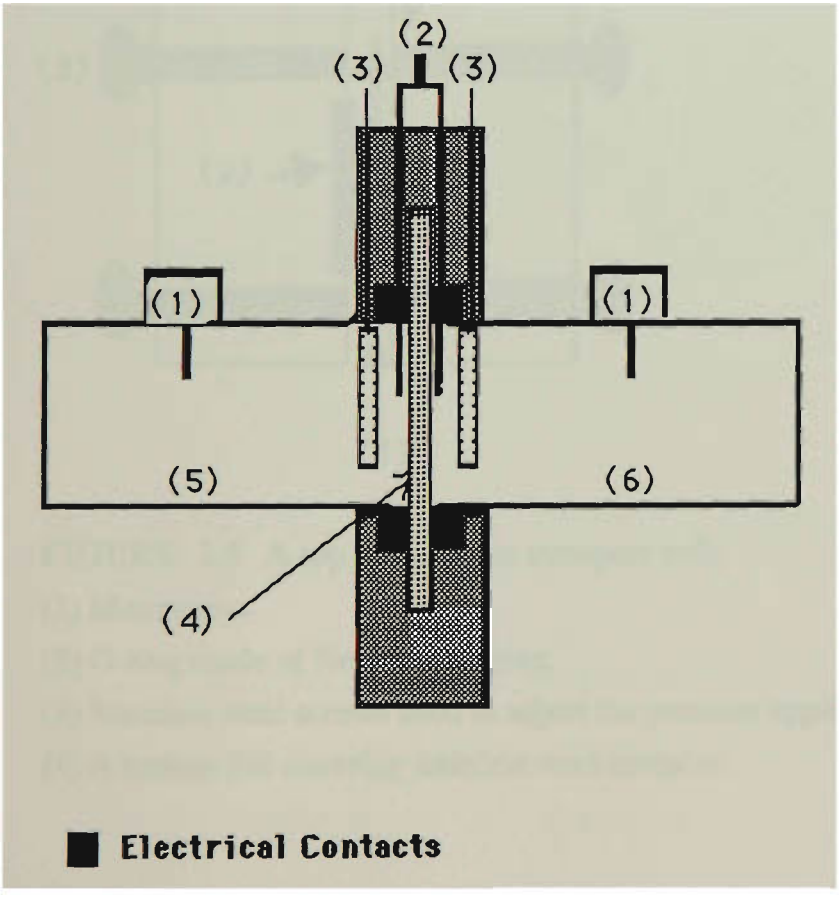

FIGURE 2.4 The cell used for transport studies:
(1) Stirrer motors
(2) Reference electrode
(3) Auxiliary electrodes-platinum mesh
(4) Membrane
(5) Receiver solution
(6) Source solution

Several aspects of the cell design were optimised in the course of this work:

Cell configuration. As shown in Figure 2.5 the membrane was held between two blocks made from Teflon (25% glass reinforced). It was found that when the cell was sealed using stainless steel screws the pressure applied caused the membrane to become brittle at the edges. Using an O-ring at the point of contact with the Teflon block eliminated this problem (Figure 2.5).

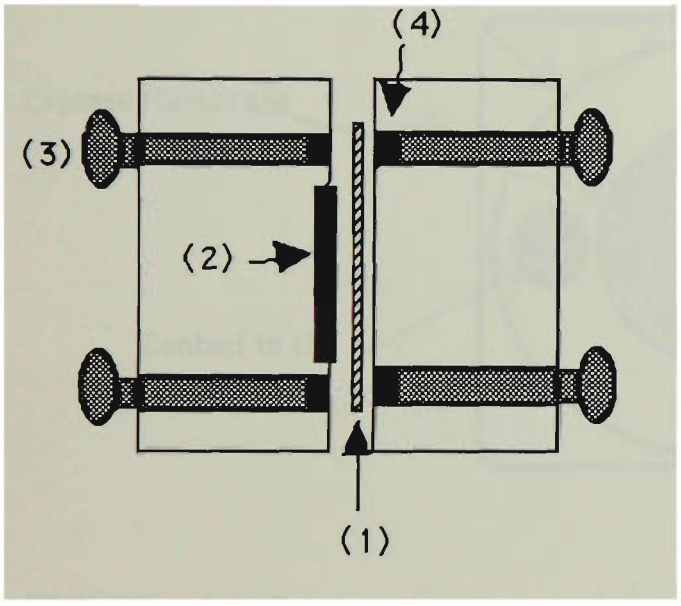

FIGURE 2.5 A top view of the transport cell:
(1) Membrane.
(2) O-ring made of Neoprene rubber.
(3) Stainless steel screws used to adjust the pressure applied to the membrane.
(4) A carbon foil covering stainless steel contacts.

Electrodes. The working electrode material was the membrane under investigation (Geometric surface area= 7.1 cm^2). The auxiliary electrode required an open structure since the cell was stirred. Therefore a platinum mesh electrode (18 mesh/cm with wire diameter of 195 μm) was used (2.0 x 2.0 cm).

Electrical contact to the membrane. Electrical contacts was via two circular connections at the unexposed part of the membrane (Figure 2.6).

Contact pressure can be adjusted by means of using two screws connected to the outside of the cell. Each contact had surface area of A= 0.8 cm^2 and were 4.4 cm from each other. The size, nature and the pressure applied to the contact were found to be important in electrochemically controlled transport studies. These results are described below.

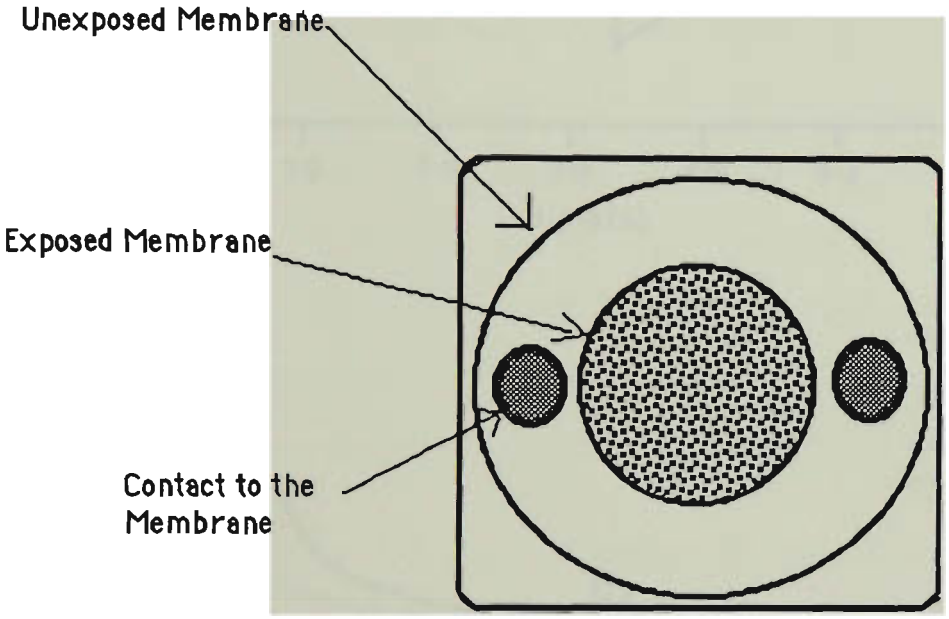

FIGURE 2.6 Cross-sectional view of electrical contacts applied to the membrane. Contacts were on both sides of the membrane.

Due to iR drop parts of the membrane removed from the immediate electrical contact do not experience the potential applied. As the ratio of contact area versus membrane surface area (exposed to solution) increased this problem diminished. This is illustrated by chronoamperometric responses obtained for two different membranes such as PPy/PTS (polypyrrole/p-toluenesulfonate) and polypyrrole/polyvinyl sulfonate (PPy/PVS) using contacts with different surface area (Figure 2.7 (a,b)). With both membranes as the surface area of the contact decreased the current response declined.

(PPy/PVS)

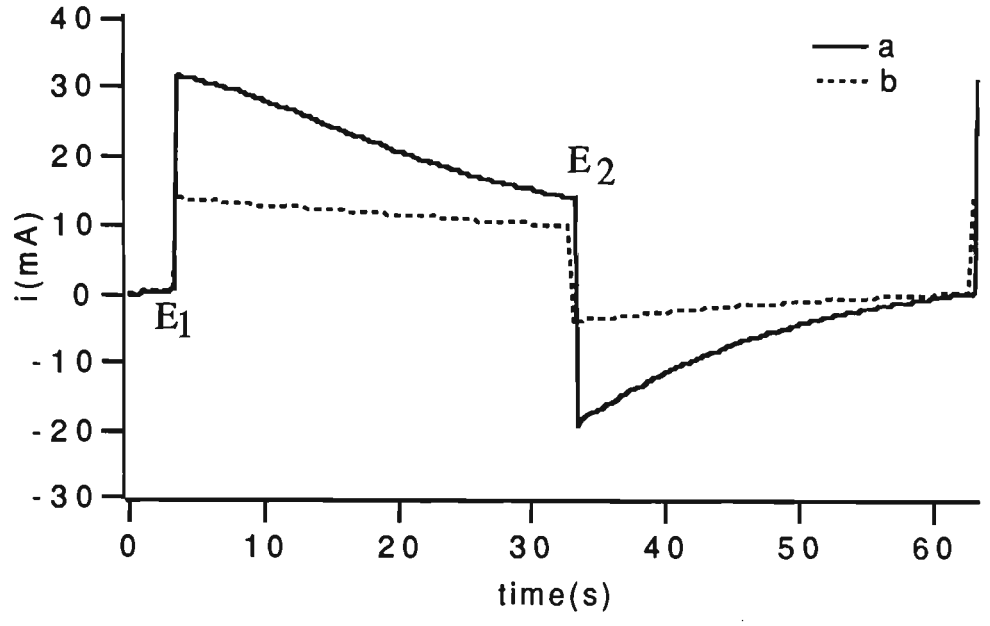

(PPy/PTS)

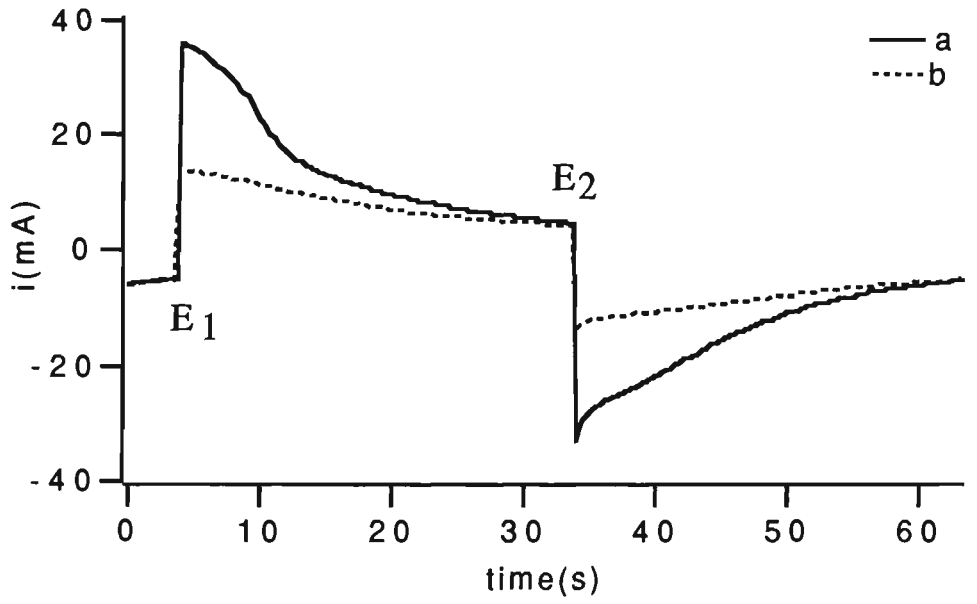

FIGURE 2.7 Chronoamperometric response of PPy/PVS and PPy/PTS membranes during transport of 0.20 M sodium benzene sulfonate (BS) using contacts with R value of (ratio of contact surface area to membrane area exposed) (a) 0.222 (b) 0.111.
A pulsed potential of E_1=0.40 to E_2=-0.6 and t_1=t_2=30 s was applied to the membranes.
The membranes were prepared as part of the investigation described in Chapter 4.

The pressure applied to the contacts during transport was found to play a crucial role. In general as the pressure on the contacts increased the current flow upon application of potential during the course of transport increased (Figure 2.8).

It was found that the resistance measured between contacts attached to either side of the membrane was directly related to the applied pressure. As the pressure increased this resistance decreased until it reached a constant value. For example using the diffusion cell described above (Figure 2.6) a minimum resistance of ~110 Ω was measured for PPy/PTS membranes while for PPy/PVS membranes this value was about 140 Ω. It should be noted that the resistance was measured relative to the transport cell and these values are valid if the given dimensions of the membrane and contacts are used.

It was found that as the resistance between two sides of the membrane decreased (by adjusting the applied pressure) the oxidation/reduction current increased (Figure 2.8). Consequently the charge consumed during oxidation/reduction increased (Table 2.1). However care had to be taken since excess pressure damaged the membrane.

(PPy/PVS)

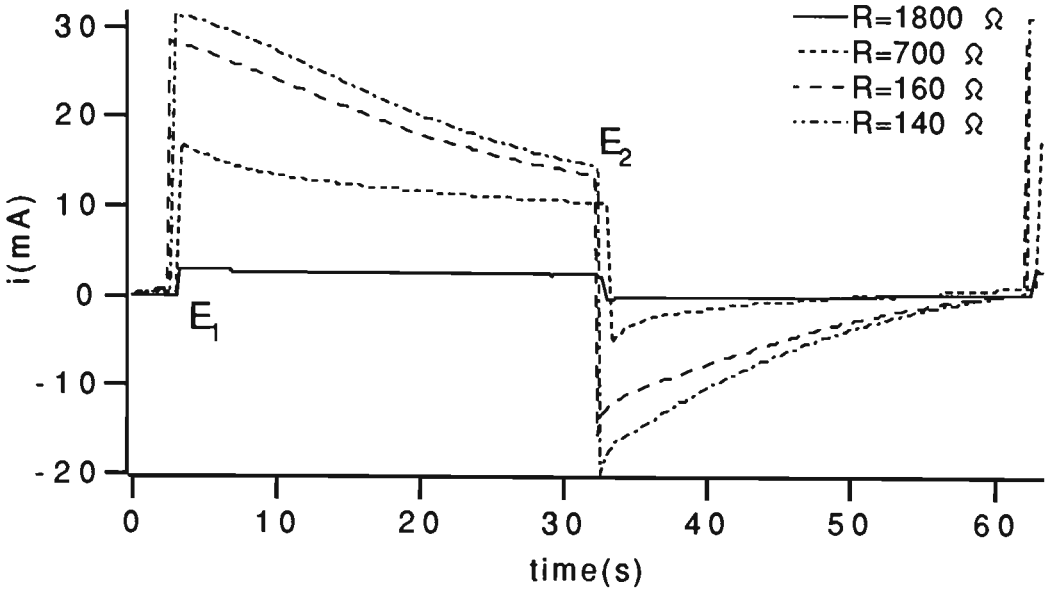

(PPy/PTS)

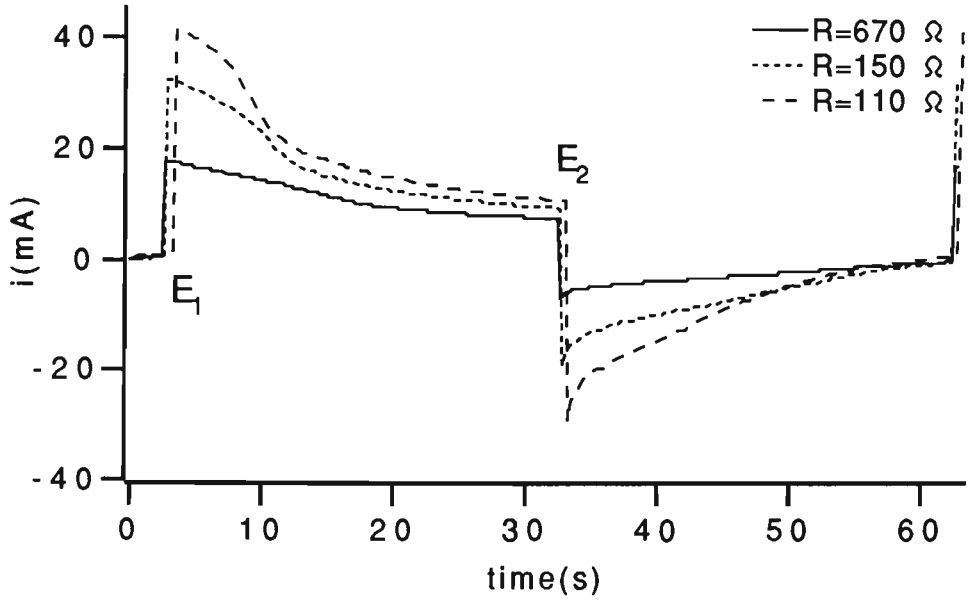

FIGURE 2.8 Chronoamperometric response of PPy/PVS and PPy/PTS membranes during transport of 0.20 M BS with different contact resistances.

A pulsed potential of E_1=0.40 to E_2=-0.60 and t_1=t_2=30 s was applied to the membranes. Resistance adjusted by altering contact pressure. Note that all resistance measurements were carried out with respect to the transport cell shown in Figure 2.6.

TABLE 2.1 The relationship between resistance and charge passed during transport of 0.20 M BS across (a) PPy/PVS and (b) PPy/PTS membranes.

(a)

Resistance(Ω)	135	160	210	300	700	1400	1800
Q(Ox)-mC	432	365	258	240	141	36	28
Q(Red)-mC	426	366	245	226	210	67	49

(b)

Resistance(Ω)	110	125	135	195	260	670	1000
Q(Ox)-mC	415	399	370	360	256	219	176
Q(Red)-mC	400	357	336	324	242	200	189

A pulsed potential of E_1=0.40 to E_2=-0.60 and t_1=t_2=30 s was applied to the membranes.

The charges were calculated by integration of the chronoamperograms.

The resistance was measured in the transport cell shown in Figure 2.6.

The chemical and physical nature of the contact was also important. It was found that employing soft materials such as carbon foil gave better contact compared to hard materials such as stainless steel. For example using PPy/PTS membrane the minimum attainable resistance measured between two contacts was 110 Ω for carbon foil while it was 280 Ω for stainless steel contacts.

On the basis of the above descriptions the transport cell shown in Figure 2.6 was designed and used throughout the studies. In this design four circular contacts (via carbon foil) were applied to the membrane under investigation.

Electrical contact was made to both sides of the membrane from both sides. In order to get more reproducible results (in terms of the charge passed through the cell) the resistance between two contacts was always adjusted to a constant value prior to an experiment. This constant value was the minimum resistance attainable for each membrane. With polyaniline membranes (see Chapter 3) another cell design was used. This was essentially the same as described above but the distance between the exposed membrane and contacts was minimised.

2.4 CHARACTERISATION TECHNIQUES

Scanning Electron Microscopy (SEM). The most popular technique for morphological observation of polymers is Scanning Electron Microscopy (SEM), as evidenced by the variety of materials studied[168]. The resolution of SEM is typically of the order of 5 nm, this being limited by the stability of the power supply. This corresponds to a magnification[169] from 20 up to 100000.

The preparation of membrane sample was straightforward. Small pieces of the membrane under investigation were cut carefully with a sharp blade. They were glued into an aluminium tray using a conducting silver paint. A thin layer of gold was deposited on the top of the membrane. All images were obtained using a Hitachi S 450 instrument.

Atomic Force Microscopy (AFM). AFM enabled us to image surface topography of the membranes in either air or in electrolyte solution. This technique was invented by Binnig, Quate and Gerber in 1986[170]. The first[171] images obtained using AFM were reported in 1987. In this work atomic-scale

features on the surface of graphite were shown. Subsequently this technique was developed to measure surface forces and image surface topography[172-175].

One of the major advantages of AFM over SEM is its ability to image non conducting samples under various ambient conditions, such as in solution. Unlike SEM no conducting coating (ie. silver or gold) is required in order to take images. Consequently these permit the taking of non-destructive images of structures in the atomic level.

It has been shown that individual proteins and protein complexes can be imaged with atomic force microscopy down to a resolution where even molecular details are visible under physiological conditions[176]. This work also demonstrates the non destructive nature of the technique at this resolution.

The AFM photos shown in Chapter 4 of this work were obtained using the AFM (Nonscope 2, Digital instrument Inc) at the Australian National University (ANU).

Conductivity measurements. In order to measure the conductivity of the membranes, a standard test method as designed by ASTM (D 4496-87) was employed. The cell used for the conductivity measurements was made at the University of Technology, Sydney. The cell contained four electrodes held in an insulating epoxy matrix. The electrodes were flat and between two outer electrodes a constant current of 1 ± 0.001 mA was applied then the potential differences between the two inner electrodes was recorded (Figure 2.9). The two inner electrodes were fixed at distance of 0.987 ± 0.002 cm. The electrodes were fabricated from brass with wire contacts made from common antimony/lead solder to give a resistance of 0.07 Ω.

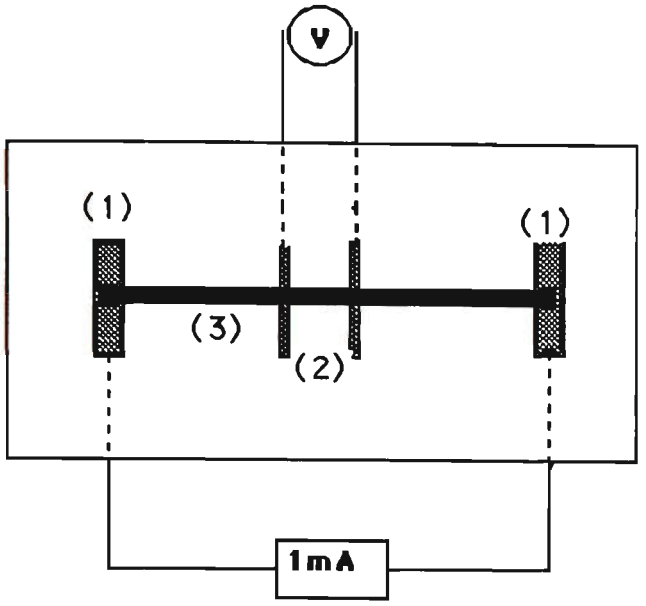

FIGURE 2.9 A schematic of the cell used for four-point probe conductivity measurements:
(1) Outer electrodes (a constant current of 1 ± 0.001 mA was applied)
(2) Inner electrodes (the potential differences were measured between the electrodes)
(3) A polymer strip.

The four-probe volume resistivity (R_V in units of Ω cm) of the membranes was measured as:

$$R_V = \frac{X.Y}{Z} * \frac{\delta_E}{i} \qquad (2.1)$$

where:

X= thickness of conducting polymer film (cm), Y= width of conducting polymer film (cm), Z= distance between inner electrodes (cm), δ_E= potential difference over inner electrodes (mV), i= current passed through outer electrodes (mA).

The film conductivity σ was then calculated by:

$$\sigma = \frac{1}{R_V} \qquad (S\ cm^{-1}) \text{ or } (\ \Omega^{-1}cm^{-1}) \qquad (2.2)$$

Throughout this work samples with a width of 0.2 cm and a length of 6.5 cm were used. The film thickness was measured by a digital micrometer (Mitutoyo) with a resolution of 1 μm.

Mechanical properties. The tensile strength is the most widely reported mechanical property for polymeric material. These properties are usually measured using an ASTM standard method. A specimen is held in the jaws of a tensile testing machine. Then it is extended at a known steady rate and the force developed in it, is recorded in the machine. The test is usually continued until the specimen breaks. If the cross-sectional dimensions of the specimen are known, the force can be converted to stress and the stress/elongation curve is obtained. Tensile strength is the maximum stress or load per unit area in units of Pa or MPa. It is calculated as follows:

$$S = \frac{P}{TxB} \tag{2.3}$$

where S is tensile strength (MPa) and P is the maximum load (Newton), T is thickness (mm) and B is the sample width (mm).

Young' s modulus (E) is another useful parameter used to describe the mechanical strength of polymers. It is the load required to stretch a specimen of unit cross-sectional area by a unit amount. It is defined as the ratio of stress to strain and is determined from the initial straight-line portion of the stress-strain curve, as follows:

$$E = \frac{\sigma}{\varepsilon} \tag{2.4}$$

where E is the Young's modulus (MPa), σ is tensile stress (MPa) and ε is the strain. σ and ε are determined by:

$$\sigma = \frac{F}{A_0} \tag{2.5}$$

F is tensile force (or load) and A_o is the cross sectional area of the specimen (T. B).

$$\varepsilon = \frac{L\text{-}Lo}{Lo} \qquad (2.6)$$

Lo is the initial length and L is the extended length. The term of L-Lo is defined as extension, which is usually measured directly by testing machine.

Throughout this work a universal testing machine was used (Instron 4302) at room temperature with a strain rate of 1 mm min^{-1}. Each specimen of the conducting membrane was cut with the dimensions of 10 x10 x 0.01 mm. The specimen was held in the jaws of a 100 Newton tensile cell using adhesive tape. Then the measured force was converted to the tensile strength and Young' s modulus.

Cyclic voltammetry. Cyclic voltammetry (CV) has proven very useful in obtaining information about electrode reactions. The technique involves measurement of current at the working electrode as a function of the applied potential.

It enables the electrode potential to be rapidly scanned and the current is monitored[167, 177, 178]. Figure 2.10 shows a potential-time signal for cyclic voltammetry. The repetitive triangular potential excitation signal for CV causes the potential of the working electrode to swept between two designated values (the switching potentials). Application of the potential with such a triangular waveform to a polymer modified electrode (in this case polypyrrole) results in current response (Figure 2.11). This voltammogram suggests that if the potential is oscillated between two values (e.g. 0.40, -1.00 V) the ion exchange process described in Equations 1.1 and 1.2 (Chapter 1) is induced.

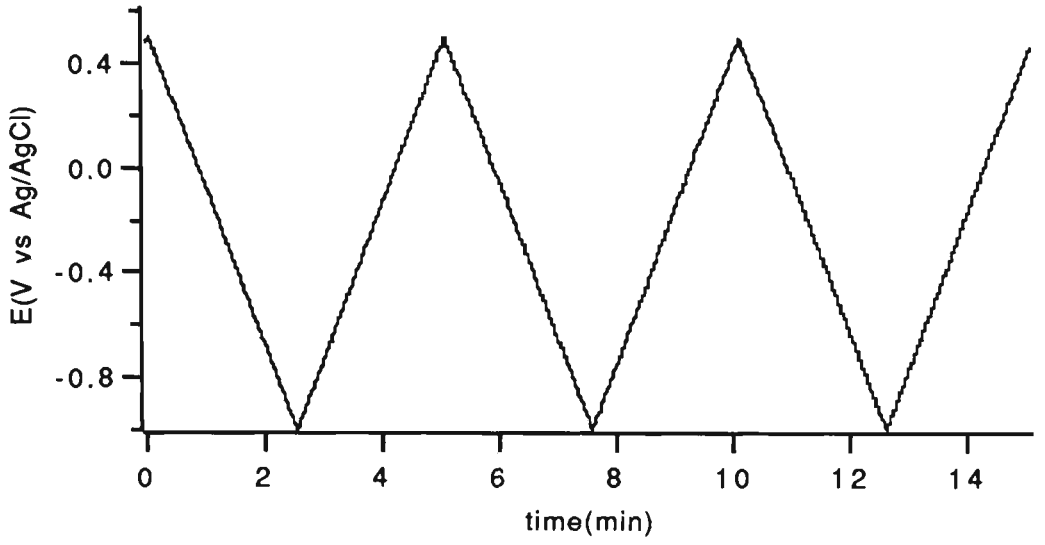

FIGURE 2.10 The potential waveform for cyclic voltammetry.

The important parameters of a cyclic voltammogram are the magnitude of the anodic peak (i_{Pa}), the cathodic peak current (i_{Pc}), the anodic peak potential (E_{Pa}), and the cathodic peak potential (E_{Pc}).

Throughout this work cyclic voltammetric studies were carried out using a conventional three-electrode electrochemical cell with a platinum counter electrode and a Ag/AgCl reference electrode. The working electrode was the polymer modified electrode (see individual chapters).

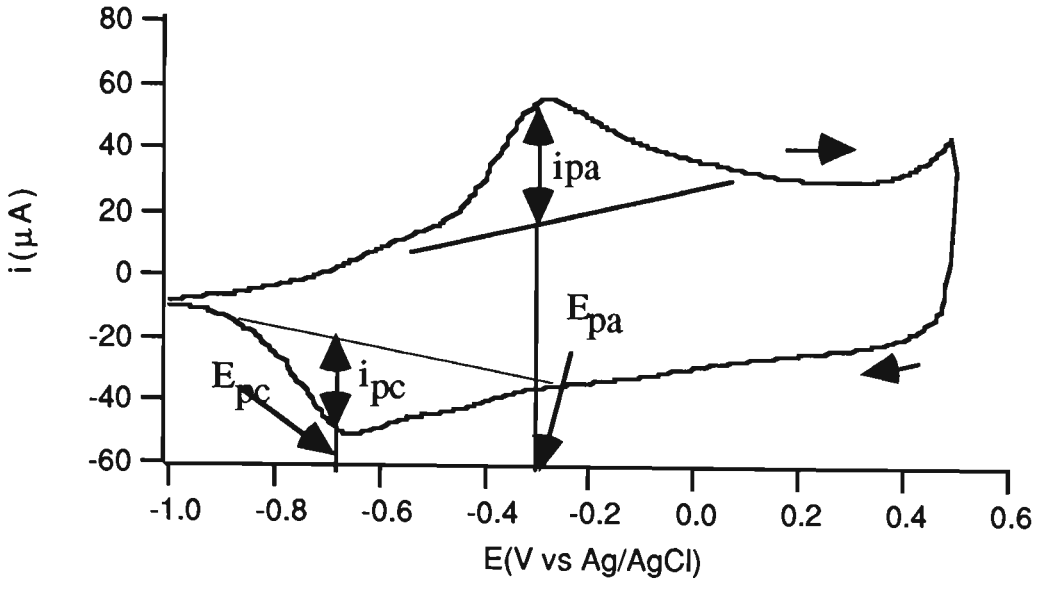

FIGURE 2.11 Cyclic voltammogram showing oxidation-reduction of polypyrrole/ PTS in 0.20 M NaCl. Scan rate=10 mV s^{-1}.

Polymer was grown electrochemically from a solution containing 0.20 M pyrrole and 0.05 M PTS. A gold film electrode and constant current of 2.0 mA cm^{-2} were used for 60 s.

CHAPTER 3

TRANSPORT ACROSS POLYANILINE MEMBRANES

3.1 INTRODUCTION

Despite the strong attention paid to the electrochemical and spectroscopic properties of polyaniline, the mechanical properties have not been investigated in any detail. To date no one has succeeded in electrosynthesising free-standing films of polyaniline with adequate mechanical properties, although a number of attempts[106, 179] have been reported in this regard. For example Kitani and co-workers[179] have prepared polyaniline films by electrochemical reduction of ordinary polyaniline film in organic solvents. However, to peel the polymer from the electrode a minimum thickness of ~500 μm was required. In addition, to maintain the mechanical properties, the film must be in the reduced form[179]. Therefore other methods including chemical casting have been considered. MacDiarmid and co-workers[130] reported the partial solubility of polyaniline in the emeraldine base form, in NMP (N-methyl-2 pyrrolidinone) a solvent commonly used to dissolve azo dyes[180]. Polyaniline film could be cast from this solvent and they reported a conductivity of 1-5 S cm^{-1}.

In 1989, Cao and co-workers investigated the influence of chemical polymerisation conditions on the properties of the polyaniline[113]. They reported the relation between oxidation conditions and properties such as the conductivity and the molecular weight of the resultant powder. This work represented the first systematic study of the relationship between the chemical polymerisation conditions and the principles governing the macromolecular properties of polyaniline such as molecular weight and conductivity.

In this Chapter the preparation of polyaniline membranes using either electrochemical or chemical methods was considered. Using chemical polymerisation the method described by Cao and co-workers was further considered with a view to produce free-standing films of polyaniline. In particular, improving the conductivity and mechanical properties of polyaniline

films cast from NMP was a major objective. After preparation of the membranes the transport of different acids and some simple inorganic salts across the membranes was investigated.

3.2 EXPERIMENTAL

3.2.1 REAGENTS AND MATERIALS

Analytical reagent (AR) grade chemicals were used throughout, unless otherwise stated. Reagent-grade ammonium persulphate, aniline and ammonium hydroxide were purchased from BDH chemicals. Acids were purchased from Ajax Chemicals. 1-methyl-2-pyrrolidinone (NMP), p-Toluenesulfonic acid monohydrate (PTSA), anthraquinone-2,6-disulfonic acid disodium salt (Anth-2,6D) and low molecular weight polyvinylsulfonic acid (PVS), sodium salt (25% w/v in water) were purchased from Aldrich chemicals. Sodium dodecyl sulphate (SDS) was supplied by Sigma.

Aniline was distilled prior to use and all the other chemicals were used as received.

3.2.2 INSTRUMENTATION

All cyclic voltammetric studies were carried out as described in Section 2.4 using a BAS 100A Electrochemical Analyser and/or A CV-27 voltammograph with a MacLab/4 chart recorder. A Princeton Applied Research (PAR) Model 363 potentiostat was used for electropolymerisation and to apply the electrical stimulus during transport studies. A high vacuum pump (Javac Co., Australia) was used to dry the polyaniline films. An Instrumentation Laboratory atomic absorption spectrometer (1L-551) was used to determine cations.

3.2.3 EXPERIMENTAL PROCEDURES

Film Preparation. Polyaniline was grown using a potential cycling method with the potential scanned between -0.20 and 0.80 V. A scan rate of 50 mV s^{-1} was employed. The electrolyte consisted of acid (1.00 M) and aniline (0.20 M). Alternatively polyaniline was deposited under potentiostatic or galvanostatic conditions, with a constant potential of 0.80 V (vs Ag/AgCl) or a constant current of 2.0 mA cm^{-2}. The potential was kept below 0.80 V since it has been shown by cyclic voltammetry that degradation products appear at higher potentials[118].

Characterisation of polymer membranes. The conductivity and the tensile properties of polyaniline membranes were determined as described in Chapter 2. SEM photos were obtained as per Section 2.4. Cyclic voltammograms of the polyaniline membranes were obtained as in Chapter 2 with a gold electrode (0.5 x 0.5 cm) covered by polyaniline.

Transport Studies. The cell utilised in the transport studies was as shown in Figure 2.4. The cell consisted of two compartments (volume of 30 mL each) separated by polyaniline membranes. The membrane area was 3.14 cm^2. The concentration of acids in all cases was 0.40 M. One side of the cell was filled with the acid and other side with an equal volume of Milli-Q water. The decrease in the pH of the receiver solution was measured as a function of time. In the case of transport of inorganic species a concentration of 0.40 M salt (Na^+, K^+ or Cu^{2+}) and 0.05 M HNO_3 were used as source solution with Milli-Q water in the receiver side.

Sample analysis. Sodium, potassium and copper were analysed using an atomic absorption spectrometer. A calibration curve was obtained prior to analysis. The relation between concentration of cations and the absorbance

was linear in the range of 0.4-2.8 ppm with correlation coefficient (R^2) of above 0.997. The concentration of acids was measured by a Linbrook pH meter.

Potentiometric titration. The potentiometric titration of polyaniline was carried out using the polyaniline working electrode (cast from NMP solution over a piece of gold film) and a Ag/AgCl as reference electrode. Supporting electrolyte contained 0.10 M KCl (25 mL) and 0.10 M HCl was added slowly. The delay between two consecutive additions was approximately 10 minutes. The potential change was plotted against volume of titrant using a Linbrook potentiometer.

3.3 RESULTS AND DISCUSSIONS

3.3.1 ELECTROCHEMICAL SYNTHESIS AND CHARACTERISATION

Using a constant potential method aniline was polymerised in the presence of HNO_3 (Figure 3.1). Well defined responses due two separate oxidation (A,B) and reduction (A') processes were observed (see Section 1.3.2). Polyaniline was alternatively prepared using a constant potential or constant current (Figure 3.2). It was noted that potential cycling methods produced more adherent films while the product with a constant potential seemed to be powdery and easily removed from the electrode. None of these products could be peeled off due to poor mechanical properties. These results are in agreement with previous observations[125].

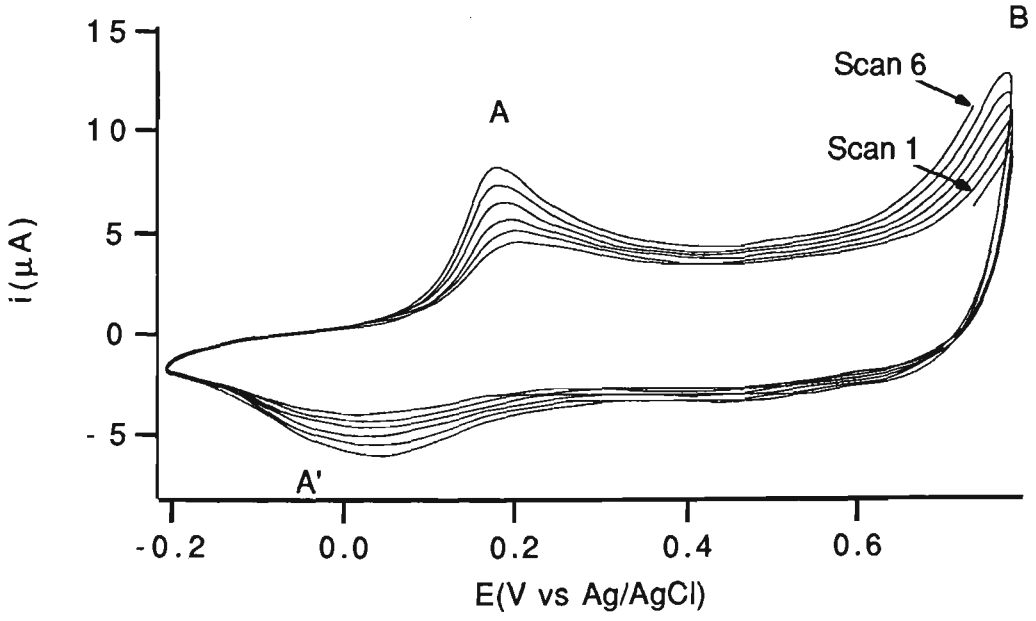

FIGURE 3.1 Cyclic voltammograms of 0.20 M aniline in 1.00 M HNO_3 at a glassy carbon disk electrode during polymer growth for the first 6 cycles.
Scan rate =50 mV s^{-1}.

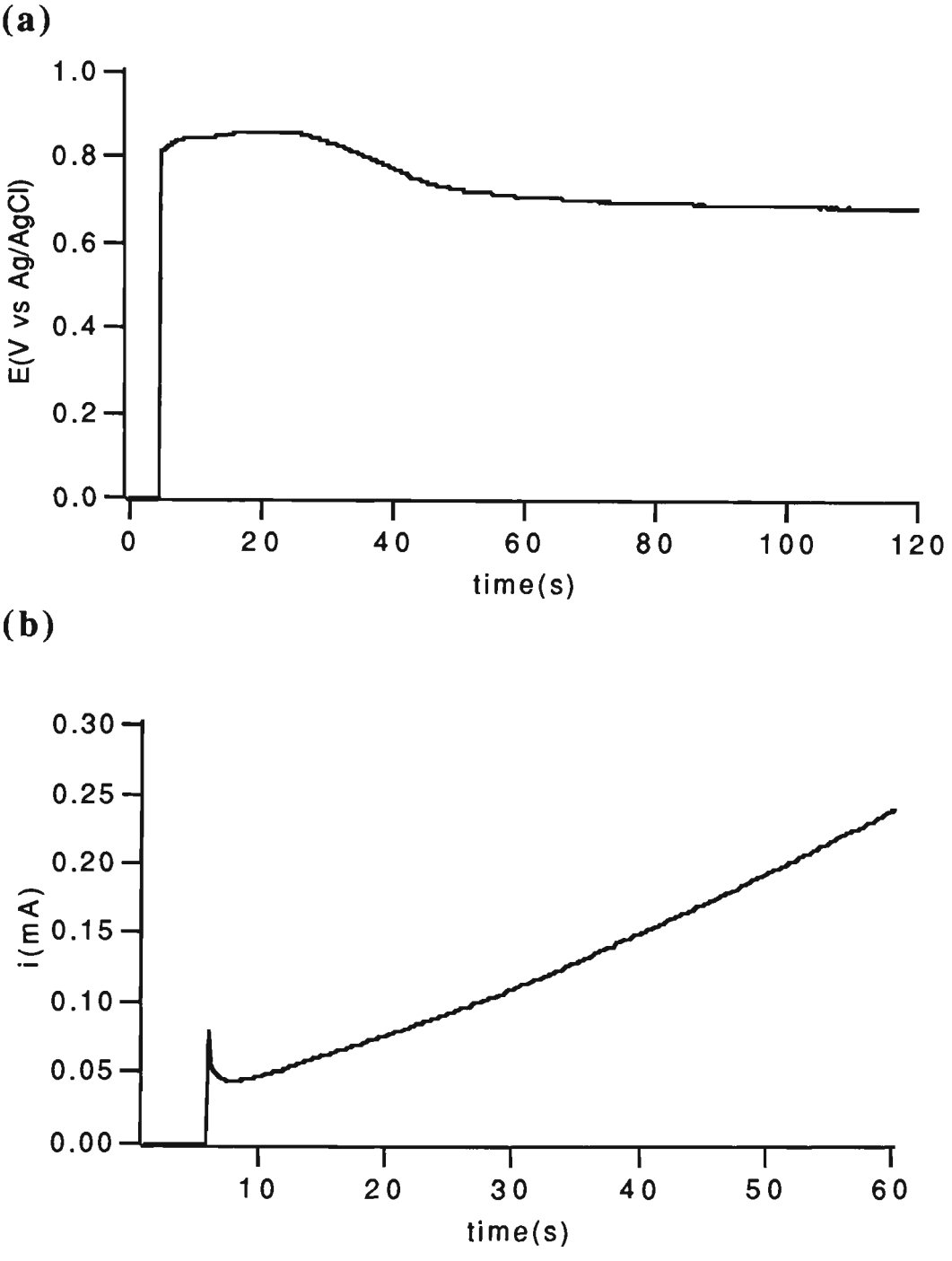

FIGURE 3.2 Chronopotentiometric (a) and chronoamperometric (b) responses recorded at a glassy carbon disk electrode for the oxidation of 0.20 M aniline in solution containing 1.00 M HNO_3.

A constant current of 2.0 mA cm^{-2} and constant potential of 0.80 V was used.

It has been shown that the type of anion determines the structure of the polymer[123]. Therefore in attempts to improve the mechanical properties of the polyaniline film the preparation of the polymer was carried out in the presence of different counterions. In the course of this work both organic and inorganic counterions were employed. Both the potential cycling and constant potential method were used.

It was found that a continuous film of polyaniline (i.e. the film uniformly deposited over the entire electrode) can be prepared in the presence of strong inorganic acids and p-Toluensulfonic acid (Table 3.1).

TABLE 3.1 The effect of the counterion on properties of polyaniline films.

Counterion	Aniline(M)	Counterion concentration (M)	Film formation
Cl^-(HCl)	0.50	1.00	+
HSO_4^-/H_2SO_4	0.50	1.00	+
NO_3^-	0.50	1.00	+
ClO_4^-	0.30	1.00	+
*Antq(2,6)-D	0.20	Saturated	-
*SDS	0.20	0.50	-
*PTSA	0.20	1.00	+
*PVS	0.20	25.0 g L^{-1}	-

(+) indicates formation of continuous film, (-) indicates absence of continuous film.
*See experimental Section.

CV behaviour similar to that observed for HNO_3 (Figure 3.1) was obtained for all the strong inorganic acids. In all cases the films prepared were too fragile to measure a tensile stress or Young's modulus. Consequently, they were not suitable for use as a free-standing membrane, and further characterisation was not carried out.

The polymerisation of aniline was also carried out in the presence of organic counterions. A solution containing 0.20 M aniline and any of the organic counterions (except PTSA) had a pH value greater than 6. With such high pH solution, polyaniline did not grow (Figure 3.3) and the oxidation current disappeared after a few scans due to the lack of electroactivity/conductivity.

Similarly the chronoamperometric response of aniline in the presence of PVS indicates a lack of deposition (Figure 3.4). In both cases polymer growth was limited due to the lack of conductivity of the polymer film in the high pH media. As polyaniline looses its conductivity in high pH media (i.e pH>4). This can be overcome by reducing the pH in some way.

A strong protonic acid (i.e HCl: pH<2) was added to reduce the pH. Thus a continuous film of polyaniline was readily produced however, due to the poor mechanical properties the polymer film could not be peeled off the electrode. It is believed that the co-counterion (i.e. Cl^- from the HCl used to reduce pH) may have been incorporated into the polymer matrix resulting in the poor mechanical properties.

In other attempts the pH was reduced by employing a greater ratio of counterion to monomer (note that the aniline is a base). A solution containing 0.10 M aniline and saturated amounts of the counterion such as PVS and anthraquinone-2,6-disulfonic acid disodium salt were employed. No continuous film was formed and the polymer only deposited as a very thin

heterogeneous layer with a rough and flaky surface. This was extremely difficult to peel it off.

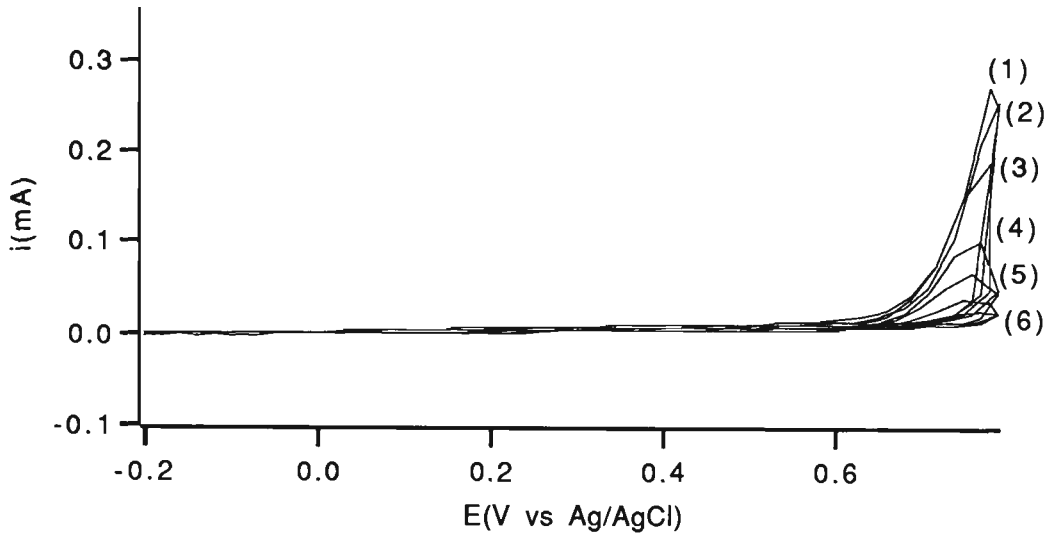

FIGURE 3.3 Cyclic voltammograms showing oxidation of aniline (0.20 M) in SDS (0.05 M). Working electrode was a glassy carbon disk electrode. Scan rate =50 mV s^{-1} The numbers on the graph (1-6) show the cycle number.

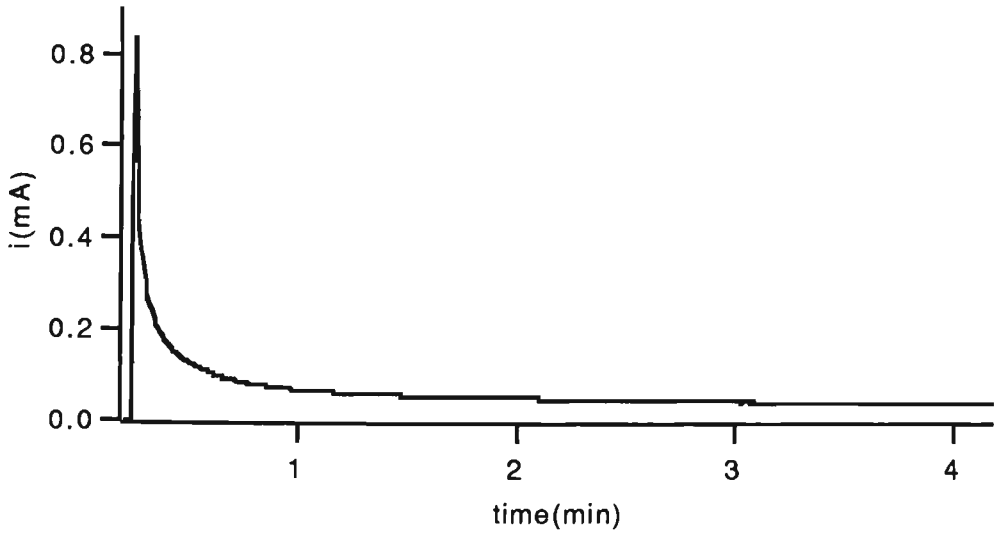

FIGURE 3.4 Chronoamperometric response for the oxidation of a 0.20 M aniline in a 25.0 g L^{-1} solution of PVS at a glassy carbon disk electrode. A constant potential of 0.80 V vs Ag/AgCl was applied.

3.3.2 CHEMICAL SYNTHESIS AND CHARACTERISATION

3.3.2.1 SYNTHESIS

The chemical preparation of polyaniline membranes was carried out in three distinct stages with a number of variables involved in each stage:

1) Powder preparation

2) Solution preparation

3) Casting and drying methods

Fine polyaniline powder was prepared in an aqueous protonic acid solution as described previously[113]. 45.6 g of ammonium persulphate was dissolved in 250 mL of 1.70 M HCl solution. This was then added to 20 mL of aniline dissolved in 250 mL of 1.70 M HCl.

Various temperatures in the range between -10 to 25 °C have been employed to prepare polyaniline powder[112, 113, 181]. We have found that the polymerisation temperature plays a crucial role since the polymer membrane produced from powder synthesised at -3 to -5 °C had superior tensile strength, ~110 MPa. Those prepared at higher temperatures +3 to 5 °C had tensile strength of the order of 85 MPa. When the temperature employed during polymerisation was over 5 °C the films prepared from the powder were brittle and too fragile to enable tensile strength to be measured. The improvement in the mechanical properties of the films produced from the powder synthesised at low temperatures may be due to the increase in molecular weight of the polymer as reported previously[114].

The oxidant was added slowly over a period of one hour to keep the temperature of polymerisation below -3 °C. The addition of oxidant was

completed in 2 hours. The polyaniline was collected and washed several times with Milli-Q water until the solvent became colourless. It was previously shown that the removal of the THF-soluble fraction from the emeraldine base leads to a significant increase in the molecular weight of the remaining powder[113], as verified by measuring the viscosity of the dissolved powder. Therefore to increase the molecular weight (mechanical properties) the prepared powder was washed in THF several times until the THF became colourless. Finally the material was dried under vacuum for at least 24 hours. To convert the emeraldine hydrochloride to a base form, which is more soluble in NMP, the precipitate was stirred with a solution of NH_4OH (1.70 M) for 2 hours. Then it was dried to constant weight under high vacuum, for a period of up to two days. The powder was further dried in an oven (60 ^oC for 12 hours). The powder was then ground with an agate mortar and pestle before being sieved through a 60 mesh sieve to obtain a very fine powder.

One gram of the powder was then slowly added (over 1 hour) to 40 mL of NMP solution, and magnetically stirred at room temperature for 7 hours. It was found that if the polymer powder was added too rapidly to the NMP, it tended to aggregate. The resulting viscous solution was pre-filtered twice through a Buchner funnel using Whatman paper # 541 to remove large particles. Finally it was filtered with Whatman paper # 542. It was found that any unfiltered insoluble material affected the homogeneity of the cast membranes resulting in the lower tensile strength. For example a range of 20-40% decrease in the tensile strength value of the films was observed when the unfiltered solution was used to cast films. A ratio of 1.0 g powder to 40 mL NMP (25.0 g L^{-1}) gave the best results with respect to the thickness and uniformity of the final prepared films. The films cast from dilute solutions (i.e 15.0 g L^{-1}) took a longer time to dry and the resultant films were not uniform. If the solution was too

concentrated (i.e 35 g L^{-1}) the filtration process was difficult and it was not possible to cast an even layer from such a concentrated solution.

The viscous solution of polyaniline was spread over a piece of glass to obtain an even layer of emeraldine base form. This was then dried under vacuum. In general slower drying gave films with more uniform thickness. When dry the film was removed from the glass by immersion in water.

NMP is soluble in methanol and spectroscopic studies have shown that the removal of all NMP from polyaniline films with methanol is possible[182]. Therefore the cast films were treated in methanol solution to remove NMP. It was necessary to remove the NMP from the film, as during the transport studies, application of potential may interfere with any impurities. When the polyaniline films were placed in methanol they shrunk by 10-15% of their original size and the films prepared from 3 mL of solution cast over a piece of glass (8 x 8 cm) gave a membrane with thickness of ~15 μm.

3.3.2.2 CHARACTERISATION

Conductivity. Polyaniline was doped by immersing in 1.00 M HCl solution for 24 hours. The film was then placed between two sheets of filter paper and was dried under high vacuum for 48 hours. It was found that the conductivity reached a constant value after this period. Conductivities in the range of 20-30 S cm^{-1} were obtained. Previous researchers have reported[98, 114, 144, 180] conductivity values in the range 1.2-20.0 S cm^{-1} for polyaniline films. Recently a conductivity of 20.0 -60.0 S cm^{-1} has also been reported[129] for polyaniline fibers. The membranes prepared here had adequate conductivity to allow application of electrical stimuli during transport studies.

Cyclic Voltammetry. Polyaniline films cast from NMP solution (see experimental) were subjected to cyclic voltammetry (CV) in different acidic media. The important quantitative data obtained from the CV's was recorded (Table 3.2).

TABLE 3.2 Electrochemical data for the polyaniline oxidation process.

Acid	Epa	Epc	ΔEp	Ipa	Ipc	$\frac{ipa}{ipc}$
	E(V vs Ag/AgCl))			$x10^{-2}$ (μA)		
H_2SO_4	0.32	0.02	0.30	18.1	19.3	0.9
HCl	0.32	0.02	0.30	17.5	15.0	1.2
HNO_3	0.30	0.15	0.15	10.3	3.6	2.9
$HClO_4$	0.25	0.10	0.15	3.3	1.4	2.4

Ep= Peak potential, Ip= Peak current, ΔEp =Peak separation (see Section 2.4). Scanned in 0.40 M acid solution. The cyclic characteristics were obtained from Figure 3.5 (A, A'). Scan rate= 50 mV s^{-1}

It is well known that during every scan the polymer undergoes two separate oxidation and reduction processes. In this case the reactions occurring were as follows:

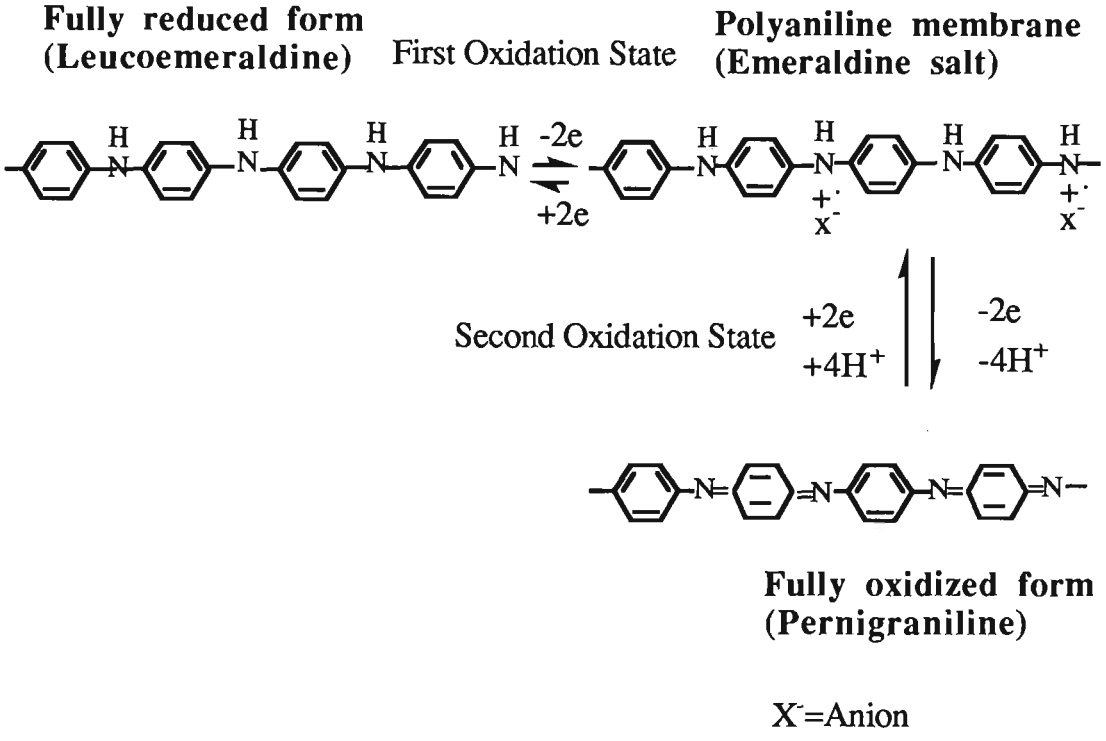

(3.1)

This is clearly found to be occurring in the films prepared here in a variety of acidic media (Figure 3.5 (a-d)). The first response (A and A') is due to the first oxidation/reduction of polyaniline (Equation 3.1). The second response (B, B') is due to oxidation of emeraldine to pernigraniline (fully oxidised form) and vice-versa (Equation 3.1).

Note ,also, in the very acidic solutions (pH<1) the amine groups in the leucoemeraldine can also be protonated to produce leucoemeraldine salt[118] however for simplicity they are not shown here.

FIGURE 3.5 Cyclic voltammograms showing oxidation-reduction of polyaniline films cast from NMP solution on a gold film electrode. Scan rate=50 mV s^{-1}
(a) in 0.40 M H_2SO_4 (b) in 0.40 M HCl (c) in 0.40 M HNO_3 (d) in 0.40 M $HClO_4$.

(a)= H_2SO_4

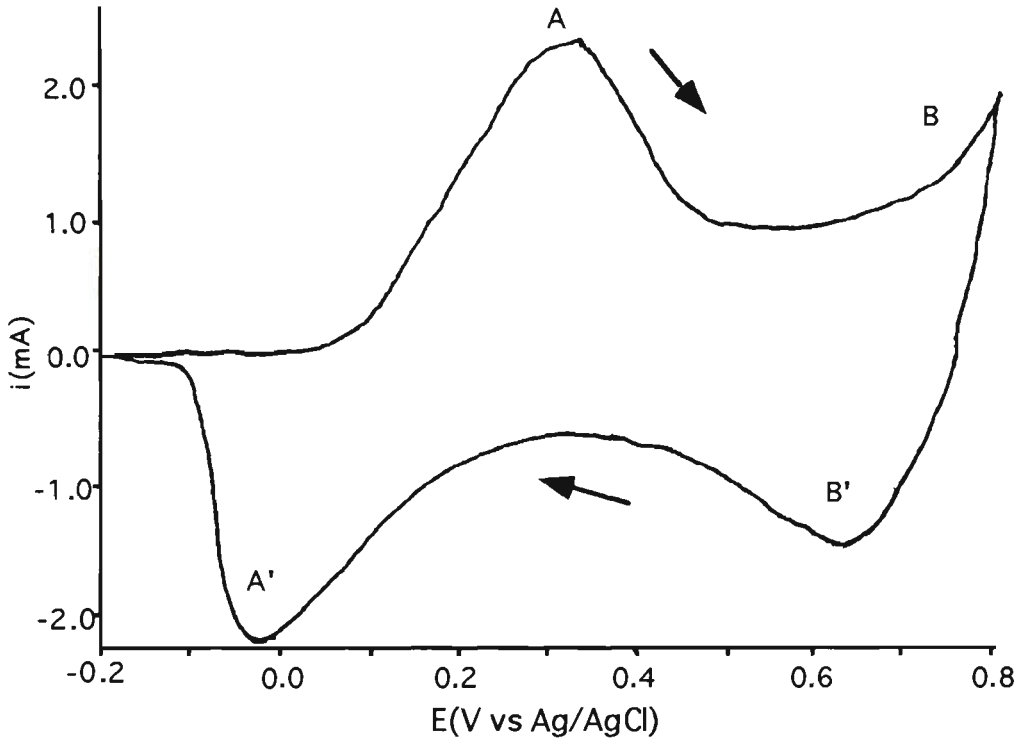

(b)= HCl

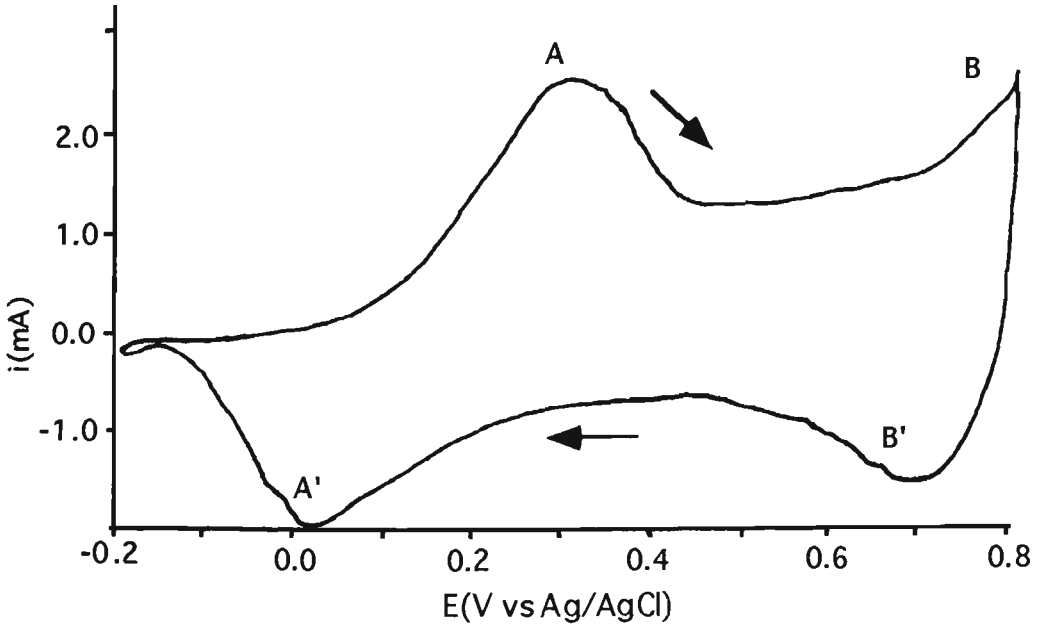

(c)= HNO_3

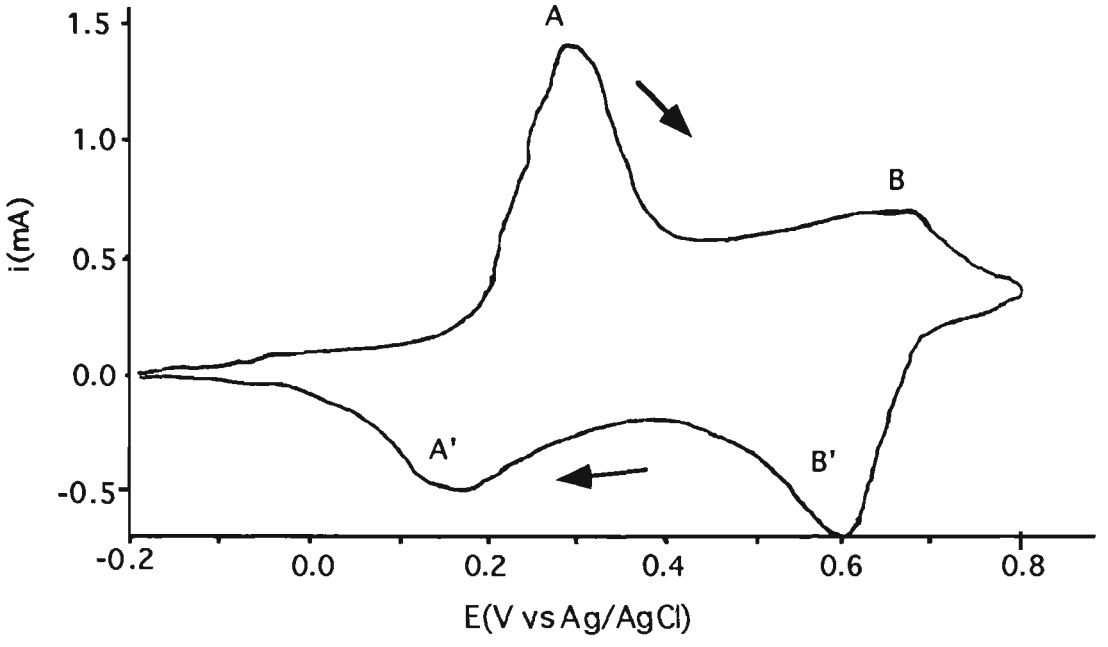

(d)=$HClO_4$

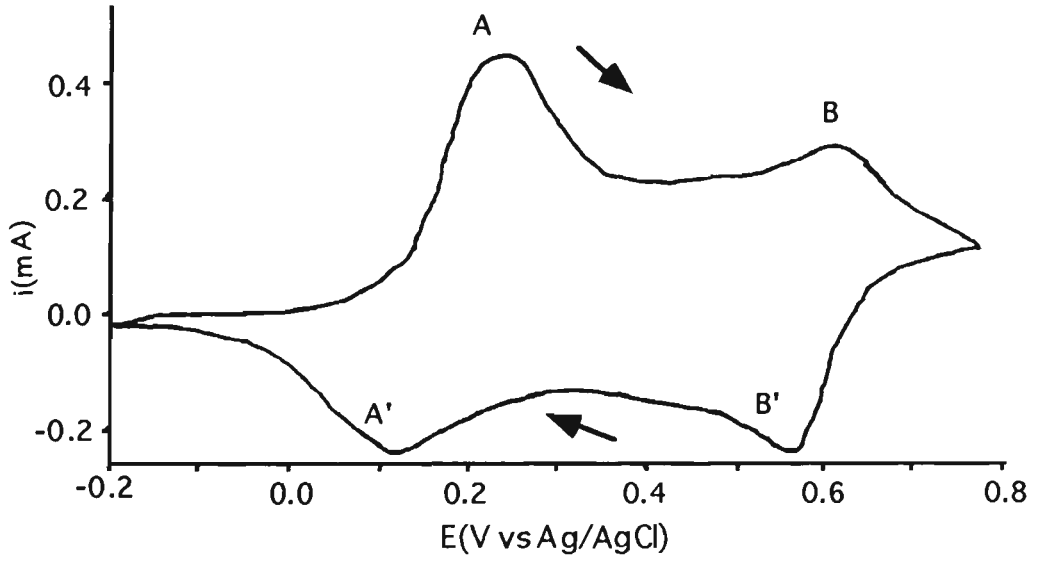

Morphology of polyaniline membranes. The morphology of polyaniline cast from NMP solution was different from polymer prepared by the electrochemical method. Both the air side (i.e. the side exposed to air during drying) and the glass side (i.e. the side in contact with glass during drying) appear dense and smooth (Figure 3.6) and there was no difference between the doped and undoped forms. However, it has been shown that polyaniline films prepared by an electrochemical method showed some differences between doped and undoped form[183]. The doped polyaniline has a continuous surface and larger grains whereas the undoped polyaniline is composed of smaller grains separated by honeycombs.

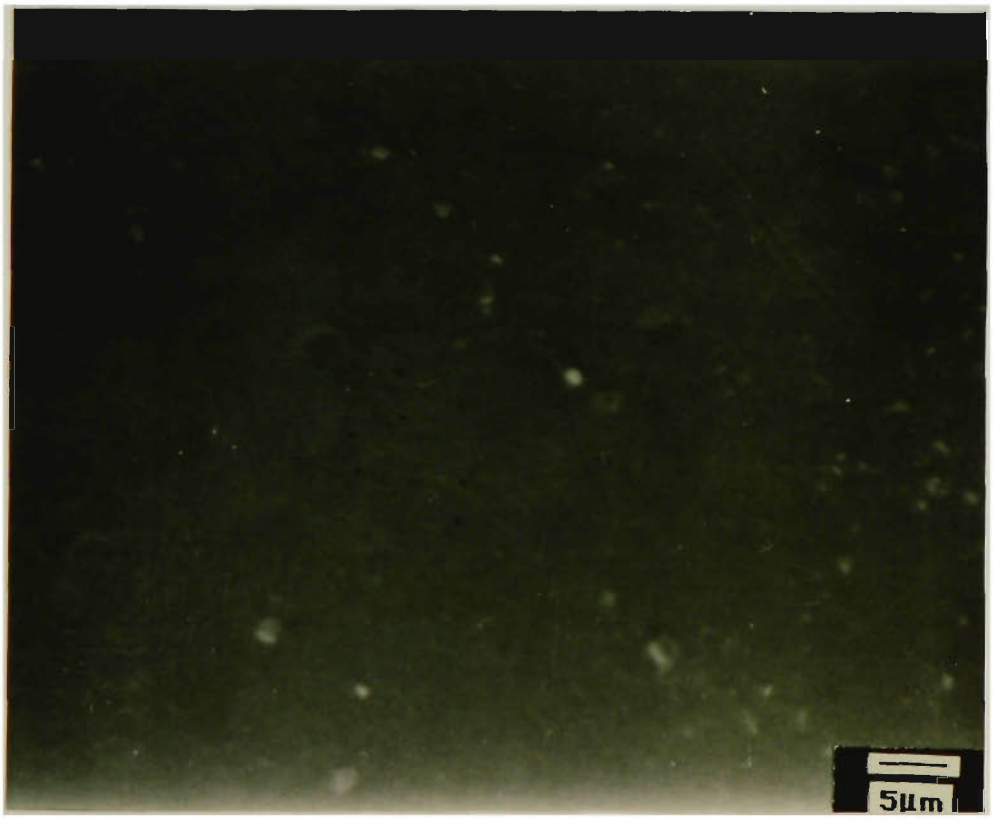

FIGURE 3.6 SEM photographs of polyaniline membranes (Polyaniline/Cl^-). Both solution and plate sides appeared to have same SEM's (see text).

The structure of the chemically cast polyaniline membranes did change when positive potential was applied (Figure 3.7). This was probably due to the oxidation of emeraldine to pernigraniline (see Equation 3.1).

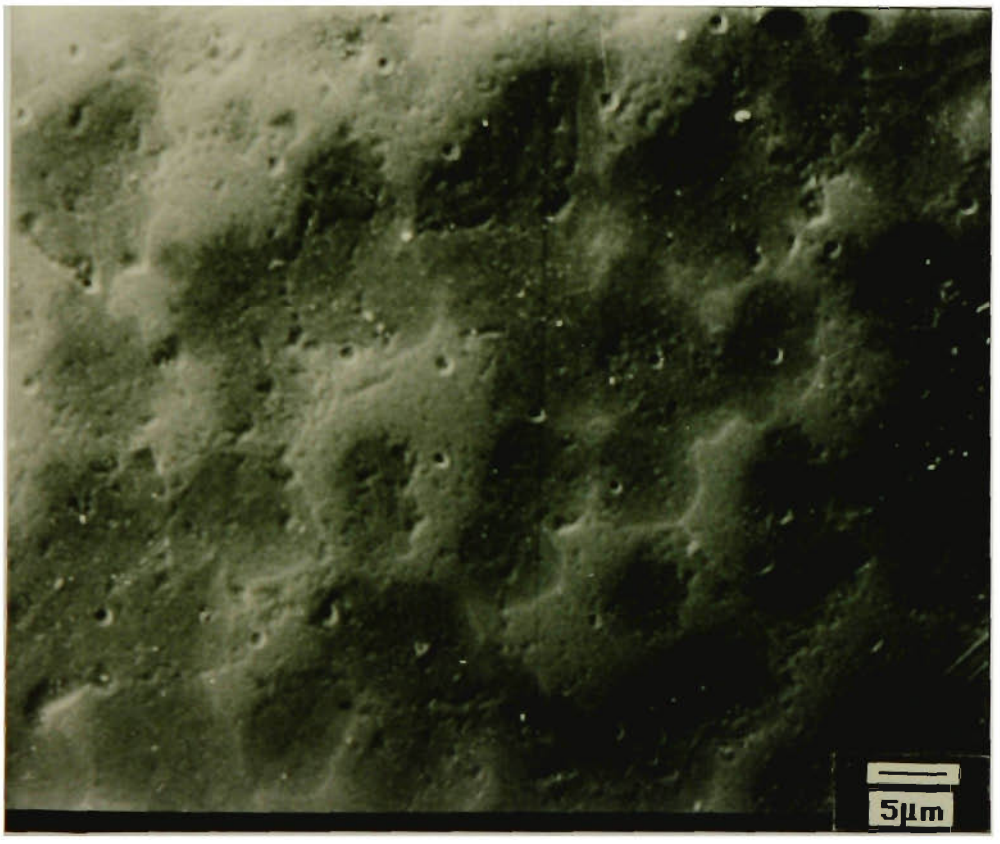

FIGURE 3.7 SEM photographs of polyaniline membranes after exposure to constant potentials during transport studies in 0.40 M HCl. A constant potential of 0.65 V was applied for 45 minutes.

Mechanical Properties. The tensile strength of polyaniline membranes was measured at room temperature using the experimental conditions described in the experimental Section. The tensile strength of polyaniline films cast from NMP was found to be 110 ±10 MPa, which was strong enough to carry out transport studies.

3.3.3 TRANSPORT ACROSS POLYANILINE MEMBRANES

The cell utilised in the transport experiments was described in Section 2.3. A potential was applied to the membrane by direct contact to the polymer. For transport of acids the polyaniline membrane was initially in the emeraldine base form (non-conductive) to ensure that no acid was released from the membrane during transport. When the cell design shown in Figure 2.6 was used there was usually a portion of the membrane not exposed to the acidic solution and this remained insulating preventing the current flowing through the cell. Therefore, in the new design the potential was applied directly to the exposed membrane using an intermediate contact material (i.e. carbon foil see Chapter 2).

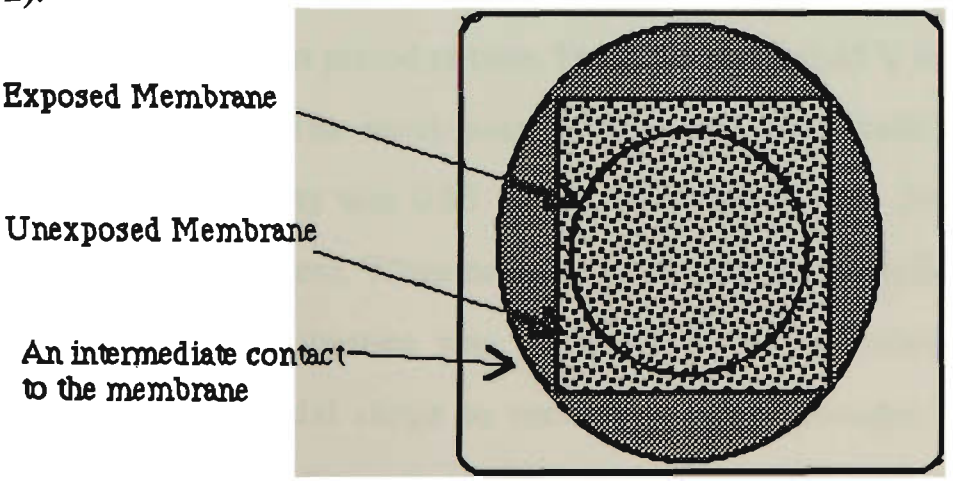

FIGURE 3.8 Electrical contact applied to polyaniline membranes using an intermediate contact (carbon foil).

3.3.3.1 TRANSPORT OF ACIDS

Since the major objective of the preparation of the membranes was to undertake transport studies with and without application of potential, it was important to find out the range of voltage that could be practically applied to the membranes during transport studies. A series of test studies was therefore carried out using the polyaniline membranes. The membrane was placed in the transport cell and 0.40 M HCl was used as the source solution with the same volume of Milli-Q water in the receiver side. Various constant potentials over the range of +0.50 to +0.85 V (vs Ag/AgCl) were applied to the membrane. It is expected that application of any potential in this range would encourage the redox reactions in polyaniline.

The concentration of H^+ in the receiver solution was monitored, in-situ by measuring pH. Any sudden decrease in pH was taken to indicate that damage to the membrane had occurred, and solution was freely flowing through any breaks in the membrane. If this occurred, the concentration of H^+ would quickly (~2 minutes) became equal in both sides of the film. It was found that application of any potential above 0.65 V damaged the structure of the membrane in a short period of time. For example, at 0.85 V the membrane lasted only 5 minutes. The most positive potential that could be applied while maintaining stability was 0.65 V, the membrane lasting for the period of this test (for 120 minutes). When negative potentials were applied no deterioration of mechanical properties was observed. It was concluded that the most appropriate potential range to encourage redox changes in the film while maintaining its stability was +0.65 to -0.20 V.

It was found that the characteristics of oxidation/reduction process (Table 3.2) varied considerably depending on the counterion of the acid employed as

electrolyte. Since these oxidation-reduction processes involve protonation and deprotonation as well as counterion incorporation and expulsion (Equation 3.1), we expected these differences in voltammetric behaviour to be reflected in the transport behaviour observed.

The structure of polyaniline suggests that the transport of H^+ through it is possible. It was found that H^+ transport occurred spontaneously and in order to keep charge neutrality the anions also have to transport as well as the protons. In order to control the transport, use of a pulse potential was considered. A pulse potential of E_1=0.65 to E_2=-0.20 V and t_1=t_2=30 s was applied to the membrane (exposed to the source solution). No significant difference in transport behaviour was observed as compared to when no pulse was applied. Therefore application of a constant potential was considered. The magnitude of the applied potential was chosen by taking into account both the mechanical stability and the potential required to oxidise/reduce the membrane as obtained by CV (Figure 3.5 (a-d)).

It was found that when a positive potential was applied the rate of transport increased. In the case of $HClO_4$, transport was negligible. For all other acids considered, the transport of H^+ ions was halted by the application of a negative potential (Figure 3.9 (1-3)), then restarted by application of the positive potential. The vertical lines in the figures represent the time when a potential was first applied to the membrane. This potential was removed after 15 minutes. The rate of transport varied depending on the acid employed. The switching behaviour was quite reversible.

FIGURE 3.9 Influence of electrical stimuli on transport of acids, (1) a constant potential of 0.65 V was applied for 15 minutes (2) a constant potential of -0.20 V was applied for 15 minutes.

(a) Transport of 0.40 M H_2SO_4.

(b) Transport of 0.40 M HCl.

(c) Transport of 0.40 M HNO_3.

Note that no transport was obtained for 0.40 M $HClO_4$.

(a) 0.40 M H_2SO_4

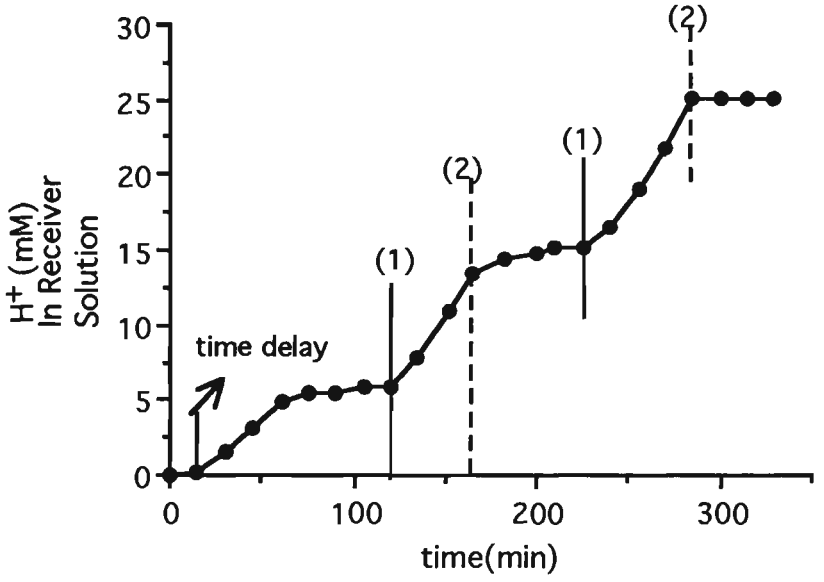

(b) 0.40 M HCl

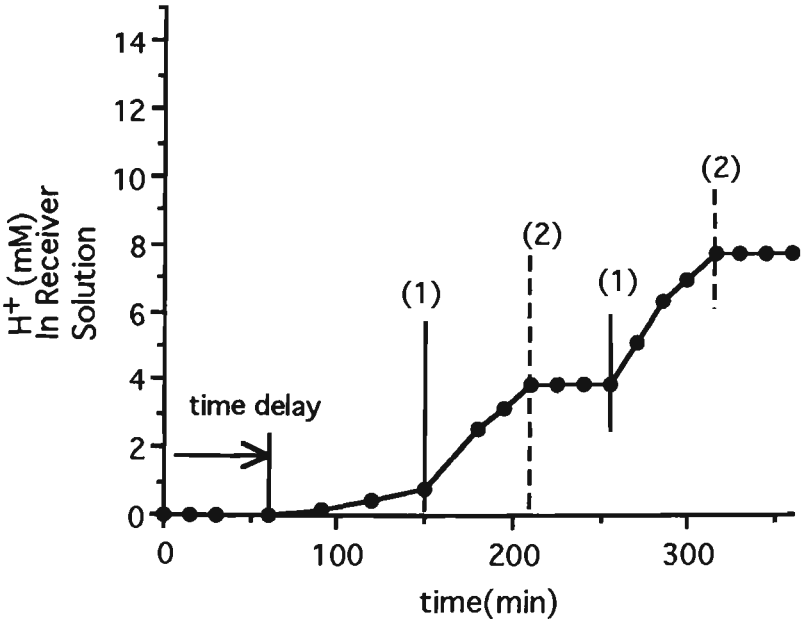

(c) 0.40 M HNO_3

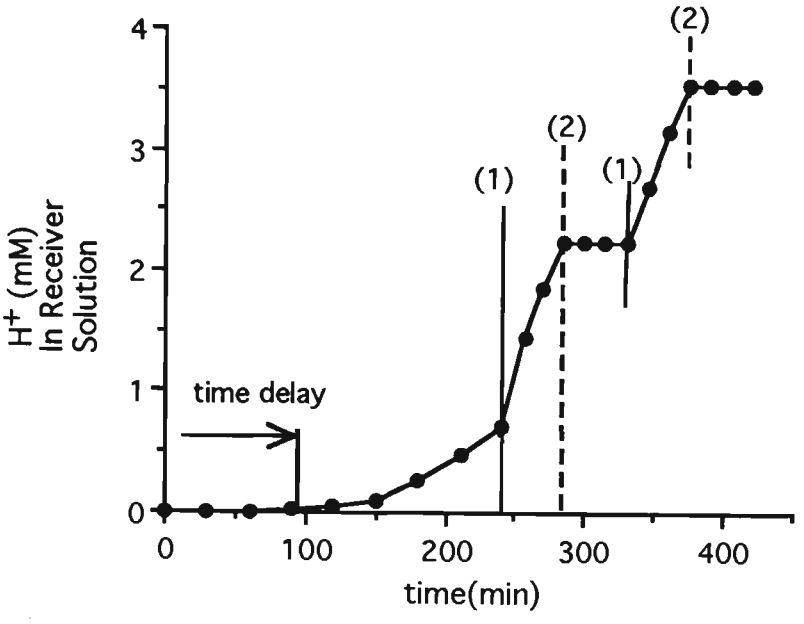

With the different potentials applied the flux was calculated using the following Equation.

$$\text{Flux} = \frac{(C_2-C_1)V}{(t_2-t_1)\,A} \qquad (3.2)$$

where C_1 and C_2 are initial and final concentrations (molar), respectively and V is the cell volume (in our case 30 mL), t_2 and t_1 are the time period over which the flux is to be measured (s) and A is the area of the membrane exposed to the solution (cm^2).

The H^+ fluxes obtained for each of the acids (Table 3.3) corresponded to the order of magnitude of the oxidation reduction currents observed during the cyclic voltammetric experiments in different acids (Table 3.2).

TABLE 3.3 Transport of acids across polyaniline membranes

Acid	Flux* (mol $cm^{-2}s^{-1}$) x 10^9		
	No E applied	+E applied (0.65 V)	-E applied (-0.20 V)
H_2SO_4	9.5	20.5	1.7
HCl	1.4	7.8	0.0
HNO_3	0.9	5.3	0.0
$HClO_4$	0.0	0.0	0.0

* The average flux obtained for three independent experiments within ± 10% error.

3.3.3.2 MECHANISM OF TRANSPORT

As shown in Figures 3.9 there was a time delay before transport started. This varied with the acid employed. The maximum delay was recorded for $HClO_4$ and the minimum for H_2SO_4. It is believed that this is the period required for the membranes to be protonated (anions also involved to maintain charge neutrality). This is quite likely since the polymer was initially in the emeraldine base form. However, to prove this further investigations were carried out.

In-situ potentiometry was carried out during the transport of 0.40 M HCl across the polyaniline membrane (Figure 3.10). It was noticed that during the delay time, the membrane's potential eventually increased (see arrow (a) in Figure 3.10). A potentiometric acid-base titration of polyaniline was then

carried out as described in the experimental Section. The potential of the polyaniline film increased from ~250 mV to ~500 mV (Figure 3.11) during protonation (non-oxidative doping). After a while no significant change was observed, suggesting that all available sites were protonated (the length of the period was dependant on the polymer mass).

Two statements may be made from the above experiments:

(1) The transformation of polyaniline from the base form to the acid form was accompanied by an increase in the rest potential (Figure 3.11)

(2) During the time delay the rest potential of the polyaniline membrane increased and no transport was observed until the polymer was fully doped (see arrow (b) in Figure 3.10).

An immediate conclusion from the above statements is that in the initial stage of transport (delay time), the polyaniline membrane was being protonated (as the rest potential increased) and after this transport started. The mechanism of transport involves protonation and deprotonation of the polymer membrane due to the concentration differences between two solutions. The maximum delay was recorded for $HClO_4$ and the minimum for H_2SO_4. The maximum flux was obtained for H_2SO_4 while the minimum was obtained for $HClO_4$. When the rate of protonation was high the rate of transport was consequently high. Apparently the high affinity between membrane and the HSO_4^- species encourages the protonation processes resulting in high H^+ flux for this acid.

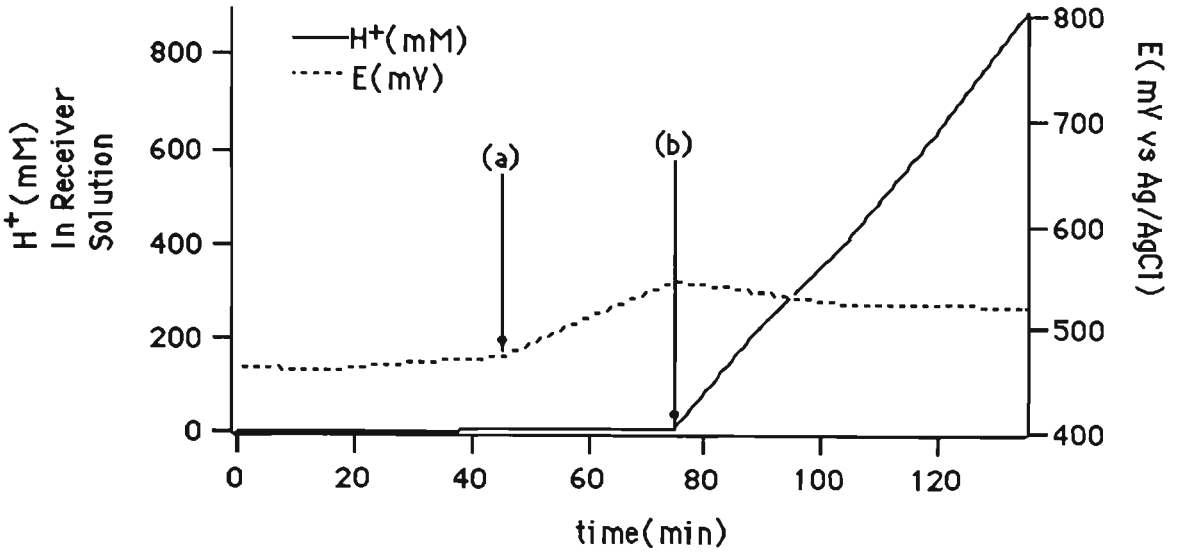

FIGURE 3.10 Potential of polyaniline membrane during transport.

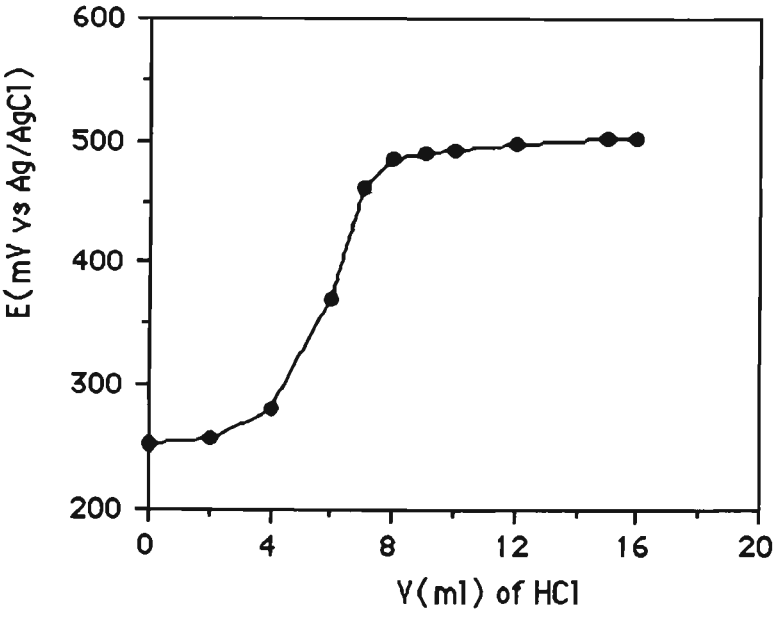

FIGURE 3.11 Potentiometric titration of polyaniline cast from a NMP solution. Titration details in experimental Section.

Application of a positive potential increased the rate of transport, while the negative potential decreased the transport. The two possible explanations for this are:

1) With application of the positive potential either the emeraldine salt form or the pernigraniline (fully oxidised form) is formed (see Equation 3.1). Formation of emeraldine salt provides more sites for proton migration. Alternatively the formation of pernigraniline cause the protons (as well as anions) to be released. With either possibility the rate of transport of H^+ is expected to increase, as observed.

2) With application of the negative potentials the fully reduced form of polyaniline is formed with neither available sites for proton migration nor release of protons, thus resulting in lack of transport.

3.3.3.3 TRANSPORT OF INORGANIC SPECIES

As Equation 3.1 suggests, in order to convert the oxidised form of polyaniline to a reduced form, or vice-versa, the media must be acidic. This is because H^+ ions must be exchanged. Therefore electrochemically controlled transport is only possible in acidic media, thus the transport of Na^+,K^+ (electroinactive species) and Cu^{2+} (electroactive) species were carried out in the presence of low concentration of nitric acid.

In the course of this work a concentration of 0.40 M inorganic salt in 0.05 M HNO_3 was employed. However there was no significant transport of Cu^{2+}, Na^+ or K^+ (<< 0.4 ppm) after 45 minutes of electrical stimulus (with both pulsed and constant potential). The cyclic voltammetry of polyaniline in the presence of Cu^{2+} and Na^+ were recorded in 0.05 M HNO_3 (Figure 3.12). It is seen that

the polyaniline was still electroactive in this media, although the nature of the response was distorted compared when pure acid was employed (Figure 3.5). Therefore the polymer membrane could be oxidised and reduced in the media containing the cations. However, there are thought to be several reasons for the lack of transport:

1) The transport of H^+ and the corresponding anions presumably occurred during doping and de-doping process. There is no evidence to show that polyaniline can be doped with other cations.

2) The redox reactions of polyaniline occur in the presence of H^+ ions. In the solution containing H^+, the cations can hardly compete with the more mobile H^+ ions.

3) The surface morphology of polyaniline membranes appeared to be dense and smooth (Figure 3.6). Such a dense structure may not allow to transport of cations.

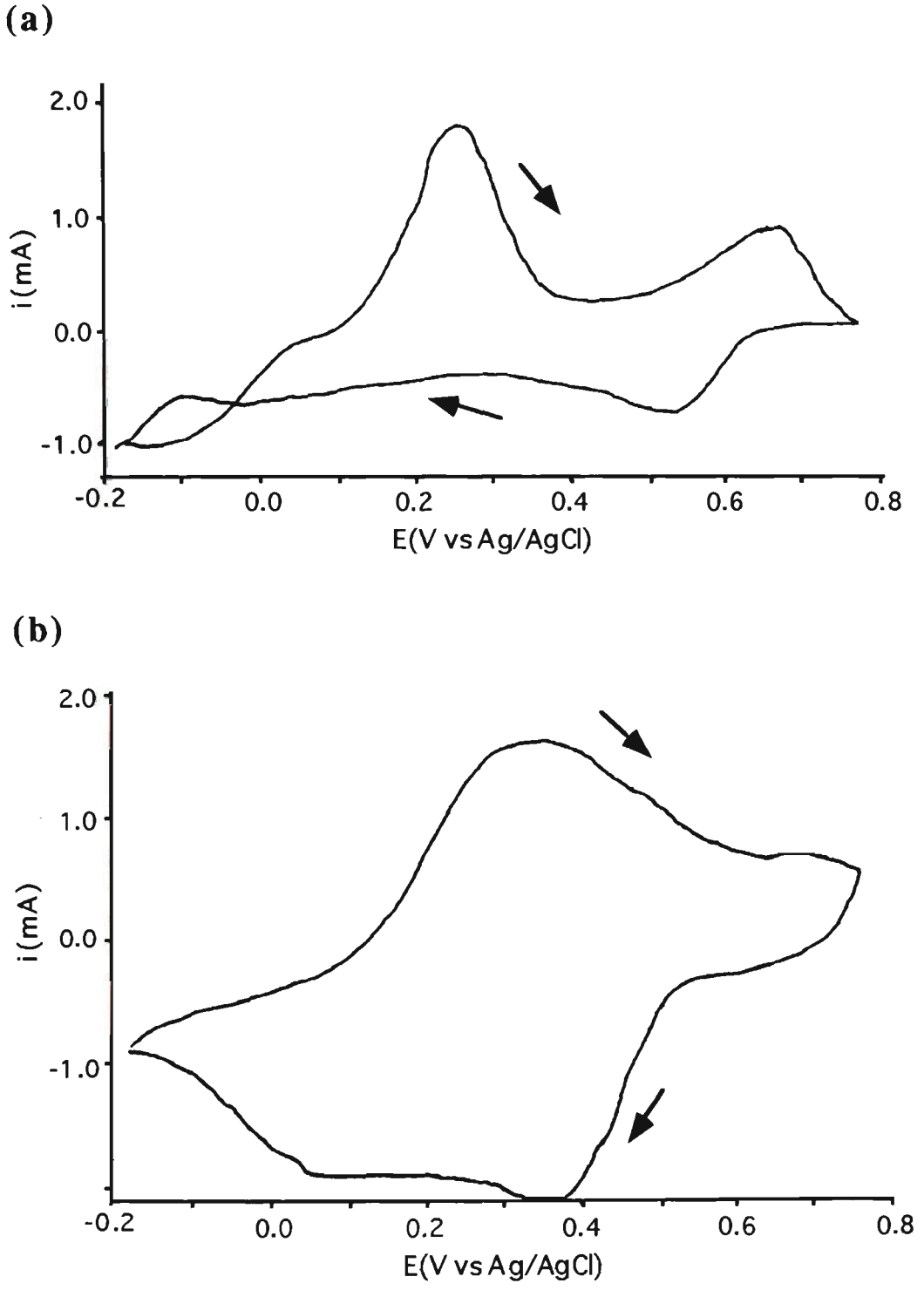

FIGURE 3.12 Cyclic voltammograms showing oxidation-reduction of polyaniline films cast from NMP solution on a gold film electrode. Scan rate=50 mV s^{-1}

(a) In 0.40 M Cu^{2+} in 0.05 M HNO_3.

(b) In 0.40 M NaCl in 0.05 M HNO_3.

3.4 CONCLUSION

The electrochemical preparation of polyaniline films was carried out in the presence of organic and inorganic counterions. In order to get films with good mechanical properties the growth conditions (synthesis mode, counterion concentration and type of counterions) were investigated. It was found that continuous films of polyaniline can be synthesised in the presence of strong inorganic acids. However, these films did not show adequate mechanical properties. Taking stock of the results obtained by us and previous workers[180] it seemed the only route open to produce free-standing polyaniline films was via casting films of chemically prepared polyaniline from an organic solvent.

In the course of this work polyaniline membranes having excellent mechanical properties (tensile strength = 110 MPa) were prepared from viscous solution of polyaniline powder in 1-methyl-2-pyrrolidinone. A film casting method was used to distribute an even layer of the film. It was found that the temperature of the polymerisation was a dominant factor with regard to the mechanical properties.

The permeability of a series of acids through the free-standing films of polyaniline was also studied. Remarkable selectivity was obtained for different acids. It was found that the rate of transport of the different acids could be controlled by application of an external potential. In the case of HCl, HNO_3 and H_2SO_4 it was found that H^+ transport occurred without application of potential. However, the rate of transport for each increased significantly when a positive potential was applied. The transport could be stopped by the application of a negative potential. This approach could be useful for either the separation or purification of acids.

CHAPTER 4

ELECTROCHEMICALLY CONTROLLED TRANSPORT ACROSS CONDUCTING POLYMER COMPOSITE MEMBRANES

4.1 INTRODUCTION

In order to extend the range of species that are able to be transported and separated by this novel electro-membrane system, preparation of other conducting membranes was investigated. To date the range of free-standing mechanically stable conducting polymer films that can be produced is small. For transport studies it is required to produce stand-alone membranes with desirable properties. Previous workers have shown that the mechanical properties of polypyrrole can be enhanced by combining the electroactive polymer with inert host polymer[91-93] or by doping with polymeric counterions[25, 97]. In this part of the work these approaches are examined with the aim of producing free-standing films with adequate membrane properties suitable for transport studies. Various factors influencing the mechanical properties of the polymer were investigated. In particular, preparation of two different membranes are reported:

Polypyrrole/Polyvinylsulfonate (PPy/PVS). The polypyrrole was doped with an immobile polyelectrolyte (PVS). When polypyrrole is reduced (Section 1.2.2) the charge neutrality of the polymer is normally conserved by outward diffusion of anions. However, when the incorporated counterion is hardly mobile the charge neutrality can be also maintained by inward movement of cations[83]. Therefore if an immobile (or less mobile) counterion is employed at the time of synthesis, the involvement of cations would be expected during redox processes. The membrane would be expected to act predominantly as a cation exchanger.

PPy/Nafion. This is a combination of an electroactive polymer (polypyrrole) with ionically conductive polymer (Nafion). Since Nafion membranes exhibit good mechanical properties, the production of stand-alone conductive membrane may be achieved.

These polymer membranes were then characterised by a variety of techniques such as Atomic Force Microscopy (AFM) and Scanning Electron Microscopy (SEM) in order to understand and optimise the physical and chemical properties for transport/separation studies.

By employing membranes with the above characteristics, an intensive investigation into the transport of ions across the composite membranes was carried out using various potential waveforms.

4.2 EXPERIMENTAL

4.2.1 REAGENTS AND MATERIALS

Reagent grade sodium chloride, potassium chloride and magnesium chloride were purchased from BDH. Nafion perfluorinated (5 % w/w) solution in a mixture of lower aliphatic alcohols and 10% water, and 1,5-Naphthalenedisulfonic acid tetrahydrate, 97% w/w (NDS) were purchased from Aldrich chemicals. Pyrrole (Py) was supplied by Sigma. P-toluene sulphonate sodium salt (PTS) was obtained from Merck. Alumina powder was purchased from the Leco Corporation (USA).

Platinum plate and platinum mesh were obtained from Engelhard (Australia), stainless steel plate and carbon foil were purchased from Goodfellow (Eng), the glassy carbon electrodes were purchased from Hart Analytical (Australia), Indium Tin Oxide (ITO) was obtained from Delta Technologies (USA), Gold coated film (intrex) was obtained from Courtaulds. The polishing pad (the finest product) was obtained from Leco corporation (USA).

A stainless steel plate (0.5 x 0.5 cm) was used throughout the cyclic voltammetric studies.

Pyrrole was distilled prior to use and all other chemicals were used as received. All solutions were prepared using Milli-Q water purification system.

4.2.2 INSTRUMENTATION

A home made pulse generator was used to apply electrical stimuli (it was designed as part of the current investigation (see R&D)). A Varian AA-20 atomic absorption spectrometer was used to determine the amount of K^+ or Na^+ transported across the membranes. Spectrophotometric analyses were carried out using a Shimadzu-250 spectrophotometer. A Ag/AgCl reference electrode was used in aqueous solution and a Ag/Ag^+ electrode was used in acetonitrile. All polymer membranes were prepared and characterised using the cell design shown in Section 2.2.

4.2.3 EXPERIMENTAL PROCEDURES

Treatment of electrodes. All electrodes were pre-treated by polishing using alumina (1.0 μm then 0.5 μm) powder on a polishing pad. The indium tin oxide electrode was used as obtained. The electrodes were rinsed with distilled water several times then they were treated in an ultrasonic bath for 30 s.

Preparation of PPy/NDS and PPy/PTS membranes. The preparation of PPy/NDS and PPy/PTS membranes were carried out in a similar manner to that described previously[87]. PPy/NDS membranes were prepared galvanostatically with a current density of 2.0 mA cm^{-2} from a solution containing 0.20 M pyrrole and 0.05 M NDS. A stainless steel plate was employed as the working electrode (Chapter 2). A charge of 1.44 C cm^{-2} was consumed during the polymerisation process. Similarly PPy/PTS membranes were prepared from a solution containing 0.20 M pyrrole and 0.05 M PTS with a charge of 1.44 C cm^{-2} consumed during polymerisation.

Characterisation of membranes and transport studies. Membranes were characterised using the techniques described in Chapter 2. The cell utilised in the transport experiments has been shown in Figure 2.4. It has two compartments with a volume of 63 mL separated by the membrane under investigation. The membrane surface area was A= 7.068 cm^2. In all transport studies a concentration of 0.01 M $MgCl_2$ was used as the background supporting electrolyte (in both receiver and source solution). The source solution also contained 0.20 M salt solution (NaCl or KCl).

Sample analysis. Analysis of Na^+ and K^+ was carried out as described in Chapter 3.

4.3 RESULTS AND DISCUSSIONS

4.3.1 SYNTHESIS OF PPy-PVS MEMBRANES

Two electrochemical modes have been employed to prepare polypyrrole films. They are galvanostatic (constant current) and potentiostatic (constant potential) polymerisation[184, 185]. However previous workers have shown that the galvanostatic method is most suited to bulk deposition of films of large surface area[35] as the films produced by this method are more uniform and reproducible[36, 184]. Since transport studies require a large surface area of uniform (in thickness) membranes produced by a reproducible method, throughout the work polymerisation at constant current was employed.

Effect of current density. As shown by the cyclic voltammograms of pyrrole in a PVS solution (Figure 4.1), a minimum potential of 0.70 V is required for the oxidation of pyrrole. Application of 2.0 mA cm^{-2} (Figure 4.2) provided the potential. With higher current densities (2.3-3.0 mA $cm^{-2)}$ no further changes were observed as verified by chronopotentiometric responses (Figure 4.2). It was found that when lower current densities (0.5-1.4 mA cm^{-2}) were employed the polymer formed adhered too strongly to the gold substrate. This made removal of the membrane from the plate difficult.

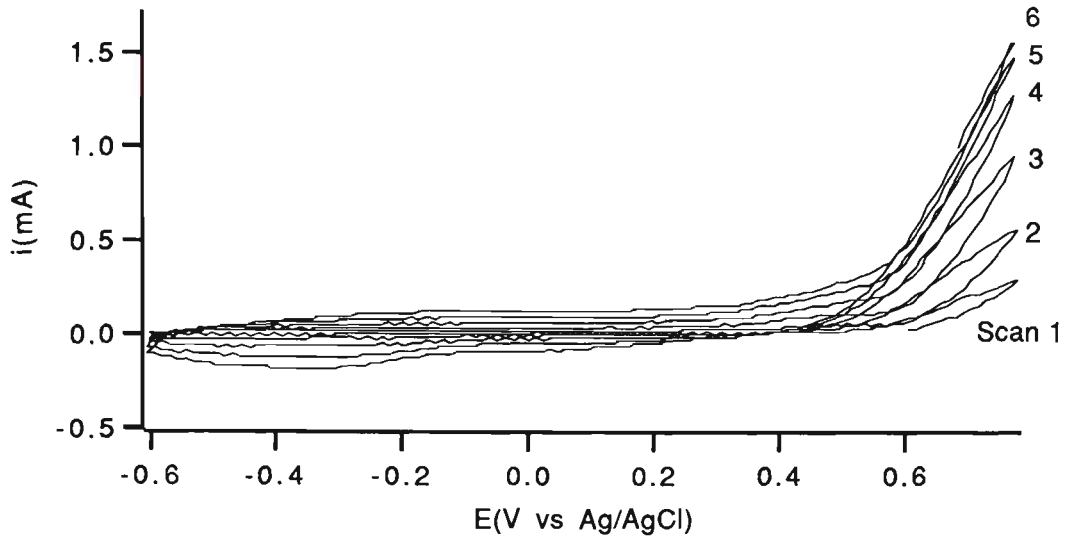

FIGURE 4.1 Cyclic voltammograms during oxidation of 0.20 M pyrrole in 10.0 g L^{-1} of PVS solution at a gold film electrode. Scan rate=50 mV s^{-1}.
The numbers on the graph (1-6) show the cycle number.

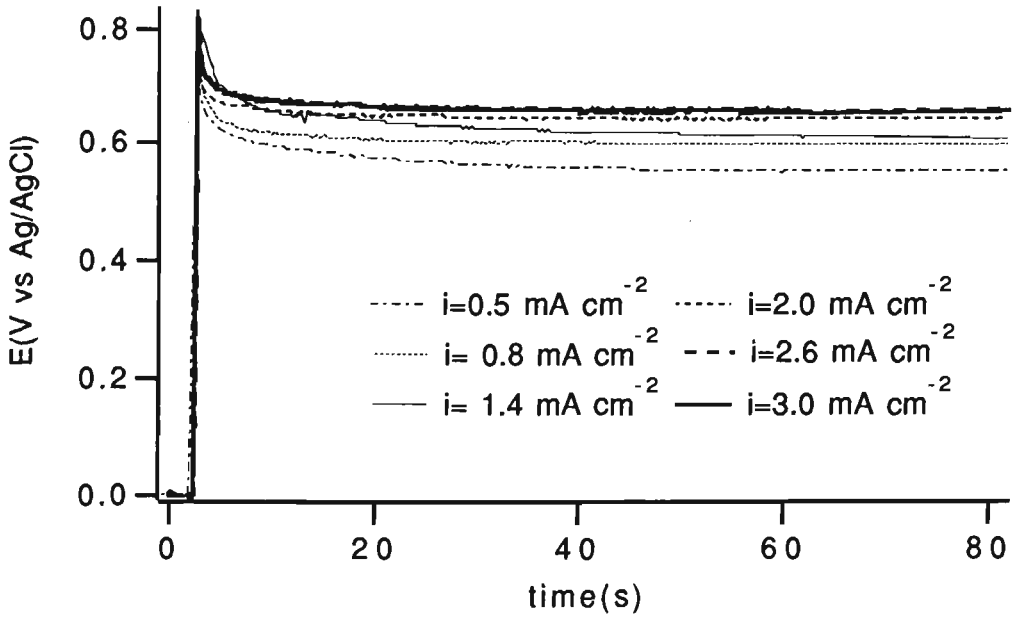

FIGURE 4.2 Chronopotentiometric responses for the galvanostatic oxidation of 0.20 M pyrrole in 10.0 g L^{-1} PVS at a gold film electrode.
Note that the responses obtained for i=2.6 and i=3.0 mA cm^{-2} overlapped each other.

The effect of electrolyte concentration. The use of various concentrations (1.0-19.0 g L^{-1}) of the electrolyte (PVS) in the polymerisation solution was investigated. It was found that the polymer grew slowly when the concentration of PVS was less than 5.0 g L^{-1}. With lower concentrations the solution was too resistive (Figure 4.3) causing an increase in the potential of growth (above 1.00 V). In addition, a long period of time (~40 minutes) was needed to prepare a film with a thickness of ~10 μm. At a much higher concentration (i.e. 19.0 g L^{-1}) no further changes of potential of growth was observed (Figure 4.3). Therefore an optimum concentration of 10.0 g L^{-1} was used.

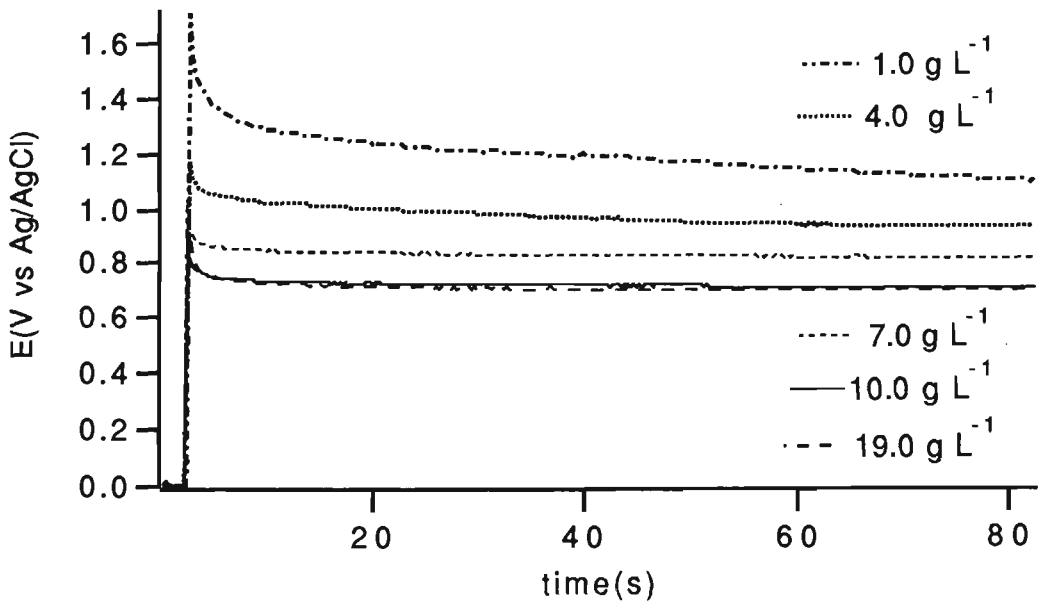

FIGURE 4.3 Effect of PVS concentration on the chronopotentiometric responses for the galvanostatic oxidation of 0.20 M pyrrole at a gold film electrode.
A current density of 2.0 mA cm^{-2} was employed.

The effect of the substrate. The potentials required to prepare the PPy/PVS polymer on various substrates are summarised in Table 4.1. Using a gold plate substrate, PPy/PVS was deposited uniformly and it was possible to peel the membrane off quite easily. However, during deposition bubbles were formed at the surface of the working electrode and this gave rise to pinholes in the membrane. It was subsequently found that the potential at the gold plate electrode, in the early stages of polymerisation, was above 0.80 V. The pH of the solution was also relatively high (pH>8.0). As pH increases the potential required to oxidise water decreases and at a pH value greater than 8 the oxidation of water occurs at potentials[186] below 0.80 V. Presumably then the oxidation of water to form O_2 was the cause of the pinholes observed when PPy/PVS was grown on a gold substrate.

Polymerisation at the ITO electrode required a potential of 1.10 V (Table 4.1) and the polymer obtained did not grow uniformly on this substrate. In addition the higher potential of growth may also result in the overoxidation of the polypyrrole formed as shown previously[56].

The carbon foil electrode material was extremely soft and porous. Consequently, although, the polymer was readily deposited it was difficult to remove the membrane from the electrode. Similarly polymer grown on a platinum electrode was uniform, but, it was very difficult to peel off the substrate.

TABLE 4.1 Polymerisation potentials obtained for growth of PPy/PVS on various substrates.

Substrate	**Carbon Foil**	**Gold Film**	**Platinum (Pt)**	**Indium Tin Oxide (ITO)**	**Stainless Steel**
Polymerisation/ deposition potential (V)	0.68	0.69	0.71	1.10	0.78

Polymerisation solution consisted of 0.20 M pyrrole and 10.0 g L^{-1} PVS. A constant current of 2.0 mA cm^{-2} was employed. Electrode surface area was 0.5 x 0.5 cm^2.

Stainless steel was found to be the best substrate because pinhole free materials could be reproducibly prepared. In addition it was easy to peel the resultant membrane from the stainless steel plate. However a problem arose because polymer adhesion at the edges of the stainless steel plate decreased as the polymerisation progressed.

In order to maintain adhesion during polymerisation, two possible solutions were investigated. The first involved the use of an additional counterion. Since sulfonated aromatic counterions had been used successfully by other workers[47] to form good films of polypyrrole, the use of NDS (shown below) was considered. NDS was chosen rather than any other sulfonated counterions such as PTS since it is assumed to be less mobile. Previous workers using larger molecules (in their case surfactants) as counterion have shown this to be the case[187].

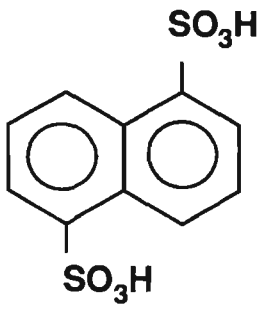

NDS= 1 ,5-Naphthalenedisulfonic acid

It was found that adhesion of the polymer film to the plate could be maintained by the addition of NDS to the polymerisation solution. Optimum results were obtained when a concentration of 7.2 g L^{-1} (0.02 M) NDS and 10.0 g L^{-1} PVS were used. The chronopotentiometric response obtained during growth (Figure 4.4) showed that the addition of NDS decreased the potential at which polymer growth occurred. This in turn may alter the surface characteristics of the stainless steel promoting adhesion.

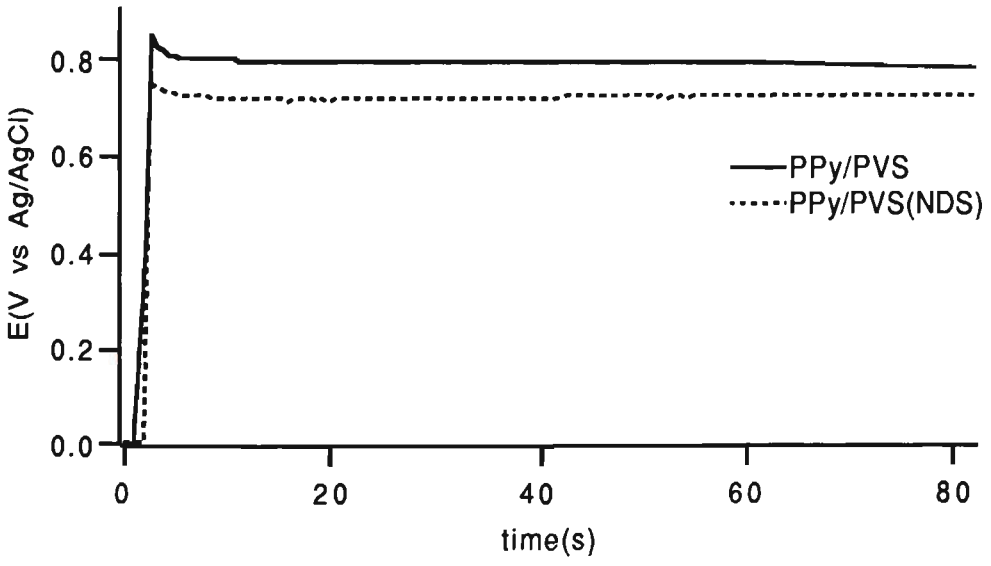

FIGURE 4.4 The effect of addition of NDS on the chronopotentiometric response for the galvanostatic oxidation of 0.20 M pyrrole in 10.0 g L^{-1} PVS at a stainless steel electrode.
A current density of 2.0 mA cm^{-2} was employed.

An alternative approach to the adhesion problem involved covering the stainless plate with a thin layer of an adhesive polymer such as PPy/NDS prior to deposition of PPy/PVS. This was achieved by deposition of polypyrrole from a solution containing 0.20 M pyrrole and 0.02 M NDS. Polymerisation was carried out galvanostatically for 75 s (i= 2.0 mA cm^{-2}). The pre-coated electrode was then used to deposit PPy/PVS. Employing this method resulted in the preparation of pinhole-free membranes with adequate adhesion during polymerisation.

Although the polymer adhesion during polymerisation could be maintained using both methods the former was used in the remainder of this work as it was practically, easier to implement. Also the films produced were more reproducible (with respect to polymer thickness= 9 ± 1 μm) and less chemicals were consumed during preparation of the membrane using this method (only one stage involved).

From the above results an optimised procedure for the preparation of PPy/PVS composite membrane was derived. A solution containing 0.20 M pyrrole, 10 g L^{-1} PVS and 7.2 g L^{-1} NDS was used. Electrodeposition of polypyrrole on to a steel plate was achieved using a constant current of 2.0 mA cm^{-2}. The polymerisation time was 18 minutes which gave a membrane with a thickness of ~9 μm. The membranes obtained were uniform and pinhole free.

4.3.2 CHARACTERISATION OF PPy/PVS MEMBRANES

The tensile strength, Young's modulus and conductivity of the composite PPy/PVS membranes are summarised in Table 4.2. The membranes exhibited good mechanical properties with adequate tensile strength. The values

obtained for the Young's modulus suggest, that the polymer was less rigid than PPy/PTS and more rigid than PPy/BF_4[188]. The conductivity and mechanical properties of the membrane were adequate for transport studies.

TABLE 4.2 Mechanical and electrical properties of composite membranes developed as described in the text [(1)].

Polymer Membrane	**Thickness (μm)**	**Conductivity (S cm^{-1})**	**Tensile Strength (MPa)**	**Young's Modulus (MPa)**
PPy/PVS	9 ± 1	14-15	70-90	630-670
PPy/Nafion	12 ± 1	10-14	40-55	300-370

(1) Membranes prepared using optimal conditions.
In all cases the range of results were obtained by using six individually prepared membrane samples.

Previous workers have reported the preparation of the PPy/PVS composite on the surface of an ITO electrode[25, 83, 97, 189]. They have reported conductivities in the range 10-21 S cm^{-1} and a maximum value of 21 MPa for the tensile strength.

As shown in Table 4.2 the films prepared in this work have a higher tensile strength than those reported previously although the average conductivity was similar.

In the course of our work a sulfonate group was present in the structure of the polyelectrolyte dopant while in all other work a sulphate group was employed.

It has been demonstrated that the sulfonate group (e.g. in p-toluene sulfonic acid) results in significantly improved mechanical properties of polypyrrole films[87, 57].

The improvement in the mechanical properties may also be due to the fact that employing a low percentage of a co-counterion such as NDS allowed the formation of the membrane at a lower potential of growth (Figure 4.4) than those obtained using the ITO electrode (Table 4.1). Exposure to these higher potentials during growth may deteriorate mechanical properties of the polymer[55] due to over oxidation.

A further feature of the method we employed was the ability to prepare thin (~9 μm) pinhole free membranes while in previous work only the preparation of very thick films (~100 μm) has been considered. Thick membranes may not have pinholes however, as the film thickness decreases the chance of formation of pinholes increases. Consequently the preparation of pinhole free membranes becomes more complicated.

Morphology of the PPy/PVS membranes. SEM micrographs of PPy/PVS membranes are shown in Figure 4.5. The morphology of the composite films was different from polypyrrole grown from solutions containing conventional dopants such as PTS and NDS. The solution side of the PVS containing membrane (i.e. side exposed to solution during growth) appears to reveal a closer packed (dense) structure composed of nodules smaller than those usually observed with other sulfonated aromatics which show a greater surface roughness (Figure 4.6). With the composite the plate side (i.e. side in contact with electrode plate during growth) appears dense and smooth as observed for other PPy's deposited from solutions containing small sulfonated counterions (Figure 4.5 (b)).

(a)

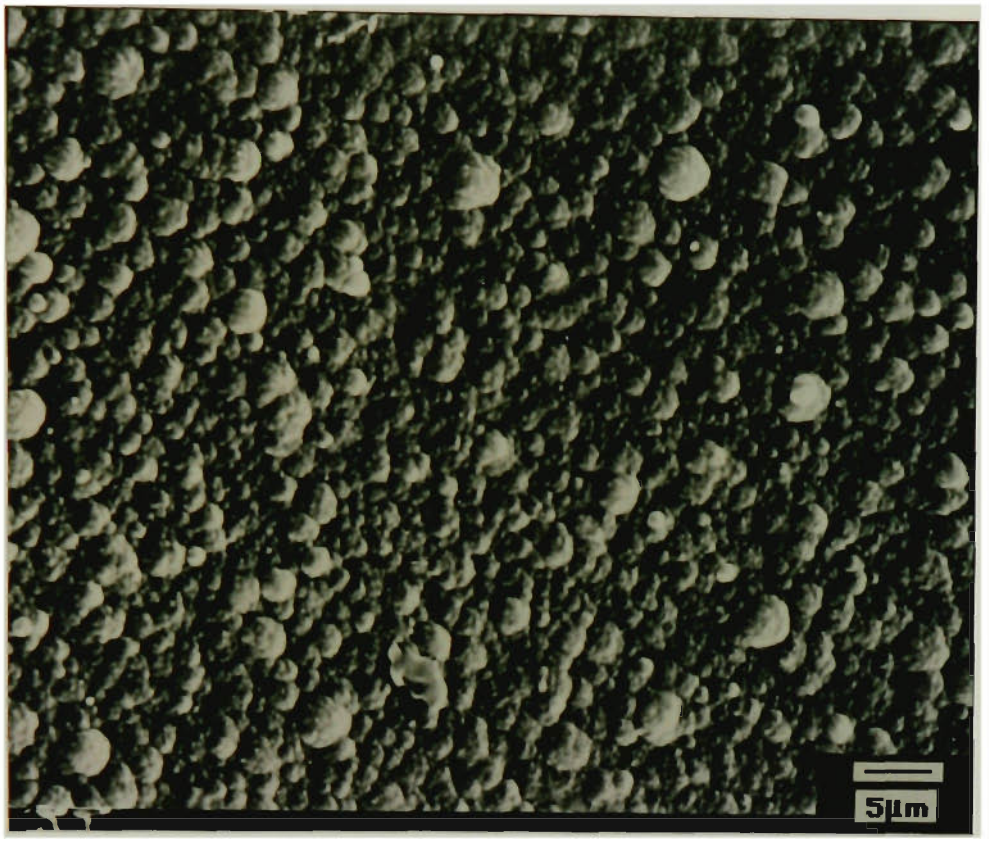

(b)

FIGURE 4.5 SEM photographs of PPy/PVS composite membrane.
(a) solution side.
(b) plate side.

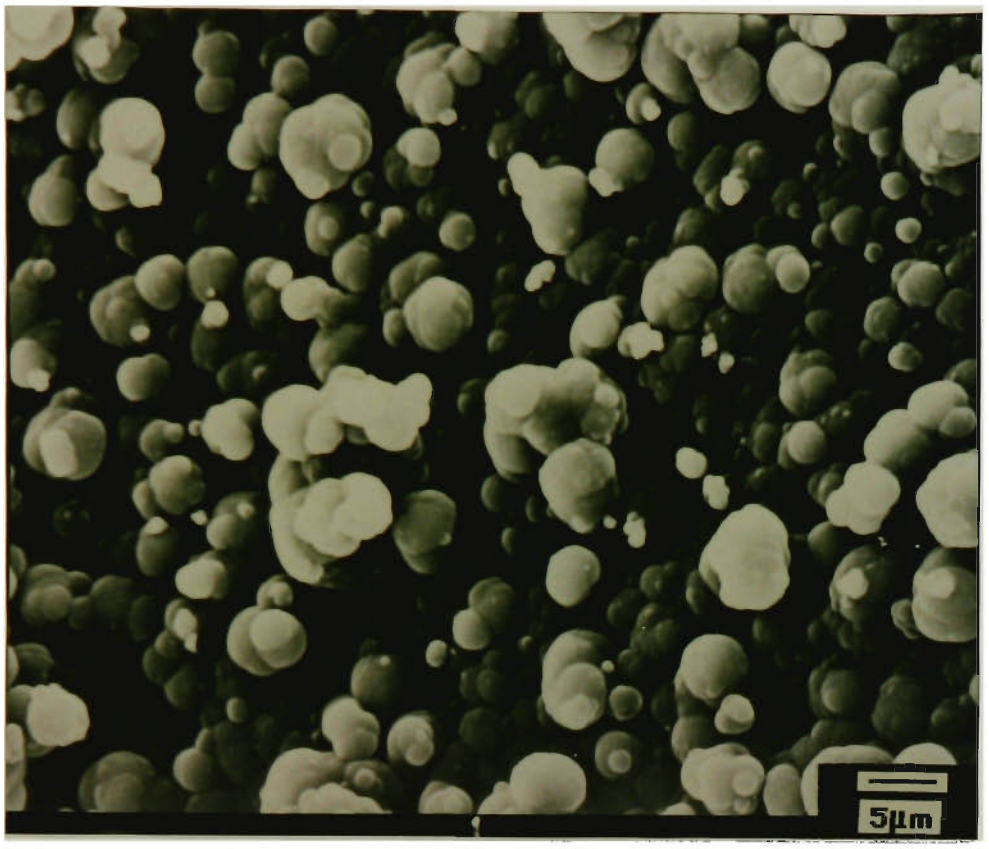

FIGURE 4.6 SEM photographs of PPy/NDS- solution side. Membrane prepared as in Section 4.2.3.

The surface morphology of the membranes was investigated further using Atomic Force Microscopy (AFM). Figure 4.7 (a) shows the top view of the solution side of the PPy/PVS membrane in 0.01 M NaCl. As with SEM the polymer exhibits a dense structure. Figure 4.7 (b) shows the surface topography of the polymer in the same solution (0.01 M NaCl). A dense and uniform structure with smaller nodules compared to conventional counterions (e.g. PTS see Figure 4.9) were the important features of the composite membrane. Similar images of closed packed surfaces were obtained when the membrane surface was imaged in air (Figure 4.8).

AFM photos of the membrane prepared with conventional and smaller sulfonated aromatics (PTS) were also imaged (Figure 4.9). The surface topography of the PPy/PTS imaged in 0.01 M NaCl shows a nodular structure in contrast to the observation made for PPy/PVS membranes.

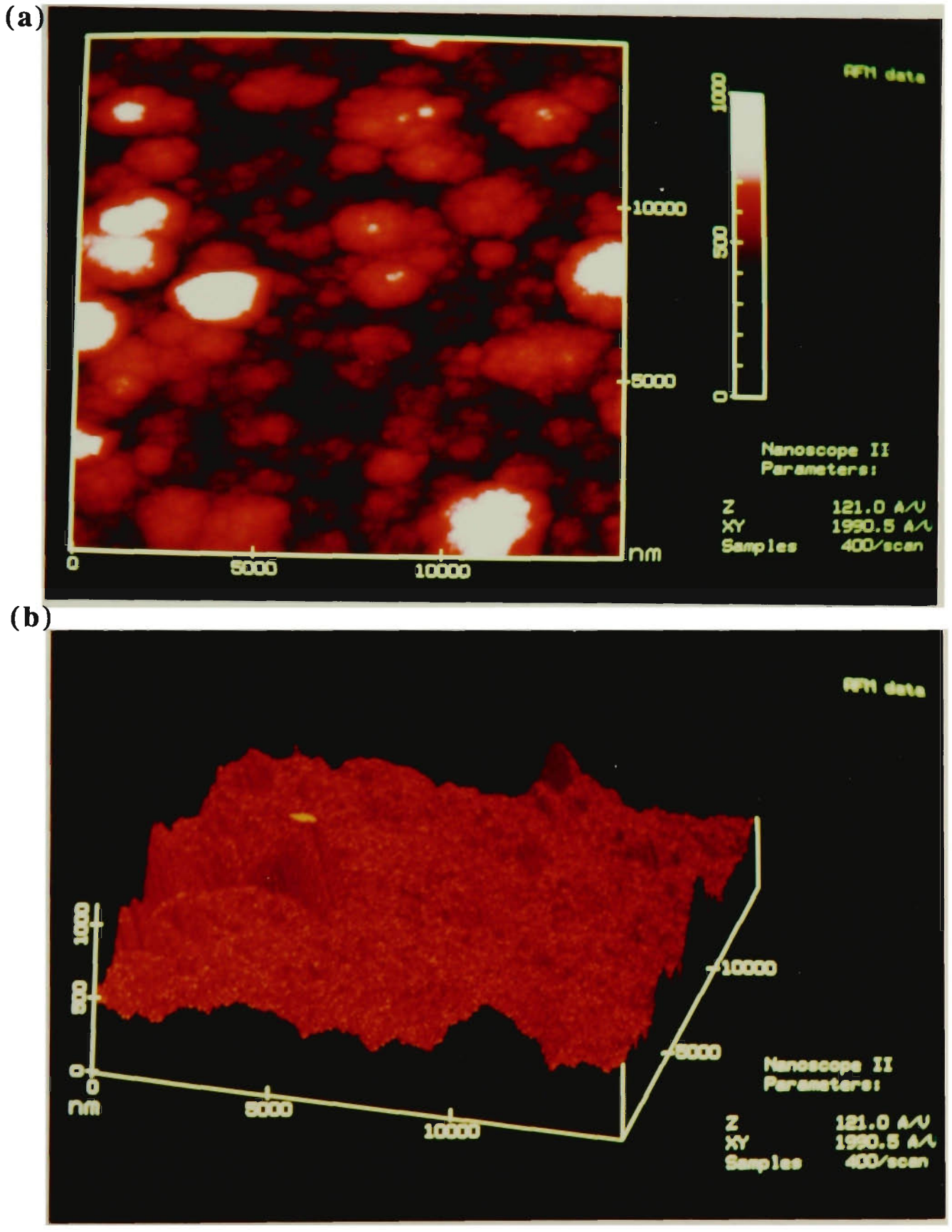

FIGURE 4.7 AFM images of the PPy/PVS membrane in 0.01 M NaCl:

(a) Top view of the solution side of PPy/PVS membrane

(b) Three-dimensional perspective view (surface topography) of PPy/PVS membrane

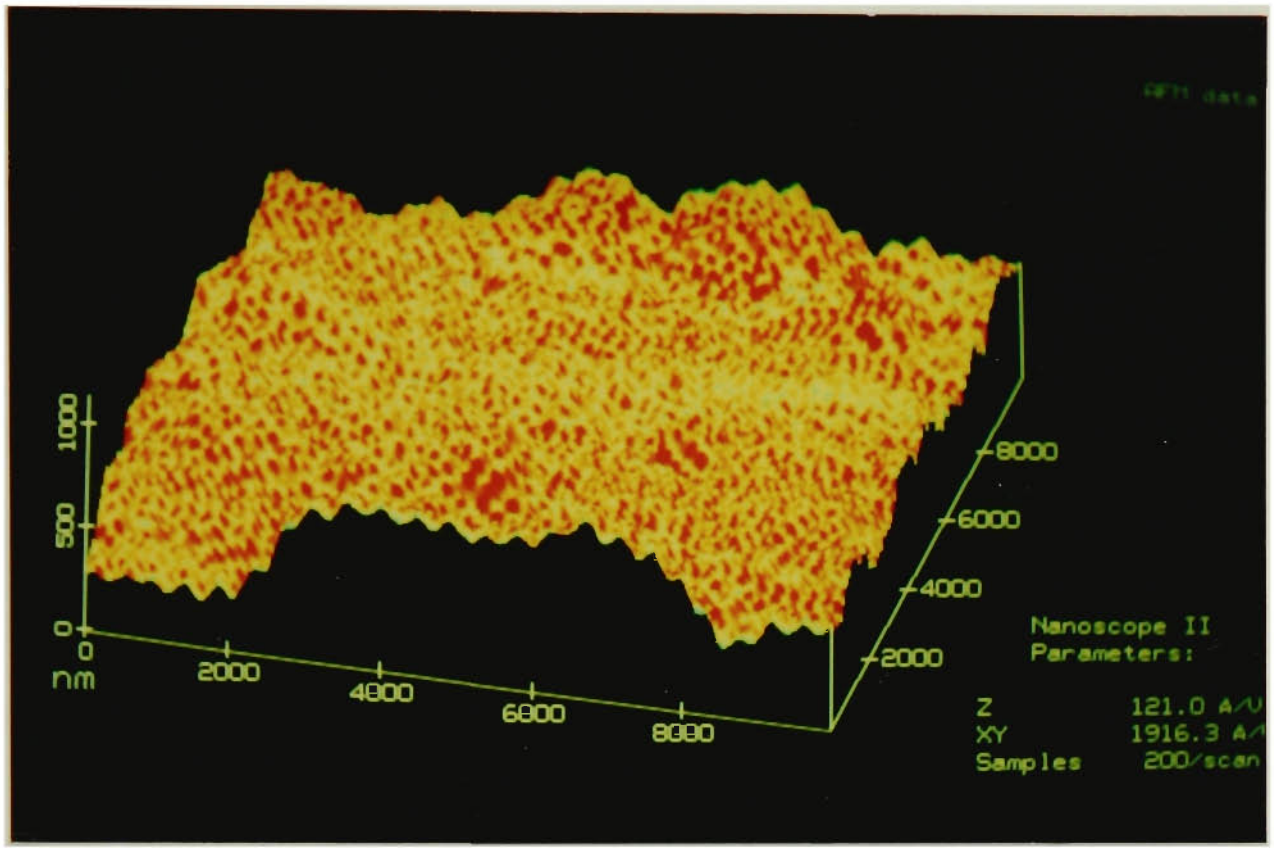

FIGURE 4.8 Three-dimensional perspective view (surface topography) of PPy/PVS membrane (solution side) in air was imaged by AFM.

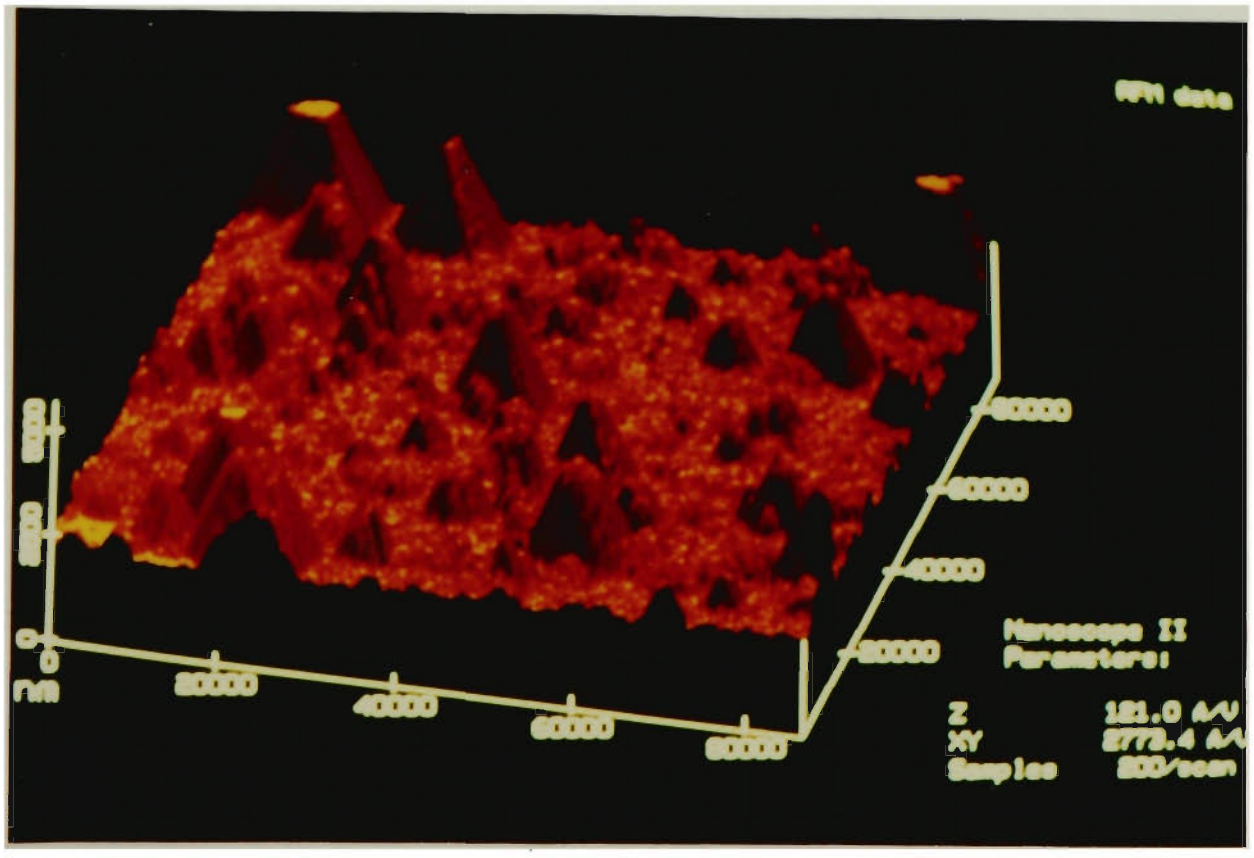

FIGURE 4.9 Three-dimensional perspective view (surface topography) of PPy/PTS membrane (solution side) in 0.01 M NaCl was imaged by AFM (membrane was prepared as in Section 4.2.3).

Chemical composition of composite polymer. The chemical composition of the free-standing film of the composite polymer is shown in Table 4.3. From the elemental analysis of the polymer the molar ratio of incorporated anion (calculated using sulfur content) to the polypyrrole unit (from nitrogen content) was estimated. The average molar ratio (for four samples) is 0.29 ± 0.02 depending on the nature of the counterion. Since not a large variation of molar ratio was observed between polyelectrolyte and conventional counterions, it may be suggested that the level of oxidation of the polymer is mainly determined by the chemical nature of the polymer and less affected by the nature of the counterion. This also suggests that SO_3^- groups on PVS are used in charge compensation. Similar results have been previously observed using small molecules as counterions[24, 42]. The elemental analysis of the polymers does not show good material balance. The weight loss may be due to the presence of oxygen, moisture and other undetermined elements such as fluorine (see structure of Nafion).

TABLE 4.3 Elemental analysis of polypyrrole films prepared using the conditions described in the text.

Membrane	C %	H %	N %	S %	Molar ratio n= S / N
PPy/PVS	47.45	3.93	11.97	7.69	0.28
PPy/NDS	52.89	3.51	11.00	7.80	0.31
PPy/Nafion	38.94	1.72	6.50	4.10	0.28

Oxygen and some other elements (such as fluorine due to Nafion itself) were not determined. All polymers were prepared by the optimised procedure described in the text.

4.3.3 THE EFFECT OF NDS EMPLOYED DURING SYNTHESIS OF THE PPy/PVS COMPOSITE

It was the primary objective of this work to produce polypyrrole membranes with an immobile counterion. The polymeric counterion (PVS) was therefore employed. However during synthesis the use of relatively mobile anions (NDS) was necessary to overcome the adhesion problem as described above. In order to estimate the effect of additional NDS on the structure and ion exchange properties of PPy/PVS further investigations were carried out. The properties of the PPy/PVS films prepared with NDS (the optimised procedure) were compared with pure PPy/PVS and pure PPy/NDS.

Surface morphology. As discussed in Section 4.3.2 the surface morphology of PPy/PVS (prepared using NDS) membranes seemed to have less surface roughness as opposed to the greater surface roughness of PPy/NDS (Figure 4.6). The surface morphology of pure PPy/PVS was similar to that prepared in the presence of NDS (Figure (4.10 a,b)). These results indicate that although some NDS was used during the synthesis of PPy/PVS, the surface morphology of the resultant film was different from PPy/NDS and similar to that obtained using pure PPy/PVS (Figure 4.10).

Note that using the gold electrode enabled the preparation of PPy/PVS membranes without using NDS. However, these membranes could not be used for transport studies due to the pinholes present (see Section 4.3.1).

(a)

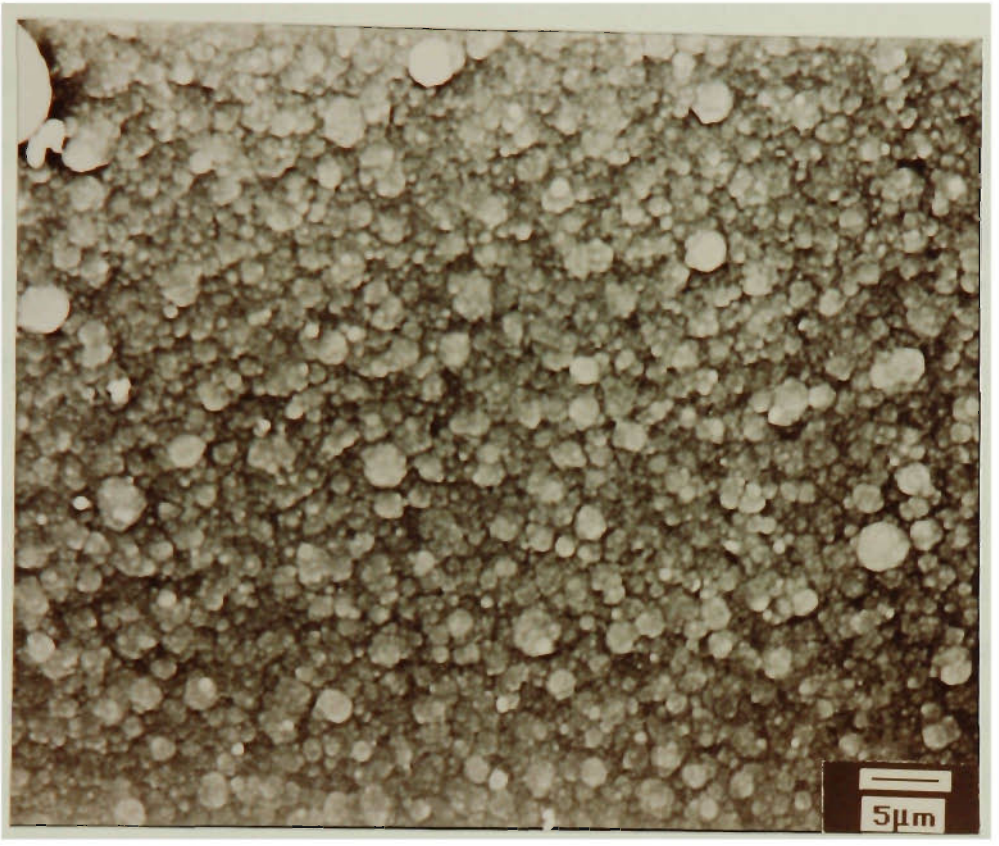

(b)

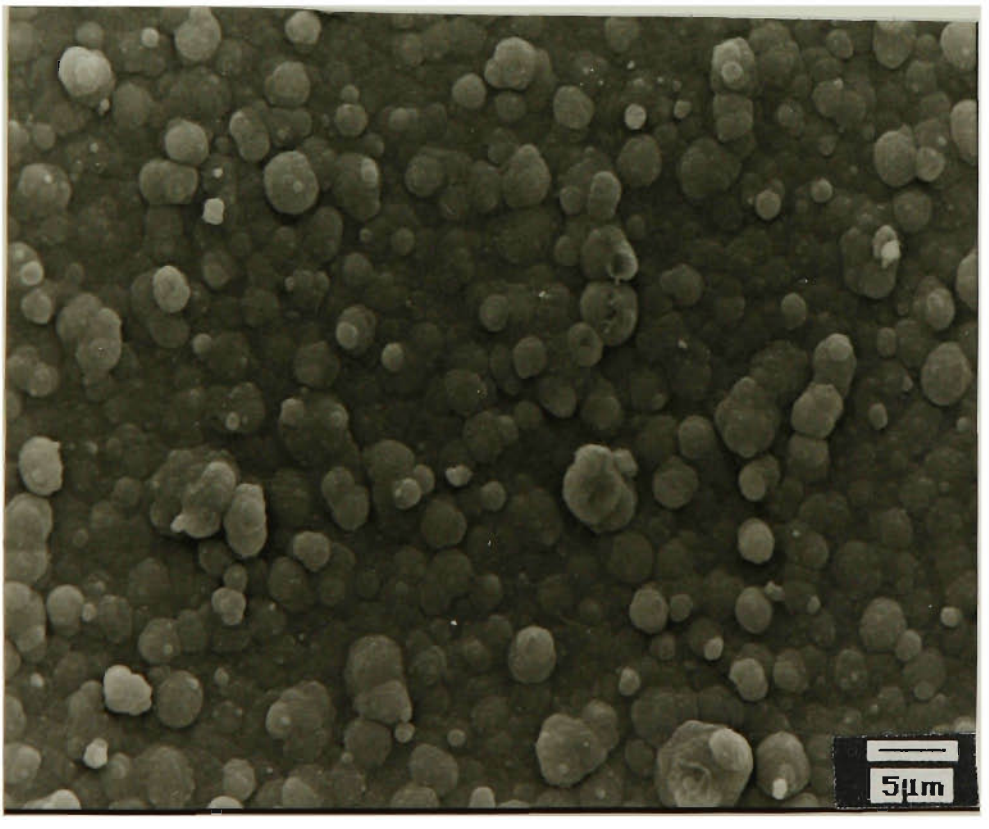

FIGURE 4.10 SEM photographs of PPy/PVS composite membrane (solution side) grown at the surface of a gold electrode:

(a) No NDS was used during synthesis.

(b) NDS was used as discussed in the optimised procedure (Section 4.3.1).

Ion exchange properties. The PPy/NDS membrane (4 x 6 cm) was placed into 50 mL of 0.20 M KCl. It was then stirred for 7 hours withdrawing samples every one hour (every 15 minutes in first hour). Each sample of solution was analysed for NDS using a U.V spectrophotometer (λ_{max}= 225.7 nm). The calibration curve obtained was linear over the range investigated (0.09-9.00 ppm) with a correlation coefficient of R^2=0.999. Therefore the minimum concentration of 0.09 ppm NDS (~0.25 μM) could be detected. It was found that the concentration of NDS, released from PPy/NDS membrane, increased (Figure 4.11) as a function of time indicating diffusion of Cl^- anions into the film with subsequent release of NDS. Based on the elemental analysis only ~ 3% of NDS was found to be replaced by anions (Cl^-) after 420 minutes. Therefore the counterion employed to synthesise a membrane such as PPy/NDS was mobile enough to be replaced by a solution anion.

The same experiment was repeated using the PPy/PVS composite membrane prepared with and without NDS (Figure 4.11). No release of NDS was observed for both membranes.

The application of a pulse potential was then considered. A pulse potential with E_1=-0.60 to E_2=0.70 V and t_1=t_2=30 s (for 45 minutes) was applied to the membrane in order to oxidise and reduce the polymer. However, no release of NDS was detected (detection limit = 0.09 ppm).

These results indicate that the NDS employed during the synthesis of PPy/PVS membranes either was not incorporated into the polymer matrix or was tightly trapped so that it could not be released by ion exchange or by reduction of polypyrrole. Therefore it would be expected that the charge neutrality would be conserved by cation movements and that the membrane would have greater

capacity of cation exchange properties compared with conventional polymers such as PPy/PTS or PPy/NDS.

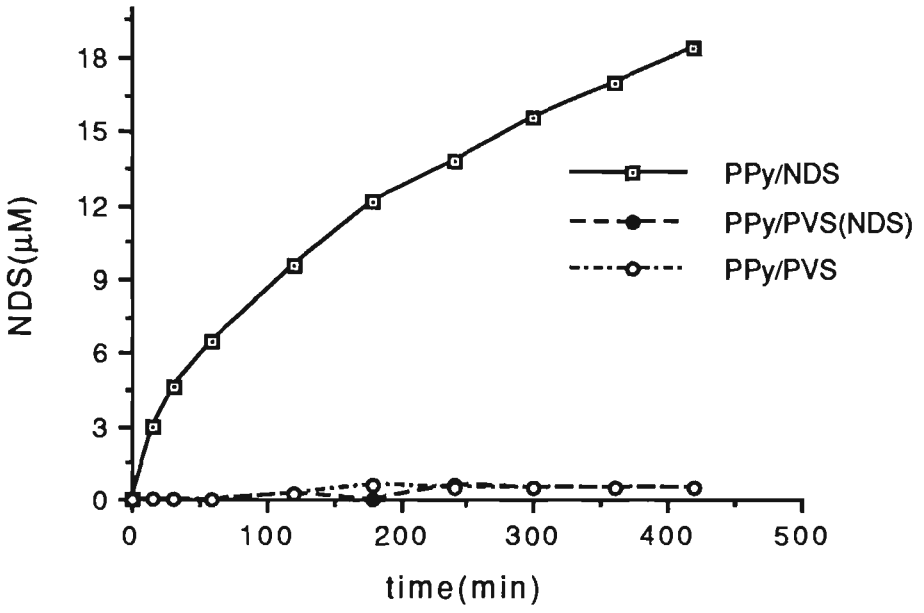

FIGURE 4.11 The release of NDS as a function of time from polypyrrole membranes in 0.20 M KCl.

4.3.4 PREPARATION OF POLYPYRROLE/NAFION MEMBRANES

Most previous syntheses of PPy-Nafion composites[94, 95, 190] (as deposited films) have been carried out from organic media and none have considered preparation of the composite as a large free-standing membrane.

In this work we considered the preparation of the composite as a free-standing membrane (7 x 5 cm) from both aqueous and non aqueous solutions.

Preparation of PPy/Nafion in non aqueous solutions. The electrode substrate (Pt, Au or Stainless Steel) was initially coated with 17.5 mg cm^{-2} of Nafion solution (diluted 2:1 with ethanol) and was left to dry for 30 minutes. Nafion is soluble in ethanol and the films cast from diluted Nafion appeared to be more uniform in thickness than those cast from concentrated Nafion. The amount of 30 μL diluted Nafion (17.5 mg) per cm^2 was found to give films with thickness of 12 ± 1 μm. The polypyrrole was deposited on the surface of the pre-coated electrode from a solution containing 0.35 M pyrrole and 0.05 M TEATFB (tetraethylammonium tetrafluroborate).

The suitability of the gold coated film, platinum and stainless steel substrates was considered. No differences in the chronopotentiometric responses of the electrodes were observed (Figure 4.12). However it was found that in acetonitrile media the gold coated film was not stable and the polymer grown on stainless steel was neither uniform in thickness (as some part of the electrode was very thick, and some thin) nor mechanically strong. With the platinum electrode the polymer was uniform however it was hard to peel off the electrode. Due to the low conductivity of the organic solvent the whole surface of the large electrode was not uniformly covered and this gave rise to pinholes. Due to the above difficulties, in particular the existence of pinholes in the membrane, further characterisation was not carried out for the films grown in non aqueous solution. Preparation of the PPy-Nafion composite from aqueous media was consequently attempted.

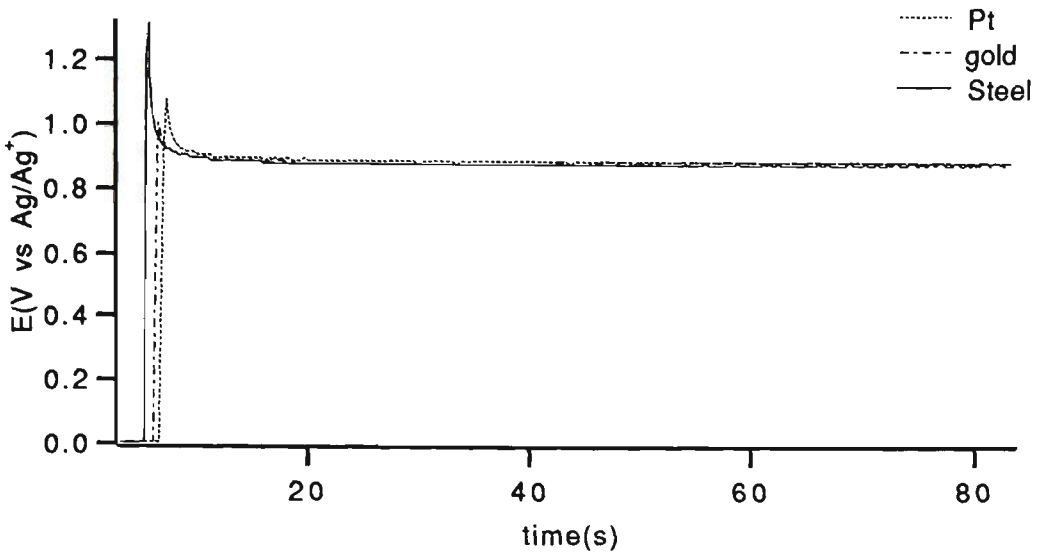

FIGURE 4.12 The effect of substrate on the chronopotentiometric response for the galvanostatic oxidation of 0.35 M pyrrole in 0.05 M TEATFB.
A current density of 2.0 mA cm^{-2} and acetonitrile as solvent were employed. The electrode was coated by Nafion (see text).

Preparation of PPy/Nafion in aqueous solutions. A known amount (17.5 mg cm^{-2}) of Nafion solution was cast onto a piece of mirror polished stainless steel plate and was allowed to dry under vacuum. The coated stainless was then used as the working electrode in the polymerisation cell containing pyrrole and the counterion. Stainless steel plate was employed since it was readily available and the membrane was easily removed after deposition.

It was found that the supporting electrolyte was an important factor in determining the properties of the PPy/Nafion composite. For example, when $LiClO_4$ or $NaNO_3$ was used as the supporting electrolyte anion the deposited polymer was found to become less adhesive at the edges of the plate as polymerisation progressed. The chronopotentiometric response in the presence of $LiClO_4$ and $NaNO_3$ show an increase in the growth potential, compared with other electrolyte used (Figure 4.13), as the polymer became less adhesive.

Further investigation revealed that using counterions with either sulphate or sulphonate functional group such as NDS or Na_2SO_4 overcame this problem.

The optimum procedure as developed was, therefore, as follows. A stainless steel plate was coated with 17.5 mg cm^{-2} of Nafion solution. Then the polypyrrole was deposited at the surface of the electrode from an aqueous solution containing 0.20 M pyrrole and 0.05 M NDS (Figure 4.13). A constant current of 2.0 mA cm^{-2} for 12 minutes was applied. Using this procedure large (5 x 7 cm) pinhole free membranes were obtained.

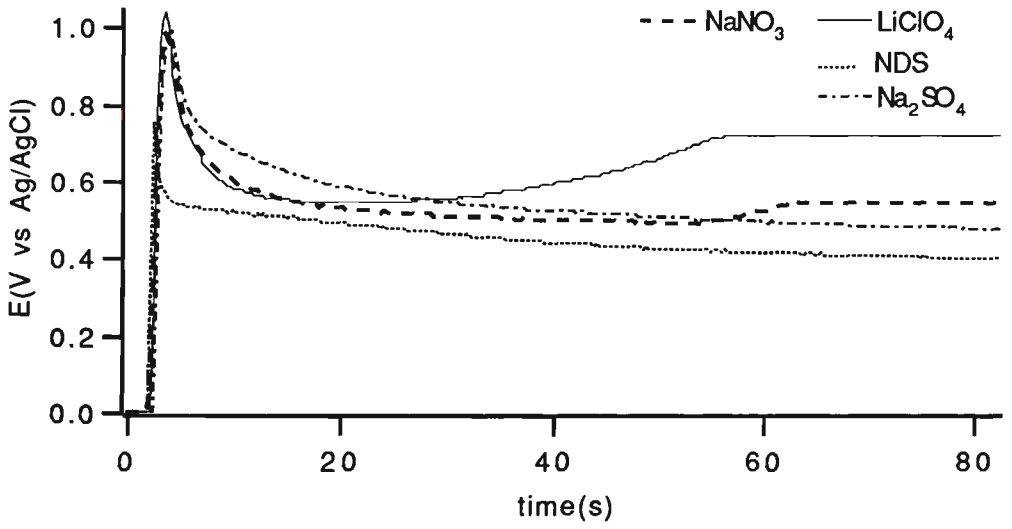

FIGURE 4.13 The effect of electrolyte on the chronopotentiometric response for the galvanostatic oxidation of 0.20 M pyrrole in 0.05 M electrolyte.
A Nafion coated stainless steel electrode and a current density of 2.0 mA cm^{-2} were employed.

The tensile strength, Young's modulus and conductivity of the composite PPy/Nafion membranes were measured (Table 4.2). The Young's modulus determined suggests that the polymer (PPy/Nafion) is more flexible and less rigid than the PPy/PVS membrane.

Scanning electron micrographs of the PPy/Nafion composites were obtained (Figure 4.14). As with PPy/PVS the plate side has a smooth appearance suggesting the presence of a dense polymer layer (SEM not shown). The solution side has a much more open appearance than those observed with PPy/PVS displaying a nodal structure.

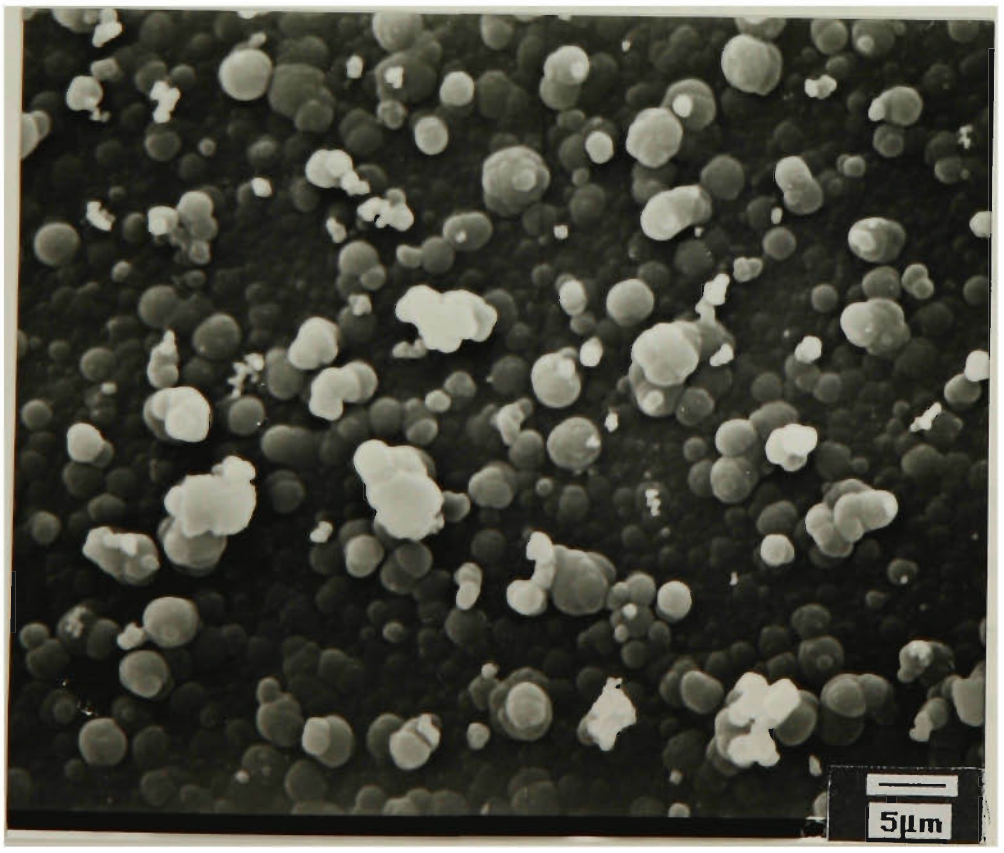

FIGURE 4.14 SEM photographs of PPy/Nafion composite prepared as described in the text (solution side).

The results obtained for the elemental analysis of PPy/Nafion is shown in Table 4.3. The ratio of counterion to pyrrole monomer units was determined. This value was similar to that obtained for the PPy/PVS. Nafion is a copolymer of tetrafluoroethylene and perfluoro 3,6-dioxa-4-methyl-7-octenesulfonylfluoride (see structure below). The carbon content of the PPy/Nafion films was significantly less than those obtained for PPy/PVS or PPy/NDS indicating the presence of Nafion containing some other elements such as fluorine.

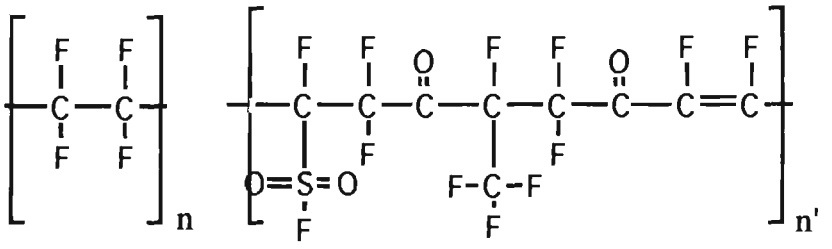

Structure of Nafion

Note that n and n' are the number of monomer units present in Nafion.

4.3.5 TRANSPORT ACROSS COMPOSITE MEMBRANES

4.3.5.1 ELECTROACTIVITY

In order to evaluate switching properties and the electroactivity of the PPy/PVS composite material cyclic voltammograms (CVs) were recorded in media containing KCl and NaCl. The CVs obtained for composite polymers were slightly different from those obtained for conventional counterions such as NDS (Figure 4.15).

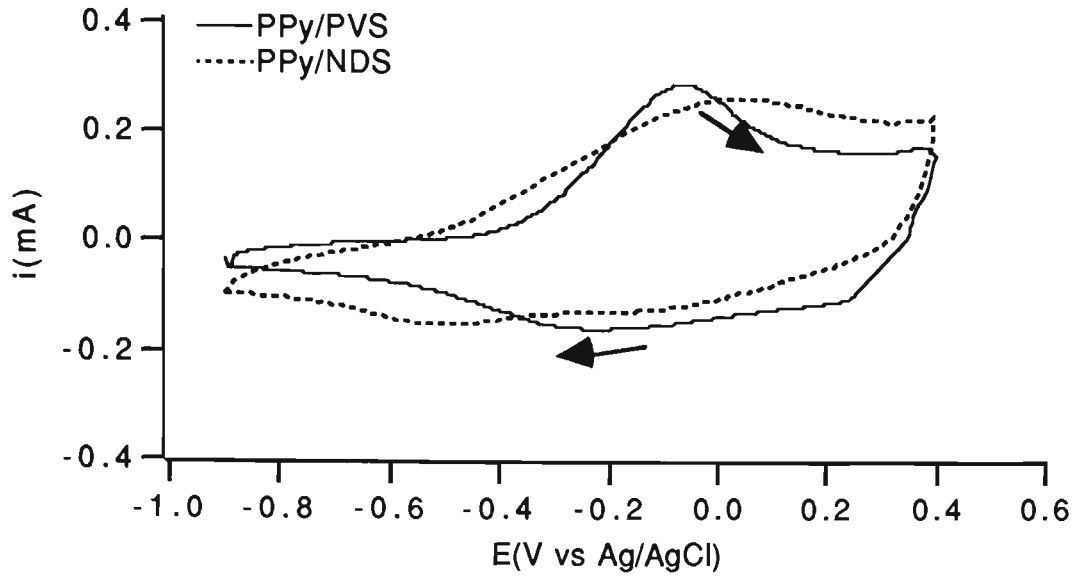

FIGURE 4.15 A comparison between cyclic voltammetric responses of polypyrrole composite (PPy/PVS) as prepared and polypyrrole grown with a conventional counterion (PPy/NDS) in 0.20 M KCl solution. Scan rate =50 mV s^{-1}.

For both PPy/PVS and PPy/NDS polymers scanned in 0.20 M KCl the peak separation ($\Delta E=E_{pa}-E_{pc}$) was larger than expected ($\Delta E=0.06$ V) for a one electron transfer reversible reaction (Table 4.4). However, these values in the case of the composites were much smaller than conventional polymers. This indicates that regardless of the mechanism, the ion movement is more efficient in the case of the composite polymer. This could be accounted for the predominant role of cations in ion transport as they were less limited by kinetic effects.

TABLE 4.4 Cyclic voltammetric characteristics of different polypyrrole based polymers in 0.20 M KCl Solution.

Polymer	**E(oxidation) (V)**	**E(reduction) (V)**	**Peak separation ΔE(ox-red)-V**
PPy/PVS	-0.05	-0.27	0.23
PPy/Nafion	-0.27	-0.41	0.14
PPy/NDS	+0.06	-0.50	0.56

All polymers were prepared as described in the text. A total charge of 120 mC cm^{-2} was used to prepare the polymers. Scan rate= 50 mV s^{-1}.

The cyclic voltammogram of the composite polymer in a solution of NaCl was also obtained (Figure 4.16). Well-defined responses due to the oxidation of PPy/PVS were observed. The oxidation peak was shifted approximately 100 mV more positive when the supporting electrolyte was changed from KCl to NaCl (Figures 4.15, 4.16). This cation dependent shift suggests that the oxidation process was accompanied by the expulsion of cations incorporated during the reduction process which is in agreement with previous observations[86]. This is quite likely since the dopant employed in the synthesis of the films (PVS) would be relatively immobile.

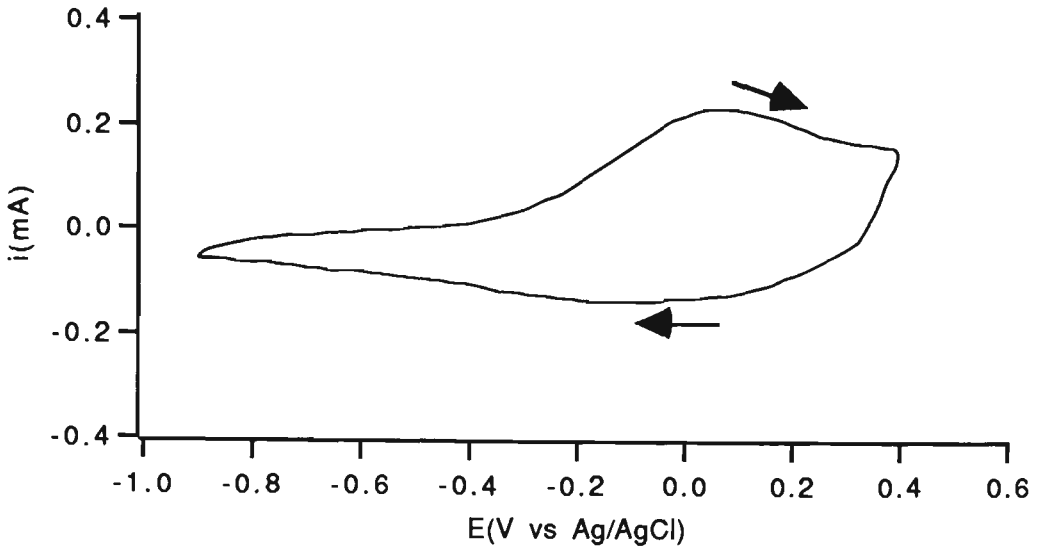

FIGURE 4.16 Cyclic voltammogram showing oxidation-reduction of the PPy/PVS composite in 0.20 M NaCl.
Scan rate = 50 mV s^{-1}

With PPy/Nafion composites well defined oxidation/reduction processes (A, A') were observed (Figure 4.17). The peak separation value obtained for PPy/Nafion (ΔE=0.14 V) was significantly smaller than the value obtained for PPy/NDS (ΔE=0.56 V). This is closer to the ideal value (ΔE=0.06 V) predicted for a one electron transfer reversible reaction. Hence as PPy/PVS, this behaviour may be attributed to the predominant role of cations during redox reactions.

Given the immobile nature of the incorporated counterions it is most likely that the voltammetric responses observed with both PPy/PVS and PPy/Nafion are due to cation incorporation and expulsion as the polymer is reduced and oxidised respectively. The smaller peak separations obtained for both composites, as explained, are further evidence for such an assumption.

(a)

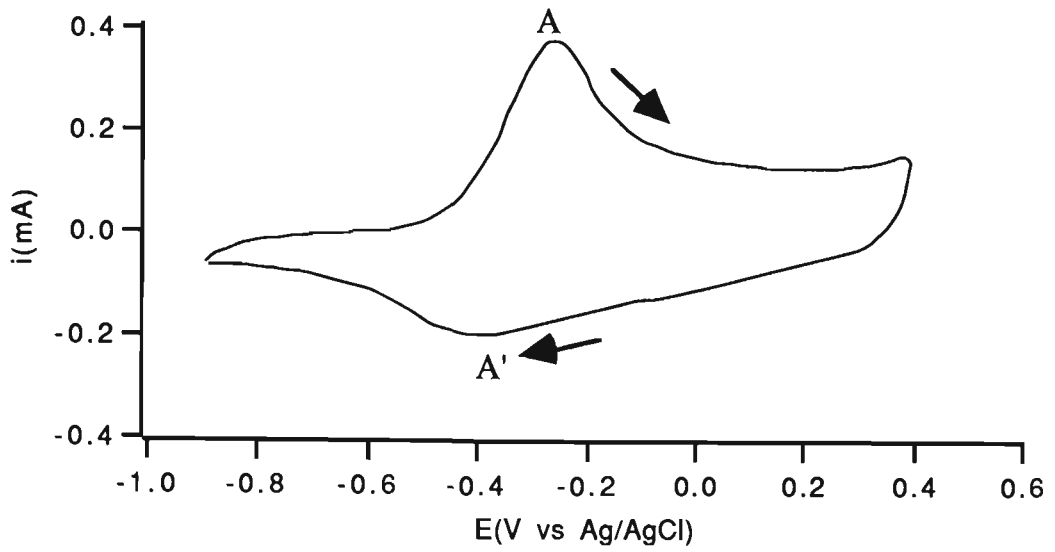

(b)

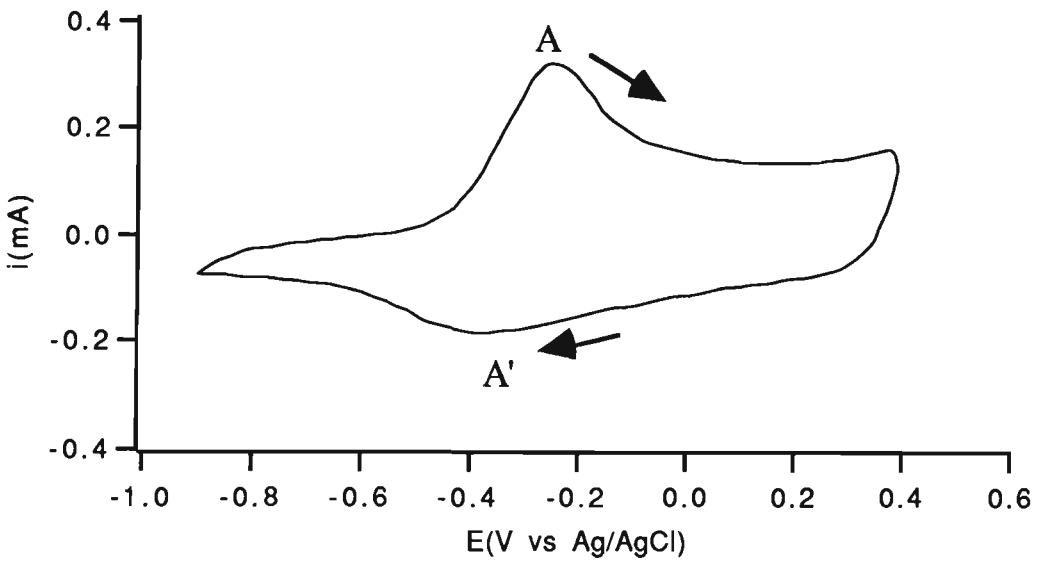

FIGURE 4.17 Cyclic voltammograms showing oxidation-reduction of the PPy/Nafion composite.

In (a) 0.20 M KCl (b) 0.20 M NaCl. Scan rate = 50 mV s^{-1}.

4.3.5.2 TRANSPORT STUDIES

Using the electromembrane diffusion cell the controlled transport of potassium and sodium ions was subsequently considered. With the PPy/PVS membrane it was found that there was no transport of any species when no potential was applied to the membrane. Similarly, the application of either a positive or a negative constant potential gave no transport.

The use of a pulsed potential to initiate transport was then considered. This involved the application of repetitive pulses of sufficient amplitude (+0.70 V $\leftrightarrow$ -0.60 V vs Ag/AgCl) to oxidise and reduce the polymer. The membrane served as the working electrode and a pulsed potential with a pulse width = 30 seconds was applied. The oxidative and reductive pulsed potentials were applied to the polymer exposed to the source solution to encourage incorporation and expulsion of ions.

A proposed scheme for ion movement during transport using this method (Method A) is shown in Figure 4.18. When the polymer is reduced the charge neutrality is maintained by expulsion of anions (step 1) or incorporation of cations (step 2). Conversely when the polymer is oxidised charge neutrality is conserved by incorporation of anions (step 3) or expulsion of cations (step 4). However expulsion of cations could occur either in the receiver side or source side. Subject to the mobility of the counterion employed at the time of synthesis (Chapter 1) and the solution anion, the dominance of each step is determined. Normally both A^-/M^+ must be transported to maintain charge balance in the receiving solution.

(A) DURING REDUCTION

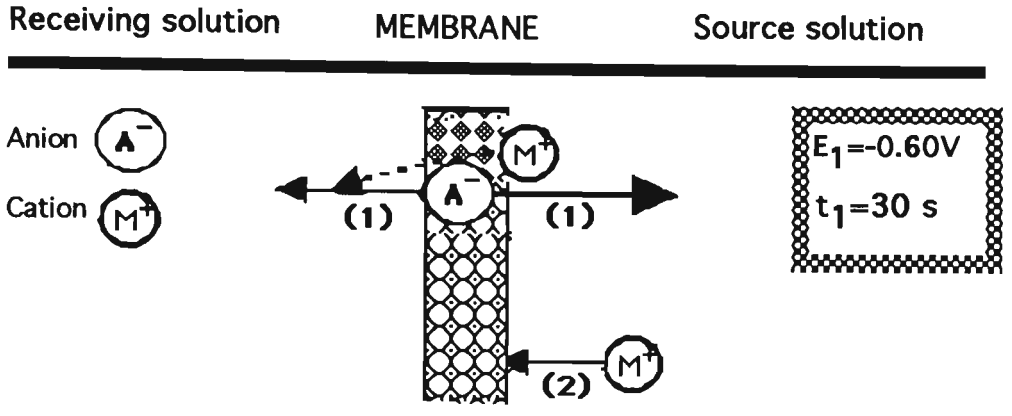

(B) DURING OXIDATION

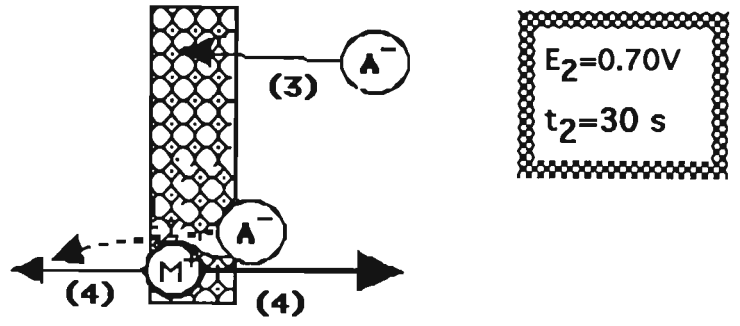

FIGURE 4.18 Proposed scheme for ion movement during transport using method A. A pulsed potential of E_1=-0.60 to E_2=0.70 V and t_1=t_2=30 s was applied to the source side of the membrane under investigation.

(A): Ion movement during reduction:

(1) Expulsion of anions either into the receiver (accompanied by cation) or source side.

(2) Incorporation of cations.

(B): Ion movement during oxidation:

(3) Incorporation of anions.

(4) Expulsion of cations either into the receiver (accompanied by anion) or source side.

In previous work from our laboratory this potential waveform routine resulted in ion incorporation and expulsion resulting in transport across conventional membranes[87]. For example application of the pulse potential (method A) to a PPy/PTS membrane resulted in transport of Na^+(Flux=1.74×10^{-10} mol cm^{-2} s^{-1}). However using the PPy/PVS membrane transport was still not observed. Since the cyclic voltammograms suggested that incorporation and expulsion of cations or anions occurred, the lack of transport of these species across the membrane was puzzling. There were thought to be several reasons for this.

(1) The lower conductivity of these membranes (approx. 14 S cm^{-1}) compared with PPy/PTS membranes (approx. 100 S cm^{-1}) may reduce the efficiency of electrochemical control.

(2) The PPy-PVS may have such a high affinity for the cation that transport is prevented.

(3) With this potential waveform routine (Figure 4.18) the release of cations in the receiver side was subject to movement of anions (steps 1, 4). In other words the transport of the cations must be accompanied by the anions to maintain charge neutrality. A lack of mobile anions in the structure of PPy/PVS membranes would prevent this and in fact application of this waveform to the PPy/PVS membranes would result in the incorporation and expulsion of cations (or protons) in the source side with no subsequent transport through the membrane (Figure 4.19).

(A) DURING REDUCTION

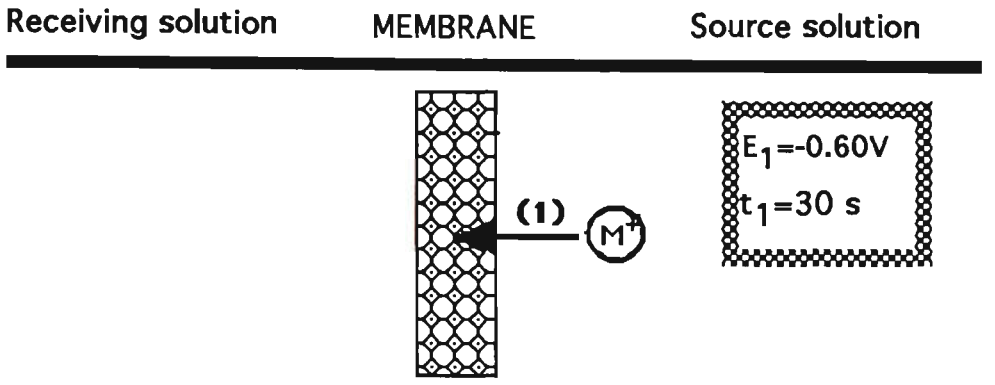

(B) DURING OXIDATION

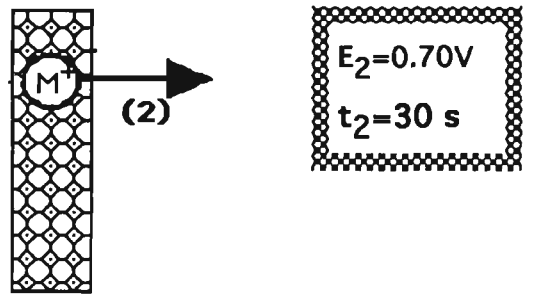

FIGURE 4.19 A simple schematic showing the movement of species when method A was applied to PPy/PVS membranes.
A pulsed potential of E_1=-0.60 to E_2=0.70 V and t_1=t_2=30 s was applied to the source side of the membrane.
(A): Ion movement during reduction: (1) Incorporation of cations from the source side.
(B): Ion movement during oxidation: (2) Expulsion of cations into the source side.

Some of these problems may be alleviated by use of a more efficient cell design where electrical contact is made at more points and from both sides of the membrane. Therefore a new cell was designed and built as described in Section 2.3 (cell design and development).

Application of a new pulsed potential method (method B). In attempts to initiate transport of cations an electrochemical system that allows potential control of each side of the membrane to be initiated independently (but not simultaneously) was then considered.

An electronic controller which enables the source side of the membrane to be reduced for a fixed time (30 seconds) and then electrically disconnected and alternatively the receiver side to be oxidised for a fixed period (30 seconds) and then disconnected was constructed (see Appendix). In this way (method B) electrical field and its polarity could be alternated between the receiver and source side of the cell.

When the membrane exposed to the source solution is reduced potentiostatically cations will be incorporated (Figure 4.20, step 1). Since the receiver side is always forcibly oxidised, expulsion of the cation on this side of the membrane is encouraged (step 3). Given the immobile nature of PVS no movement of anions is expected. However movement of anions if present, would not prevent transport of cations (Figure 4.20, steps 2,4). Using the new cell set-up other electrochemical reactions can now be brought into play to provide charge balance in the receiver solution.

(A) DURING REDUCTION

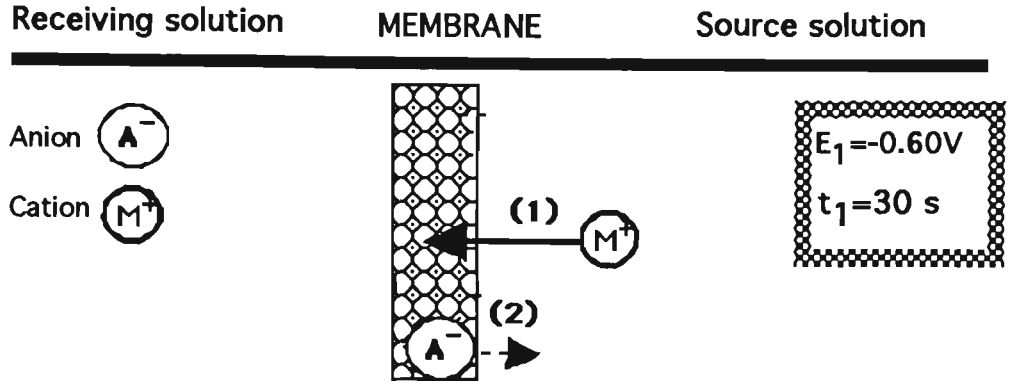

(B) DURING OXIDATION

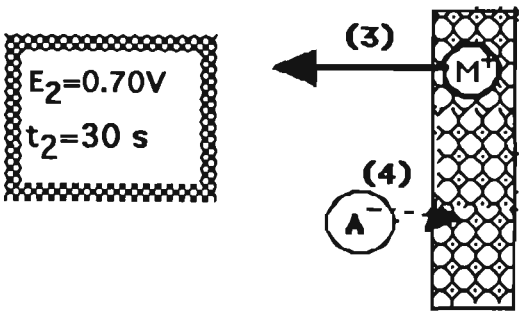

FIGURE 4.20 Proposed scheme for ion movement during transport using method B. On the source side of the membrane -0.60 V was applied for 30 seconds then disconnected for 30 seconds. On the receiver side of the membrane +0.70 V was applied when the source side was disconnected. This sequence was repeated.

(A): Ion movement during reduction on source side:

(1) Incorporation of cations

(2) Possible expulsion of anions (in the case of immobile PVS this would hardly occur)

(B): Ion movement during oxidation in receiver side:

(3) Expulsion of cations into the receiver side

(4) Possible incorporation of anions (in the case of immobile PVS this would hardly occur)

The use of this new system resulted in the transport of K^+ and Na^+ across the PPy-PVS membrane. The applied potential waveform initiated the transport of cations across the composite polymers while removing the potential halted the transport (Figure 4.21).

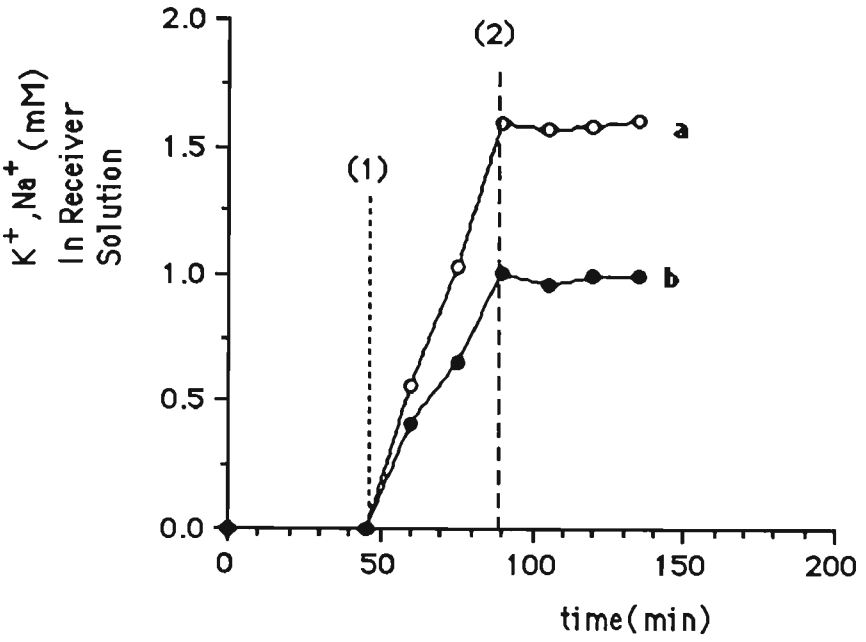

FIGURE 4.21 Transport of 0.20 M salt (0.10 M NaCl, 0.10 M KCl) across a PPy/PVS membrane with a twin pulsed potential applied (method B).
On the source side of the solution -0.60 V was applied for 30 seconds then disconnected for 30 seconds. On the receiver side of the solution +0.70 V was applied when the source side was disconnected. This sequence was repeated.
At time (1) the potential sequence is applied.
At time (2) it is removed.
(a) Transport of K^+
(b) Transport of Na^+

The concentration of cation in the receiver side was measured as a function of time. Then the average fluxes were calculated based on Equation 3.2. When the concentration of cations in the receiver side was plotted against time during transport, a linear relationship was obtained with a correlation

coefficient (R^2) of above 0.994 for all the composite membranes under investigation.

It was found that the membrane is selective to the cations (Table 4.5) and a selectivity factor (α) of 1.69 ($\alpha = \frac{\text{Flux } (K^+)}{\text{Flux } (Na^+)}$) was obtained. This indicates the existence of competition between cations in the mixture.

The experiment was repeated with three separately grown membranes. The results were reproducible within ± 9% for either the PPy/PVS or the PPy/Nafion composites. Throughout the work the plate side of the membrane (i.e. the side that remained in contact with electrode during polymerisation) was exposed to the source side. However further investigation had revealed that the transport behaviour was independent of the side of the membrane exposed to the source solution as the same results (within the experimental error) were obtained with the results shown in Table 4.5.

TABLE 4.5 Transport of Na^+ and K^+ across PPy/PVS membranes

	Flux (mol $cm^{-2}s^{-1}$) x 10^9			
Exp NO	**(1)**	**(2)**	**(3)**	**Average**
K^+	4.62	5.24	5.54	5.13
Na^+	2.80	3.18	3.12	3.03

Pulsed potential of E_1=-0.60 to E_2=0.70 V and t_1=t_2=30 s was applied to the source and receiver side respectively, as shown in Figure 4.20.

When transport of K^+ and Na^+ was studied separately, no significant difference in flux was observed for PPy/PVS membranes (Table 4.6). This may indicate that the selectivity obtained for the mixture was due to the competition between cations in the mixture of solution.

TABLE 4.6 Transport results for PPy/PVS and PPy/Nafion membranes.

Membrane	Flux* (mol $cm^{-2}s^{-1}$) x 10^9	
	PPy/PVS	PPy/Nafion
K^+	7.70	6.90
Na^+	7.82	2.51
K^+ (Mix)	5.13	3.10
Na^+(Mix)	3.03	1.33

*Average of results for three membranes. Experimental conditions were as in Table 4.5.

Similar results were observed for PPy/Nafion membrane. Again, the new cell design and electronic controller were required to facilitate transport. Figure 4.22 shows the results obtained from a typical experiment. Fluxes are summarised in Table 4.6. In this case selectivity factor (α) of 2.33# was obtained.

It has been previously shown (H. Small, Ion chromatography, Plenum press, New York , 1989) that conventional cationic exchange membranes such as sulfonated polystyrenes are selective to some cations. For example, a selectivity coefficient of K^+/Na^+ = 1.43 has been reported for Na^+ and K^+ ions. The selectivities of 2.33 and 1.69 presented here (for PPy/Nafion and PPy/PVS membranes) are even better than these conventional ion-exchange systems.

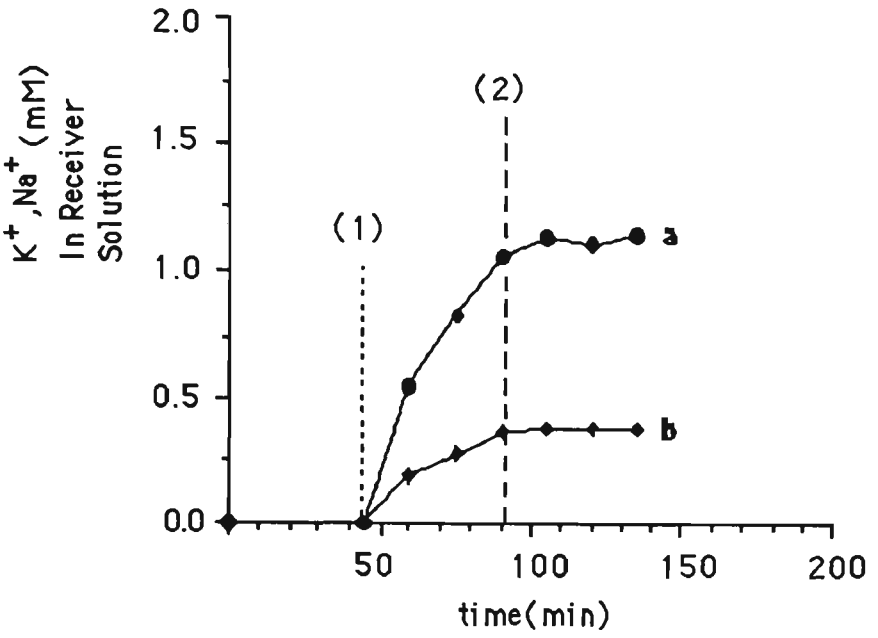

FIGURE 4.22 Transport (0.10 M NaCl, 0.10 M KCl) across a PPy/Nafion membrane with a twin pulsed potential applied. The potential applied as in Figure 4.20.
At time (1) the potential is applied.
At time (2) it is removed.
(a) Transport of K^+
(b) Transport of Na^+

Unlike PPy/PVS, Nafion membranes are selective to the cations whether the cations were studied from a mixture or separately (Table 4.6). It is probably due to the cation exchange properties of Nafion.

Transport of the cations was accompanied by an increase in pH on the receiver side and a decrease on the source side (Table 4.7). This is due to reduction and oxidation of water occurring at the auxiliary electrodes on either side of the membrane as the auxiliary electrode is polarised at very negative and positive potentials (over ± 1.00 V). The reduction of dissolved oxygen in the water may also increase the pH.

The reduction reactions occurring at the auxiliary electrode in the receiver side are:

$$2H_2O + 2e \longrightarrow H_2 + 2OH^- \qquad E^0=-0.828\ V \qquad (4.1)$$

$$O_2 + 2H_2O + 4e \longrightarrow 4OH^- \qquad E^0=0.401\ V \qquad (4.2)$$

The oxidation reaction occurring at the auxiliary electrode in the source side are:

$$2H_2O - 4e \longrightarrow O_2 + 4H^+ \qquad E^0=0.815\ V \qquad (4.3)$$

TABLE 4.7 The changes in solution pH before (a) and after (b) transport in both receiver and source solutions.

Membrane	Receiver pH(a)	Receiver pH(b)	Source pH(a)	Source pH(b)
PPy/PVS	5.1	9.6	5.3	3.4
PPy/Nafion	5.1	9.9	5.1	3.0

The transport conditions were as in Table 4.5. Note that the changes in pH of the receiver solution was not equal to the source solution. This indicates that two separate reactions are occurring in the two different electrolyte (source and receiving) solutions.

Since the same supporting electrolyte ($MgCl_2$) was used in both solutions the detection of Cl^- was not possible (although with this set up no transport of anions is expected). The transport and detection of anions is investigated in the next Chapter.

Comparison of the methods (A and B). Application of both methods A and B initiated transport of K^+ across conventional (PPy/PTS) membranes (Table 4.8). However using method B the rate of transport was significantly increased (~twenty times). When method A was employed the release of cations in either source or receiver side was possible (steps 1,4 in Figure 4.18). This would have decreased the rate of transport. However, using method B this possibility is minimised therefore the rate of transport increased.

Comparison of the membranes (PPy/PTS with composites). The flux obtained for the transport of K^+ (Table 4.8) across composite membranes (PPy/PVS and PPy/Nafion) was higher than that obtained for PPy/PTS under the same method of pulsing (method B). This improvement in transport is presumably due to the higher cation exchange capacity of the composite membranes.

TABLE 4.8 Transport of 0.20 M KCl across PPy/PVS and PPy/PTS membranes using different pulsed potential methods.

	Flux* of K^+ (mol cm^{-2} s^{-1}) x 10^9		
Membrane	**PPy/PVS**	**PPy/Nafion**	**PPy/PTS**
Method A	0.00	0.00	0.17
Method B	7.70	6.90	3.30

*Average results were obtained for three membranes. Source solution contained 0.20 M NaCl. 0.01 M $MgCl_2$ was used as background electrolyte in both side.

Method A: See Figure 4.18.

Method B: See Figure 4.20

4.4 CONCLUSION

Electrosynthesis procedures that allow production of free-standing pin-hole free conducting polymer composite membranes have been developed. PPy/PVS and PPy/Nafion composite membranes with good mechanical and electrical properties were prepared.

For successful electrochemically facilitated transport across conducting polymer membranes high affinity of the solute for the polymer matrix is required for ion incorporation yet high release rates in the receiver side are required to allow transport. In order to achieve this a new electrochemical controller based on a twin pulsed applied potential was designed and constructed. This device enabled the reduction and oxidation of the polymer to be separately initiated in different parts of the cell. When these composite membranes were used in combination with the new electrochemical controller, transport of cations was initiated. Such transport was controlled by electrochemical means and in fact it could be switched on or off.

It was found that due to the larger cation exchange capacity of the composite membranes more transport of cations was obtained compared with PPy/PTS.

The findings of this Chapter revealed that the transport of cations across the membranes was due to incorporation in the source side followed by expulsion in the receiver side. Application of a similar method would be expected to initiate transport of anions. However for such transport the anions would be required to be incorporated in the source side and to be released in the receiver side. This is the subject of the next Chapter.

CHAPTER 5

ELECTROCHEMICALLY CONTROLLED TRANSPORT OF SMALL ORGANIC MOLECULES ACROSS CONDUCTING POLYMER MEMBRANES.

5.1 INTRODUCTION

In Chapter 4 an electrochemical method that allowed transport of cations across composite membranes was introduced. It was a new device based on applying a time resolved potential pulse routine to either side of membrane. It was thought that employing this method may also encourage transport of anions as they can be incorporated/released with a similar mechanism to that of cations, during oxidation or reduction reactions.

For the purpose of this study polypyrrole doped with a relatively mobile counterion (PTS) was considered, since it has been shown that polypyrrole formed with PTS is capable of both cation and anion exchange properties[80]. In addition, the polymer has been shown to exhibit good mechanical properties[57, 87].

The anions chosen for this investigation have a sulfonated benzene ring. The effect of the presence and position of other substituents on the benzene ring on the transport across PPy/PTS membranes was considered.

Transport of anions across PPy/PVS membranes was also considered to evaluate the anion exchange properties of the membrane, although it is expected to be low as shown from our previous results in Chapter 4. This was carried out as a means of comparison with the anion exchange behaviour of PPy/PTS membranes.

5.2 EXPERIMENTAL

5.2.1 REAGENTS AND MATERIALS

All reagents were of analytical reagent (AR) grade purity unless otherwise stated. Reagent grade sodium benzene sulfonate (BS), 3-sulfobenzoic acid, sodium salt (3SBA), 4-sulfobenzoic acid, sodium salt (4SBA), 4-hydroxy benzene sulfonic acid, sodium salt (4-HBSA) and 1,3 benzene disulfonic acid, sodium salt (1,3BDSA) were purchased from Aldrich chemicals. Sodium 4-toluene sulfonate (PTS) was purchased from Merck. Methyl Alcohol (HPLC grade) was obtained from Mallinckrodt. Pic A low UV reagent was purchased from Waters (Millipore). The other chemicals were purchased as described in the previous Chapters.

The pyrrole (Py) was distilled before use. All eluents and solutions were filtered through a 0.45 μm filter prior to HPLC analysis.

All solutions were made up using a deionised water from a Milli-Q water system delivering 18 MΩ cm water.

5.2.2 INSTRUMENTATION

A Beckman 114 solvent delivery module and variable wavelength detector (Linear) with a Waters μ-Bondpak C_{18} column (3.9 x 300 mm) were used for HPLC analysis.

Cyclic voltammetric studies were carried out as described in Section 2.4. A gold electrode with surface area of 0.25 cm^2 was used as the working electrode. In-situ charge measurements during transport studies were recorded

using a MacLab™ recorder (ADI Instruments) with Chart 4™ software. All other instruments used were as described previously.

5.2.3 EXPERIMENTAL PROCEDURES

Sample analyses. Sodium was analysed by atomic absorption. The amount of organic anion transported was determined using HPLC (High Performance Liquid chromatography). Reverse phase ion pairing chromatography[191] was employed using Pic A solution (0.005M). In all experiments a flow rate of 1 mL min $^{-1}$ was used. A μ-Bondpak C_{18} column was employed as stationary phase and a UV detector (254 nm) was used.

The solvent composition used for each anion is shown in Table 5.1 Calibration curves were obtained for the samples to be analysed prior to analysis. Chromatographic peak height was used for quantitative purposes. Calibration curves for all anions were linear over the range investigated (1-9 ppm) with a correlation coefficient (R^2) of above 0.998.

Membrane Preparation. The procedure used to prepare the PPy/PTS membranes was similar to that described in Section 4.3.1. The PPy/PTS membrane was prepared by electropolymerisation from a solution containing 0.20 M pyrrole and 0.05 PTS. A constant current of 2.0 mA cm^{-2} was employed for 12 minutes. A highly polished stainless steel plate was used as the working electrode. The preparation of the PPy/PVS membranes was as described in the previous Chapter (see Section 4.3.1).

TABLE 5.1 The solvent composition used for chromatographic analysis of each anion.

Anion	Methanol (%)	Water (%)
BS	40	60
PTS	40	60
4HBSA	20	80
4SBA	35	65
3SBA	35	65
1,3BDSA	20	80

The solvent composition was optimised to obtain the best separation between the given anion and the counterion released (or transported) through the polymer membrane.

Transport Studies. The cell utilised in the transport experiments has been described in Chapter 2. It consisted of two compartments (volume 63 mL each) separated by the membrane under investigation. A concentration of 0.20 M organic salt as source solution and 0.01 M magnesium chloride (as background supporting electrolyte in both sides) were used in all studies. The details of the electrical stimuli applied to initiate transport are described in the individual Sections (see R & D). Table 5.2 shows the structure of the organic anions whose transport was investigated.

TABLE 5.2 Structure of sulfonated aromatics whose transport was investigated.

BS	PTS	4HBSA
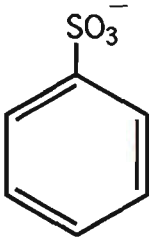		
4SBA	**3SBA**	**1,3BDSA**
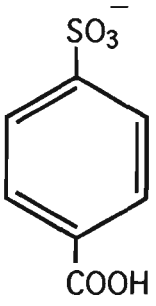	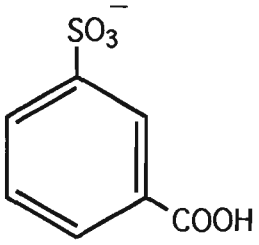	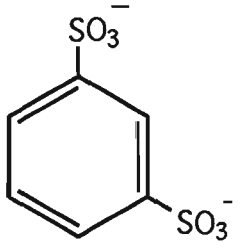

5.3 RESULTS AND DISCUSSIONS

5.3.1 TRANSPORT OF ORGANIC ANIONS ACROSS PPy/PTS MEMBRANES

The PPy/PTS membranes prepared were mechanically strong and electrically conductive, as is necessary for use as free-standing films in transport studies (Table 5.3).

TABLE 5.3 Mechanical and electrical properties of membranes used for the transport of organic anions.

Membrane	Thickness (μm)	Tensile (MPa) Strength	Conductivity (S cm^{-1})
PPy/PTS	7	80	60
PPy/PVS	8	70	14

Membranes prepared as per the experimental Section.

The transport of a range of sulfonated aromatic compounds (Table 5.2) was considered. Initially the cyclic voltammetry of the PPy/PTS polymer in electrolytes comprised of these organic salts was studied. The purpose was to determine the range of potentials promoting redox reactions of the polymer in the given media. In all cases (except for electrolytes containing 3SBA and 4SBA) oxidation/reduction processes (A, A'), due to the electroactivity of the polymer in the given media, were observed. Figure 5.1 (a) represents behaviour that was obtained for the entire range of the anions. However, in the case of 3SBA and 4SBA (acidic counterions) the responses were not well defined (Figure 5.1 (b)).

(a) 0.20 M BS

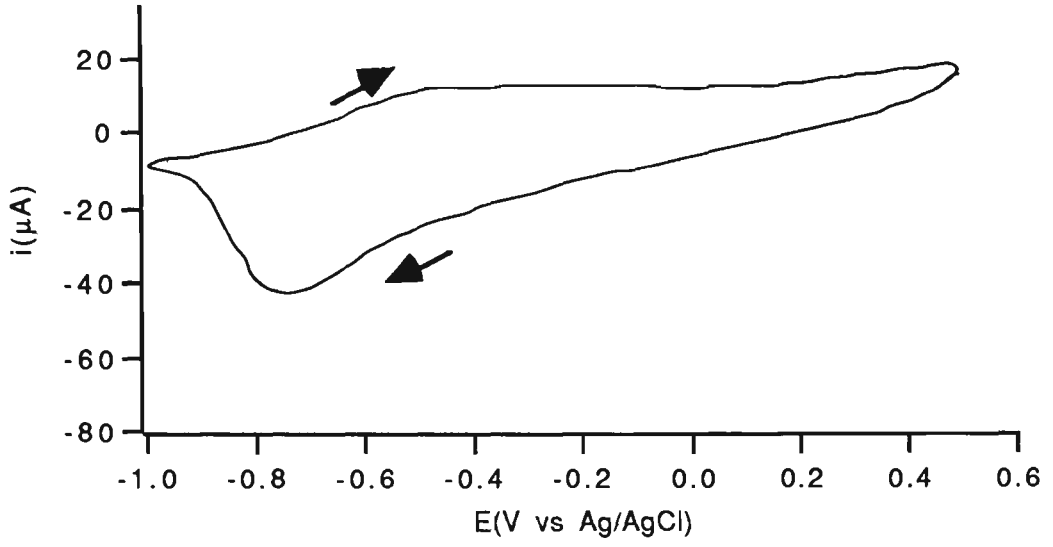

(b) 0.20 M 3SBA

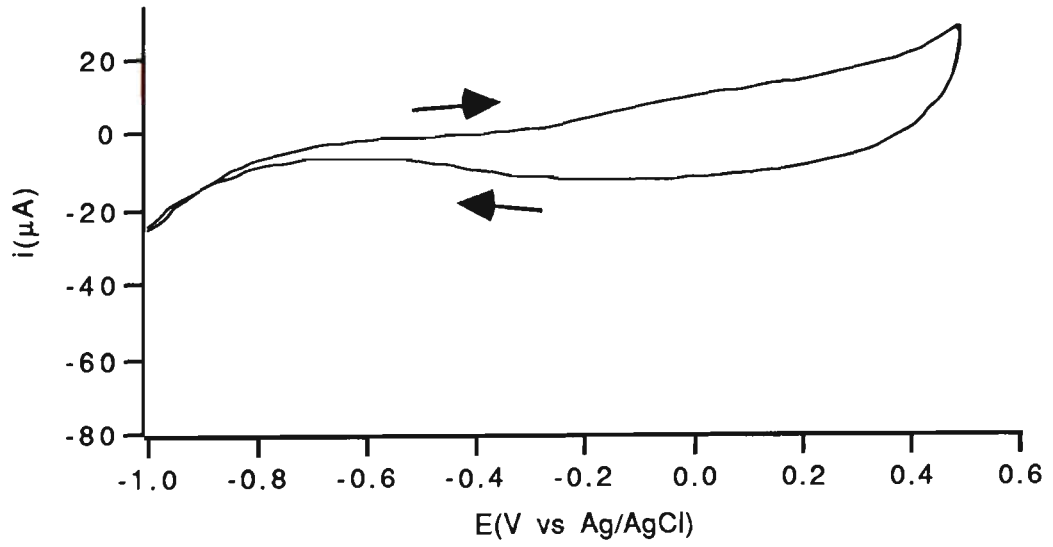

FIGURE 5.1 Cyclic voltammograms showing oxidation/reduction of PPy/PTS in various organic media. Scan rate = 10 mV s^{-1}

(a) 0.2 M BS

(b) 0.2 M 3SBA

These voltammograms suggest that in all cases if the potential is oscillated between +0.40 V and -1.00 V then the ion exchange process described in Equations 1.1 and 1.2 (Chapter 1) should occur and transport could be initiated. However it was found that when a pulsed potential of E_1=-1.00 to E_2=0.40 V and t_1=t_2=30 s was applied to the membrane in the media containing the organic salts (except PTS and BS) the membrane was ruptured before completion of the experiment. This deterioration of the mechanical properties was most likely due to the chemical change in composition induced by rapid replacement of the original counterion (PTS) with the solution anions. The replacement could cause a structural re-arrangement in which the new structure (with the organics having an electron withdrawing nature) is less stable. In addition, heat produced due to iR effects could also affect the mechanical strength.

It was found that the membranes were quite stable in all cases when a pulsed potential of E_1=-0.60 to E_2=0.40 V and t_1=t_2=30 s was applied. Therefore, in order to obtain comparable results for different anions a pulse potential of E_1=-0.60 to E_2=0.40 V was applied to the PPy/PTS membranes unless otherwise stated.

Transport experiments were then carried out. It was found that without electrical stimuli applied to the membrane transport could not be initiated for any of the organic ions considered. The application of a pulsed potential routine with different cell configurations was then considered. The initial studies involved the transport of BS as a test system.

1) Method (A): The membrane was continuously oxidised and reduced in the source side (Figure 4.18).

2) Method (B): The membrane was oxidised in the receiver side for a fixed time then reduced in the source side (Figure 4.20).

Method A. It was found that application of this pulsed potential waveform (Figure 4.18) initiated transport, but only at a low rate. With this potential waveform the membrane exposed to the source side was repetitively oxidised and reduced. Table 5.4 shows the results obtained for transport of BS across the PPy/PTS membrane. The fluxes were calculated using Equation 3.2. Both cations and anions were transported across the membrane but the rate of transport was quite low compared with our previous results (Table 4.6).

The mechanism of transport involves incorporation/expulsion of both anions and cations as the polymer membrane is continuously oxidised and reduced in a conducting electrolyte solution (Figure 4.18). However, following the incorporation of the species in the source side the expulsion into either the receiving or source solution could occur. Expulsion of species into the receiving solution requires the species to cross the membrane. For these large, hydrophobic anions this set up was not suitable for efficient transport. Most species did not cross the membrane but returned to the source solution. The flux observed for anions was less than for cations since some of the PTS, originally incorporated into the membrane, was also released (4.85×10^{-5} M).

TABLE 5.4 Application of a pulsed potential* (method A) to the PPy/PTS membranes to initiate transport of organic anion (BS).

	Flux (mol cm^{-2} s^{-1}) x 10^9	
Membrane	**BS**	**Na^+**
PPy/PTS	0.02	0.28

*A pulsed potential of E_1=-0.60 to E_2=+0.40 V and t_1=t_2=30 s was applied to the membranes using the set up shown in Figure 4.18 (method A). In this arrangement the source side was repetitively oxidised and reduced.
Flux calculated over the period the potential was applied, ie: 45 minutes.

Method B. The use of this potential waveform allowing the membrane to be reduced by application of a negative potential to the source side and oxidised by application of a positive potential to the receiver side was introduced previously (Figure 4.20). Application of this waveform to the PPy/PTS membranes resulted in the transport of cations, but transport of anions (BS) was still negligible (Table 5.5). Interestingly a high rate of transport for cations was observed (approximately 150 times larger than anions). The lack of transport of BS with this method can be explained by considering that with this set up there is no possibility of anion incorporation in the source side and consequently no release of anions in the receiving side occurred (Figure 4.20).

As with PPy/PVS (Chapter 4) the charge neutrality in both sides of the membrane was maintained by the electrochemical reactions occurring at auxiliary electrodes (Equations 4.1-4.3). This caused an increase in pH on the receiver side and a decrease on the source side.

TABLE 5.5 Application of a pulsed potential* (method B) to the PPy/PTS membranes to initiate transport of BS.

Membrane	Flux (mol cm^{-2} s^{-1}) x 10^9 BS	Na^+
PPy/PTS	0.02	2.95

*A pulsed potential E_1=-0.60 to E_2=+0.40 V and t_1=t_2=30 s was applied to the membranes using the set up shown in Figure 4.20 (method B). In this set up the membrane was reduced by application of a potential to the source side for a fixed period of time then the receiver side oxidised.
Flux calculated over the period the potential was applied, ie: 45 minutes.

Method C. Application of another waveform, defined as "method C", was then considered. In this set up the potential waveform shown in Figure 4.20 was reversed. This set up involved reduction of the polymer at the receiver side using potential pulses of -0.60 V for a duration of 30 seconds. The pulse was then removed (system was short circuited) for 30 seconds and this sequence repeated (Figure 5.2). At times when the reducing pulse was removed from the receiver side an oxidising pulse (+0.40 V for 30 seconds) was applied on the source side. When the membrane exposed to the source side is oxidised potentiostatically, anions will be incorporated (Figure 5.2, step 3). Since the receiver side is always forcibly reduced, expulsion of the incorporated anions on this side of the membrane is encouraged (step 1). This resulted in dramatic increases in flux for BS (Table 5.6).

(A) DURING REDUCTION

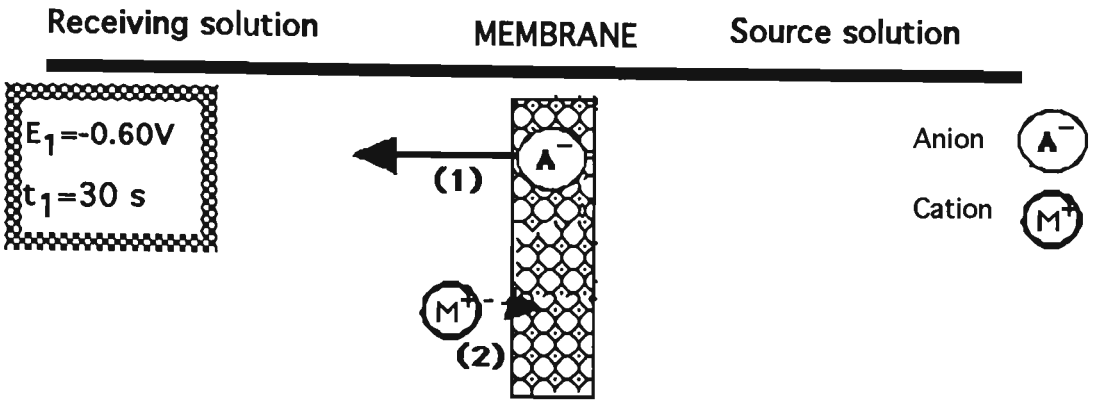

(B) DURING OXIDATION

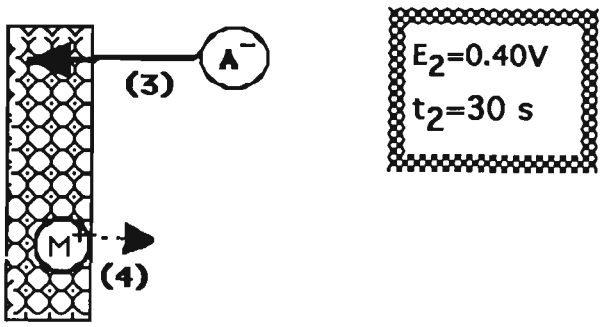

FIGURE 5.2 Proposed scheme for ion movement during transport of anions using method C.

On the source side of the membrane 0.40 V was applied for 30 seconds then it was disconnected for 30 seconds. On the receiver side of the membrane -0.60 V was applied when the source side was disconnected. This sequence was repeated.

(A): Ion movement during reduction of the receiver side:

(1) Expulsion of anions into the receiver solution

(2) Possible incorporation of cations

(B): Ion movement during oxidation of the source side:

(3) Incorporation of anions

(4) Possible expulsion of cations

TABLE 5.6 Application of a pulsed potential* (method C) to the PPy/PTS membranes to initiate transport of BS.

Membrane	Flux (mol cm^{-2} s^{-1}) x 10^9	
	BS	Na^+
PPy/PTS	1.49	0.00

*A pulsed potential E_1=-0.60 to E_2=+0.40 V and t_1=t_2=30 s was applied to the membranes using the set up shown in Figure 5.2 (method C). In this set up the membrane was reduced by application of a potential to the receiver side for a fixed period of time before the source side was oxidised. Flux was calculated over the period the potential was applied, ie: 45 minutes.

The results of the different methods described above indicate that the transport of anions was encouraged when method C was employed. Using a mechanism of transport which involves the incorporation and expulsion of species, the observations can be explained. For transport of cations the best results were obtained when the cations were incorporated in the source side and expelled in the receiver side. Application of method B provides such conditions (Table 5.5). However this method did not result in the transport of anions, so the transport of anions occurs when the anions were incorporated in the source side and released in the receiver side. Only application of method C allowed this (Table 5.6). By employing method (A) neither the transport of cations nor anions was significant. The expulsion of the incorporated species could occur on either side of the membrane, rather than the receiving solution only, thus resulting in a low flux (Table 5.4).

Method C was employed for the transport of anions throughout the remainder of this work since this method gave the highest value of flux for the transport of anions (Table 5.6).

More detailed studies on the transport of organic ions were then carried out using the PPy-PTS membranes with the potential waveform routine as described in Figure 5.2 (method C). As for BS, no transport was observed without any applied stimulus for any of the organic ions investigated. The results for the transport of anions employing method C are summarised in Table 5.7. The release of PTS from the membrane during transport studies was also considered during these transport experiments (Table 5.8).

It was found that the largest fluxes were obtained when electrolytes containing BS and PTS were employed. For other anions (containing electron withdrawing groups) fluxes were considerably reduced.

TABLE 5.7 Fluxes for the transport of the different organic anions across PPy/PTS membranes.

Electrolyte / **Anion**	**BS**	**PTS**	**4HBSA**	**4SBA**	**3SBA**	**1,3BDSA**
Flux ($mol\ cm^{-2}\ s^{-1}$) x 10^9	1.49	1.47	0.31	0.23	0.12	0.02

The transport was carried out using method C (Figure 5.2). Anions were determined using HPLC (Section 5.2.3). The fluxes shown here are the average of three independent experiments and were reproducible within ±7% error.

The amount of PTS released from the membrane during transport was also measured. It was found that for the anions giving low fluxes the amount of PTS released was high. This indicates that while the organic ion under investigation was not transported, it was incorporated into the membrane material, causing PTS to be released in performance to the applied potential. With subsequent potential pulses the PTS was released in preference to the incorporated anion. The smaller the rate of transport of the test species the greater the rate of PTS released (Table 5.8). However, the results obtained for 3SBA were an exception to this trend. This was probably due to the low affinity of the PPy/PTS for 3SBA.

The amount of PTS released during transport of anions correspond to ~30% of total number of anion in the polymer. For example, in the case of transport of BS, 25% of total available sites of PTS was released (as calculated by elemental analysis). This shows that the majority of PTS sites under these circumstances are not readily available for ion exchange.

TABLE 5.8 PTS released through the PPy/PTS membranes during transport of different organic anions.

Electrolyte **Anion**	**BS**	**4HBSA**	**4SBA**	**3SBA**	**1,3BDSA**
[PTS] C(M) x 10^5	5.1	5.3	6.2	4.5	7.7

PTS concentration was monitored after the electrical stimuli was applied for 45 minutes. Three experiments were considered. Experimental conditions were as Table 5.6.

Lowest fluxes were obtained with 1,3BDSA, which is likely to be due to the fact that this species contains two charged sites that have to be incorporated into the polymer structure. For polymers grown with monovalent anions this is known to be difficult[86]. From ion exchange principles, release of divalent anions, if incorporated, would also be more difficult. The cyclic voltammogram of the PPy/PTS recorded in the medium containing 1,3BDSA (Figure 5.3) showed that ion movement is more efficient (smaller peak-peak separation) compared to all the other organic anions (Figure 5.1). If the cations which are more mobile and less limited by kinetic effects take part in the ion exchange process, then ion movement would be more efficient. This, as well as the transport results, may indicate that PPy/PTS acts as a cation exchanger in solution of 1,3BDSA. Further investigations (using EQCM) showed this to be the case (Chapter 6).

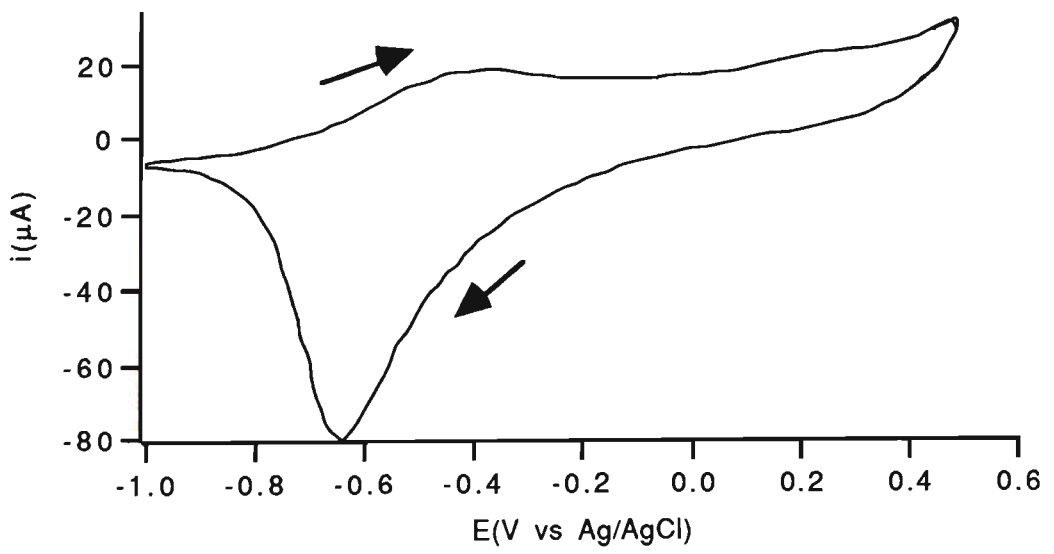

FIGURE 5.3 Cyclic voltammograms showing oxidation/reduction of PPy/PTS in 0.20 M 1,3BDSA. Scan rate = 10 mV s^{-1}

An interesting result was obtained in that the position of the functional group had a marked influence on the flux attainable with 3SBA or 4SBA, indicating that a high degree of electrochemical selectivity may be achieved (Table 5.7). The higher flux was obtained for 4SBA, which has the functional group in the para position.

$$\sigma = \frac{\text{Flux}_{(\text{P-COOH})}}{\text{Flux}_{(\text{M-COOH})}} = 2.0$$

Due to a greater inductive effect, the charge density on the sulphonate group on 3SBA may have been less than in 4SBA. This could reduce the affinity of anion incorporation in the polymer, resulting in a lower flux.

Although no cation transport was observed it was found that dramatic changes in solution pH accompanied the transport experiments (Table 5.9). In all cases the pH of the receiving solution decreased. This decrease in pH was presumably due to the electrochemical oxidation of water at the auxiliary electrode during transport (see Equation 4.3) This is necessary to maintain charge neutrality. The pH in the source side increased (Equation 4.1 and 4.2) due to electrochemical reduction of water at the surface of the auxiliary electrode. However, in the case of acidic anions (3SBA and 4SBA) such increase in the pH of the source solution was not detectable due to the high concentration of H^+ in the given media.

5.3.1.1 SEPARATION OF ORGANIC ANIONS

In order to investigate the possibility of separation of two organic anions using the conducting membranes further investigations were carried out. A solution containing 0.10 M PTS and the same concentration of another organic anion was employed as the source solution. The amount of both anions was

determined in the receiver side as function of time while the electrical stimulus was employed. In all cases, except for the BS/PTS system, reasonable selectivity factors were obtained (Table 5.10). For example, separation of 1,3BDSA and PTS were successfully carried out with a selectivity factor (α) of 27.50.

$$\alpha = \frac{\text{Flux PTS}}{\text{Flux (1, 3 BDSA)}} = 27.50$$

TABLE 5.9 The changes in solution pH before (a) and after (b) transport.

Anion	Receiver pH(a)	Receiver pH(b)	Source pH(a)	Source pH(b)
PTS	5.6	2.6	6.5	9.9
BS	5.6	2.8	5.8	9.5
4HBSA	5.6	3.0	5.4	6.3
4SBA	5.6	2.9	2.4	2.4*
3SBA	5.6	3.0	2.4	2.4*
1,3BDSA	5.6	2.9	7.2	8.6

* Due to high concentration of H^+ in source solution the changes in pH could not be detected.

The highest flux was obtained for BS while the lowest was obtained for 1,3BDSA (Table 5.10). The order was similar to that obtained for the individual transport of anions (Table 5.7).

TABLE 5.10 Separation of different organic anions from PTS using the PPy/PTS membrane.

Anion	Mean Fluxes (mol cm^{-2} s^{-1}) x 10^9		Selectivity factor $\alpha = \frac{\text{Flux PTS}}{\text{Flux Anion}}$
	Anion	PTS	
BS	0.76	0.87	1.14
4HBSA	0.17	0.47	2.76
4SBA	0.08	0.22	2.75
3SBA	0.07	0.33	4.71
1,3 BDSA	0.02	0.55	27.50

Experimental conditions as Table 5.6.

Figure 5.4 shows the profile obtained for transport of both anions across the membranes. In the given example, transport of PTS and 4HBSA was considered. PTS was readily transported while the rate of transport of 4HBSA was low due to the presence of -OH substitution. The -OH substitution has an electron withdrawing effect and reduces the charge density on $-SO_3$ resulting in a low affinity for anion incorporation. Consequently the incorporation of the 4HBSA anions with the polymer matrix was insignificant, resulting in low flux values. This effect is reflected in pK_a values of substituted benzenesulfonic acid. For example pK_a for benzene sulfonic acid is 0.70 but addition of an electron donating substituent (i.e. $-NH_2$) increased the pK_a value (pK_a for sulfanilic acid=3.23). By contrast, the pK_a was decreased when an electron withdrawing group such as $-NO_3$ (3-Nitro benzensulfonic acid= strong acid) was employed.

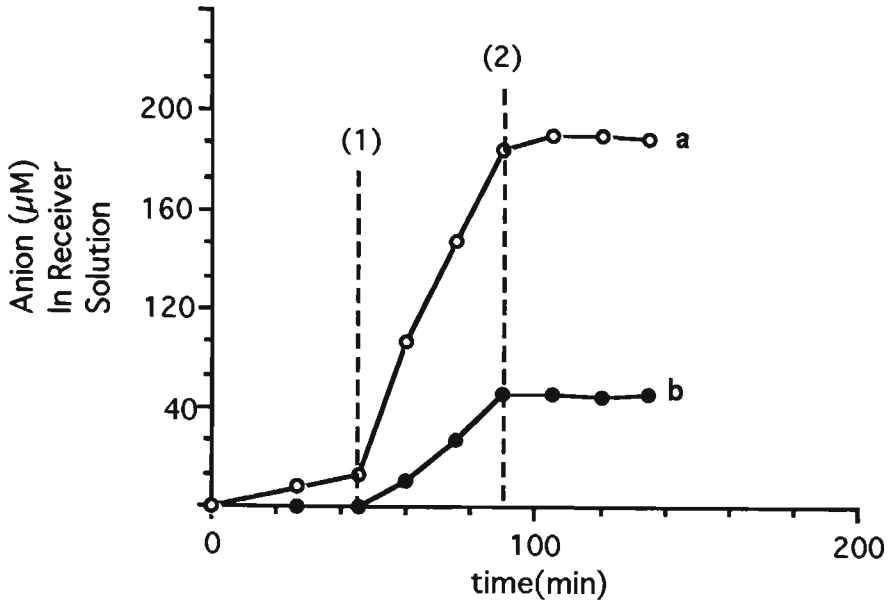

FIGURE 5.4 Transport across a PPy/PTS membrane using a pulsed potential routine (method C).
The potential was applied as Figure 5.2. The electrolyte was a mixture of organic salts (0.10 HBSA + 0.10 M PTS).
At time (1) the potential is applied.
At time (2) it is removed.
(a) Transport of PTS.
(b) Transport of 4HBSA.

The effect of different ions on the transport of PTS from a mixture of PTS and the corresponding anion was investigated (Figure 5.5). It was found that the transport of PTS varied depending on the nature of the other anion present. PTS was readily transported when accompanied by BS. While in all other cases the transport of PTS decreased. The mechanism of transport involves the incorporation of anions in the source side (Figure 5.2) followed by expulsion in the receiver side. These processes occur via the ion exchange sites. Apparently occupation of these sites by some of the anions affected the transport of PTS. The individual transport of these anions showed that they were hardly released when incorporated (Table 5.7). When incorporated with

no subsequent release, the ion exchange sites occupied by these anions no longer act as sites for transport of PTS, but presumably as cation exchanger and transport of PTS was subsequently decreased.

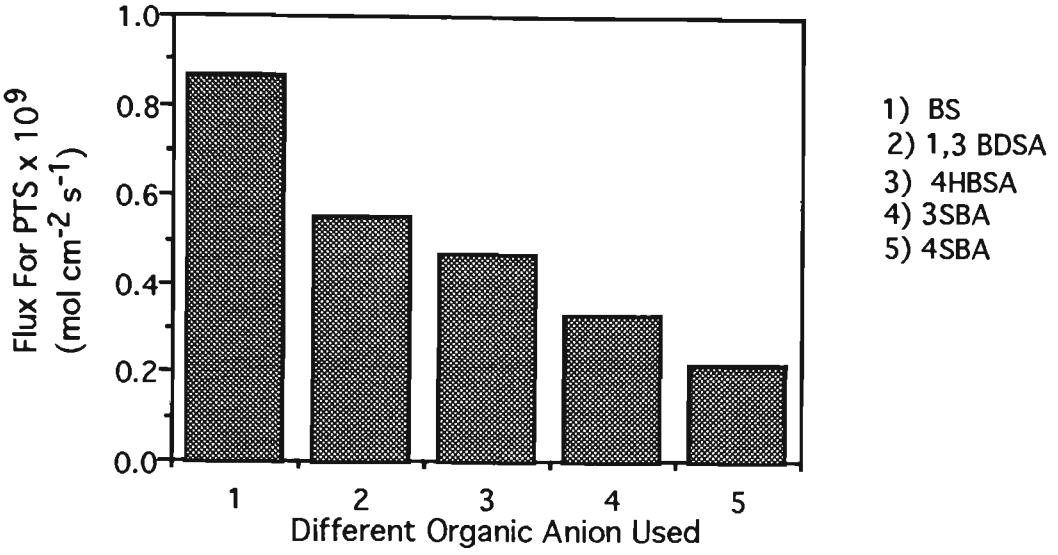

FIGURE 5.5 Transport of PTS in the presence of different organic anions. Transport experiment was carried out as described in the text. A mixture of 0.10 M PTS and 0.10 M anion was employed.

5.3.1.2 ELECTROCHEMICAL SELECTIVITY VERSUS CHEMICAL SELECTIVITY

Separation of a mixture of the anions considered in this work was demonstrated using HPLC (see Experimental Section). The capacity factors (k') were then calculated using the Equation below:

$$k' = \frac{t_r - t_0}{t_0} \qquad (5.1)$$

where t_r is the retention time (s) of the anions and t_0 is the dead time. The capacity factors for the separation of different anions/PTS are shown in Table 5.11. The ratio of capacity factors $\frac{k'_1}{k'_2}$ is an indication of the chemical

selectivity (α) obtained using ion pair chromatography based on hydrophobic interactions. These values were then compared with the selectivities obtained with the electromembrane separation method used in this work. The separations obtained using polymer membranes were in some case better (i.e. BDSA) than those obtained using the chromatographic method (Table 5.10 and 5.11). With both methods poor selectivity was observed for the mixture of BS and PTS.

TABLE 5.11 Capacity factors for the different organic anions mixed with the PTS.

Anion	BS	4HBSA	4SBA	3SBA	1,3BDSA
k'(PTS)	1.82	2.07	1.78	2.00	2.47
k'(anion)	0.98	0.39	0.36	0.46	0.71
$\alpha = \frac{k'_{PTS}}{k'_{Anion}}$	1.86	5.30	4.94	4.35	3.48

5.3.1.3 TRANSPORT EFFICIENCIES

Further investigations were carried out to evaluate the efficiency of transport of anions across conducting polymers. These results were valuable in particular when the mechanism of transport was considered. The chronoamperometric responses obtained for the PPy/PTS membrane during transport were recorded (Figure 5.6). Similar behaviour was observed in the presence all other organic anions whose transport was considered in this Section.

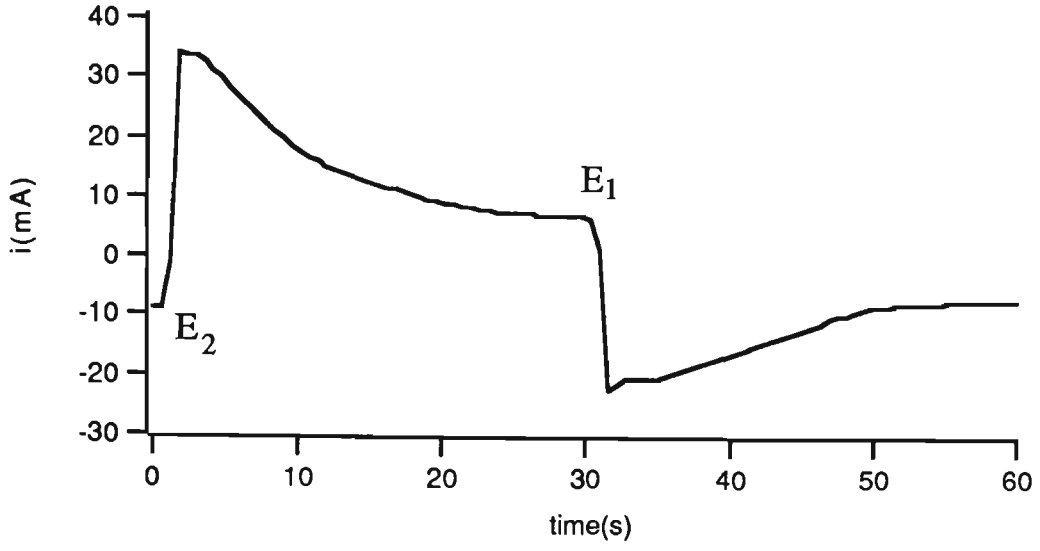

FIGURE 5.6 Chronoamperometric response (one cycle) of PPy/PTS membrane in 0.2M BS during transport of BS.
A pulse potential of E_1=-0.60 to E_2=0.40 V and t_1=t_2=30 s (method C) was applied to the receiver and source side respectively.

The total charge consumed during the complete course of transport was calculated by integration of the curve (chronoamperogram) over a period of 45 minutes. The average charge consumed for the transport of anions is shown in Table 5.12. The same calculations were repeated for the transport of a mixture of anion and PTS (Table 5.13). In both cases the maximum charge passed was obtained when BS was present. Maximum transport was also obtained for BS. Note that the charge consumed during reduction was not equal to that during oxidation, presumably due to the irreversible nature of the reactions as previous CV suggested (Figure 5.1). Also the oxidation reactions occurred in source side containing 0.2 M organic salt, while the reduction occurred in receiver side.

TABLE 5.12 The average charge consumed during the transport of organic anions across PPy/PTS membranes.

Anion	Q(C) Oxidation	Q(C) Reduction
BS	18.6	-19.5
PTS	15.7	-16.1
4HBSA	12.8	-7.9
4SBA	8.6	-8.3
3SBA	8.1	-5.7
1,3 BSDS	10.2	-8.7

The charge calculated for the period the pulsed potential (method C) was applied (i.e 45 minutes).

TABLE 5.13 The average charge consumed during the transport of mixtures of organic anions with PTS across PPy/PTS membranes.

Anion	Q(C) Oxidation	Q(C) Reduction
BS	19.8	-20.9
4HBSA	12.8	-7.9
4SBA	6.7	-5.1
3SBA	8.5	-6.8
1,3BDSA	13.8	-11.8

The charge calculated for the period the pulsed potential (method C) was applied (i.e 45 minutes).

The mechanism of the transport involves incorporation of anions from the source solution followed by expulsion into the receiver solution. Hence, the ratio of the number of moles of anion transported to the number of moles of electrons consumed during reduction (the stage when anions are expelled) could be used as an indication of the electrochemical efficiency of transport. Thus the efficiency of transport was calculated using the Equation:

$$E_f = \frac{m_t}{m_e} \% \qquad (5.2)$$

where m_t is the moles of anions transported during 45 minutes and m_e is the moles of electrons consumed during application of the reductive potential for the same period of time (i.e. the number of moles expected to be consumed for transport as calculated using Faraday's law).

The transport efficiencies obtained for the transport of a mixture of anions and PTS was determined (Table 5.14). Maximum efficiency was obtained for BS and the minimum for 1,3BDSA.

In general only about 15% of the charge consumed during transport carried anions to the receiver side. Possible explanations for such low efficiencies are:

1) In order to simplify the model, Q due to the charging current was not taken into account. However, due to the nature of the applied potential (pulsed potential) the total current includes a portion which was not involved in the transport of anions (charging current). Therefore subtracting this effect would result in an increase in the efficiency.

2) As shown in Figure 5.2 (step 2) part of the total charge consumed during reduction may also be consumed by the incorporation of cations. It has been shown that PPy/PTS undergoes both anion and cation exchange processes during redox reactions[80]. The incorporation of cations (or protons) during

reduction (instead of expulsion of anions) would decrease the calculated efficiencies for transport.

3) Some Faradaic reactions such as the reduction of oxygen may also occur at the negative potentials applied.

TABLE 5.14 Transport Efficiencies (E_f) for the transport of 0.10 M PTS plus the corresponding organic anion (0.10 M) across PPy/PTS membranes.

Anion	Moles of electron consumed (m_e) x 10^4	Moles of anions transported (m_t) x 10^4	$E_f = \frac{m_t}{m_e}$ %
BS	2.16	0.31	14.35
4HBSA	0.82	0.12	14.63
4SBA	0.52	0.06	11.54
3SBA	0.70	0.08	11.42
1,3BDSA	1.23	0.11	8.94

5.3.1.4 EFFECT OF ELECTROCHEMICAL PARAMETERS ON THE TRANSPORT

In an attempt to investigate the effect of pulse width (duration) and pulse height on transport further investigations were carried out. The transport of anions from a solution containing a mixture of 0.10 M BS and 0.10 M PTS was considered.

A pulsed potential waveform with various widths was then applied to the membrane while the pulse height was kept constant (Table 5.15). It was found that as the pulse width increased the flux obtained for either BS or PTS also increased until it reached a maximum value at pulse widths of ~30 s. An unusual increase of flux for PTS was observed when a short pulse (5 s) was employed. This may have been due to the release of PTS (incorporated during synthesis) from the membrane.

At shorter pulse length there was not sufficient time to allow incorporation or expulsion. When the pulse widths increased the flux for both anions also increased since species had enough time to be incorporated/expelled. However at larger widths the maximum amount of incorporation could not be exceeded and the flux decreased. The chronoamperometric response also shows that a pulse width of ~30 s is optimal with respect to the electrochemical reaction (Figure 5.6).

TABLE 5.15 The effect of pulse width on transport (PTS+BS) across PPy/PTS membranes.

Pulse Width (s)	**Flux** (mol $cm^{-2}s^{-1}$) x 10^{10} BS	PTS	**Selectivity factor** $\alpha = \frac{\text{Flux PTS}}{\text{Flux Anion}}$
5	5.45	11.20	2.06
15	7.81	7.85	1.01
30	7.90	8.65	1.09
45	6.54	6.65	1.02
60	4.10	4.40	1.07

*A pulsed potential E_1=-0.60 to E_2=0.40 V (t_1=t_2 as above) was applied to the membranes using the set up shown in Figure 5.2 (method C).

The effect of pulse height was also investigated. As mentioned previously application of pulsed potentials greater than E_1=-1.00 to E_2=0.40 V to the PPy/PTS membranes was not practical due to the deterioration of the mechanical stability of the membranes in media containing the organic anions, except in the case of PTS and BS. Therefore, the effect of various pulse heights was only investigated using PTS or BS (Table 5.16). As the pulse height increased in the negative direction the flux for both anions (BS or PTS) also increased. However, selectivity was not improved. As the CV suggests (Figure 5.1 (a)) the observed increase in the fluxes was presumably due to the completion of the redox reactions occurring at more negative potentials. Application of more positive potentials was not attempted since the CV indicated that 0.40 V was sufficient to oxidise the polymer.

TABLE 5.16 Transport of a mixture of 0.10 M BS and 0.10 M PTS across PPy/PTS membrane.

Flux* **(mol cm^{-2} s^{-1}) x 10^9**		
BS	**PTS**	$\sigma = \frac{\text{Flux PTS}}{\text{Flux Anion}}$
1.05	1.16	1.10

*A pulsed potential E_1=-1.00 to E_2=0.40 V t_1=t_2=30 s was applied to the membranes using the set up shown in Figure 5.2 (method C). In this set up the membrane was reduced by application of a potential to the source side for a fixed period of time before the receiver side was oxidised. Flux was calculated over the period the potential was applied, ie: 45 minutes

The effect of the membrane side exposed to source solution. Scanning electron micrographs have revealed different surface topographies on each side of the PPy/PTS membranes[87]. Throughout this work the plate side of the membrane (i.e. the side that remained in contact with the electrode during polymerisation) was exposed to the source solution. However, as shown in Table 5.17 the transport behaviour was independent of the side of the membrane exposed to the source solution indicating that a symmetric membrane was produced with respect to the transport characteristics under the conditions used.

TABLE 5.17 Transport of 0.20 M BS across PPy/PTS membranes.

	Flux* (mol cm^{-2} s^{-1}) x 10^9
A	1.60
B	1.49

* Experimental conditions as in Table 5.6.

(A) Solution side of the membrane exposed to source side.

(B) Plate side of the membrane exposed to the source side.

5.3.2 TRANSPORT OF ANIONS ACROSS PPy/PVS MEMBRANES

Using benzene sulfonate as a test case, it was found that without a potential applied to the PPy/PVS membranes no transport of anions was obtainable. In addition, application of the stimuli (Figure 5.2) that facilitated transport of anions across the PPy/PTS membrane did not do so across the composite polymers. With this potential waveform the membrane was oxidised at the source side for a fixed period of time then it was reduced in the receiver side (Figure 5.2). The lack of transport of anions was most likely due to the immobile nature of PVS which is tightly trapped in the membrane and therefore no movement of anions (steps 1,3) was possible. When the membrane is oxidised/reduced cation movement is used to maintain charge neutrality (steps 2,4). These observations are in agreement with the results shown in Chapter 4 (see method A).

In order to compare the ion exchange capacities of both PPy/PTS and PPy/PVS membranes, the transport of BSNa as a test system was investigated (Table 5.18). It was found that:

1) Transport of either anions or cations was possible across PPy/PTS membranes while only cations were allowed to move across PPy/PVS membranes.

2) Cations were more readily transported across PPy/PVS than PPy/PTS membranes. This is presumably due to enhanced cation exchange capacity of PPy-PVS, in agreement with the observation made in Chapter 4.

TABLE 5.18 Transport of 0.20 M BSNa across PPy/PTS and PPy/PVS membranes with different potential waveforms applied.

	Flux (mol cm^{-2} s^{-1}) x 10^9			
Method employed	**Method B**		**Method C**	
	BS	Na^+	BS	Na^+
PPy/PTS	0.02	2.92	1.49	0.00
PPy/PVS	0.00	4.65	0.07	0.00

Method B See Figure 4.20.
Method A See Figure 5.2.

5.3.3 MECHANISM OF TRANSPORT

The redox reactions encouraging transport across both PPy/PTS and PPy/PVS membranes can be illustrated by:

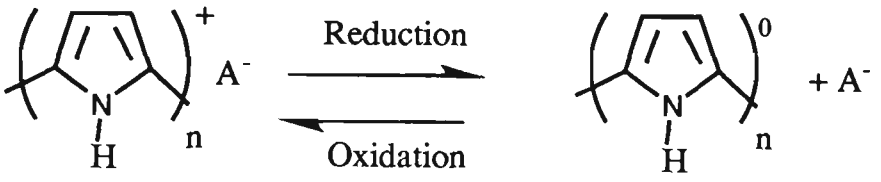

(5.3)

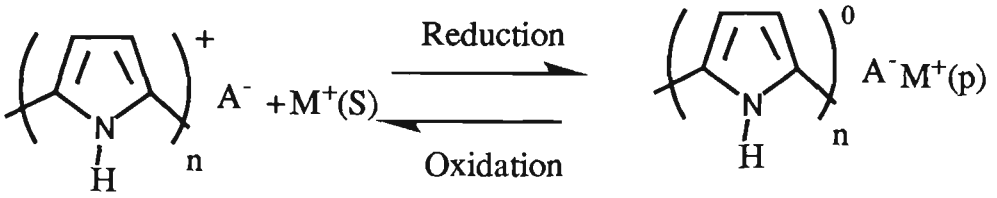

(5.4)

where A^- is the counterion incorporated during synthesis and/or anion incorporated from the electrolyte solution and M^+ is the cation in the electrolyte solution in which the polymer is oxidised/reduced. As previously discussed (Section 1.2.2), when A^- (the counterion that is within the polymer) is mobile enough to be expelled into the solution the behaviour described by Equation 5.3 predominates. However when the counterion is relatively immobile it does not leave the polymer during reduction and the cation from the solution ($M^+(S)$) is incorporated into the polymer ($M^+(p)$) to maintain charge neutrality (Equation 5.4).

It was shown that the transport of both cations and anions across PPy/PTS was possible (Table 5.18). Transport of anions and cations occurred as per Equations 5.3 and 5.4 respectively. It can be assumed that PPy/PTS contains

some mobile anions (Figure 5.7) which can readily move in/out of the polymer (loosely held anions) as well as some deeply trapped anions (inner layer). The parts of the membrane containing mobile counterions would act as binding sites to encourage transport of anions. However, in the inner layers charge neutrality is maintained by cation movements (Figure 5.7 & Equation 5.4). The fact that the transport efficiency of the anions was low (Table 5.14) was partly due to the incorporation/expulsion of cations (Equation 5.4) in the inner layer during transport of anions.

The mechanism of the transport in the case of PPy/PVS was also involved with the reactions shown in Equations 5.3 and 5.4. However, the fact that the transport of anions was negligible while the transport of cations readily occurred (Table 5.18) indicates that the reaction shown in Equation 5.4 predominates.

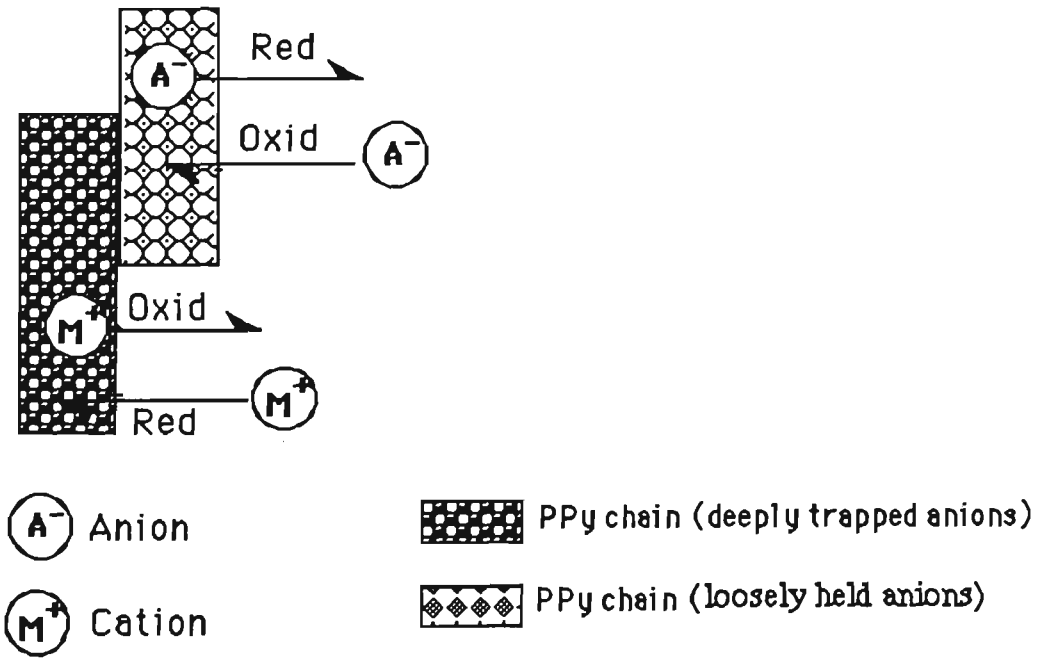

FIGURE 5.7 A schematic of ion movement in PPy/PTS upon oxidation/ reduction.

With both PPy/PTS and PPy/PVS the reduction of the polymer in the source side, facilitating transport of cations, resulted in an decrease of the solution pH. This indicates that while the incorporation of cations was occurring in the membrane the water was oxidised at the auxiliary electrode (Equation 4.3). Transport of anions was accompanied by the oxidation of the membrane in the source side. This resulted in an increase of pH in the source solution as the water was reduced to produce OH^- anions at the auxiliary electrode (Equation 4.1). A converse change in the solution pH occurred in the receiver side with generation of H^+ ions.

5.4 CONCLUSION

In this Chapter it has been shown that electrochemically controlled transport of organic anions across conducting polymer membranes is possible. Transport of sulfonated aromatics with various functional groups was investigated. It was found that the rate of transport of compounds with substituents of an electron withdrawing nature was markedly lower than those that had no substituent or with a substituent of an electron donating nature. In addition, it was found that the position of the functional group had a marked influence on the transport, indicating that a high degree of selectivity is attainable. The transport of species with two charged sites was insignificant, suggesting a strong affinity for the oxidised polypyrrole.

Separation of the organic compounds using the membranes was also investigated. Various selectivity factors were obtained indicating that electrochemically controlled separation of organic compounds can be achieved.

Two different classes of membranes were employed, one with a relatively mobile counterion (PPy/PTS) and the other less mobile (PPy/PVS). It was found that the anions were readily transported across PPy/PTS membranes. However, transport of the anions across PPy/PVS membranes was insignificant. The rate of transport of cations was much higher with PPy/PVS membranes. This indicates that due to the immobile nature of PVS the membrane formed with this counterion tends to be more useful as a cation exchanger. However, a shortage of mobile anions in the polymer matrix prevented transport of anions across the membranes. These results support the observations made in Chapter 4 where the preparation of a composite material (PPy/PVS) for the purpose of cation transport was considered.

From the present findings, it can be suggested that when the transport of anions is desired, PPy/PTS membranes should be employed while with the transport of cations PPy/PVS membranes should be selected.

The application of a different cell set up was also demonstrated in these investigations. It was shown that the cell configuration was extremely important with respect to the rate of transport. The best cell configurations were illustrated for the transport of cations and anions.

Although the results shown in this Chapter and Chapter 4 provided some information about the mechanism of transport and the ion exchange properties of the membranes, the use of an electrochemical technique that can evaluate the results seems to be needed. The newly established technique of Electrochemical Quartz Crystal Microbalance (EQCM) is suitable for this and is discussed in Chapter 6.

CHAPTER 6

MECHANISTIC STUDIES USING ELECTROCHEMICAL QUARTZ CRYSTAL MICROBALANCE (EQCM)

6.1 INTRODUCTION

This Chapter introduces and evaluates the technique of Quartz Crystal Microbalance (QCM). This is a low cost piezoelectric technique where small changes in mass can be detected by measuring the frequency of oscillation of a quartz crystal[192]. This technique has recently attracted much attention in the area of conducting polymers [41, 193, 194].

Background. In 1880, the Curie brothers discovered the piezoelectric effect[195]. They showed that when certain crystals, including quartz and rochelle salts ($NaKC_4H_4O_6.4H_2O$), were compressed in particular directions an electrical potential was produced between the deformed surfaces. The magnitude of this potential was proportional to the applied stress[195]. This behaviour is referred to as the piezoelectric effect. Shortly after the initial discovery the converse piezoelectric effect was verified. In this phenomenon application of a voltage across the crystal caused a corresponding mechanical strain. The converse piezoelectric effect is the basis of QCM.

The piezoelectric effect remained a purely academic concept until 1946, when Langevin[196] employed quartz plates to serve as emitters and receivers of high-frequency waves under water leading to the development of sonar.

This discovery was the spark that initiated the transformation of the piezoelectric effect from a scientific curiosity to a widely exploited phenomenon with applications in both science and engineering. In 1957 Sauerbrey showed that these devices could be used to measure mass changes at a crystal surface[197]. He derived an expression relating the changes in frequency to the mass of material deposited on the metal coated crystal.

Twelve years later the use of a QCM as an electrochemical method to monitor small changes by the electrodeposition of metals onto a gold electrode was

demonstrated by Jones and Meiure[198]. They determined the concentration of trace metals (e.g. cadmium) using a quartz crystal electrode. A current was allowed to pass for a known period of time and the crystal was removed from the cell, washed and dried. The mass increase was then determined from the changes in frequency.

Until 1980 it was thought that these crystals would not oscillate in liquids due to excessive energy loss to the solution from viscosity effects[192]. At that time Konash and Bastiaans[199] demonstrated the application of the piezoelectric crystal as a mass detector in a liquid environment. They then employed QCM in conjunction with liquid chromatography. Shortly after Nomura and co-workers demonstrated the first in-situ applications of the QCM in analytical chemistry[200, 201]. In the first attempt the change in the frequency of a horizontal quartz crystal in contact with a single drop of solution was measured when the gold electrode of the crystal was dissolved by reaction with cyanide in alkaline solution[201]. The changes of frequency were linearly related to cyanide concentration in the range of 10^{-3} -10^{-4} M at pH 10.4. In another report[200] in-situ determination of silver in solution by the frequency change of a piezoelectric quartz crystal was demonstrated. After these investigations the in-situ application of the QCM to electrochemical systems was referred to as electrochemical quartz crystal microbalance (EQCM).

QCM has been used to study the structure of conventional polymers. For example interactions of solvents with thin polymer films (such as polymethyl methylacrylate) have been demonstrated[202]. It was shown that the polymer swelling could be monitored using this technique.

QCM has also been used in the area of biochemistry[203]. A quartz crystal was used as a viscosity detector for the detection of blood coagulation factors. Due to the blood coagulation, the solution viscosity changed and was monitored

using QCM. A linear relationship was obtained between concentration of the blood coagulation factors and coagulation time.

The EQCM technique was first used for characterisation of conducting polymers in 1984, when Kaufman and co-workers showed that on reduction of a polypyrrole/perchlorate film, charge compensation was achieved by diffusion of the lithium cation into the polymer and not the perchlorate anion into solution[204].

EQCM has also been used to study anodic electropolymerisation of pyrrole[41, 205-207]. A detailed study determining the efficiency of the polymerisation/deposition process as a function of film thickness and the rate of electrodeposition has been described[41]. It was shown that the early stages of film formation were affected by the solubility of the oligomers formed and that the ultimate polymerisation efficiency was electrolyte dependent.

This technique has also been used to study mass transport and ionic motion across polypyrrole films[80, 85, 204, 208]. EQCM gave valuable information about the interaction of polycationic proteins with electroactive polypyrrole/polystyrene sulfonate films[193, 209]. Polypyrrole was also employed as a gas sensor in conjunction with EQCM[194]. A series of experiments was designed to test both selectivity and sensitivity of a polymer-coated sensor towards the target gases. The different response profiles were recorded for the gases under investigation.

Ion movement during the doping/dedoping process in polypyrrole has also been studied using EQCM[210]. The corresponding frequency-charge relationships were plotted for different electrolytes. A linear relationship with approximately the same slope for charging and discharging was found. From

this slope the stoichiometry of ion movement (the ratio of anion to cation) during the redox process was calculated.

Since the first report on polypyrrole this technique has been used successfully for characterisation of polyaniline, copolymers and composite polymers. Buttry demonstrated determination of ion population and solvent content as a function of redox state and pH in polyaniline[211]. The data were shown to be consistent with a model for polyaniline in which the initial oxidation at a potential of ca. 0.20 V vs SCE creates charged sites by oxidation of amine moieties along the polymer chain to give the conductive form of the polymer. Others have used EQCM to study redox reactions in polyaniline[212- 214].

The technique has also been used to aid identification of ionic species that are involved in redox reactions during switching of the polymer between its insulating and conducting forms. In polyaniline/Nafion composites the frequency changes observed in solution containing various cationic species suggest that cation transport is predominant[215].

Counterion injection and release is known to accompany oxidation-reduction of polypyrrole films. Recent studies of some polypyrrole composite films with EQCM have revealed more details on both counterion movement and simultaneous solvent and or cation movement[36]. Analysis of EQCM data for the fully cycled films showed that cations were being inserted and removed at more negative potentials (i.e. -0.30 to -0.70 V vs SCE) while anions were being inserted and removed at more positive potentials[36](i.e. -0.30 to 0.30 V).

Theory of quartz crystal microbalance. The converse piezoelectric effect is the basis of the QCM where application of an electric field across a non-centrosymmetric (acentric) crystal produces a shear strain proportional to the applied potential. Crystal symmetry dictates that strain induced in a

piezoelectric material by an applied potential of one polarity will be equal and opposite in direction to that resulting from the opposite polarity[216]. This is depicted in Figure 6.1 for the shear motion of the AT-cut quartz resonator.

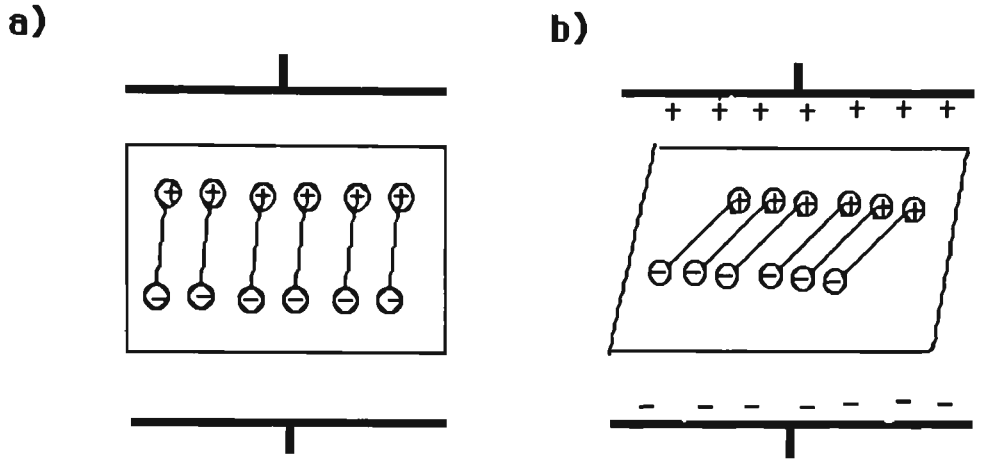

FIGURE 6.1 Schematic representation of the converse piezoelectric effect for shear motion.
(a) No field applied
(b) Electrical field applied.
The electric field includes reorientation of the dipoles of the acentric material, resulting in a shear deformation of the material. Redrawn from reference 216.

In quartz this deformation is elastic. The opposite polarity produces an identical strain, but in the opposite direction. An alternating potential across the crystal causes a vibrational motion in the quartz crystal, with amplitude parallel to the surface of the crystal. It is important to know that only crystals cut with the proper angles (i.e AT-cut) with respect to the crystallographic axis exhibit shear displacement[216].

As a result of vibrational motion of the quartz crystal a transverse acoustic wave is produced that propagates across the thickness of the crystal at the surface. A standing wave condition can therefore be applied:

$$f_o = \frac{V_{tr}}{2tq} = \frac{\mu_g^{1/2}/d_g^{1/2}}{2tq} \quad (6.1)$$

where f_o is the frequency of quartz crystal, V_{tr} is the transverse velocity of sound in AT cut quartz (3.34×10^4 m s^{-1}), t_q is the thickness of the crystal, d_g is the density of the quartz and μ_g is the shear modulus of the quartz.

Sauerbrey[197] utilised this idea as the basis of a sensitive microbalance technique. He showed that when a uniform layer of a foreign material is added to the surface of the quartz crystal, this will affect the frequency of the oscillation, if the assumption is made that the acoustic properties of the foreign layer are identical to those of quartz. This system can be treated as a "composite resonator". Sauerbrey showed that the thickness $t_q(m)$ of the quartz plate is related to its mass according to the Equation :

$$t_q = \frac{M}{dg.A} \quad (6.2)$$

where A is the area of the quartz plate undergoing oscillation and M is the mass (g) of the oscillating quartz.

A fractional change in thickness (Δt_q) then results in a fractional change in frequency (Δf):

$$\frac{\Delta f}{fo} = \frac{\Delta t_q}{t_q} \quad (6.3)$$

Substituting t_q from Equation 6.1 into Equation 6.3 results:

$$\frac{\Delta f}{fo} = \frac{2fo\,\Delta tq}{Vtr} = \frac{-2fo\,\Delta tq}{\mu g^{1/2}/dg^{1/2}} \quad (6.4)$$

Combining Equations 6.2 and 6.4 yields:

$$\Delta f = \frac{-2f_0^2\,\Delta m}{A\,(\mu g.dg)^{1/2}} \quad (6.5)$$

Equation 6.5 is the most useful formula for the EQCM, where Δm is the mass change and Δf is the measured frequency shift. Substituting for the various constants for an AT-cut crystal gives Equation 6.6:

$$\Delta f = \frac{-2.26.10^6 \ f_0^2 \Delta m}{A} \qquad (6.6)$$

where f_0 is the fundamental frequency of the crystal (Hz) and Δm is the mass of deposited material (g) and A is the coated area (cm^2).

Equation 6.6 predicts that in an AT cut 10 MHz crystal the mass sensitivity per unit area to be 0.226 Hz cm^2 ng^{-1}. Thus a crystal having a projected area of 0.25 cm^2 should have an absolute mass sensitivity of 0.904 Hz ng^{-1}.

In Chapter 5 it was demonstrated that the transport of a wide range of sulfonated aromatic compounds was possible. We therefore initiated an investigation aimed at establishing the relationship between the macroscopic properties of the polymer in the presence of the organic species as observed by transport studies and the microscopic properties using EQCM. A mechanism of transport is then postulated. Such studies were also carried out for composite polymers. No EQCM studies were carried out on polyaniline since the nature of the method used to prepare the membranes (chemical casting) was quite different from the electropolymerisation that can be applied with QCM.

6.2 EXPERIMENTAL

6.2.1 REAGENTS AND MATERIALS

All chemicals and instruments were as previously described (Chapters 2-5). All solutions were filtered using a 0.45 μm Nylon filter membrane and degassed prior to use.

6.2.2 EQCM APPARATUS

Figure 6.2 shows a block diagram of the EQCM instrument used in this work. The resonant frequency of the quartz oscillator is converted to a proportional voltage via a F-V converter and recorded using a MacLab™/4 analog to digital converter and Macintosh computer. The charge was determined using CV-27 BAS coulometer.

The quartz crystal is mounted in the electrochemical cell (Figure 6.3). The oscillator circuit, including the crystals, is enclosed in a Faraday cage. With our set up a minimum mass change of 10 ng could be monitored.

6.2.2.1 CRYSTALS

The 10 MHz crystals were purchased from International Crystal Manufacturing Company (ICM), Oklahoma, USA. According to the supplier the density and shear modulus of the crystals was 2.65 g cm^{-3} and 2.98 x 10^{11} dynes cm^{-2} respectively.

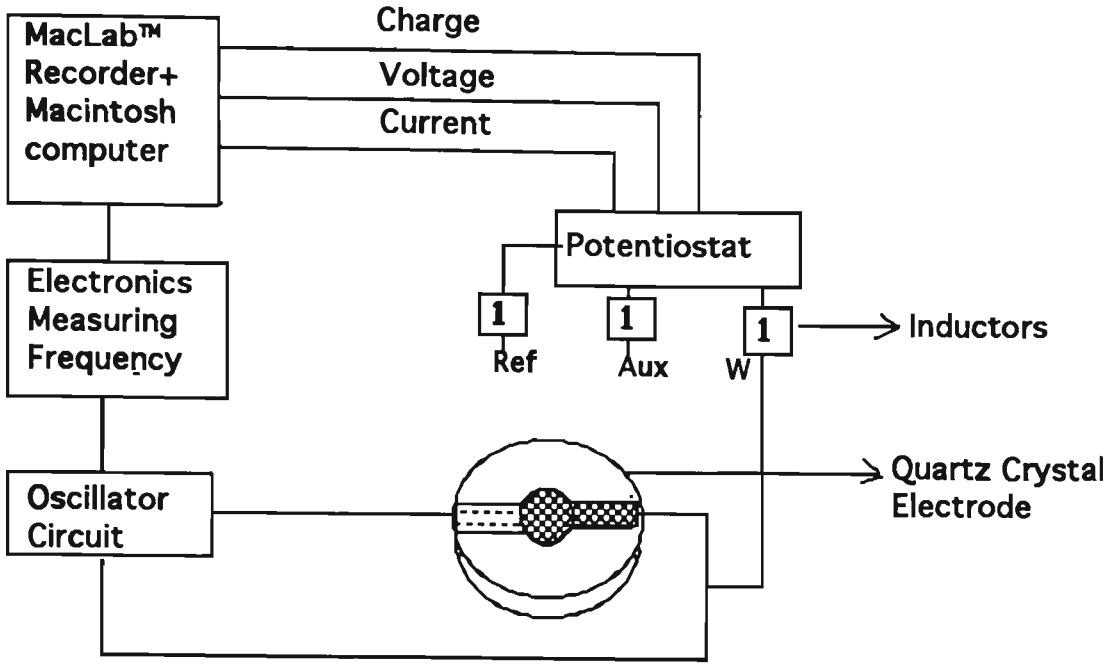

FIGURE 6.2 Block diagram of EQCM Apparatus.

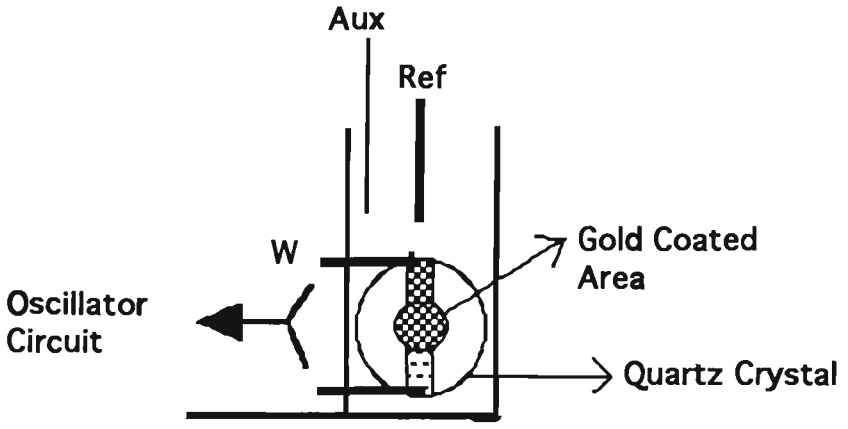

FIGURE 6.3 The Electrochemical cell used for EQCM.

The effect of temperature variation was minimised by the use of AT cut crystal plates. The crystal was sandwiched between two vacuum deposited gold electrodes. The working electrode was the vapor-deposited gold electrode on the quartz crystal face in contact with solution. It was connected to a potentiostat via 10 mH inductors to isolate oscillator electronics from noise introduced by the potentiostat. We found that the circuit without the inductors would not oscillate in a stable fashion. The electrode had a circular

region with a projected area of 0.20 cm^2. This circular region was connected to the electrical circuit by using a gold flag electrode (Figure 6.2). The area of the flag was typically 0.04 ± 0.01 cm^2. Therefore, the geometric working electrode area was about 0.24 ± 0.01 cm^2. The other face of the crystal with the same surface area was exposed to air.

Experiments were carried out in a three electrode system (Figure 6.3). The leads to the reference and auxiliary electrodes also had 10 mH inductors inserted between the potentiostat and the electrodes. The quartz crystal plate was sealed to the cell with a silicone rubber sealant. The connections between cell and circuit were made in a manner that minimises the capacitance effect. The crystals were mounted in the cell in a position that the effect of liquid height on crystal frequency is minimised. Such an effect was therefore negligible in our studies. All these items were designed and constructed in the Electronic Workshop at the University of Wollongong.

6.2.2.2 OSCILLATOR CIRCUIT

The oscillator circuit used (Appendix) is essentially the same as that designed by S. Bruckenstein and M. Shay[217]. However, some modification of the original design was carried out as a part of the current study.

In both designs, the oscillation frequency of the EQCM crystal was measured with respect to a reference crystal which is external to the electrochemical cell. The output was then sent either to a frequency-to-voltage converter or frequency counter. Since the magnitude of the initial difference in frequency between working crystal and reference crystal is large (typically ~20 KHz) in comparison to the frequency change due to the electrochemical reactions, a stable and adjustable frequency off-set phase-locked loop circuit was used in

conjunction with the original circuit. The frequency resolution was improved using this circuit. Schematics for the home designed offset circuit and the original circuit are shown in Appendix.

We have found that the working crystal did not lock into its operating frequency when some conducting polymers were used (e.g. PPy/PVS). This was corrected by replacing the values of capacitor (3) used in the oscillator loop in the original circuit[217]. This was done by tuning the 25 pF capacitor up or down by a few pF.

6.2.3 FILM PREPARATION

The films were prepared in the same manner as that employed to prepare membranes (Chapters 4, 5).

PPy/PTS was prepared by electropolymerisation from a solution containing 0.20 M pyrrole and 0.05 M PTS. A constant current of 2.0 mA cm^{-2} was employed.

PPy/PVS was prepared using a solution containing 0.20 M pyrrole, 10.0 g L^{-1} PVS and 7.2 g L^{-1} NDS with a constant current of 2.0 mA cm^{-2}.

6.3 RESULTS AND DISCUSSIONS

Calibration of the EQCM. The mass sensitivity of the EQCM was investigated by deposition of silver from $AgNO_3$ solution. Silver was deposited from a solution of 0.001 M $AgNO_3$ in 0.20 M perchloric acid with a constant potential of 0.10 V vs Ag/AgCl (it should be noted that the correlation between Q and m is strictly valid only at constant potentials). The charge was determined in-situ using a coulometer (see experimental Section). The expected mass deposited was calculated using Faraday's law and assuming 100% current efficiency. Faraday's law states that the mass of different substrates deposited at the electrode by a given quantity of electricity is proportional to the respective equivalent mass. From the charge passed in the electrodeposition of silver ions at constant potential, the corresponding mass was obtained by :

$$\Delta m = \frac{A_{Ag}\Delta Q}{ZF} \qquad (6.7)$$

where A_{Ag} is the atomic weight of silver (107.87 g mol^{-1}), Z is electrovalency (+1) and F the Faraday constant (F=96485 C mol^{-1}).

The frequency shift due to the deposition of silver ions was measured with the EQCM and the corresponding mass changes were calculated by Faraday's law. By plotting ΔF, measured by EQCM during deposition, versus the amount of mass calculated by Equation (6.7), the slope yields the mass sensitivity (Figure 6.4).

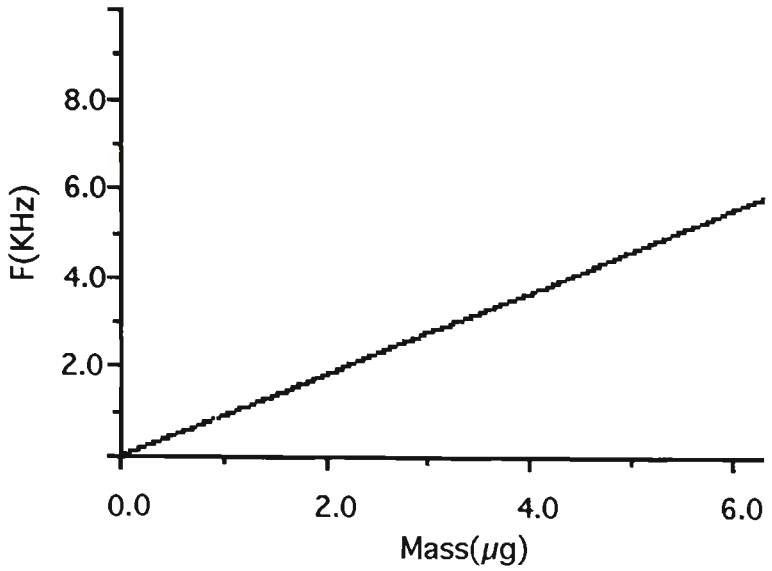

FIGURE 6.4 Frequency-mass relationship for deposition of Ag from a 0.001M solution of $AgNO_3$ solution. Mass changes were calculated from Equation 6.7 and frequency shift measured by EQCM. The slope of the graph gives the mass sensitivity of the EQCM.

In order to evaluate the reproduciblity of the results the experiment was carried out on four different crystals and each experiment was repeated three times. An average mass sensitivity of 0.97 Hz ng^{-1} with a standard deviation of ±0.07 Hz ng^{-1} was obtained (Table 6.1). Thus a crystal having a projected electrode area of 0.24 cm^2 should have a mass sensitivity per unit area of 0.23 Hz ng^{-1} cm^2. These data are in good agreement (within ± 5%) with the value of 0.22 Hz ng^{-1} cm^2 predicted by Equation 6.6.

TABLE 6.1 Absolute mass sensitivity (Hz ng^{-1}) of EQCM obtained from 4 separate experiments.

Crystals	Mass Sensitivity (Hz ng^{-1})			
	Exp(1)	Exp(2)	Exp(3)	Mean
Crystal (1)	0.93	0.93	0.93	0.92
Crystal (2)	1.09	0.93	0.93	0.98
Crystal (3)	0.98	0.95	0.94	0.96
Crystal (4)	1.20	0.93	0.97	1.03

The geometric working electrode area was 0.24 ± 0.01 cm^2.

Charge-frequency relationship. In order to apply Equation 6.6 the assumption has been made that the acoustic properties of the foreign layer are identical to those of the quartz. This assumption is valid only if a rigid material is deposited. It has been shown that polymer films can be treated as rigid and free from elastomeric effects if a linear change of frequency with charge is observed during polymerisation[36, 80, 216].

In our case the rigidity of the films was examined by plotting the frequency change upon deposition of the film versus the charge consumed during polymerisation. A linear relationship between the charge and frequency change was observed for almost the entire range investigated for the PPy/PTS polymers. A typical graph of the relationship between charge and frequency for PPy/PTS growth is shown in Figure 6.5. This indicates that the polymers

could be treated as rigid and free of viscoelastic effects, and validates the use of Equation 6.6 over the mass range of interest.

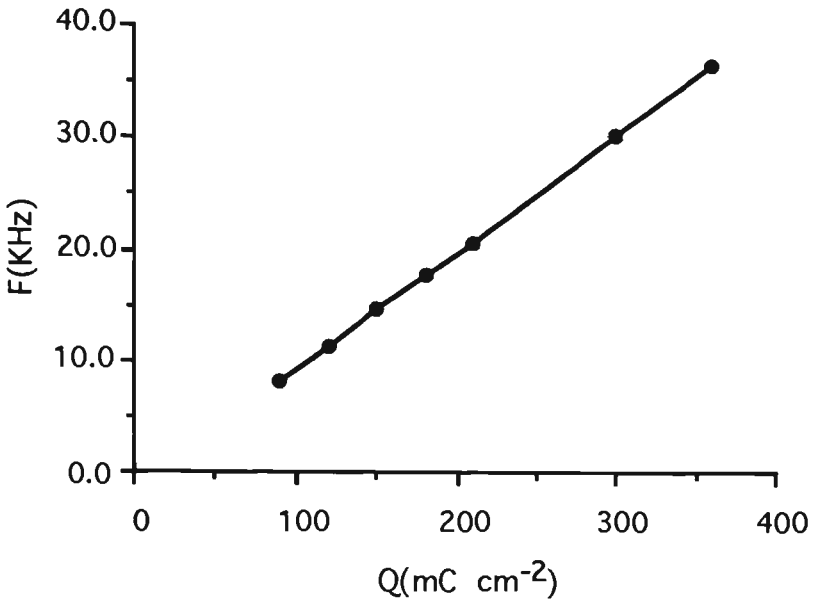

FIGURE 6.5 Relationship between the total charge passed during the growth of PPy/PTS and the resulting frequency shift.

Reproducibility of Polymer Growth. In order to illustrate the reproducibility of the charge versus mass measurements during polymer growth, ten separate experiments were performed on different days. The total charge consumed during each polymerisation was 120 mC cm^{-2}. This corresponded to an average mass change of 11.90 ± 0.14 μg for 10 different experiments.

Effect of polymer thickness. The effect of polymer thickness on the response to the mass change was investigated by application of a pulsed potential. The charge consumed for the electropolymerisation was varied from 90 mC cm^{-2} to 360 mC cm^{-2} resulting in corresponding differences in thickness. Since there was no method available for direct measurement of polymer thickness at the surface of the crystal electrode, charge densities consumed during polymerisation were used as a thickness indicator, with thickness

increasing with increasing charge consumption. A pulse potential was then applied to polymers of different thickness in the presence of a 0.20 M BS solution. The film stability was evaluated by pulsing for several minutes.

Figure 6.6 (a) shows a typical response obtained for the polymer grown with 90 mC cm^{-2}. It was found that the mass of the polymer decreased on reduction and increased on oxidation. This was the case for the entire range of polymer thicknesses. However, only for the thinner polymers (where less than 150 mC cm^{-2} charge was consumed during polymerisation) were the mass changes reversible (Figure 6.6 (a,b)). The mass increase during oxidation was equal to the decrease in mass upon reduction.

The thicker polymers did not exhibit such behaviour (Figure 6.6 (c,d)). In fact as the polymer thickness increased the nature of the response was distorted. Figure 6.6 (d) shows the result observed for a very thick polymer prepared with 360 mC cm^{-2} charge. The large net weight loss was observed over a short period of time.

Thicker polymers have greater surface areas and therefore a larger mass exchange between polymer and solution is expected in a short period of time. It is believed that when a large mass is expelled from the polymer in a short period of time, the polymer rigidity is affected. Consequently, a deviation of the acoustic impedance of the film from that of the crystal would be expected. This deviation may cause a distortion of the signal as the crystal may no longer oscillate in the appropriate frequency band. In addition, it has been shown that high mass loading on the crystals cause the acoustic impedance of the crystal to change[216]. The remainder of this work was therefore carried out using thin polymers (polymers prepared with 120 mC cm^{-2} charge consumed during polymerisation) where the response was tested as being stable for over 2 hours.

FIGURE 6.6 The PPy/PTS mass change with the application of a pulse potential in 0.20 M BS. Total charge consumed for deposition of the polymer was:
(a) Q=90 mC cm^{-2}
(b) Q=120 mC cm^{-2}
(c) Q=210 mC cm^{-2}
(d) Q=360 mC cm^{-2}
Note that zero mass corresponds to polymer without applied potential.

(a) Q=90 mC cm^{-2}

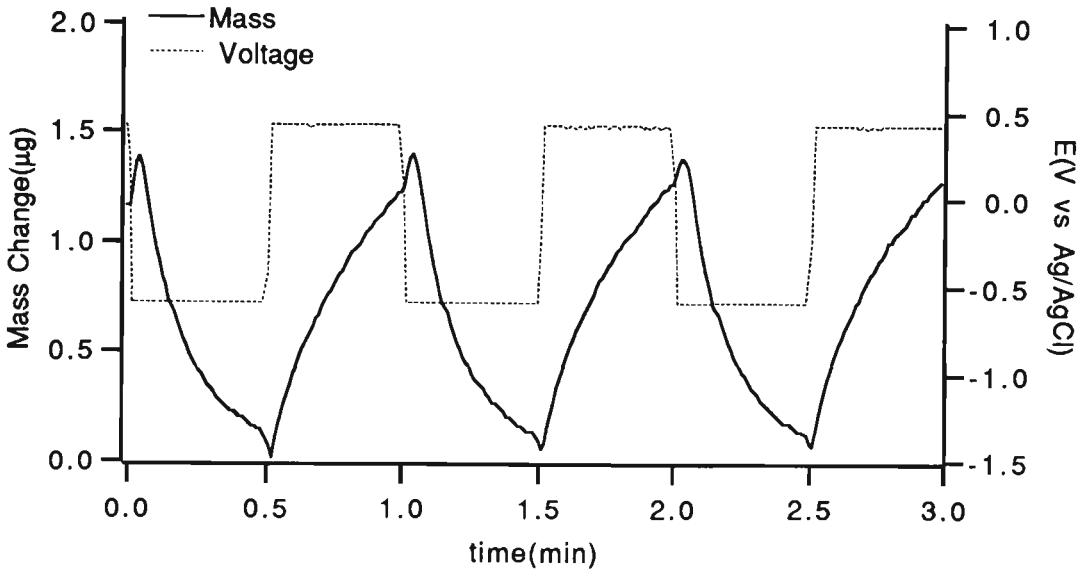

(b) Q=120 mC cm^{-2}

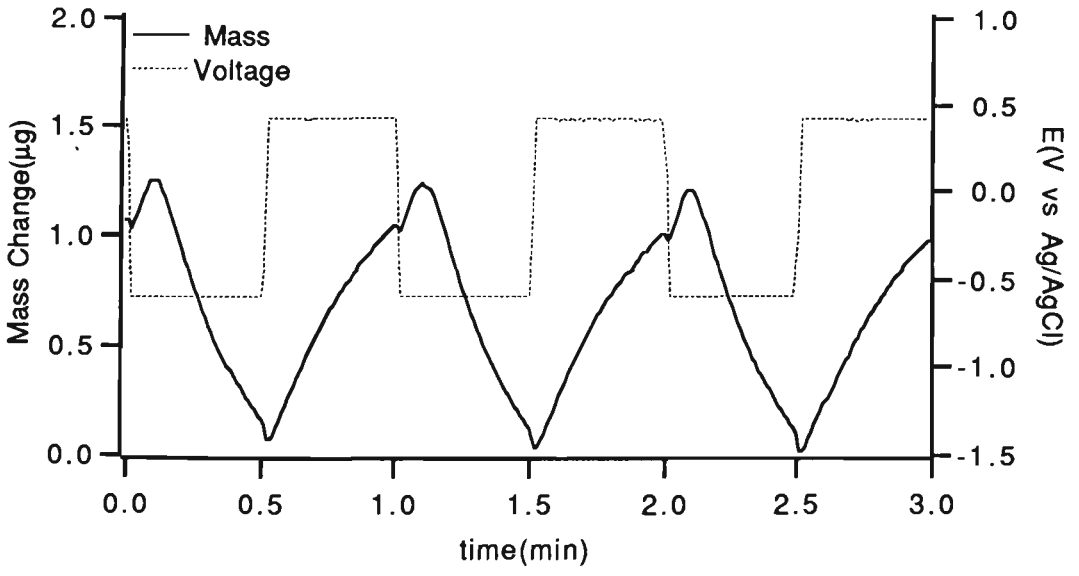

(c) Q=210 mC cm^{-2}

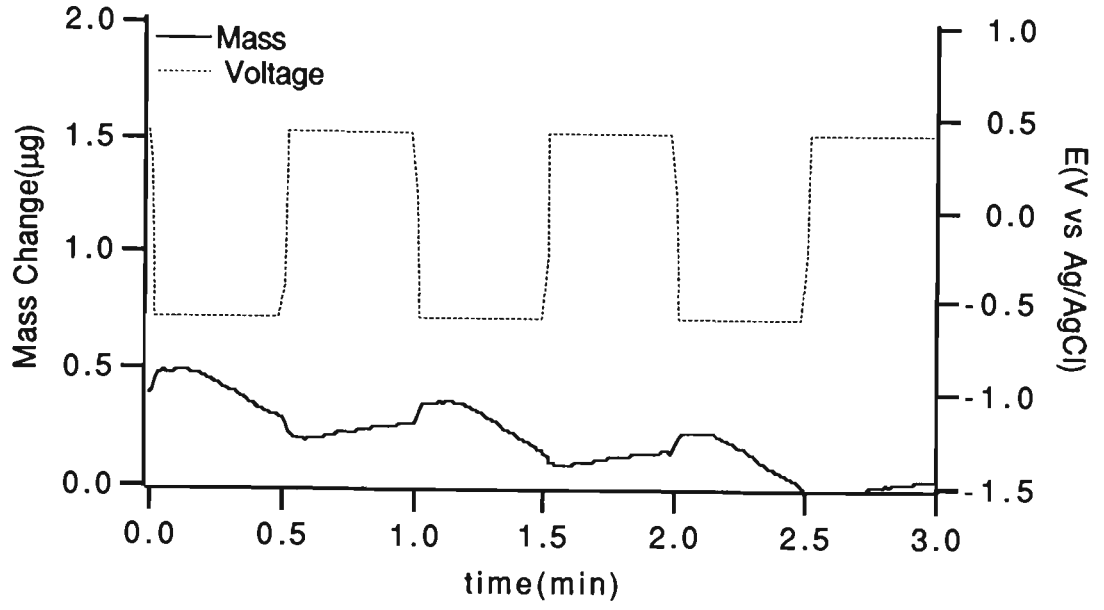

(d) Q=360 mC cm^{-2}

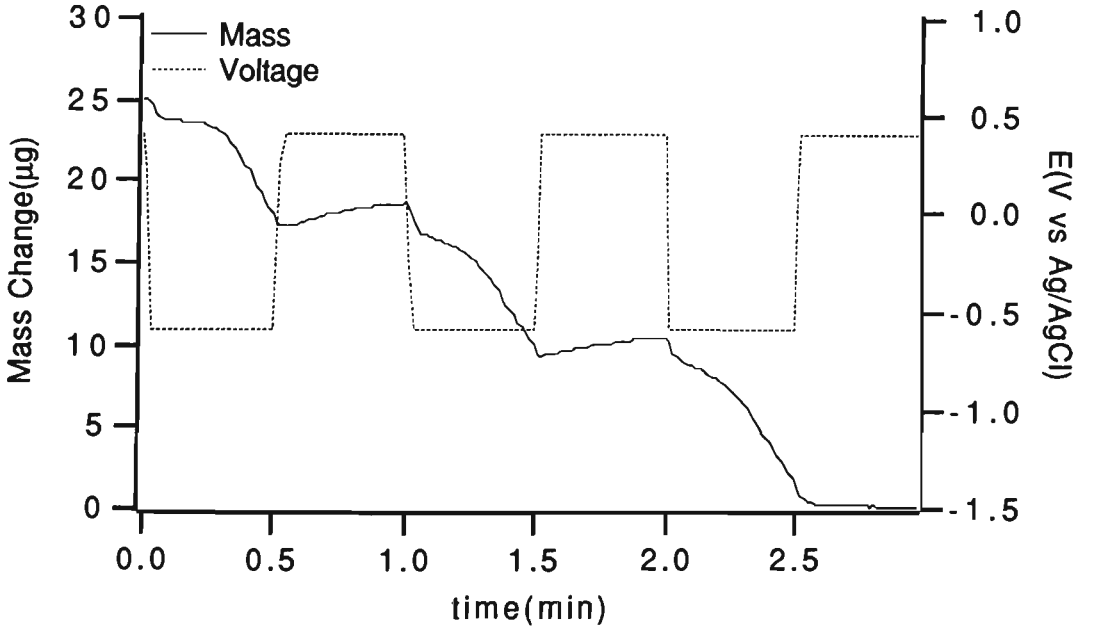

6.3.1 PULSE POTENTIAL STUDIES

The PPy/PTS films were prepared as per Section 6.2.3. A pulse potential of E_1=-0.60 V to E_2=0.40 V and t_1=t_2=30 s was applied to the polymer in the presence of the different organic salts (BS, PTS, 3SBA, 4SBA, 4HBSA, 1,3BDSA) whose transport was considered in Chapter 5. To enable comparison with the transport experiments described in the previous Chapter the pulse potential routine was applied for a period of 45 minutes.

It was found that in general a rapid increase in polymer mass accompanied the first reduction step (presumably due to solvent diffusion), then a regular mass change was recorded upon oxidation and reduction. However, the net polymer mass (the mass difference between two consecutive oxidation or reduction pulses) changed slightly over the period of the experiment (i.e. 45 minutes). The average mass drift varied from 2 to 15% of the main response depending on the nature of the electrolyte used (Table 6.2).

In the case of 3SBA, 4SBA, 1,3BDSA, 4HBSA this shift was positive and in the case of BS it was negative. This may be accounted on the basis of molecular weight of the counterion. In the presence of anions with higher molecular weight (Table 6.2) than the original counterion (PTS) a positive mass shift was obtained indicating the replacement of the original counterions (PTS) by the solution anion. A negative shift was experienced for BS showing replacement of PTS with anions having lower molecular weight (Table 6.2).

Free solvent may also diffuse into the polymer resulting in a mass shift. However, this shift would have been similar for all anions as the same polymer and solvent were employed for all experiments in this section. The fact that the trends were quite different indicates that the process did not predominate.

TABLE 6.2 Mass drift for EQCM studies of PPy/PTS in 0.20 M of supporting electrolyte.

Anion	**Average mass[1] drift per cycle (μg)**	**Average mass[2] change per cycle (μg)**	**% Mass drift to mass change in each cycle**
BS	-0.05	1.25	4.00
4HBSA	0.02	0.21	9.50
3SBA	0.01	0.06	16.66
4SBA	0.05	0.31	16.12
1,3BDSA	0.05	1.98	2.52

[1]Mass drift (the mass difference between two consecutive pulses) was calculated after a pulsed potential of E_1=-0.6V to E_2=0.40 V and t_1=t_2=30 s was applied to the polymer (PPy/PTS).

[2]Mass change was the differences between maximum changes in a cycle and the base line.

(-) Shows that the mass of the polymer decreased when the potential was applied. The average mass drift was obtained for 44 measurements.

These observation of mass drift shows that although most of the available counterions were replaced by solution anions in the first few pulses, there were still some sites available for ion exchange (Figure 6.7). For example in the case of BS ~70% of the total mass was exchanged in the first 9 pulses and the remainder (~ 30%) was exchanged over the next 35 pulses.

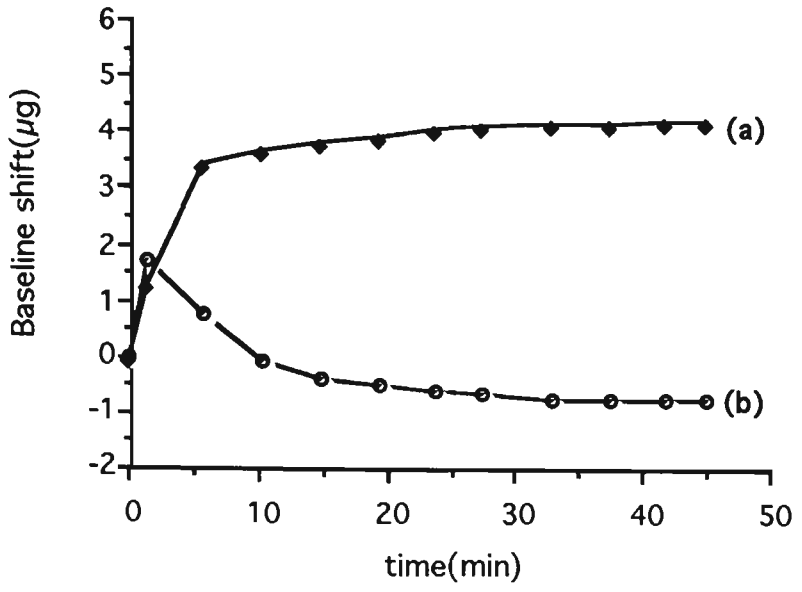

FIGURE 6.7 The net weight of PPy/PTS during pulsed potential experiments.
(a) in 0.20 M 4SBA solution
(b) in 0.20 M BS solution.
Each experimental data point represents the polymer weight between two consecutive pulses over the period of the experiment. A pulsed potential of E_1=-0.60 to E_2=0.40 V and t_1=t_2=30 s was applied to the polymer.

Analysis of the EQCM data for PPy/PTS in the presence of monovalent organic anions showed that the polymer exhibited two different types of behaviour. Where PPy/PTS was in a solution containing either BS, PTS or 4HBSA (Group 1) mass increases upon oxidation and decreases upon reduction were obtained (Figure 6.8). While for Group 2 (3SBA, 4SBA) the reverse response was observed. That is, a mass decrease upon oxidation and an increase upon reduction.

Upon oxidation, charge neutrality can be maintained by outward diffusion of cations or inward diffusion of anions. The solvent may also accompany cations[36] and anions. The fact that for Group 1 compounds the mass of polypyrrole increased upon oxidation suggests that anion diffusion into the

polymer was dominant. The expulsion of the cation from the polymer was not a significant process since this process would have resulted in a decrease in polymer mass. Therefore PPy/PTS in the presence of BS, PTS or 4HBSA acted as an anion exchange polymer under the experimental conditions employed.

Although the trend in mass change for all members of Group 1 was similar, the absolute change in mass varied depending on the nature of the anions. The maximum change was observed with BS and the minimum change for 4HBSA. This may indicate that although the PPy/PTS is defined as anion exchanger in the presence of group 1 compounds, the anion exchange capacity of the polymer in the presence of BS is greater than when PTS or 4HSBA are present.

When the PPy/PTS response in the presence of the anions (Group 1) was studied in more detail it was found that in the early stages of a reductive pulse (for BS and 4HBSA) there was a small mass increase immediately prior to the decrease. Conversely, in the early stages of an oxidative pulse the mass decreased for a very short period of time and then increased (Figure 6.9). We believe that these changes correspond to cation movement since this is the only available possibility to maintain charge neutrality. However, these mass changes were small compared with the main response.

(a) In 0.20 M BS

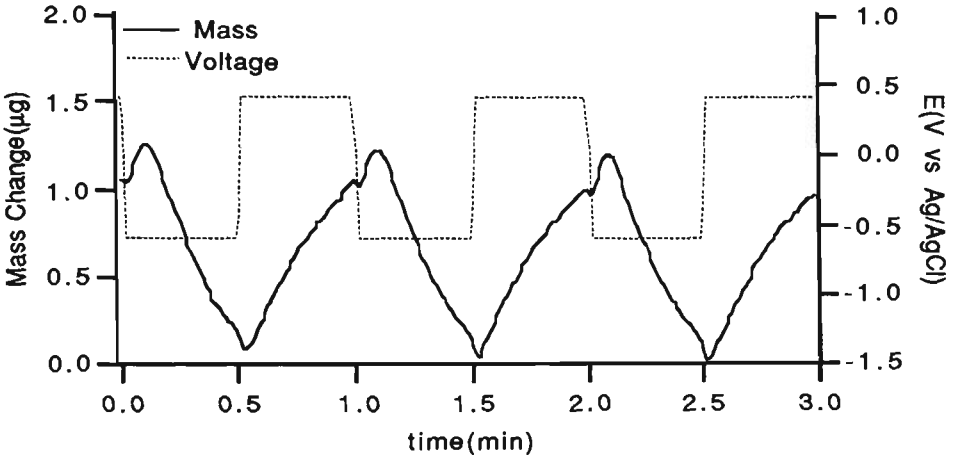

(b) In 0.20 M 4HBSA

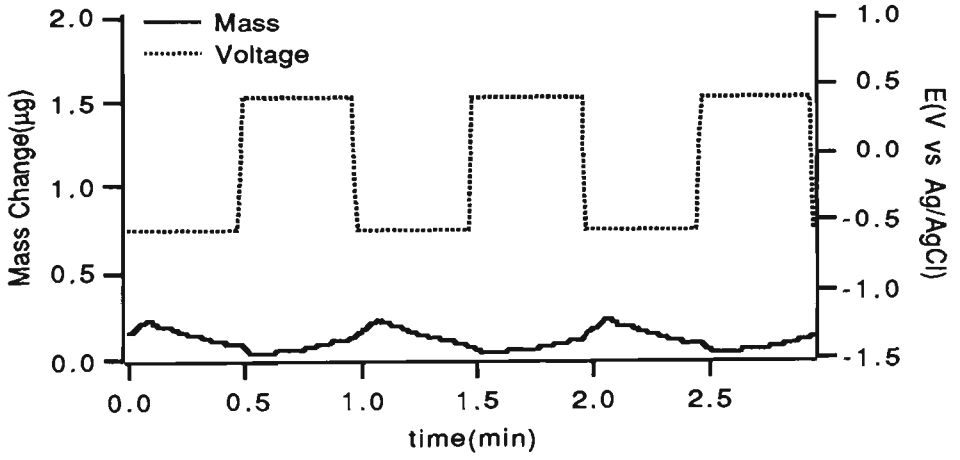

(c) In 0.20 M PTS

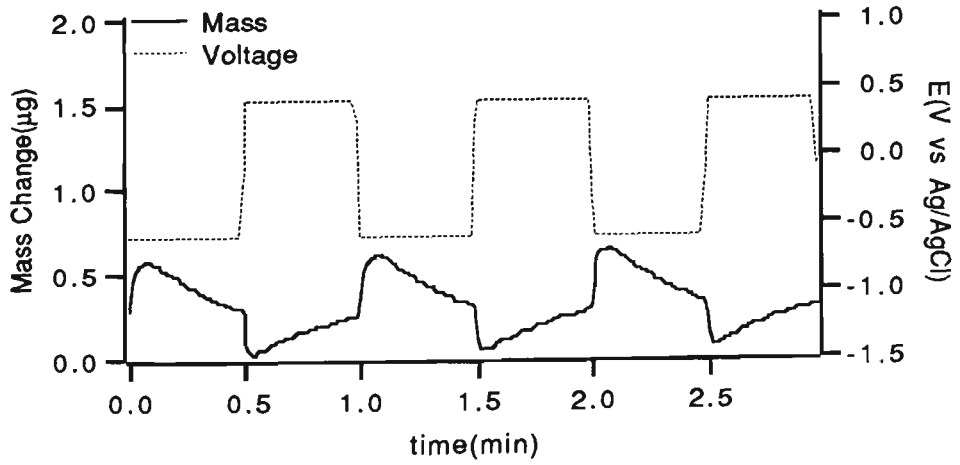

FIGURE 6.8 Mass change for PPy/PTS upon reduction and oxidation for Group 1 compounds. In 0.20 M (a) BS (b) 4HBSA (c) PTS

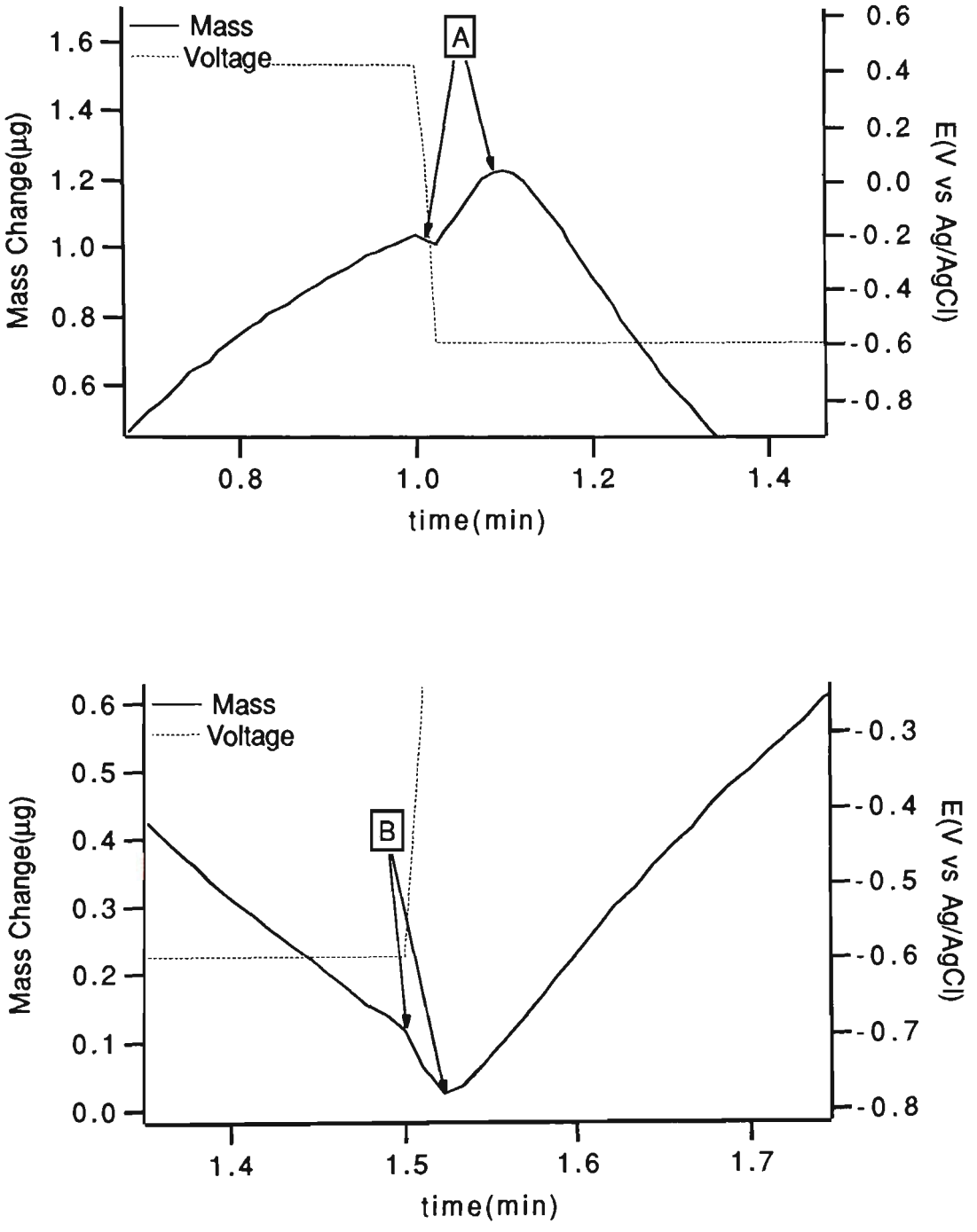

FIGURE 6.9 Enlargement of Figure 6.8 (a).
A A small mass increase in the early stages of reduction.
B A small mass decrease in the early stages of oxidation.

Mass changes in the presence of Group 2 compounds were also recorded (Figure 6.10). Unlike with responses obtained with Group 1 compounds the mass increased upon reduction and decreased upon oxidation of PPy/PTS polymer. In the case of 4SBA (Figure 6.10 (a)) these mass changes are large, but for 3SBA (Figure 6.10 (b)) the changes are very small. It is well known that the polymer charge has to be balanced upon oxidation and reduction, and this can be achieved by incorporation of cations or expulsion of anions during reduction. The former process would increase the mass of the polymer while the latter will result in a mass decrease. Since the mass of the polymer increased during reduction the charge neutrality of the polymer was maintained by insertion of cations (and the solvent) into the polymer. The tosylate (or solution anion) tends to remain in the polymer matrix as the mobile sodium ions exchange between polymer and solution. Hence, the PPy/PTS polymer acts as a cation exchanger in the presence of Group 2 compounds.

Figure 6.11 shows PPy/PTS pulsed in a solution of 1,3BDSA (a divalent anion). The mass of the polymer rapidly increased during reduction and decreased on oxidation. Due to the large mass increase in reduction a large portion of cations (as well as solvent) must be incorporated into the polymer to keep charge neutrality. This might suggest that the 1,3BDSA was strongly trapped in the polymer matrix so that further redox reactions mainly involved cation movement. This is likely since the two charges present in 1,3BDSA would result in a strong affinity for polypyrrole. For this anion the transport was also negligible (Table 5.7). These EQCM results reveal that the insignificant transport observed was due to the strong interaction of the anions with the polymer matrix and therefore cation incorporation/expulsion was the charge balancing mechanism in this case.

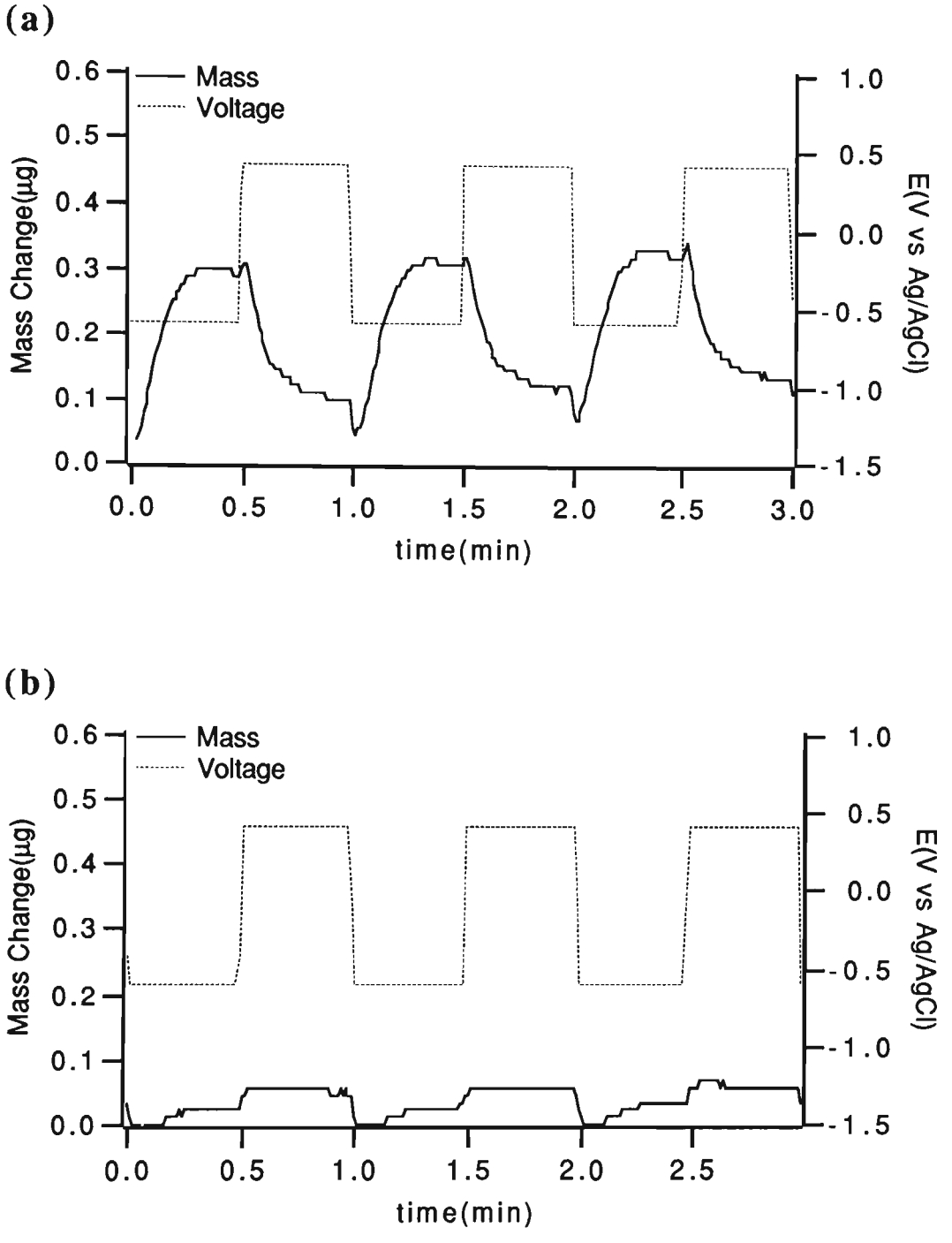

FIGURE 6.10 PPy/PTS mass change upon reduction and oxidation in the presence of Group 2 compounds.

(a) in 0.20 M 4SBA

(b) in 0.20 M 3SBA.

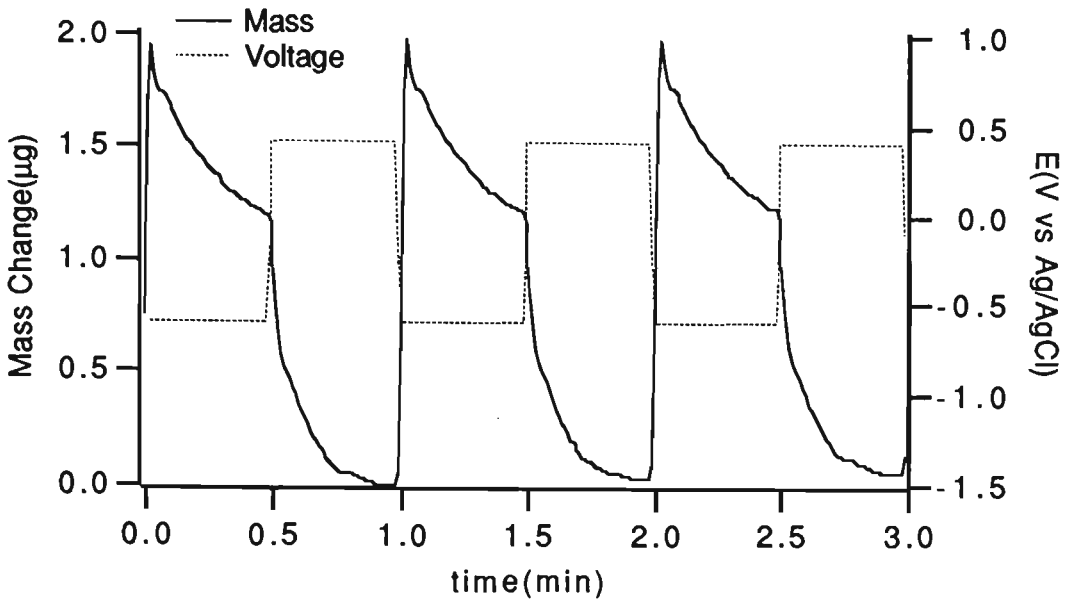

FIGURE 6.11 Mass changes of PPy/PTS due to reduction and oxidation in 0.20 M 1,3BDSA.

Based on the EQCM observations the different reactions occurring during oxidation and reduction may be summarised (Table 6.3). In Chapter 5 it was suggested that the structure of PPy/PTS consists of two layers (Figure 5.7). The charge neutrality in the inner layer, the layer containing deeply trapped anions, is maintained by cation movement whereas the loosely held anions can readily move into/out of the polymer.

In the early stages of reduction the polymer mass increased (stage 1) indicating movement of cation (and solvent) into the polymer (inner layer). With continuing reduction the polymer mass decreased (stage 2) corresponding to anion expulsion from the outer layers of the polymer.

The mass decrease in stage 3 is associated with the expulsion of cations, however the combination of anion incorporation and cation expulsion can also occur (stage 4). Since molecular weight of the cation (Na^+) is ~10 times smaller than the anion, in all stages the role of cations would be dominant. For example, if 10 moles of cations take part in stage 1, less than 1 mole of anion would be expected to be involved in stage 2 providing the same mass change.

Overall, mass increased on reduction and decreased on oxidation. Therefore, the polymer in this medium is considered a cation exchanger.

TABLE 6.3 The proposed reactions occurring when a pulse potential is applied to PPy/PTS in 0.20 M 1,3BDSA solution. X=(PTS) or (1,3BDSA).

Stage	Proposed Equations	EQCM Results
1 (Reduct)	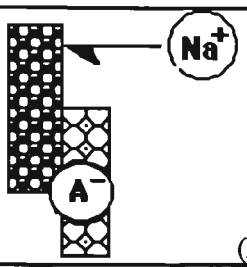 $(PPy)^+(X)^- + (Na^+, XH2O) \rightarrow (PPy)(X)^-Na^+, XH2O$	Mass increase
2 (Reduct)	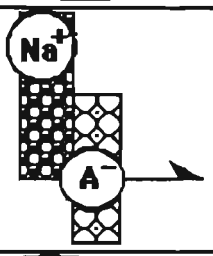 $(PPy)^+(X)^- \rightarrow (PPy) + (X)^-$ (Solution)	Mass decrease
3 (Oxid)	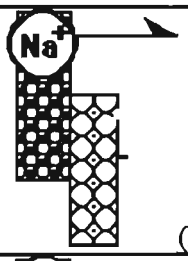 $(PPy)(X)^-Na^+, XH2O \rightarrow (PPy)^+(X)^- + Na^+, XH2O$	Mass decrease
4 (Oxid)	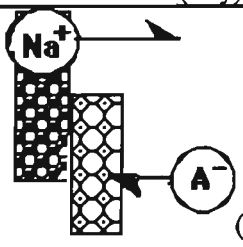 $(PPy)(X)^-Na^+, XH2O \rightarrow (PPy)^+(X)^- + Na^+, XH2O$ $(PPy) + (X)^- \rightarrow (PPy)^+(X)^-$	Mass decrease

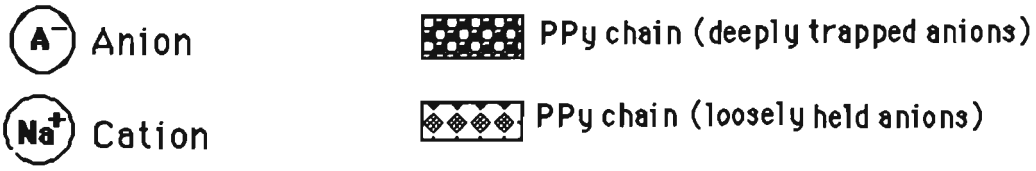

6.3.1.1 QUANTITATIVE ANALYSIS OF THE EQCM DATA

In order to get a more quantitative insight into the exchange of material between polymer and solution during oxidation/reduction processes we calculated the mass changes obtained from the EQCM measurements ($\Delta m_{(EQCM)}$) and from Faraday's Law (Δm_f) using Equations 6.6 and 6.7 respectively (Table 6.4). As shown in this section in the case of group 1, anion exchange processes were dominant. If anions were the only species inserted into the polymer during the oxidation the mass change would have reached the maximum value of $\Delta m_{(f)}$ which can be calculated from the charge (integrated current). However, the real mass change ($\Delta m_{(EQCM)}$) was always less than $\Delta m_{(f)}$ as is shown in Table 6.4.

TABLE 6.4 The mass changes calculated by charge and EQCM results during application of a pulse potential to PPy/PTS polymer in the presence of different anions.

Anion	$\Delta m_f(\mu g)$	$\Delta mQCM(\mu g)$	$\frac{\Delta mQCM}{\Delta mf}$
BS	2.87	0.95	0.33
PTS	2.32	0.26	0.11
4HBSA	2.27	0.08	0.03

The deviation of real mass change ($\Delta m_{(EQCM)}$) from the expected mass change ($\Delta m_{(f)}$) may have arisen from a process in which cations are expelled from the polymer to compensate for the anions which were trapped deep inside the bulk of the material. Errors in the calculation due to charging current may also be a

reason for such a deviation since current flow due to charging current was not subtracted from the faradaic current. However, it would be expected that the amount of charging current would be similar for all the species (Table 6.5). The charge measured due to charging current in the presence of different anions at a bare glassy carbon electrode was essentially the same (within ± 4%).

TABLE 6.5 The average charge consumed at the surface of a bare glassy carbon electrode in the presence of 0.20 M organic salt.

Anion	Q(Oxidation)-mC	Q(reduction)-mC
BS	0.72	-0.65
4HBSA	0.68	-0.68
PTS	0.73	-0.65

A pulsed potential of E_1=-0.60 to E_2=0.40 V and t_1=t_2=30 s was applied for 30 s. The corresponding charges were then calculated by integration of the current for the period the potential was applied. The averages obtained for 4 measurements are reported.

The ratio of $\Delta m_{(EQCM)}$ to $\Delta m_{(F)}$ represents the magnitude of the deviation from anion exchange properties, where a greater value in this ratio shows greater anion exchange capacity and a smaller ratio represents a smaller anion exchange capacity.

Table 6.4 shows these ratios ($R[\Delta m_{(EQCM)}/\Delta m_{(F)}]$) obtained for PPy/PTS in the presence of BS, PTS and 4HBSA. The highest value was obtained for BS while the lowest value observed was for 4HBSA. The data present the average of 4 different measurements. The same order of magnitude in flux was obtained

for the transport of these anions across PPy/PTS polymer (Table 5.7). These results indicated that the species that display higher anion exchange capacity (Group 1) also gave larger value of fluxes in transport while the species with less anion exchange capacity (more cation exchange capacity) resulted in lower values of flux. This agreement is further proof that the transport of anions was due to the incorporation/expulsion of anions. This information provides evidence to help substantiate the proposed mechanism of transport.

6.3.1.2 EFFECT OF PULSE WIDTH AND PULSE HEIGHT

The effect of the applied potential pulse routine on the changes in mass observed at a PPy/PTS polymer was investigated further using different pulse widths and pulse heights.

The mass responses obtained for a PPy/PTS film in a solution containing 0.20 M BS were recorded using various potential pulse widths (Figure 6.12 (a)). It was found that the polymer mass decreased upon reduction and increased upon oxidation as discussed previously. The application of pulses with different widths did not change this overall trend. However, the magnitude of the response (i.e. the maximum mass change) was found to be dependent on the pulse width. The total mass exchanged between polymer and solution increased as the pulse width increased up to 40 s. Application of longer potential pulses had no further effect on the response.

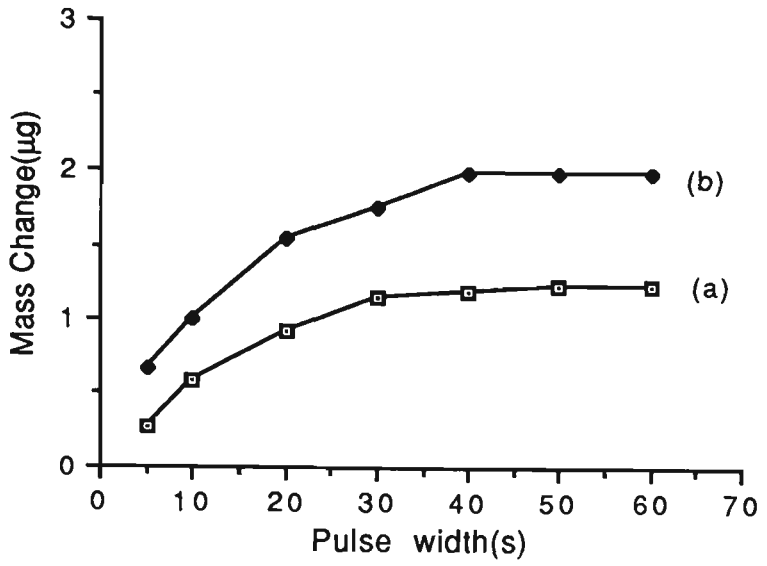

FIGURE 6.12 The maximum mass changes obtained for PPy/PTS during reduction -oxidation with various potential pulse widths.
(a) 0.20 M BS
(b) 0.20 M 1,3BDSA

The responses observed for PPy/PTS in a solution containing 1,3BDSA were also recorded (Figure 6.12 (b)). For the entire range (5-60 s) a similar trend was observed, that is the mass increased upon reduction of the polymer and decreased on oxidation (as shown in Figure 6.11). However, as for BS, the magnitude of the response increased as the pulse became longer until a maximum value was approached at 40 s. No further increase was observed with longer pulses.

In other experiments using both BS and BDSA as the test systems, various potential pulse heights were applied to the polymer. In the case of BS a similar trend was recorded as the mass increased during the application of an oxidative potential and decreased upon reduction. However, with more negative or more positive potentials greater mass changes were observed (Table 6.6 (a,b)). A large mass change was observed when a potential of -1.00

V was applied presumably due to the completion of the oxidation/reduction reaction as suggested by CV (see Figure 5.1).

TABLE 6.6 Effect of potential pulse height on mass changes observed for PPy/PTS in 0.20 M BS.
Application of:
(a) various negative pulses
(b) various positive pulses

(a)

$(E_1)^*$	-0.60 V	-0.70	0.80	-0.90	-1.00
Mass Change (μg)	1.32	1.42	1.54	1.66	2.21

*E_2 kept constant at 0.40 V.

(b)

$(E_2)^*$	0.50 V	0.60	0.70
Mass Change (μg)	1.32	1.42	1.54

*E_1 kept constant at -0.60 V.
In all experiments $t_1=t_2=30$ s. Mass changes were measured between two consecutive pulses.

An interesting result was obtained when the experiment was carried out using 0.20 M 1,3BDSA as supporting electrolyte. As shown before, PPy/PTS in a solution of 1,3BDSA acted as a strong cation exchanger. Similar behaviour was

observed here until the applied pulse was less than -0.90 V. At more negative potentials the response was reversed (Figure 6.13 (a)). The polymer mass decreased upon reduction (arrow E_1(a)) and increased upon oxidation (E_2(a)). Unlike the response obtained with E_1=-0.60 to E_2=0.40 V (t_1=t_2=30 s) the polymer exhibited anion exchange properties when the applied pulse was more negative ($E_1 \leq$ -0.90 V). Such behaviour was not observed when more positive potentials were applied. Although these results suggest that the transport of 1,3BDSA may be possible if a pulsed potential of E_1=-0.90 to E_2=0.40 V was applied, this could not be verified due to deterioration of the mechanical properties of the membranes at negative potentials.

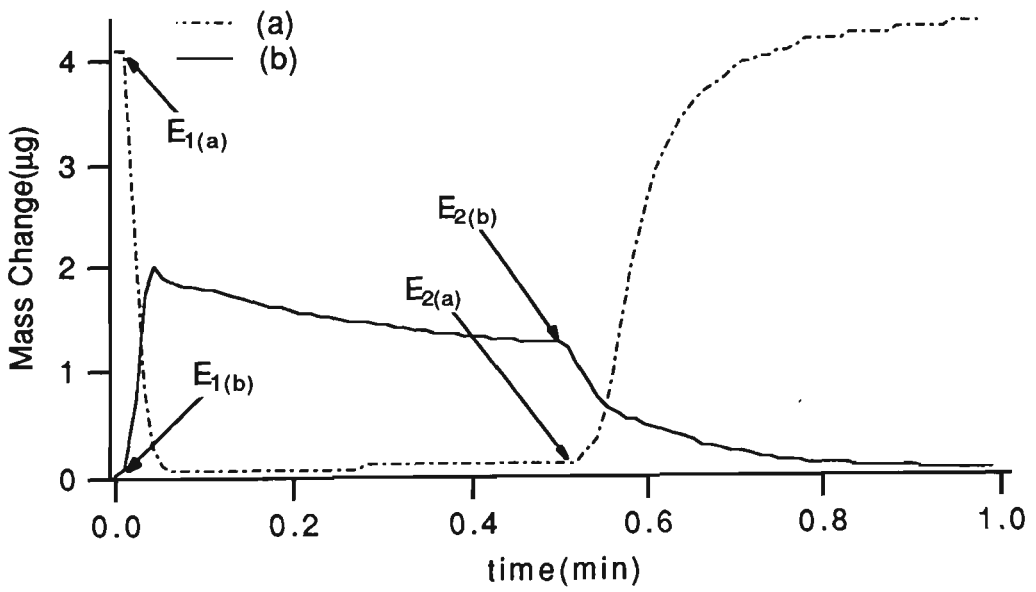

FIGURE 6.13 Effect of potential pulse range on mass changes observed for PPy/PTS in 0.20 M 1,3BDSA.

(a) E_1=-0.90 to E_2=0.40 V and t_1= t_2=30 s.

(b) E_1=-0.60 to E_2=0.40 V and t_1= t_2=30 s.

6.3.2 CYCLIC VOLTAMMETRIC STUDIES

In order to reveal more details of the redox reactions of PPy/PTS in the presence of the different anions, the mass changes and cyclic voltammetric measurements were performed at the same time.

A PPy/PTS film was cycled in 0.20 M BS (Figure 6.14). The films were very stable and no significant net weight change was observed over the experimental period.

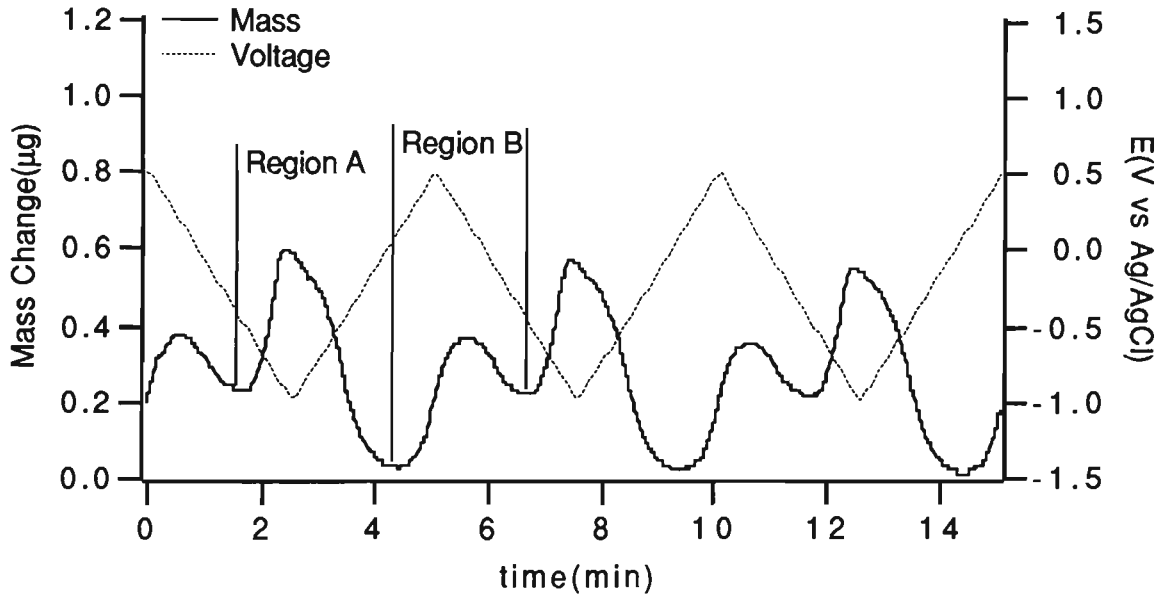

FIGURE 6.14 Mass change of PPy/PTS cycled in a solution of 0.20 M BS. Scan rate = 10 mV s^{-1}

It was found that during potential cycling mass changes were observed in two different regions (Figure 6.14). In region A when scanned toward negative potentials the mass increased at potentials more negative than -0.50 V, then it decreased when the scan was reversed. Another peak appeared (region B) with application of oxidative potentials at +0.20 V or more. It is believed that the peaks in region A and B are cation and anion dependent, respectively. This was confirmed by further investigations.

The effect of scan rate on the mass changes of the polymer was considered (Figure 6.15 (a-c)). As the scan rate increased, the peak in region A (more cathodic) remained largely unchanged while the peak in region B (more anodic) gradually disappeared (Figure 6.15 (c)). With a scan rate of 50 mV s^{-1} the anodic peak (region B) still remained but when the scan rate was increased to 200 mV s^{-1} the anodic peak (B) completely disappeared. The same trend was observed when higher scan rates were employed (Table 6.7).

With increased scan rates the decrease in response (region B) is due to kinetic effects as the diffusion of large anions (BS) was limited. But the peak in the reduction region due to cation motion was not affected by the scan rate as the cations (Na^+) are more mobile. These observations show that during redox reactions in polypyrrole the charge neutrality is maintained by cation transport at more negative potentials (region A) followed by a dominant anion movement at higher levels of oxidation (region B).

(a) Scan rate=5 mV s^{-1}

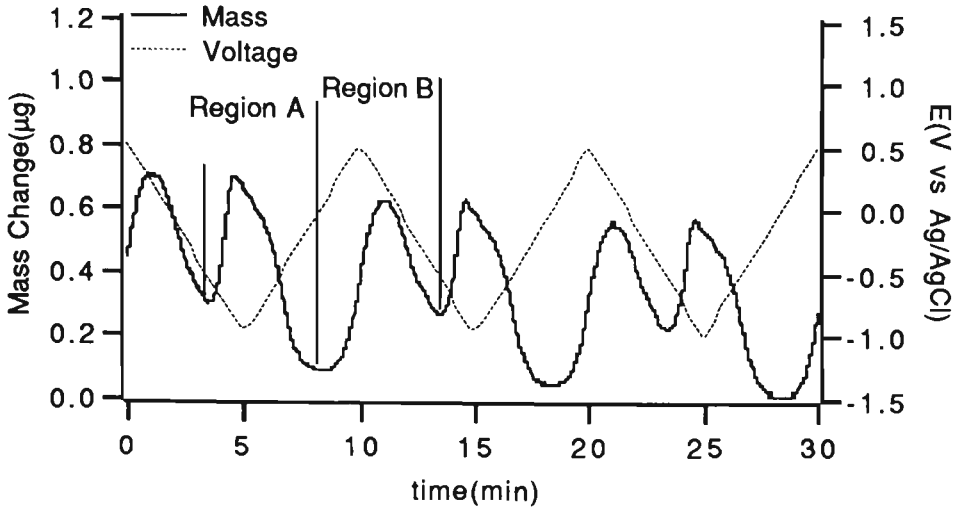

(b) Scan rate=50 mV s^{-1}

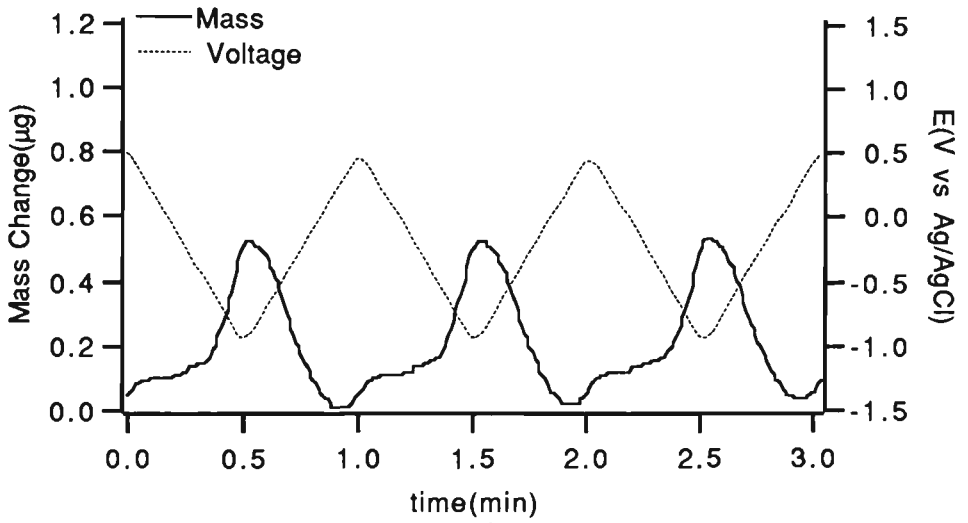

(c) Scan rate=200 mV s^{-1}

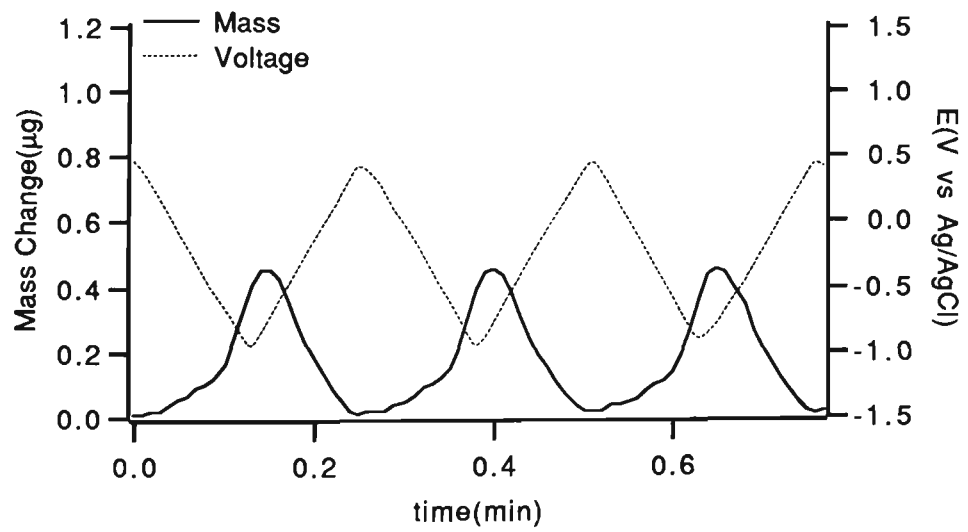

FIGURE 6.15 Mass changes of PPy/PTS electrode cycled in a solution of 0.20 M BS. Scan rate = (a) 5 mV s^{-1} (b) 50 mV s^{-1} (c) 200 mV s^{-1}.

TABLE 6.7 The effect of scan rate on the redox properties of PPy/PTS cycled in 0.20 M BS.

Scan rate ($mV\ s^{-1}$)	**$\Delta m(\mu g)$ Cathodic peak (Region A)**	**$\Delta m(\mu g)$ Anodic peak (Region B)**
5	0.36	0.57
10	0.33	0.35
20	0.36	0.20
50	0.43	0.10
100	0.52	0.00
200	0.49	0.00
500	0.32	0.00
1000	0.20	0.00

Cathodic mass changes (Δm)= Maximum mass changes observed during reduction (Region A). Anodic mass changes (Δm)= Maximum mass changes observed during oxidation (region B).

6.3.2.1 EFFECT OF SMALL ANIONS

Further investigations were carried out using small, mobile anions such as Cl^- but employing the same cation (Na^+). Large mass changes occurred in the anodic region (region B) of the cycle (Figure 6.16). In contrast to previous results (large and less mobile anions) when the scan rate was increased the peak in this region did not disappear (Table 6.8). An explanation of this is that as the Cl^- anions are more mobile (than BS) they readily diffuse into the polymer matrix without limitation from kinetic effects (within experimental conditions). An immediate conclusion from these observations is that in region B anions are incorporated/expelled to maintain charge neutrality. Regardless of the mechanism the peak is clearly anion dependent.

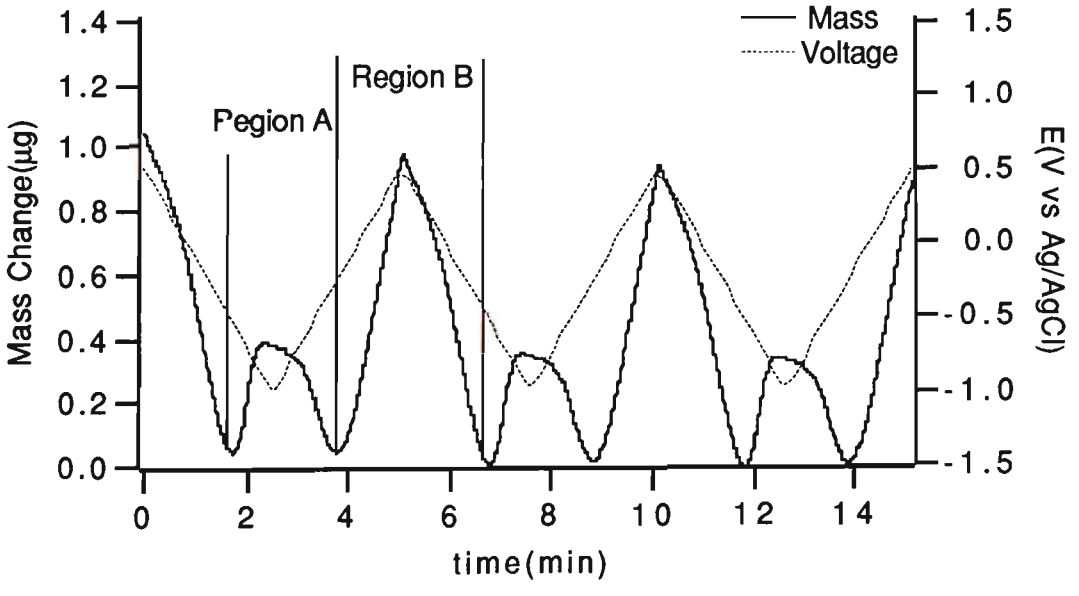

FIGURE 6.16 Mass changes of PPy/PTS cycled in a solution of 0.20 M NaCl. Scan rate=10 mV s^{-1}

TABLE 6.8 PPy/PTS cycled in the presence of a small anion (Cl^-) with various scan rates.

Scan rate ($mV\ s^{-1}$)	**Δm(μg) Cathodic peak (Region A)**	**Δm(μg) Anodic peak (Region B)**
5	0.37	1.06
10	0.35	0.88
20	0.37	0.86
50	0.45	0.82
100	0.45	0.76
200	0.45	0.71
500	0.41	0.60
1000	0.25	0.40

0.20 M NaCl was used as supporting electrolyte solution. Mass changes were calculated as in Table 6.7.

This interpretation was confirmed by studying the cation dependence of the response. Figure 6.17 shows PPy/PTS cycled with the same anion while a different cation was employed. It was found that by changing the cation from Na^+ to Mg^{2+} the peak in region B did not change, however the peak in region A disappeared. This can be explained in terms of the diffusion of the cations

into the polymers (i.e. Mg^{2+} is less mobile). This shows that the peak in the reduction region is clearly cation dependent.

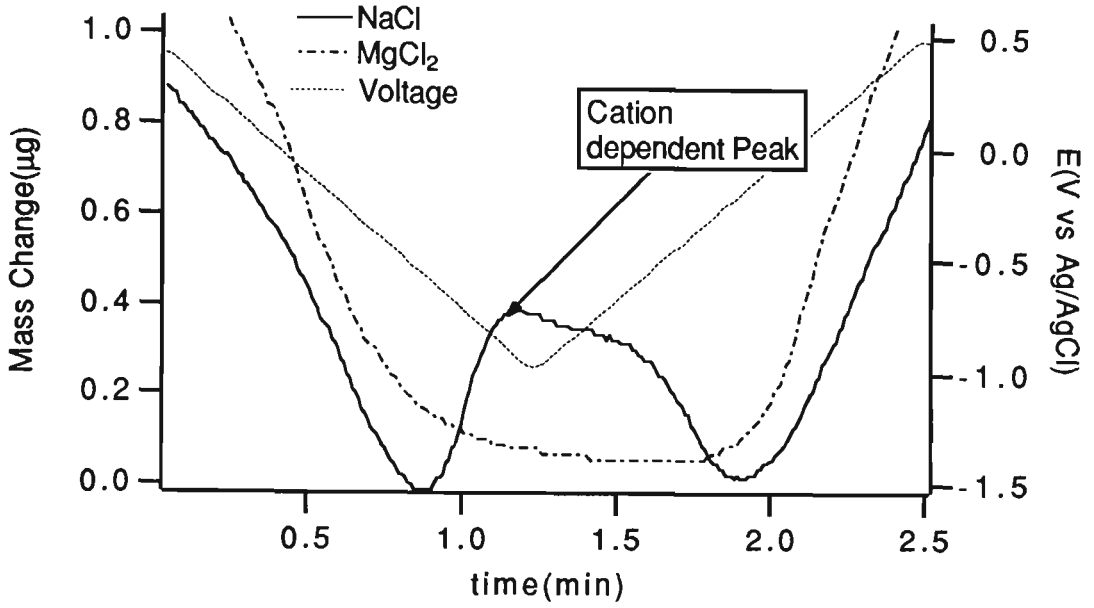

FIGURE 6.17 PPy/PTS cycled in a solution containing 0.20 M $MgCl_2$ or 0.20 M NaCl. Scan rate=20 mV s^{-1}.

6.3.2.2 EFFECT OF ORGANIC ANIONS

The results presented in Section 6.3.1 in conjunction with Section 6.3.2 are evidence that when a potential is applied to PPy/PTS in a solution of different salts (organic and inorganic) the peak in the anodic region (region B) at about 0.20 V is due to anion incorporation (anion dependent) and the peak in the cathodic region (at about -0.70 V) is cation dependent (region A). Therefore, the lack of a peak in region B would indicate poor anion exchange properties of the polymer in the given medium.

From the above results we know that PPy/PTS cycled in a solution of BS shows anion exchange properties. The existence of similar properties in the

case of the different organic anions was therefore investigated (the transport of these anions across PPy/PTS membranes was investigated in Chapter 5).

To study these properties, PPy/PTS was cycled in the presence of different organic anions (Figure 6.18). The existence of the peak in the anodic region (region B) indicates that anion exchange processes occurred in the case of BS and 4HBSA but no response was observed for 3SBA. These observations are again in agreement with the results obtained for the transport of these species. The order of magnitude of the flux obtained for the transport of these anions is (BS > 4HBSA > 3SBA), the same order of magnitude as that obtained for the mass change due to the anion exchange process. Absence of an anion dependent peak in the oxidation region of the cycle equates to the lower values of flux obtained (e.g. 3SBA see Table 5.7).

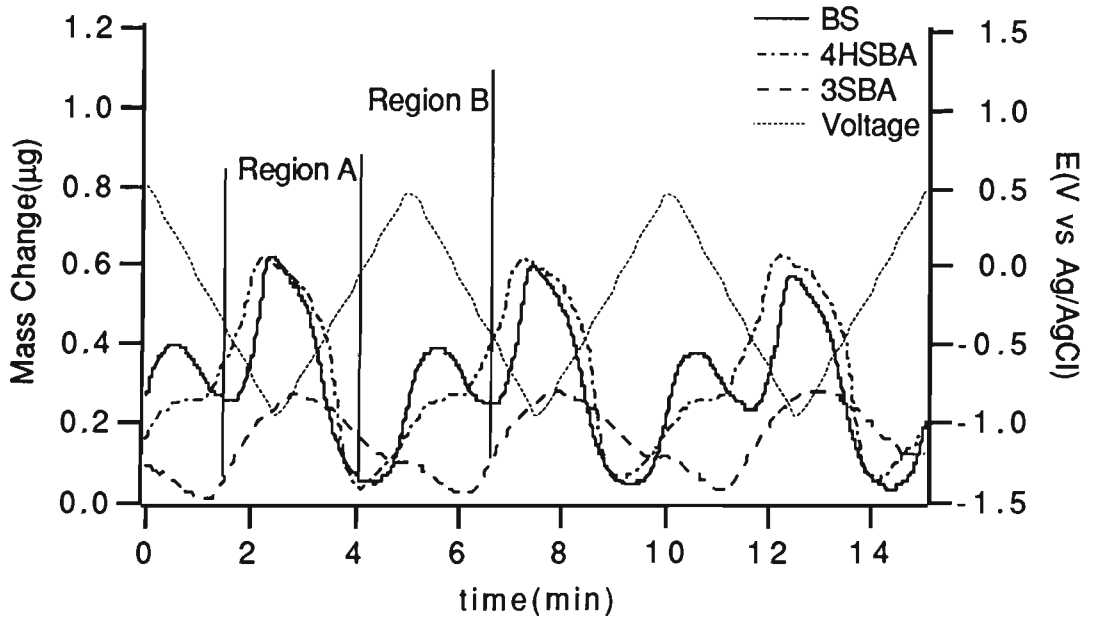

FIGURE 6.18 Mass changes for PPy/PTS in the presence of different organic anions Scan rate=10 mV s^{-1}.

6.3.3 EQCM STUDIES OF COMPOSITE POLYMERS

In Chapter 4 the development of an electropolymerisation procedure which allows the preparation of mechanically stable conductive, pinhole-free membranes based on polypyrrole/polyvinylsulfonate was described. These membranes were found to be more capable of cation rather than anion transport (Chapters 4 and 5). It was thought that this capability was due to the immobile nature of the PVS dopant. In order to get a clear insight into the polymer-solution interaction further investigations were carried out using EQCM.

Charge-frequency relationship. As discussed in Section 6.3 in order to apply Equation 6.6 to the frequency measurement for the polymer, it must be rigid and free of viscoelastic effects. The rigidity of the PPy/PVS was tested by plotting frequency shift against the total charge consumed during polymerisation. As is shown in Figure 6.19, a linear response was obtained between charge and frequency shift. Thus the polymer was treated as rigid and free of viscoelastic effects.

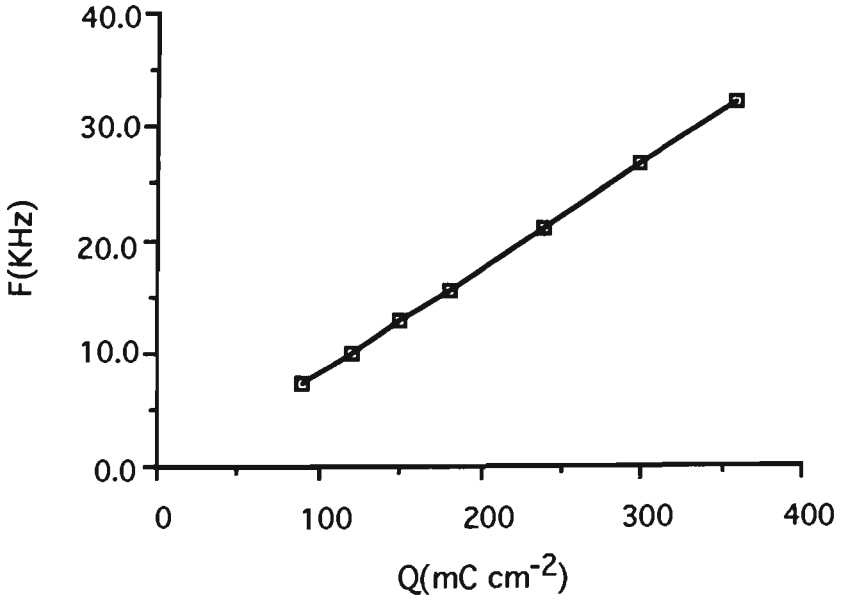

FIGURE 6.19 Relationship between the total charge passed during the growth of PPy/PVS and the resulting frequency shift.

The effect of polymer thickness. In Section 6.3 the effect of polymer thickness on the mass changes observed for PPy/PTS was discussed. It was shown that as the polymer thickness increased the response was distorted, however the same trends were obtained for both thick and thin polymers.

In the case of PPy/PVS no distortion of response was observed for thick polymers. However, the mass-change as a function of potential was markedly different with thin and thick polymers (Figure 6.20). Thin PPy/PVS showed a mass increase on oxidation and a decrease on reduction indicating anion exchange behaviour (Figure 6.20 (a)).

More complicated behaviour was observed for thick polymers (Figure 6.20 (b)). The polymer mass as a function of potential underwent 4 distinct transitions (1-4). During reduction the mass rapidly decreased (1) then increased (2). Conversely, during oxidation the polymer mass initially increased (3) then decreased (4). Such complicated behaviour is thought to be due to the presence of anions with varying mobilities. A PPy/PVS polymer consists of loosely held PVS chains (outer layer) as well as more tightly held PVS chains (inner layer). In a thin polymer anions can readily move into/out of the polymer. In thick polymers the inner layer is effectively isolated from the solution interface (with respect to anion mobility). This makes movement of the large anions into/out of the inner layer quite difficult. Consequently the original PVS present in this layer is less likely to be replaced by solution anions. The PVS then provided binding sites for cation exchange and the complex responses were due to the presence of both layers.

(a)

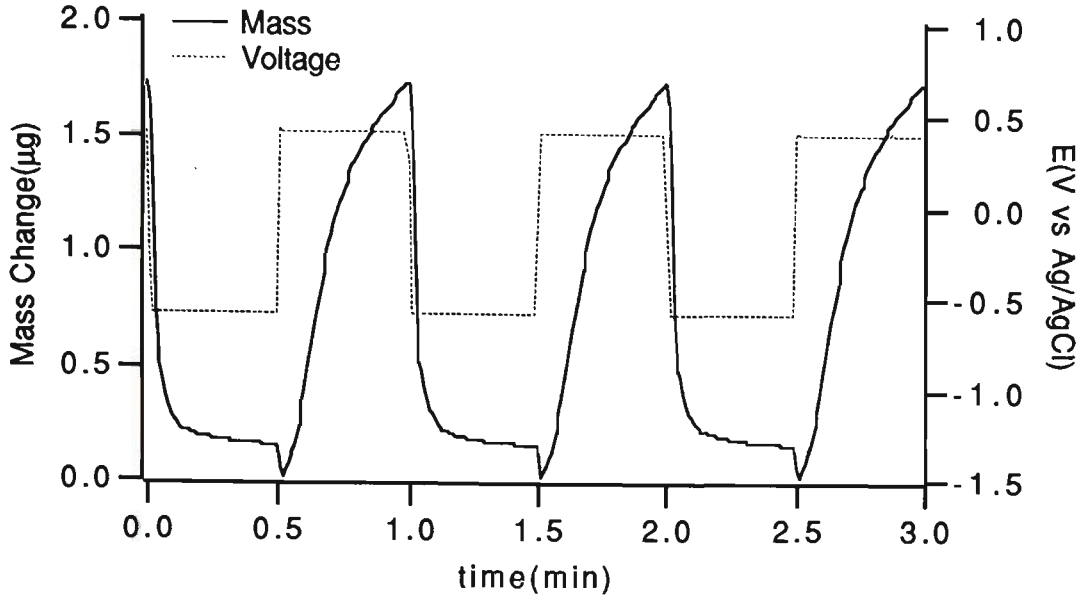

(b)

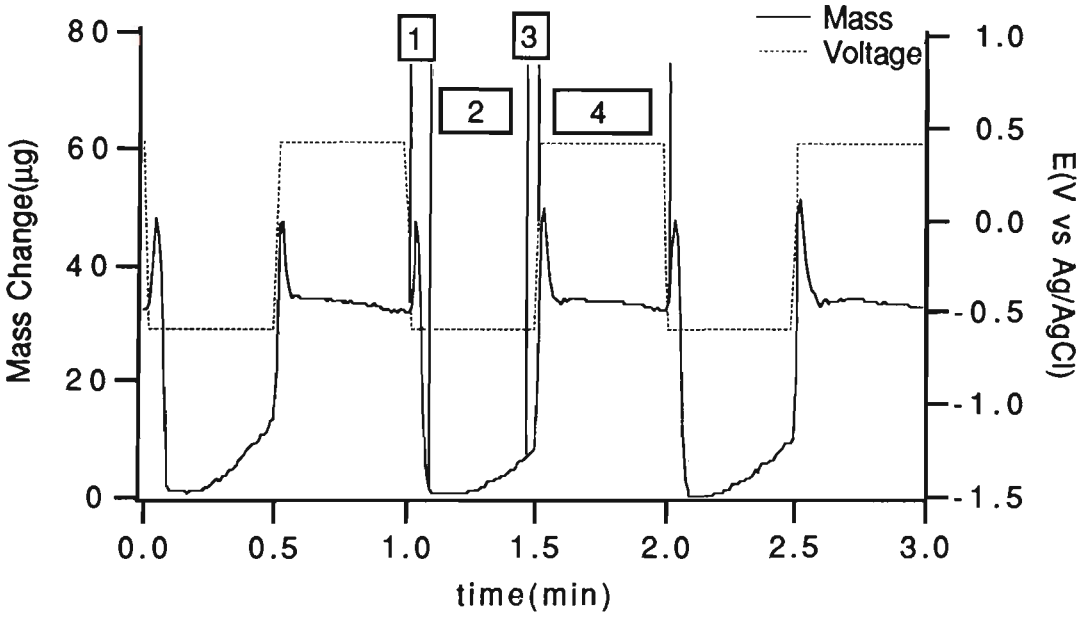

FIGURE 6.20 Mass change of PPy/PVS in a solution of 0.20 M BS during oxidation/reduction.

A pulsed potential of E_1=-0.60 to E_2=0.40 V and t_1=t_2=30 s was applied to the polymer (PPy/PVS). Total charge consumed during polymerisation was:

(a) 120 mC cm^{-2}

(b) 240 mC cm^{-2}

On the basis of the EQCM observations a model for the structure of PPy/PVS is proposed (Figure 6.21). In this model reduction process involved two stages: An initial mass decrease (1) followed by an increase in mass (2). During reduction, charge neutrality can be maintained by expulsion of anions or incorporation of cations. The fact that the mass decreased indicates expulsion of anions into the solution while a mass increase was due to cation movement into the polymer.

The oxidation of PPy/PVS also involves two stages where mass at first increased (3) then it decreased (4). During oxidation charge neutrality can be maintained by outward diffusion of cations or inward diffusion of anions. Since in the first stage mass increased, the anions predominantly moved into the outer layer and as a result mass increased. On continuing oxidation the mass decreased due to the outward diffusion of cations from the inner layer (deeply trapped PVS). This proposed model is in agreement with the observations made by Lien and co-workers[36].

As the polymer thickness increases the inner layer becomes more isolated from the solution interface and it was observed that the cation exchange capacity of the polymer increased. Hence the very thick PPy/PVS membranes exhibited more cation transport whilst little or no anion transport was observed. It can be assumed from this model that in an ideal situation, transport of anions is feasible if a very thin membrane is employed. However, in real systems (thick, mechanically stable membranes) this would hardly occur.

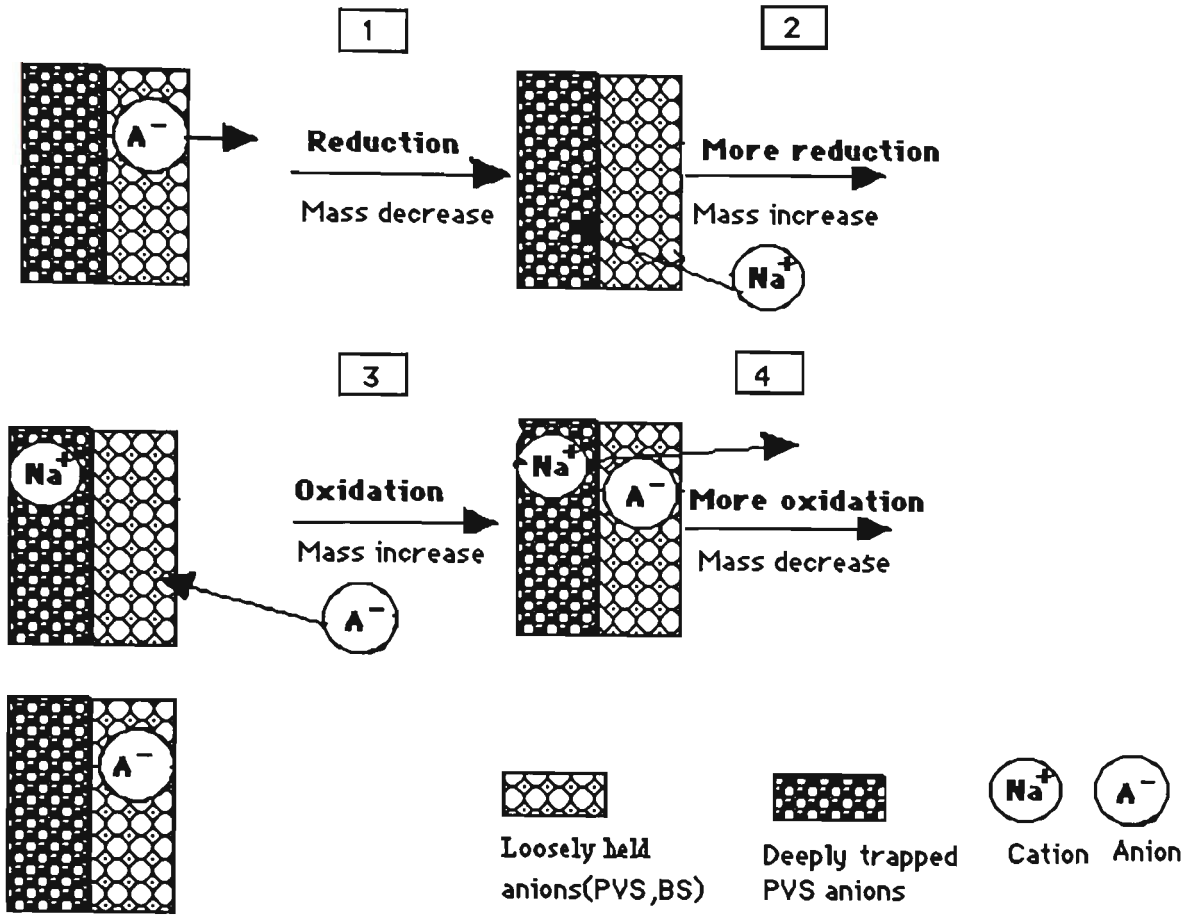

FIGURE 6.21 A proposed model for the structure of PPy/PVS polymer based on EQCM observation.

Cyclic voltammetric studies. The purpose of this section is to investigate enhanced cation exchange properties of PPy/PVS compared with PPy/PTS, as already shown by transport studies. PPy/PVS was cycled in a solution containing 0.20 M BS. Similar to the results obtained for PPy/PTS, polymer mass changes were observed in two different regions of the voltammogram. As Figure 6.22 shows there was a peak during reduction of the polymer at potentials more negative than -0.10 V (region A) followed by an oxidation peak at potentials more positive than +0.20 V (region B). In Figure 6.22 the PPy/PVS mass response to changes of potential was compared with

PPy/PTS when both polymers were cycled in 0.20 M BS using a scan rate of 50 mV s^{-1}.

The cation dependent peak in region A (potentials beyond -0.10 V) was observed for both polymers. However, the peak showing mass changes for PPy/PVS was very broad covering potentials between -0.10 to -1.00 volts. In the case of PPy/PTS the peak was narrow, covering only a small part of the voltammogram between -0.70 to -1.00 volts. That is, diffusion of cations into the PPy/PVS occurs over a wide range of negative potentials to maintain charge neutrality during reduction. This may indicate that the cation exchange capacity of PPy/PVS is greater than that of PPy/PTS.

As shown in Chapters 4 and 5 the PPy/PVS membranes encouraged more transport of cations compared with PPy/PTS. The EQCM results indicates that the more tightly trapped PVS chains in bulk polymer encourage the polymer to undergo cation exchange during the redox process.

(a)

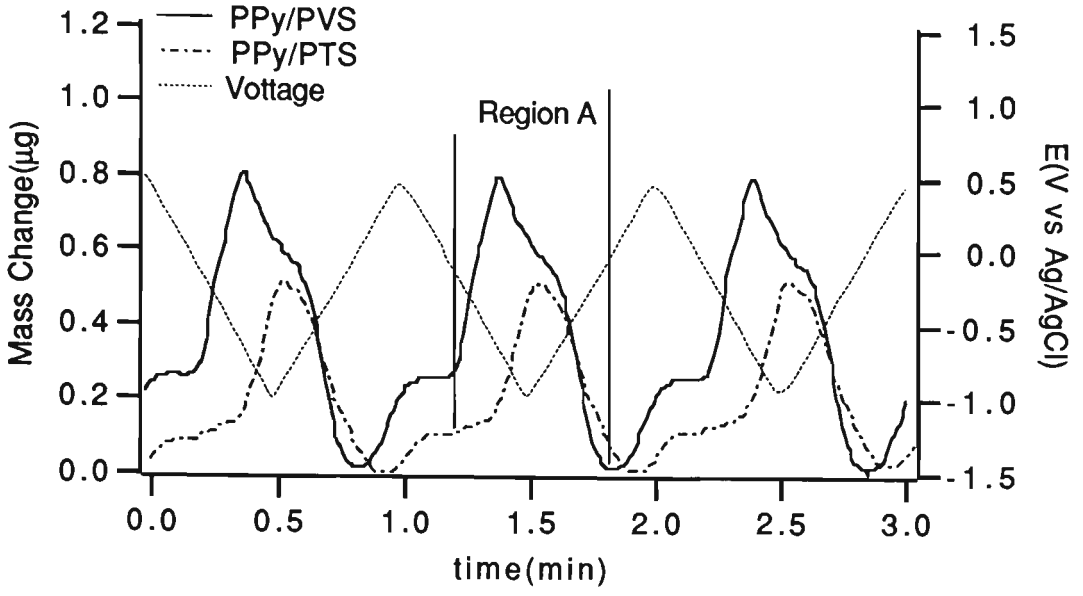

(b)

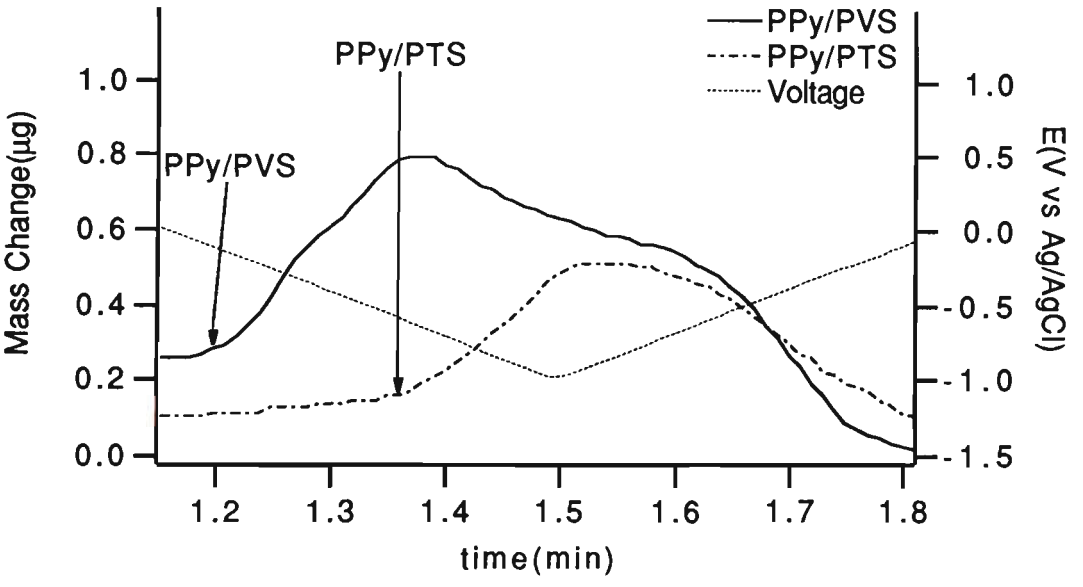

FIGURE 6.22 :

(a) Mass changes of PPy/PVS, PPy/PTS in a solution of 0.20 M BS.

Scan rate=50 mV s^{-1}. Total charge consumed for deposition of the polymer was Q=90 mC cm^{-2}.

(b) Enlarged FIGURE 6.22 (a) in region A. Arrows show the start of mass increase in the region A (cation dependent) for both polymers.

6.4 CONCLUSIONS

The technique of EQCM was successfully established. Using a variety of experimental approaches the relationship between macroscopic properties of polypyrrole based polymers and microscopic properties was studied in detail.

Simultaneous electrochemical and microgravimetric measurements gave a good understanding of the properties and behaviour of polypyrrole based polymers.

Ion motion during redox reactions of polypyrrole films (cycling or pulsing) was shown to be dependent on the nature of supporting electrolyte and the incorporated anion in the polymer. The PPy/PTS polymer was shown to be predominantly an anion exchanger in the presence of BS, PTS and 4HBSA while it was mainly a cation exchanger in the presence of 3SBA, 4SBA and 1,3BDSA. This implies that ion exchange properties of the polymer can be modified even after the polymer is synthesised.

The results obtained in this Chapter support many of the observations made in Chapters 4 and 5. In Chapter 5 it was suggested that the transport of anions was motivated by anion incorporation and expulsion during the redox processes. Similar experiments were repeated using EQCM. It was shown that the anion exchange capacity was greater for species whose transport were relatively high (e.g. BS).

For PPy/PTS cycled in a solution of organic anions such as BS It was found that during potential cycling mass changes were observed in two different regions (A and B). The peak in region B (oxidative region) was anion dependent. Using a variety of measurements we have shown that when there was no anion dependent peak (as observed by EQCM) the value of flux (obtained by transport studies) was low (e.g. for 3SBA). While a strong peak (e.g. for BS) corresponded with high value of flux in transport experiments.

The magnitude of this anion dependent peak (region B) is a good indicator to predict anionic transport properties of the membranes.

In the case of transport of cations, the PPy/PVS exhibited higher value of flux. This can be predicted by the existence of a very broad cation dependent peak (in region A) for the polymer.

On the basis of the observations made by EQCM a model for the surface structure of PPy/PVS composite was proposed.

CHAPTER 7

GENERAL CONCLUSIONS

The development of membrane systems whose transport properties can be regulated by environmental stimuli was the main objective of the current investigation. Conducting electroactive polymers such as polyaniline and polypyrrole are capable of responding to external stimuli. For example, application of a potential to these polymers induces changes in their redox state. This produces chemical and physical changes in the system such as processes of incorporation and expulsion of counterion between the solution and the polymer phase.

As a primary aim the production of free-standing films of the polymers was considered. Synthesis of a variety of conducting membranes with adequate mechanical and electrical properties was addressed. The transport and separation of different species was then carried out across the membranes with a view to control the rate of transport of target species across the membranes. Finally, mechanistic studies were carried out to understand further the mechanism of the transport.

The combined results in Chapter 3 and 4 described the efforts that have been made to improve mechanical and electrical properties of the conducting polymers. In particular, two classes of the polymers were investigated in detail.

Polyaniline. It was found that continuous films (i.e. films with uniformly deposited polymer over the entire electrode) of polyaniline could be synthesised in the presence of strong inorganic acids. However, these films did not show adequate mechanical properties to produce free-standing films of polyaniline. A film-casting method from viscous solution of polyaniline powder in 1-methyl-2-pyrrolidinone was therefore employed. It was found that the temperature of the polymerisation was a dominant factor in regard to the mechanical properties. Polyaniline membranes having excellent mechanical

properties (tensile strength = 110 MPa) were prepared. The membranes were also conductive (20-30 S cm^{-1}).

Composite polymers. Electrosyntheses that allowed production of free-standing (pin-hole free) composite membranes based on conducting polymers were developed. A variety of factors influencing the properties of the films were investigated. The concentration of polyelectrolyte, the current density in which the polymerisation took place, the substrate and the effect of co-counterions were optimised to produce a free-standing film that was conductive and pinhole free. PPy/PVS and PPy/Nafion composite membranes with good mechanical and electrical properties were prepared. For example tensile strength and conductivity for PPy/PVS membranes were respectively 70-90 MPa and 14-15 S cm^{-1}.

An intensive investigation was carried out to initiate and control transport across these membranes.

The development and optimisation of a cell for such transport studies was described in Chapter 2. The importance of electrical contacts, their size, nature and the pressure applied, was demonstrated by chronoamperometric studies during transport.

Initially, transport of some simple cations such as Na^+, K^+ and inorganic acids was considered (Chapters 3 and 4). The use of a potential (constant or pulsed) to initiate transport was then investigated. This involved application of repetitive pulses of sufficient amplitude to oxidise and reduce the polymer.

In the case of polyaniline membranes remarkable selectivity was obtained for different acids. It was found that the rate of transport of the different acids could be controlled by application of an external potential. In the case of HCl, HNO_3 and H_2SO_4 it was found that H^+ transport occurred without application

of potential. However, the rate of transport for each increased significantly when a positive potential was applied. The transport could be stopped by the application of a negative potential.

With composite polymers the conventional method of pulsing did not result in any transport. A new electrochemical controller based on a twin pulsed applied potential was therefore designed and constructed. This device enabled the reduction and oxidation of the polymer to be separately initiated in different parts of the cell. When these composite membranes were used in combination with the new electrochemical controller, transport of cations was initiated. Such transport was controlled by electrochemical means and in fact could be switched on or off.

In Chapter 5 it was shown that electrochemically controlled transport of organic anions across conducting polymer membranes was possible. In this work transport of sulfonated aromatics with various functional groups was investigated. It was found that the rate of transport of compounds with substituents of an electron withdrawing nature was markedly lower than those that had no substituent or with a substituent of an electron donating nature. In addition, it was found that the position of the functional group had a marked influence on the transport indicating that a high degree of selectivity was attainable. The transport of species with two charged sites was insignificant suggesting a strong affinity with the oxidised polypyrrole.

Separation of these organic compounds using the membranes was also investigated. Selectivity factors were obtained indicating that electrochemically controlled separation of organic compounds can be achieved.

Based on the results obtained for transport of anions and cations the membranes were classified as having two different behaviours. One having a relatively mobile counterion (PPy/PTS) and the other a less mobile counterion (PPy/PVS). It was found that the anions were readily transported across PPy/PTS membranes. However, transport of the anions across PPy/PVS membranes was insignificant. The rate of transport of cations was much higher with PPy/PVS membranes. The immobile nature of PVS as a counterion means that the membranes formed with this counterion tend to be more useful as a cation exchanger. Consequently, it can be suggested that when the transport of anions is desired, PPy/PTS membranes should be employed while for the transport of cations a PPy/PVS membrane is to be selected.

The application of a different cell set up was also demonstrated in Chapters 4 and 5. It was shown that the cell configuration was extremely important with respect to the rate of transport. The best cell configurations were illustrated for the transport of cations and anions.

Finally, in Chapter 6 simultaneous electrochemical and microgravimetric measurements (by EQCM) gave a good understanding of the properties and behaviour of polypyrrole based polymers. The results presented in this Chapter supported many of the observations made in Chapters 4, 5. In Chapter 5 it was suggested that the transport of anions was motivated by anion incorporation and expulsion during the redox processes. Similar experiments were repeated using EQCM. It was shown that the anion exchange capacity was greater for species whose transport were relatively high (e.g. benzene sulfonate (BS)). In addition, using a variety of measurements, we have shown that when there was no anion dependent peak (as verified by EQCM) the value of flux (obtained by transport studies) was low (e.g. for 3-sulfobenzoate (3SBA)). In contrast, a strong anion dependent peak (e.g. for BS) corresponded with a high value of

flux in transport experiments. This is a good indicator to predict transport properties of the membranes. On the basis of the observation made by EQCM a model for the surface structure of PPy/PVS composite was proposed.

Overall, the results presented in this thesis have added a new dimension in separation technology. It introduces a fascinating area in which transport of target species can be regulated in-situ. As a consequence of this, separation of various mixtures can be achieved. Many industrial applications may take advantage of this novel approach in future, for example, separation of precious or heavy metals from industrial waste streams. Also using EQCM ion exchange behaviour of some polymers were revealed in detail. The relationship between macroscopic properties of polypyrrole based polymer membrane (as observed by transport studies) and the microscopic properties of the polymer (as observed by EQCM) has been established. This should aid future studies to target possible applications for this technology.

REFERENCES

1. F. A. Bovey and F. H. Winslow, Macromolecules: An Introduction to Polymer Science, Academic Press, New York- San fransisco, London, (1979).

2. P. J. Clarke, *Plastics For Schools: Applied Polymer Science,* Allman and Son, London (1970).

3. D. J. Walton, *Materials and Design,* 11 (1990) 142- 152.

4. P. J. Riley and G. G. Wallace, *Materials Australasia,* (1991) 12- 13.

5. T. Ito, H. Shirakawa and S. Ikeda, *Journal of Polymer Science,* 12 (1974) 11- 20.

6. H. Shirakawa and S. Ikeda, *Polymer Journal,* 2 (1971) 231- 244.

7. C. K. Chiang, C. R. Fincher, Jr., Y. W. Park, A. J. Heeger, H. Shirakawa, E. J. Louis, S. C. Gau and A. G. MacDiarmid, *Physical Review Letters,* 39 (1977) 1098- 1101.

8. J. E. Frommer and R. R. Chance, in *Encyclopaedia of Polymer Science and Engineering, Volume 5,* J. I. Kroschwitz (Ed.), John Wiley and Sons Inc., New York, (1986).

9. H. Munstedt, G. Kohler, H. Mohwald, D. Naegele, B. Aktiengesellschaft, L. Rhein, R. Bitthin, G. Ely and E. Meissner, *Synthetic Metals,* 18 (1987) 259- 264.

10. A. Mohammadi, O. Inganas and I. Lundstrom, *J. Electrochem. Soc.: Electrochemical Science and Technology,* 133 (1986) 947- 949.

11. A. Michalska, A. Lewenstam, A. Ivaska and A. Hulanicki, *Electroanalysis,* 5 (1993) 261- 263.

12. H. Ge, J. Zhang and G. G. Wallace, *Analytical Letters*, 25 (1992) 429-441.

13. A. Angeli, *Gazz. Chim. Ital.*, 46 (1916) 279. As cited in " G. K. Chandler and D. Pletcher, *Special Reports Electrochemistry , Roy. Soc. Chem.* 10 (1985) 117- 150".

14. K. K. Kanazawa, A. F. Diaz, W. D. Gill, P. M. Grant, G. B. Street, G. P. Gardini and J. F. Kwak, *Synthetic Metals*, 1 (1979/ 1980) 329- 336.

15. T. H. Chao and J. March, *Journal of Polymer Science: Part A: Polymer Chemistry*, 26 (1988) 743- 753.

16. E. T. Kang, K. G. Neoh and K. L. Tan, *Mol. Cryst. Liq. Cryst.*, 173 (1989) 141- 150.

17. M. M. Castillo- Ortega, M. B. Inoue and M. Inoue, *Synthetic Metals*, 28 (1989) C65- C70.

18. J. Tanguy, N. Mermilliod and M. Hoclet, *Synthetic Metals*, 18 (1987) 7 12.

19. N. Bates, M. Cross, R. Lines and D. Walton, *J. Chem. Soc., Chem. Commun.*, (1985) 871- 872.

20. C. M. Elliott, A. B. Kopelove, W. J. Albery and Z. Chen, *J. Phys. Chem.*, 95 (1991) 1743- 1747.

21. G. Bidan, A. Deronzier and J. C. Moutet, *J. Chem. Soc., Chem. Commun.*, (1984) 1185- 1186.

22. J. I. Chen, R. A. Moody. J. C. Huang and S. K. Tripathy, *Mol. Cryst. liq. Cryst.*, 190 (1990) 19- 26.

23. S. Panero, P. Prosperi and B. Scrosati, *Electrochimica Acta*, 37 (1992) 419-423.

24. M. Salmon, A. F. Diaz, A. J. Logan, M. Krounbi and J. Bargon, *Mol. Cryst. Liq. Cryst.*, 83 (1982) 265-276.

25. T. Iyoda, A. Ohtani, T. Shimidzu and K. Honda, *Chemistry Letters*, (1986) 687- 690.

26. T. F. Otero and E. De Larreta, *Synthetic Metals*, 26 (1988) 79- 88.

27. S. Rapi, V. Bocchi and G. P. Gardini, *Synthetic Metals*, 24 (1988) 217-221.

28. D. Bloor, R. D. Hercliffe, C. G. Galiotis and R. J. Young, *Mechanical properties of polypyrrole plates*, Elsevier Applied Science, London, New York, (1986).

29. M. Yamaura, K. Sato and T. Hagiwara, *Synthetic Metals*, 39 (1990) 43-60.

30. M. J. V. Sluijs, A. E. Underhill and B. N. Zaba, *J. Phys. D: Appl. Phys.*, 20 (1987) 1411- 1416.

31. M. Iseki, K. Saito, K. Kuhara and A. Mizukami, *Synthetic Metals*, 40 (1991) 117- 126.

32. A. F. Diaz, K. K. Kanazawa, J. I. Castillo and J. A. Logan, *Polym. Sci. Technol.*, 15 (1981) 149- 153.

33. Y. H. Park and M. H. Han, *Journal of Applied Polymer Science*, 45 (1992) 1973- 1982.

34. V. Krishna, Y. H. Ho, S. Basak and K. Rajeshwar, *J. Am. Chem. Soc.*, 113 (1991) 3325- 3333.

35. J. Unsworth, P. C. Innis, B. A. Lunn, Z. Jin and G. P. Norton, *Synthetic Metals*, 53 (1992) 59- 69.

36. M. Lien, W. H. Smyrl and M. Morita, *J. Electroanal. Chem.*, 309 (1991) 333- 340.

37. D. R. Rosseinsky, N. J. Morse, R. C. T. Slade, G. B. Hix, R. J. Mortimer and D. J. Walton, *Electrochimica Acta*, 36 (1991) 733- 738.

38. A. I. Nazzal, G. B. Street and K. J. Wynne, *Mol. Cryst. Liq. Cryst*, 125 (1985) 303- 307

39. G. K. Chandler and D. Pletcher, *Special Reports Electrochemistry, Roy. Soc. Chem.*, 10 (1985) 117- 150.

40. R. B. Kaner in *Electrochemical Science and Technology of polymers, Volume 2, Chapter 3*, R. G. Linford (Ed.), Elsevier Applied Science, London, New York (1990).

41. C. K. Baker and J. R. Reynolds, *J. Electroanal. Chem.*, 251 (1988) 307-322.

42. A.F. Diaz and J. Bargon, in *Handbook of Conducting Polymers, Chapter 3*, T. A. Skotheim (Ed.), Marcel Dekker, New York, USA (1986).

43. R. C. D. Peres, M. A. De Paoli, S. Panero and B. Scrosati, *Photo polymer Device Physics, Chemistry and Applications II*, 1559 (1991) 151- 158.

44. R. John, M. J. John, G. G. Wallace and H. Zhao, *Electrochemistry in Colloids and Dispersions*, (1992), 225- 235.

45. W. Wernet, H. Yamato, K. Kai, T. Koshiba, M. Ohwa and B. Rotzinger, *Solid State Ionics*, 53- 56 (1992) 1125- 1131.

46. L. Atanasoska, K. Naoi and W. H. Smyrl, *Chem. Mater.*, 4 (1992) 988-994.

47. L. F. Warren, J. A. Walker, D. P. Anderson , C. G. Rhodes and L. J. Buckley, *J. Electrochem. Soc.*, 136 (1989) 2286- 2295.

48. H. Zhao, W. E. Price and G. G. Wallace, *Polymer*, 34 (1993) 16- 20.

49. W. Breen, J. F. Cassidy and M. E. G. Lyons, *J. Electroanal. Chem.*, 297 (1991) 445- 460.

50. A. J. Hodgson, M. J. Spencer and G. G. Wallace, *Reactive Polymers*, 18 (1992) 77- 85.

51. R. Qian and J. Qiu, *Polymer Journal*, 19 (1987) 157- 172.

52. G. R. Mitchell, F. J. Davis and C. H. Legge, *Synthetic Metals*, 26 (1988) 247- 257.

53. Y. Li and R. Qian, *Synthetic Metals*, 28 (1989) C127- C132.

54. G. R. Mitchell and A. Geri, *J. Phys. D: Appl. Phys.*, 20 (1987) 1346- 1353.

55. L. J. Buckley, G. E. Wnek and D. K. Roylance, *Polymeric Material Science and Engineering*, Proceedings of the ACS division of polymeric Materials Science and Engineering, Vol. 53, Washington DC (1985).

56. A. Witkowski, M. S. Freund and A. Brajter- Toth, *Anal. Chem.*, 63 (1991) 622- 626.

57. B. Sun, J. J. Jones, R. P. Burford and M. Skyllas- Kazacos, *Journal of Materials Science*, 24 (1989) 4024- 4029.

58. A. F. Diaz and J. C. Lacroix, *New J. Chem.*, 12 (1988) 171- 180.

59. A. F. Diaz , K. K. Kanazawa and G. P. Gardini, *J. C. S. Chem. Comm.*, (1979) 635- 636.

60. A. Mirmohseni, W. E. Price and G. G. Wallace, *Polymer Gels and Networks*, 1 (1993) 61- 77.

61. Y. Lin and G. G. Wallace, *Analytica Chimica Acta*, 263 (1992) 71- 75.

62. N. M. Ratcliffe, *Synthetic Metals*, 38 (1990) 87- 92.

63. A. F. Diaz and B. Hall, *IMB J. Res. Develop.*, 27 (1983) 342- 347.

64. B. Lundberg, B. Sundqvist, O. Inganas, I. Lundstrom and W. R. Salaneck, *Mol. Cryst. Liq. Cryst.*, 118 (1985) 155- 158.

65. Y. Li and R. Qian, *Synthetic Metals*, 53 (1993) 149- 154.

66. Q. Pei and R. Qian, *Synthetic Metals*, 45 (1991) 35- 48.

67. D. S. Park, Y. B. Shim and S. M. Park, *J. Electrochem. Soc.*, 140 (1993) 609- 614.

68. W. J. Albery, Z. Chen, B. R. Horrocks, A. R. Mount, P. J. Wilson, D. Bloor, A. T. Monkman and C. M. Elliott, *Faraday Discuss. Chem. Soc.*, 88 (1989) 247- 259.

69. A. K. Meikap, A. Das, S. Chatterjee, M. Digar and S. N. Bhattacharyya, *Physical Review B*, 47 (1993) 1340- 1345.

70. M. Nechtschein, F. Devreux, F. Genoud, E. Vieil, J. M. Pernaut and E. Genies, *Synthetic Metals*, 15 (1986) 59- 78.

71. J. L. Bredas, B. Themans and J. M. Andre, *Physical Review B*, 27 (1983) 7827- 7830.

72. T. J. Lewis, *Faraday Discuss. Chem. Soc.*, 88 (1989) 189- 201.

73. R. John, PhD Thesis, *Electrochemical Studies of Heterocyclic Conducting Polymers*, University of Wollongong, Australia (1992).

74. J. L. Bredas, J. C. Scott, K. Yakushi and G. B. Street, *Physical Review B*, 30 (1984) 1023- 1025.

75. J. C. Scott, J. L. Bredas, J. H. Kaufman, P. Pfluger, G. B. Street and K. Yakushi, *Mol. Cryst. Liq. Cryst.*, 118 (1985) 163- 170.

76. G. Wegner and J. Rube, *Faraday Discuss. Chem. Soc.*, 88 (1989) 333-349.

77. S. Fletcher, *J. Chem. Soc. Faraday Trans.*, 89 (1993) 311- 320.

78. J. H. Kaufman, N. Colaneri, J. C. Scott and G. B. Street, *Physical Review Letters*, 53 (1984) 1005- 1008.

79. J. H. Kaufman, N. Colaneri, J. C. Scott, K. K. Kanazawa and G. B. Street, *Mol. Cryst. liq. Cryst.*, 118 (1985) 171- 177.

80. K. Naoi, M. Lien and W.H. Smyrl, *J. Electrochem. Soc.*, 138 (1991) 440-445.

81. M. Slama and J. Tanguy, *Synthetic Metals*, 28 (1989) C171- C176.

82. J. Tanguy, N. Mermilliod and M. Hoclet, *J. Electrochem. Soc.: Electrochemical Science and Technology*, 134 (1987) 795- 801.

83. T. Shimidzu, A. Ohtani, T. Iyoda and K. Honda, *J. Electroanal. Chem.*, 224 (1987) 123- 135.

84. T. Shimidzu, A. Ohtani, T. Iyoda and K. Honda, *Chem. Soc., Chem. Commun.*, (1986) 1415- 1417.

85. K. Naoi, M. M. Lien and W. H. Smyrl, *J. Electroanal. Chem.*, 272 (1989) 273- 275.

86. R. John and G. G. Wallace, *J. Electroanal. Chem.*, 354 (1993) 145- 160.

87. H. Zhao, W. E. Price and G. G. Wallace, *J. Electroanal. Chem.*, 334 (1992) 111- 120.

88. O. Niwa, M. Kakuchi and T. Tamamura, *Macromolecules*, 20 (1987) 749- 753.

89. K. K. Kanazawa, A. F. Diaz, M. T. Krounbi and G. B. Street, *Synthetic Metals*, 4 (1981) 119- 130.

90. W. Janßen and F. Beck, *Polymer*, 30 (1989) 352- 359.

91. M. A. De Paoli, R. J. Waltman, A. F. Diaz and J. Bargon, *Journal of Polymer Science: Polymer Chemistry Edition*, 23 (1985) 1687- 1698.

92. K. Uosaki, K. Okazaki and H. Kita, *Journal of Polymer Science: Part A: Polymer Chemistry*, 28 (1990) 399- 409.

93. O. Niwa, M. Hikita and T. Tamamura, *Synthetic Metals*, 18 (1987) 677- 682.

94. F. R. F. Fan and A. J. Bard, *J. Electrochem. Soc.: Electrochemical Science and Technology*, 133 (1986) 301- 304.

95. T. Hirai, S. Kuwabata and H. Yoneyama, *J. Electrochem. Soc.: Electrochemical Science and Technology*, 135 (1988) 1132- 1137.

96. G. Nagasubramanian, S. Di Stefane and J. Moacanin, *J. Phys. Chem.*, 90 (1986) 4447- 4451.

97. T. Iyoda, A. Ohtani, T. Shimidzu and K. Honda, *Synthetic Metals*, 18 (1987) 747- 751.

98. A. Ray, A. F. Richter, A. G. MacDiarmid and A. J. Epstein, *Synthetic Metals*, 29 (1989) E151- E156.

99. A. G. MacDiarmid and A. J. Epstein, *Faraday Discuss. Chem. Soc.*, 88 (1989) 317- 331.

100. J. Fritzsche, *J. Prakt. Chem.*, 20 (1940) 453; 28 (1943) 198. As cited in " E. M. Genies, A. Boyle, M. Lapkowski and C. Tsintavis, Synthetic Metals, 36 (1990) 139- 182".

101. A. G. Green and A. E. Woodhead, *Journal of Chemical Society*, 101 (1912) 1117- 1123.

102. A. F. Diaz and J. A. Logan, *J. Electroanal. Chem.*, 111 (1980) 111- 114.

103. A. G. MacDiarmid, J. C. Chiang, M. Halpern, W. S. Huang, S. L. Mu, N. L. D. Somasiri, W. Wu and S. I. Yaniger, *Mol. Cryst. Liq. cryst.*, 121 (1985) 173- 180.

104. S. Sarkar and I. N. Basumallick, *Transactions of the SAEST*, 23 (1988) 351- 353.

105. E. M. Genies, A. A. Syed and C. Tsintavis, *Mol. Cryst. Liq. Cryst.*, 121 (1985) 181- 186.

106. E. Genies, P. Hany and Ch. Santier, *Synthetic Metals,* 28 (1989) C647- C654.

107. D. T. Hoa, T. N. S. Kumar, N. S. Punekar, R. S. Srinivasa, R. Lai and A. Q. Contractor, *Anal. Chem.*, 64 (1992) 2645- 2646.

108. E. M. Genies, A. Boyle, M. Lapkowski and C. Tsintavis, *Synthetic Metals*, 36 (1990) 139- 182.

109. A. G. MacDiarmid, L. S. Yang, W. S. Huang and B. D. Humphrey, *Synthetic Metals,* 18 (1987) 393- 398.

110. W. W. Focke, G. E. Wnek and Y. Wei, *J. Phys. Chem.*, 91 (1987) 5813- 5818.

111. S. P. Armes and J. F. Miller, *Synthetic Metals,* 22 (1988) 385- 393.

112. A. Pron, F. Genoud, C. Menardo and M. Nechtschein, *Synthetic Metals,* 24 (1988) 193- 201.

113. Y. Cao, A. Andreatta, A. J. Heeger and P. Smith, *Polymer,* 30 (1989) 2305- 2311.

114. M. Abe, A. Ohtani, Y. Umemoto, S. Akizuki, M. Ezoe, H. Higuchi, K. Nakamoto, A. Okuno and Y. Noda, *J. Chem. Soc., Chem. Commun.*, (1989), 1736- 1738.

115. J. C. LaCroix and A. F. Diaz, *J. Electrochem. Soc.: Electrochemical Science and Technology,* 135 (1988) 1457- 1463.

116. J. C. LaCroix and A. F. Diaz, *Makromol. Chem., Macromol. symp.*, 8 (1987) 17- 37.

117. V. E. Kazarinov, V. N. Andreev, M. A. Spytsin and A. V. Shlepakov, *Electrochimica Acta*, 35 (1990) 899- 904.

118. W. S. Huang, B. D. Humphrey and A. G. MacDiarmid, *J. Chem. Soc., Faraday Trans.*, 82 (1986) 2385- 2400.

119. T. Boschi, G. Montesperelli, P. Nunziante, G. Pistoia and P. Fiordiponti, *Solid State Ionics,* 31 (1989) 281- 286.

120. A. P. Monkman, D. Bloor, G. C. Stevens and J. C. H. Stevens, *J. Phys. D: Appl. Phys.*, 20 (1987) 1337- 1345.

121. B. Wang, J. Tang and F. Wang, *Synthetic Metals,* 13 (1986) 329- 334.

122. A. Kitani, J. Izumi, J. Yano, Y. Hiromoto and K. Sasaki, Bull. *Chem. Soc. Jpn.*, 57 (1984) 2254- 2257.

123. G. Zotti, S. Cattarin and N. Comisso, *J. Electroanal. Chem.*, 239 (1988) 387- 396.

124. L. Duic and Z. Mandic, *J. Electroanal. Chem.*, 335 (1992) 207- 221.

125. D. E. Stilwell, and S. M. Park, *J. Electrochem. Soc.: Electrochemical Science and Technology,* 135 (1988) 2254- 2262.

126. D. M. Mohilner, R. N. Adams and W. J. Argersinger, Jr., *J. Am. Chem. Soc.*, 84 (1962) 3618- 3622.

127. D. E. Stilwell and S. M. Park, *J. Electrochem. Soc.: Electrochemical Science and Technology*, 135 (1988) 2491- 2496.

128. A. Andreatta, Y. Cao, J. C. Chiang, A. J. Heeger and P. Smith, *Polym. Prepr. (Am. Chem. Soc., Div. Polym. Chem.)*, 30 (1989) 149- 150.

129. A. Andreatta, Y. Cao, J. C. Chiang, A. J. Heeger and P. Smith, *Synthetic Metals*, 26 (1988) 383- 389.

130. M. Angelopoulos, A. Ray and A. G. MacDiarmid, *Synthetic Metals*, 21 (1987) 21- 30.

131. D. E. Stilwell and S. M. Park, *J. Electrochem. Soc. : Electrochemical Science and Technology*, 135 (1988) 2497- 2502.

132. T. kobayashi, H. Yoneyama and H. Tamura, *J. Electroanal. Chem.*, 177 (1984) 293- 297.

133. A. Kabumoto, K. Shinozaki, K. Watanabe and N. Nishikawa, *Synthetic Metals*, 26 (1988) 349- 355.

134. C. Q. Cui, X. H. Su and J. Y. Lee, *Polymer Degradation and Stability*, 41 (1993) 69- 76.

135. J. C. Chiang and A. G. MacDiarmid, *Synthetic Metals*, 13 (1986) 193- 205.

136. J. G. Masters, Y. Sun, A. G. MacDiarmid and A. J. Epstein, *Synthetic Metals*, 41- 43 (1991) 715- 718.

137. K. G. Neoh, E. T. Kang and K. L. Tan, *Journal of Polymer Science, part A: Polymer Chemistry*, 29 (1991) 759- 766.

138. A. J. Epstein, J. M. Ginder, F. Zuo, H. S. Woo, D. B. Tanner, A. F. Richter, M. Angelopoulos, W. S. Huang and A. G. MacDiarmid, *Synthetic Metals*, 21 (1987) 63- 70.

139. J. P. Travers, F. Genoud, C. Menardo and M. Nechtschein, *Synthetic Metals*, 35 (1990) 159- 168.

140. V. M. Geskin, Ya. A. Letuchy, B. Z. Lubentsov, L. M. Grundel, S. M. Tikhomirov and M. L. Khidekel, *Journal of Molecular Electronics*, 5 (1989) 207- 213.

141. H. H. S. Javadi, F. Zuo, K. R. Cromack, M. Angelopoulos, A. G. MacDiarmid and A. J. Epstein, *Synthetic Metals*, 29 (1989) E409- E416.

142. A. P. Monkman, D. Bloor, G. C. Stevens, J. C. H. Stevens and P. Wilson, *Synthetic Metals*, 29 (1989) E277- E284.

143. E. M. Genies and M. Lapkowski, *J. Electroanal. Chem.*, 236 (1987) 199- 208.

144. E. M. Scherr, A. G. MacDiarmid, S. K. Manohar, J. G. Masters, Y. Sun, X. Tang, M. A. Druy, P. J. Glatkowski, V. B. Cajipe, J. E. Fischer, K. R. Cromack, M. E. Jozefowicz, J. M. Ginder, R. P. McCall and A. J. Epstein, *Synthetic metals* , 41- 43 (1991) 735- 738.

145. A. Watanabe, K. Mori, M. Mikuni, Y. Nakamura and M. Matsuda, *Macromolecules*, 22 (1989) 3323- 3327.

146. J. L. Bredas, R. R. Chance and R. Silbey, *Physical Review B*, 26 (1982) 5843- 5854.

147. Y. Onodera, *Physical Review B*, 30 (1984) 775- 785.

148. S. kivelson and A. J. Heeger, *Physical Review Letters*, 55 (1985) 308- 311.

149. D. L. Cowan, V. Priest, T. R. Marrero and D. W. Slaughter, *J. Phys. Chem. Solids*, 51 (1990) 307- 312.

150. M. Mulder, *Basic Principles of Membrane Technology*, Kluwer, London, UK (1990).

151. I. H. Loh, R. A. Moody and J. C. Huang, *Journal of Membrane Science*, 50 (1990) 31- 49.

152. H. K. Lonsdale, *J. of Membrane Science*, 10 (1982) 81-181

153. I. Cabasso, in *Encyclopaedia of Polymer Science and Engineering, Volume 9*, J. I. Kroschwitz (Ed.), John Wiley and Sons Inc., New York, (1987).

154. J. G. A. Bilter, *Transport Mechanisms in Membrane Separation Processes*, Plenum Press, New York, USA (1991).

155. E. Klein, *Affinity Membranes*, John Wiley, New York, USA (1991).

156. P. Burgmayer and R. W. Murray, *J. Phys. Chem.*, 88 (1984) 2515- 2521.

157. V. M. Schmidt and J. Heitbaum, *Synthetic Metals*, 41- 43 (1991) 425-428.

158. P. Burgmayer and R. W. Murray, *J. Electroanal. Chem.*, 147 (1983) 339- 344.

159. P. Burgmayer and R. W. Murray, *J. Am. Chem. Soc.*, 104 (1982) 6139-6140.

160. C. Zhong, W. Storck and K. Doblhofer, *Ber. Bursenges. Phys. Chem.*, 94 (1990) 1149- 1155.

161. C. Zhong, K. Doblhofer and G. Wienberg, *Faraday Discuss. Chem. Soc.*, 88 (1989) 307- 316.

162. E. W. Tsai, T. Pajkossy, K. Rajeshwar and J. R. Reynolds, *J. Phys. Chem.*, 92 (1988) 3560- 3565.

163. S. Yabuki, F. Mizutani and M. Asai, *Biosensors & Bioelectronics*, 6 (1991) 311- 315.

164. E. Wang, Y. Liu, S. Dong and J. Ding, *J. Chem. Soc. Faraday Trans.*, 86 (1990) 2243- 2247.

165. M. R. Anderson, B. R. Mattes, H. Reiss and R. B. Kaner, *Science*, 252 (1991) 1412- 1415.

166. M. R. Anderson, B. R. Mattes, H. Reiss and R. B. Kaner, *Synthetic Metals*, 41- 43 (1991) 1151- 1154.

167. P. T. Kissinger and W. R. Heineman, *Laboratory Techniques in Electroanalytical Chemistry*, Marcel Dekker Inc., New York and Basel (1984).

168. A. R. Hillman in *Electrochemical Science and Technology of polymers, Volume 1, Chapter 5*, R. G. Linford (Ed.), Elsevier Applied Science, London, New York (1990).

169. B. C. Cope and M. D. Glasse in *Electrochemical Science and Technology of polymers, Volume 2, Chapter 6*, R. G. Linford (Ed.), Elsevier Applied Science, London, New York (1990).

170. G. Binnig, C. F. Quate and C. Gerber, , *Physical Review Letters*, 56 (1986) 930-933.

171. C. M. Mate, G. M. McClelland, R. Erlandsson and S. Chiang, *Physical Review Letters*, 59 (1987) 1942- 1945.

172. Y. Martin and H. K. Wickramasinghe, *Appl. Phys. Lett.*, 50 (1987) 1455-1457.

173. Y. Martin, C. C. Williams and H. K. Wickramasinghe, *J. Appl. Phys.*, 61 (1987) 4723- 4729.

174. G. Meyer and N. M. Amer, *Appl. Phys. Lett.*, 53 (1988) 1045- 1047.

175. S. Alexander, L. Hellemans, O. Marti, J. Schneir, V. Elings, P. K. Hansma, M. Longmire and J. Curley, *J. Appl. Phys.*, 65 (1989) 164- 166.

176. M. Egger, F. Ohnesorge, A. L. Weisenhorn, S. P. Heyn, B. Drake, C. B. Prater, S. A. C. Gould, P. K. Hansma and H. E. Gaub, *Journal of Structural Biology*, 103 (1990) 89- 94.

177. D. A. Skoog, *Principles of Instrumental Analysis,* Third Edition, Saunders College Publishing, USA (1985).

178. A. J. Bard and L. R. Faulkner, *Electrochemical Methods, Fundamentals and Applications,* John Wiley and Sons, New York (1980).

179. A. Kitani, M. Kaya, S. Tsujioka and K. Sasaki, *Journal of Polymer Science: Part A: polymer Chemistry*, 26 (1988) 1531- 1539.

180. A. P. Monkman and P. Adams, *Synthetic Metals*, 40 (1991) 87- 96.

181. A. G. MacDiarmid, J. C. Chiang, A. F. Richter, N. L. D. Somasiri and A. J. Epstein, in *Conducting Polymers,* L. Alcacer (Ed.), D. Reidel Publishing Company (1987).

182. E. Scherr, *Personal Communication,* University of Pennsylvania, USA (1991).

183. W. Fosong, T. Jinsong, W. Lixiang, Z. Hongfang and M. Zhishen, *Mol. Cryst. Liq. Cryst.*, 160 (1988) 175- 184.

184. T. Sata, *Electrochimica Acta*, 37 (1992) 555- 563.

185. M. Satoh, K. Kaneto and K. Yoshino, *Synthetic Metals*, 14 (1986) 289- 296.

186. C. O. Too, PhD Thesis, *Volumetric Properties of Boran Carbide Electrodes,* Imperial College of Science and Technology, University of London, UK (1983).

187. R. C. D. Peres, J. M. Pernaut and M. A. De Paoli, *J. Polym. Sci.*, 29 (1991) 225- 231.

188. K. Yoshino, M. Tabata, M. Satoh, K. Kanato and T. Ohsawa, *Technology Reports of the Osaka University,* 35, 1807 (1985) 231- 236.

189. T. Shimidzu, A. Ohtani and K. Honda, *J. Electroanal. Chem.*, 251 (1988) 323- 337.

190. R. M. Penner and C. R. Martin, *J. Electrochem. Soc.*, 133 (1986) 310-315.

191. A. A. E. Martell and R. M. Smith, *Critical Stability Constants, Vol. 3,* Plenum Press, New York and London (1979).

192. D. A. Buttry, *Electroanalytical Chemistry*, 17 (1990) 2- 85.

193. L. A. Prezyna and G. E. Wnek, *Synthetic Metals*, 41- 43 (1991) 979-981.

194. J. M. Slater, E. J. Watt, N. J. Freeman, I. P. May and D. J. Weir, *Analyst*, 117 (1992) 1265- 1270.

195. P. Curie, J. C. R. Curie, *Acad. Sci.*, 91 (1880) 294. As cited in from " D. A. Buttry and M.D. Ward, Chem. Rev., 92 (1992) 1355- 1379".

196. A. Langevin, *Piezoelectricity,* First Edition, McGraw- Hill, New York and London (1946). As cited in from " J. F. Alder and J. J. McCallim, The Analyst, 108 (1983) 1169- 1189".

197. G. Sauerbrey, *Zeitschrift fur Physik*, 155 (1959) 206- 222.

198. J. L. Jones and J. P. Mieure, *Analytical chemistry,* 41 (1969) 484-490.

199. P. L Konash and S. J. Bastiaans, *Anal. Chem.*, 52 (1980) 1929- 1931.

200. T. Nomura and M. Iijima, *Analytica Chimica Acta,* 131 (1981) 97-102.

201. T. Nomura, *Analytica Chimica Acta,* 124 (1981) 81- 84.

202. G. J. Price and J. M. Buley, *Progress in Organic Coatings*, 19 (1991) 265- 274.

203. H. Muramatsu, K. Kimura, T. Ataka, R. Homma, Y. Miura and I. Karube, *Biosensors & Bioelectronics*, 6 (1991) 353- 358.

204. J. H. Kaufman, K. K. Kanazawa and G. B. Street, *Physical Review letters*, 53 (1984) 2461- 2464.

205. C. S. C. Bose and K. Rajeshwar, *J. Electroanal. Chem.*, 333 (1992) 235- 256.

206. C. K. Baker and J. R. Reynolds, *Synthetic Metals*, 28 (1989) C21- C26.

207. C. S. C. Bose, S. Basak and K. Rajeshwar, *J. Phys. Chem.*, 96 (1992) 9899- 9906.

208. C. Dusemund and G. Schwitzgebel, *Ber. Bunsenges. Phys. chem.*, 95 (1991) 1543- 1546.

209. G. E. Wnek, L. A. Prezyna and J. J. Lee, *Polymer Preprints*, 30 (1989) 178- 180.

210. R. Bilger and J. Heinze, *Synthetic Metals*, 41- 43 (1991) 2893- 2896.

211. D. Orata and D. A. Buttry, *J. Am. Chem. Soc.*, 109 (1987) 3574- 3581.

212. H. Daifuku, T. Kawagoe, T. Matsunaga, N. Yamamoto, T. Ohsaka and N. Oyama, *Synthetic Metals*, 41- 43 (1991) 2897- 2900.

213. J. Rishpon, A. Redondo, C. Derouin and S. Gotttesfeld, *J. Electroanal. Chem.*, 294 (1990) 73- 85.

214. S. Cordoba- Torresi, C. Gabrielli, M. Keddam, H. Takenouti and R. Torresi, *J. Electroanal. Chem.*, 290 (1990) 269- 274.

215. D. Orata and D. A. Buttry, *J. Electroanal. Chem.*, 257 (1988) 71- 82.

216. D. A. Buttry and M. D. Ward, *Chem. Rev.*, 92 (1992) 1355- 1379.

217. S. Bruckenstein and M. Shay, *Electrochimica Acta*, 30 (1985) 1295-1300.

APPENDIX

Operational program for dual pulse driver:

Schematic 1 shows the operational diagram used to control the potential program throughout the transport studies. At time (0 to 30 s) the polymer membrane was reduced by inducing an appropriate current between points A and B. This current was produced by application of a reductive potential (i.e. -0.60 V vs Ag/AgCl) to the membrane. At time (30 to 60 s) the circuit between A and B was disconnected. However, in this period of time the polymer membrane was oxidised by application of a oxidative potential to the receiving side, as a result of this a current flowed between A and C. Note that in this period of time no current flowed between A and B. This sequence was then repeated. The circuit diagram used to drive this potential program is shown in schematic 2.

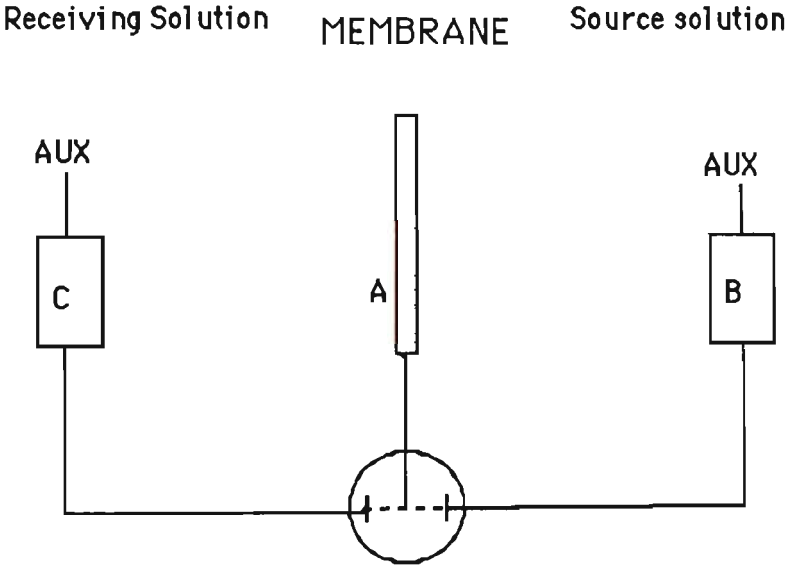

Schematic 1 The potential program diagram used for transport studies.

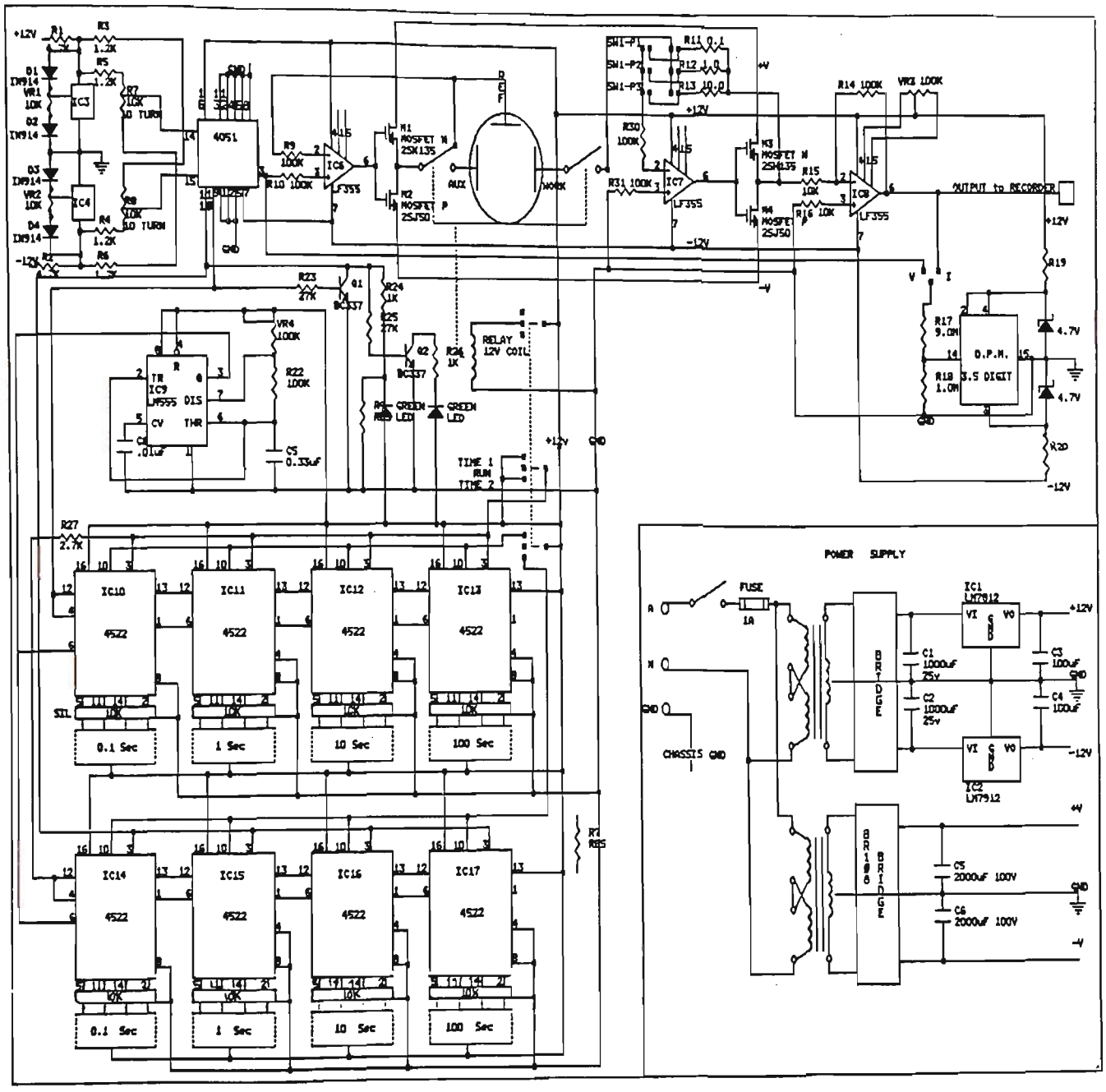

Schematic 2 The circuit diagram used to generate potential program shown in schematic 1 (transport studies).

The circuits used for EQCM

(A) Oscillator circuit

(B) Offset circuit

(A)

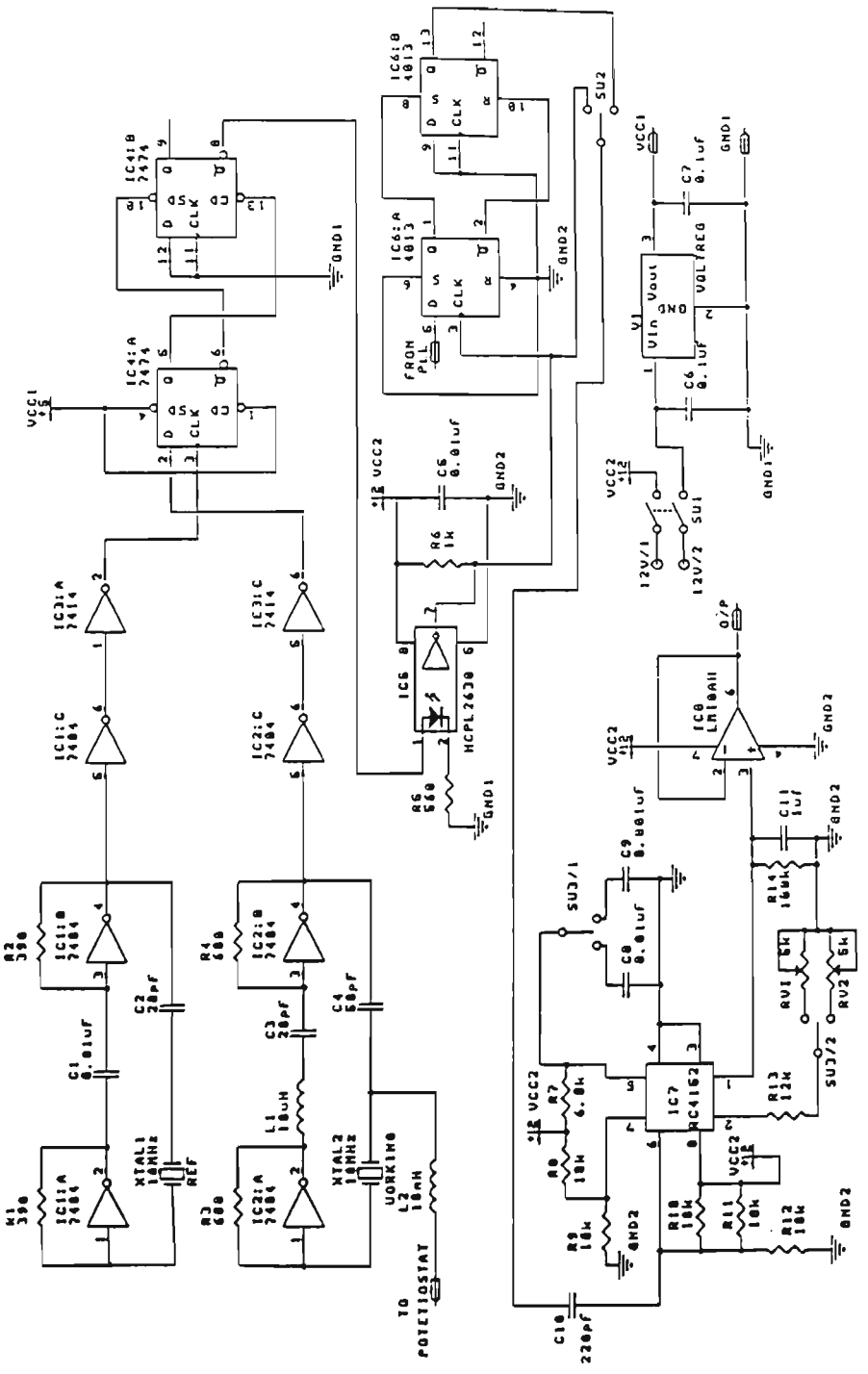

(B)

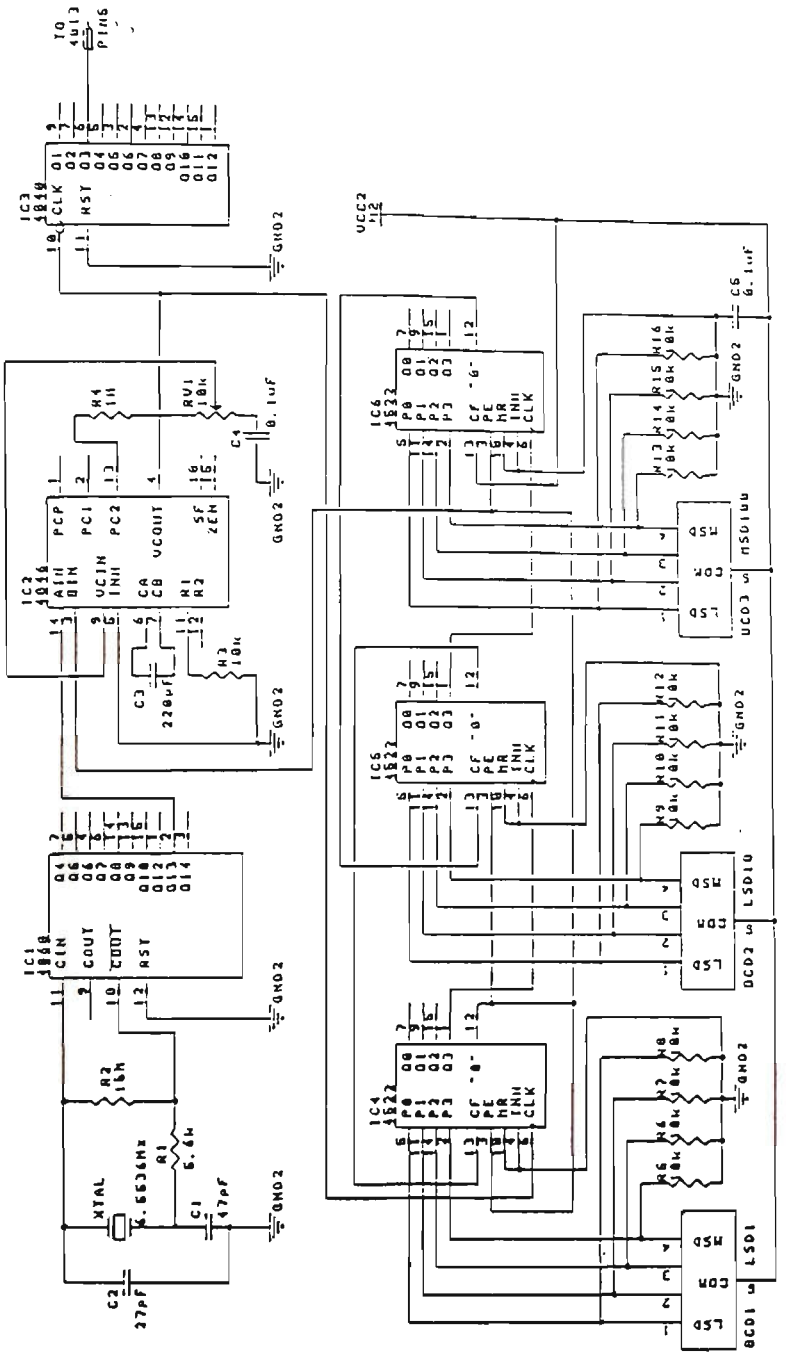
IC1
4060
IC2
4046
IC3
4040
IC4
4522
IC5
4522
IC6
4522
IC7
4522
XTAL
5.6536MHz
R1
5.6K
R2
10K
R3
10K
R4
1M
RV1
10K
C1
47pF
C2
27pF
C3
220pF
0.1uF
VCC2
+12
GND2
LSD10
LSD01